UNIVERSIDADE DE SÃO PAULO

ESCOLA POLITÉCNICA

Rubens Eliseu Nicula de Castro

MODELING A SUGARCANE BIOREFINERY PROCESS AND ASSESSMENT OF THE USE OF INDUSTRIAL RESIDUE: BAGASSE AND STRAW

São Paulo

2022

RUBENS ELISEU NICULA DE CASTRO

MODELING A SUGARCANE BIOREFINERY PROCESS AND ASSESSMENT OF THE USE OF INDUSTRIAL RESIDUE: BAGASSE AND STRAW

Corrected Version

Thesis presented to the Escola Politécnica of Universidade de São Paulo to obtain the degree of Doctor in Science.

Concentration area: Chemical Engineering

Advisor: Prof. Dr. Claudio Augusto Oller do Nascimento

São Paulo

2022

Este exemplar foi revisado e corrigido em relação à versão original, sob responsabilidade única do autor e com a anuência de seu orientador.

São Paulo, 01 de Setembro de 2022

Assinatura do autor: 

Assinatura do orientador: 

Catalogação-na-publicação

Castro, Rubens
MODELING A SUGARCANE BIOREFINERY PROCESS AND ASSESSMENT OF THE USE OF INDUSTRIAL RESIDUE: BAGASSE AND STRAW / R. Castro -- versão corr. -- São Paulo, 2022.
239 p.

Tese (Doutorado) - Escola Politécnica da Universidade de São Paulo. Departamento de Engenharia Química.

1.SIMULAÇÃO 2.CANA-DE-AÇÚCAR 3.ETANOL 4.BIOENERGIA 5.BIOCOMBUSTÍVEIS I.Universidade de São Paulo. Escola Politécnica. Departamento de Engenharia Química II.t.

RUBENS ELISEU NICULA DE CASTRO

MODELING A SUGARCANE BIOREFINERY PROCESS AND ASSESSMENT OF THE USE OF INDUSTRIAL RESIDUE: BAGASSE AND STRAW

Thesis presented to the Escola Politécnica of Universidade de São Paulo to obtain the degree of Doctor in Science.

Approved on July 29th 2022

Examination Committee:

Prof. Dr. Claudio Augusto Oller do Nascimento

Universidade de São Paulo

Prof. Dr. Rubens Maciel Filho

Universidade Estadual de Campinas (UniCamp)

Dr. Douglas Castilho Mariani

Soteica do Brasil

Dra Raquel de Freitas Dias Milão

Senai-RJ

Reinaldo Giudici

Universidade de São Paulo

ACKNOWLEDGEMENTS

Foremost, I would like to express my sincere gratitude to my advisor Prof. Dr. Claudio Augusto Oller do Nascimento for the support, motivation and enthusiasm during the time of the research. Besides, I also thank Prof. Dr. Rita Maria de Brito Alves for her patience, insightful comments, and immense knowledge.

My sincere thanks also go to my labmates. I could not have imagined having better people around me for my Ph.D. study.

Last but not least, I would like to thank my family. Without the support and love of my family I know I could not have accomplished this thesis. My parents, Vinicio and Lourdes, I am so blessed to be your son. My wife, Vivian, and my son Jorge, for all the support, patience and understanding when undertaking my research and writing.

ABSTRACT

CASTRO, R.E.N **Modeling a Sugarcane Biorefinery Process and Assessment of the Use of Industrial Residue: Bagasse And Straw.** 2022. Thesis (Doctor in Science) - Escola politécnica, Universidade de São Paulo, São Paulo, 2022.

This thesis assesses the sugarcane industrial process. First, it presents a broad understanding of sugar and bioethanol production in Brazil; in this part, the reasons why ethanol becomes a successful alternative to partially replace petroleum fuel and the potential to expand its production are evaluated. Then, a simulation platform is established to simulate the sugarcane industry. Sugar, ethanol, and electricity production are simulated considering the current process; parameters and production efficiencies are compared with those of the industrial process. In this platform, multiple-effect evaporation is shown to be a key operation that plays an important role in saving industrial thermal energy; saving thermal energy means saving bagasse, which is the feedstock for advanced fuel production. The sugarcane simulation platform is then interconnected with some advanced biofuel production processes, such as second-generation ethanol and biogas. The production of biogas and second-generation ethanol using bagasse and straw is evaluated and compared with the production of electricity; this assessment considered the use of these fuels in a light vehicle. In this part, it is concluded that depending on the criteria used to analyze, one fuel would be preferred to another. A general conclusion is that the sugarcane industry plays an important role in the Brazilian energy matrix and the use of agricultural and industrial residues has great potential to increase the share of environmentally friendly fuel.

Keywords: sugarcane industry; simulation platform; advanced biofuels.

RESUMO

CASTRO, R.E.N **Modeling a Sugarcane Biorefinery Process and Assessment of the Use of Industrial Residue: Bagasse And Straw.** 2022. Tese (Doutorado em Ciências) - Escola politécnica, Universidade de São Paulo, São Paulo, 2022.

Esta tese avalia o processo industrial da cana-de-açúcar. Inicialmente, é apresentado um amplo entendimento da produção de açúcar e bioetanol no Brasil; foram avaliados os motivos pelos quais o etanol se tornou uma alternativa de sucesso para substituir parcialmente o petróleo e também o potencial de expansão de sua produção. Em seguida, é mostrado como foi elaborada a plataforma de simulação para simular o setor sucroenergético. A produção de açúcar, etanol e eletricidade foi simulada considerando parâmetros e eficiências de produção e então comparados com os do processo industrial. Depois, é apresentado como a evaporação de múltiplos efeitos desempenha um papel chave na economia de energia térmica da industria; economizar energia térmica significa economizar bagaço, que é a matéria-prima para a produção de combustível avançado. Por fim, a plataforma de simulação foi então conectada com os processos produção de biocombustível avançado, como etanol de segunda geração e biogás. A produção de biogás e etanol de segunda geração usando bagaço e palha é comparada com a produção de energia elétrica; essa avaliação considerou o uso desses combustíveis em um veículo leve. Nesta parte, conclui-se que dependendo dos critérios utilizados para análise, um combustível seria preferível a outro. A conclusão geral é que o setor sucroenergético desempenha um papel importante na matriz energética brasileira e o uso de resíduos agrícolas é fundamental para aumentar a participação de combustíveis ecologicamente correto no país.

Palavras-chave: industria sucroalcooleira; plataforma de simulação; biocombustíveis avançados.

LIST OF FIGURES

Figure 1 - Fuel and anhydrous ethanol production; ethanol-powered car and flex-fuel car sold in Brazil; and the price of the oil barrel 21

Figure 2 - Fraciton of anhydrous ethanol added to gasoline. 22

Figure 3 - Productivity of sugarcane and planted area 26

Figure 4 - Schematic flowchart of a sugarcane industry 46

Figure 5 - Schematic flowchart of a sugarcane industry 49

Figure 6 - Schematic flowchart of a sugarcane industry 50

Figure 7 - Ethanol Sugar and Power production 51

Figure 8 - Specific Gravity correlation for sugarcane juice 56

Figure 9 - Schematic flow diagram of a condenser 65

Figure 10 - Schematic sugarcane preparation and conveyor system for a mil extraction process 66

Figure 11 - Schematic diagram of milling extraction 70

Figure 12 - Schematic diagram of the mass inlet and outlet milling unit tandem 71

Figure 13 - Schematic diagram of milling train 76

Figure 14 - Mill roll showing wedges for adjustment of rollers 78

Figure 15 - Schematic drag conveyor intermediate carrier 81

Figure 16 - Schematic flow diagram of a Juice screen process 81

Figure 17 - Juice separation scheme 83

Figure 18 - Regenerative heat exchange scheme 84

Figure 19 - Single juice treatment scheme (only ethanol is produced) 86

Figure 20 - Double juice treatment scheme without evaporation of ethanol juice 87

Figure 21 - Double juice treatment scheme 87

Figure 22 - Schematic flow diagram of a Milk of Lime preparation 88

Figure 23 - Schematic flow diagram of a steam heat exchanger 90

Figure 24 - Schematic flow diagram of juice decanter 94

Figure 25 - schematic main flows at mud filtration 96

Figure 26 - Process steam flow diagram and the main consumer of thermal energy 99

Figure 27 - Two boiling scheme sugar process 100

Figure 28 - Sugar crystallization stages 103

Figure 29 - Schematic diagram of a vacuum pan 106
Figure 30 - Schematic diagram ethanol process 115
Figure 31 - Broth preparation scheme 115
Figure 32 - Broth cooling 117
Figure 33 - Schematic diagram of CO_2 washer 123
Figure 34 - Flow diagram of the ethanol distillation process 127
Figure 35 - Schematic diagram of distillation overall feed streams 129
Figure 36 - Schematic diagram of bagasse circuit and high-pressure steam production ... 130
Figure 37 - Schematic diagram of a boiler 131
Figure 38 - Schematic diagram of a deaerator 140
Figure 39 - Schematic flow diagram of combustion gas treatment 141
Figure 40 - schematic flow in a spray type tower gas scrubber 142
Figure 41 - Schematic flow diagram of juice decanter 144
Figure 42 - Schematic flow diagram for a closed circuit cooling tower 147
Figure 43 - Schematic flow diagram for a closed-circuit cooling spray system 149
Figure 44 - Schematic flow diagram of a water treatment plant and demineralization 151
Figure 45 - Schematic hot water flowchart identifying mains consumers and producers . 153
Figure 46 - Schematic process water flowchart identifying mains consumers 153
Figure 47 – Interconnection among the areas 154
Figure 48 - B-1 vacuum pan run 160
Figure 49 - B-2 vacuum pan run 161
Figure 50 - A-3 vacuum pan run 161
Figure 51 - A-4 vacuum pan run 162
Figure 52 - A-5 vacuum pan run 162
Figure 53 - A-6 vacuum pan run 163
Figure 54 - Fermentation schedules 164
Figure 55 – Fed-batch 72 hours fermentation 164
Figure 56 - Temperature change during simulation 165
Figure 57 –Steam diagram 172
Figure 58 - Temperature distribution in a five-effect evaporation train 173
Figure 59 - Multiple effect evaporation representing the steam bleed in the Sugarmill ... 175
Figure 60 – Algorithm to solve multiple-effect evaporation in a Sugarmill industry 185

Figure 61 – Steam consumed during the crystallization process, steam fed in MEE and steam pressure produced at each multiple-effect evaporation body 186
Figure 62 - Steam consumed at the crystallization process 187
Figure 63 - Total exhaust steam consumed in a 48-hour simulation and Delta, lower and upper limit around average steam consumption. 189
Figure 64 - Electricity production 190
Figure 65 - Problem summary 198
Figure 66 - Surplus lignocellulosic material being converted into electricity 201
Figure 67 - Surplus lignocellulosic material being converted into second-generation ethanol 201
Figure 68 - Surplus lignocellulosic material being converted into biogas 202
Figure 69 - Cashflow diagram 213
Figure 70 - Total distance one can drive in a light vehicle using different types of fuel obtained from bagasse 217
Figure 71 - The net present value of the investment in the surplus bagasse processing plant 218
Figure 72 - CO2 equivalent emitted from the surplus bagasse being processed to use in a light vehicle 219
Figure 73 - Total water abstraction considering a Sugarcane mill industry when a process that converts bagasse and straw into fuel for light vehicles is added 220
Figure 74 - Representation of the performance of electricity, second-generation ethanol, and biogas used as fuel in light vehicles. 221
Figure 75 - Ethanol cars mileage rate. (*a*) city mileage rate (*b*) highway mileage rate 232
Figure 76 - Biogas cars mileage rate. (*a*) city mileage rate (*b*) highway mileage rate 232
Figure 77 - Electric cars mileage rate. (*a*) city mileage rate (*b*) highway mileage rate 232
Figure 78 - CO2 emitted during the process of producing and using each fuel 233
Figure 79 - Ethanol price paid at Paulínea - SP fuel distribution center 235
Figure 80 - Vehicular natural gas average price at São Paulo State 236
Figure 81 - Average price paid at power auctions 236

LIST OF TABLES

Table 1 - Parameters used to obtain the electricity production from sugarcane bagasse ... 35

Table 2 - Parameters used to obtain the consumption rating of two vehicles ... 38

Table 3 - Parameters used to obtain the consumption rating of two vehicles ... 38

Table 4 - Specifications and operations conditions used in this simulation ... 51

Table 5 - Specific Gravity for sugarcane juice ... 56

Table 6 - Uniquac parameters ... 62

Table 7 - Power consumption in cane preparation ... 69

Table 8 – Ratio of fiber to bagasse (*Bfib*) ... 73

Table 9 – Ratio of brix between the juice and the inlet stream (*Exef*) ... 74

Table 10 - The ratio of fiber between bagasse and the fed stream ... 74

Table 11 - Mill gearing ... 78

Table 12 - Stages and steps for crystalization B ... 102

Table 13 - Stages and steps for crystalization A ... 102

Table 14 – Basic elements for the bagasse wood-chips and lignin ... 133

Table 15 - Emission factor and unreacted carbon ... 134

Table 16 - Parameters used at simulation ... 166

Table 17 – Stages and steps for crystalization B ... 179

Table 18 - Stages and steps for crystalization A ... 179

Table 19 - Parameters for the first-generation ethanol and sugar production and CHP (backpressure turbine) processes. ... 200

Table 20 - Parameters for the thermo-power unit with a condensation turbine ... 203

Table 21 - Parameters used in the simulation for second-generation ethanol production 204

Table 22 - Parameters used in the simulation for biogas production ... 206

Table 23 - Mileage rate for light vehicles ... 208

Table 24 - Emission factors used to obtain the GHG emission ... 211

Table 25 - Parameters used to obtain the net present value of the investments ... 215

Table 26 - Distance per kg of sugarcane ... 217

Table 27 - CO2 emission given in kg of CO2 equivalent ... 234

CONTENT

CHAPTER 1: INTRODUCTION 14

1.1 Contextualization and Motivation 14
1.2 Objectives 16
1.3 Thesis Organization 16
References 17

CHAPTER 2: ASSESSMENT OF SUGARCANE-BASED ETHANOL PRODUCTION 19

Abstract 19
2.1 Introduction 19
2.2 Why has bio-ethanol become a successful alternative to partially replace petroleum fuels? A short history 20
2.3 Efficiency of the sugarcane ethanol production and what is expected in a near future 25
2.3.1 Sugarcane crop 25
2.3.2 Sugarcane transportation 27
2.3.3 Cane reception preparation and extraction 27
2.3.4 Juice treatment 30
2.3.5 Juice concentration 30
2.3.6 Fermentation 31
2.3.7 Downstream processing 32
2.3.8 Vinasse and biogas 33
2.3.9 Combined heat and power 34
2.3.10 Second-generation ethanol 36
2.3.11 Second-generation ethanol versus CHP 37
2.4 Conclusion 38
Acknowledgments 39
References 39

CHAPTER 3: OPEN SUGARCANE PROCESS SIMULATION PLATFORM 45

Abstract 45
3.1 Introduction 45
3.2 Process Overview 46
3.3 Model 48
3.4 Results 50
3.5 Conclusion 52
Acknowledgments 52
References 52

CHAPTER 4: REPORT: SUGARCANE PROCESS SIMULATION PLATFORM 54

4.1 Introduction 54
4.2 Thermodynamic properties: 55
4.2.1 Water 55

4.2.2 Sugary solutions 55
4.2.3 Fiber 58
4.2.4 Ethanol 58
4.3 General unit operation 62
4.3.1 Centrifugal Pump 62
4.3.2 Vacuum pump 63
4.3.3 Rubber belt conveyor 63
4.3.4 Barometric condenser 64
4.4 Cane reception and preparation 66
4.4.1 Feeder table 67
4.4.2 Steel Slat 67
4.4.3 Rubber belt conveyor 68
4.4.4 Shredder and knifing 68
4.4.5 Others power requirements 69
4.5 Extraction 69
4.5.1 Mil Tandem 71
4.5.2 Drag conveyor 79
4.5.3 Screen 81
4.6 Juice separation 83
4.7 Regenerative Heat Exchange 84
4.7.1 Mass and energy balance 84
4.7.2 Power 85
4.8 Juice treatment 86
4.8.1 Sulfitation 87
4.8.2 Liming and milk of lime preparation 88
4.8.3 Heating 90
4.8.4 Flash 93
4.8.5 Clarification 94
4.8.6 Filtration 95
4.8.7 Power consumption 98
4.9 Multiple effect evaporation 98
4.9.1 Mathematical model 99
4.9.2 Power 99
4.10 Sugar process 99
4.10.1 Sugar process recipe 101
4.10.2 Mathematical model 105
4.11 Ethanol process 114
4.11.1 Broth preparation 115
4.11.2 Broth cooling 116
4.11.3 Fermentation 118
4.11.4 CO_2 Scrubber 122
4.11.5 Yeast centrifuge 124
4.11.6 Yeast treatment 125
4.11.7 Distillation 126
4.12 Combined heat and power 130
4.12.1 Boiler 131
4.12.2 Steam turbine generator 137

4.12.3 Condenser 138
4.12.4 Deaerator 139
4.13 Combustion gas treatment 141
4.13.1 Boiler gas wet scrubber 142
4.13.2 Liming and milk of lime preparation 143
4.13.3 Clarification 144
4.13.4 Filtration: 145
4.14 Cooling water utility 147
4.14.1 Cooling tower 147
4.14.2 Cooling spray 149
4.15 Water treatment and demineralization 150
4.15.1 Water treatment 151
4.15.2 Demineralization 151
4.15.3 Power 152
4.16 Water abstraction 152
4.16.1 Power 153
4.17 Convergence algorithm between areas 154
4.18 Conclusion 155
References 155
Appendix A – Results from a sugar production simulation 160
Appendix B – Results from a fermentation simulation 164

CHAPTER 5: DYNAMIC SIMULATION OF MULTIPLE-EFFECT EVAPORATION 167

Abstract 167
Nomenclature 168
5.1 Introduction 169
5.1.1 Process overview 171
5.2 Method 174
5.2.1 Modeling of the Evaporator 174
5.2.2 Thermodynamic Properties and Heat Transfer Coefficient 177
5.2.3 Sugar Batch Crystallization Process 178
5.2.4 Interactive algorithm 183
5.3 Results 185
5.3.1 Flexible Steam Pressure 186
5.3.2 Fixed Steam Pressure 187
5.3.3 Lower and upper boundaries condition 188
5.3.4 Electricity production 189
5.4 Conclusion 190
Acknowledgments 191
References 191

CHAPTER 6: ASSESSING THE SUGARCANE BAGASSE AND STRAW AS A BIOFUEL TO PROPEL LIGHT VEHICLES 195

Abstract 195
6.1 Introduction 195
6.2 Methods 198

6.2.1 Bagasse processing into usable fuel for light vehicles 199
6.2.2 Mileage rate 207
6.2.3 Monte Carlo analysis 208
6.2.4 Gas emissions, water usage, and health 209
6.2.5 Financial appraisal 212
6.3 Results and discussion 216
6.3.1 Total mileage 216
6.3.2 Financial appraisal 218
6.3.3 CO_2 emission 219
6.3.4 Water abstraction 220
6.4 Conclusion 222
Conflicts of interest 223
Acknowledgments 223
References 223
Supplementary Information 232

CHAPTER 7: FINAL CONSIDERATIONS 237

7.1 General conclusions 237
7.2 Future work suggestions 238
References 238

CHAPTER 1: INTRODUCTION

This introductory chapter presents the contextualization and the motivation of this thesis, then the general and specific objectives are stated, and finely how the text in this thesis is organized.

1.1 Contextualization and Motivation

The sugarcane industry plays a vital role in global energy security, economic growth, social inclusion, and food supply. It is the source of 86 % of the total global sugar production (OECD-FAO, 2021). Additionally, in 2021, the world produced 103 million cubic meters of bioethanol (RFA RENEWABLE FUELS ASSOCIATION, [*s. d.*]), which replaced at least 69 million cubic meters of gasoline. It is a remarkable sector, especially in subtropical regions, and is expected to grow in production to meet the growing demand for sugar and bioethanol.

Currently, society is highly dependent on oil, which will not last forever. It is not only finite but also hazardous to the world due to greenhouse gas emissions. Therefore, it is urgent to find alternatives to replace it with renewable sources. Renewable energy comes from a source that is naturally replenished. Sugarcane or any other biomass is considered a renewable energy source because its inherent energy comes from the Sun via photosynthesis and can grow in a relatively short time.

To increase the production of ethanol and sugar, the sugarcane sector must not only increase land field plantation, but also be sustainable. Sustainability means reducing the impacts of its activities on the environment, promoting corporate and social responsibility, increasing transparency by improving the flow of information, and promoting greater inclusion and less social imbalance. Sustainability has three pillars: economic (profit), social (people), and environmental (planet). For a corporation without economic sustainability, no other requests are possible, since companies cannot afford to pay for them. Sugarcane bioethanol is profitable when the oil price is more than US$ 45,00 per barrel (RODRIGUES, 2008). The sugarcane industry has on average a positive social impact compared to the oil industry, such as employment generation and income distribution for actors involved in the supply chain (RIBEIRO, 2013). Furthermore, the environmental impact is the main positive impact of the sugarcane industry, since CO_2 from the use of ethanol and bagasse is reabsorbed

by photosynthesis during sugarcane growth in the following season. (GOLDEMBERG; COELHO; GUARDABASSI, 2008)

To achieve all sustainability goals, research and development are necessary in all fields. Sugarcane productivity is improved by genetic modification of the sugarcane plant: varieties can be genetically built to produce more fiber (such as "cane energy"), more sucrose, be less susceptible to pests, use less water and fertilizers, or handle management aspects such as mechanized plantation and harvest. Additionally, the transportation of sugarcane to industry and the industrial process, which is the main focus of this work, must respect all aspects of sustainability.

Therefore, to assess the sugarcane industry, the efficiency of the process must be evaluated by multiple competing criteria such as economic aspects, energy consumption, and environmental impacts. Besides, process performance and efficiency depend primarily on decisions made in the early stages of process development. Therefore, a simulation platform that simulates the industrial process is crucial for such assessments.

In this context, a simulation platform to simulate an industrial process for the production of first-generation ethanol and sugar was developed. The development of this model is based on mass and energy balances and parametric equations. The parameters were taken from the literature and industry. The sugarcane industry was simulated both continuously and dynamically. The dynamic simulation aims to obtain the energy consumption of the entire industry considering that the refinery contains batch and continuous unit operations working simultaneously. The simulation platform is then used to investigate the social, economic, and environmental impacts of the use of industrial and agricultural cellulosic residues. The mathematical model to simulate the conversion of these residues into second-generation ethanol, biogas, and electricity was then interconnected to the first-generation platform.

It is important to note that this simulation platform is not fixed and must be constantly improved to reflect new technologies and other changes in the sector, such as product demand and law regulations. In addition to this, it is intended to be expanded in the future to include agricultural production and the supply chain of suppliers and consumers.

1.2 Objectives

The general objective of this thesis is to assess the sugarcane industry using a developed simulation tool. Motivated by the aforementioned aspects, the specific objectives of this thesis are:

- Develop a simulation platform to simulate the production of first-generation ethanol, sugar, and electricity. Conversion efficiencies were compared and adjusted to reflect the current industrial process.
- Simulate the production of second-generation ethanol and biogas using bagasse and straw. The uncertainty associated with the conversion efficiency was captured using the Monte Carlo approach.
- Investigate the social, economic, and environmental impacts of the use of industrial and agricultural cellulosic residues.

1.3 Thesis Organization

This thesis is written in the format of a collection of articles and papers. Chapter 1 (this chapter) refers to the introduction, describing the contextualization and motivation, objectives, and how the thesis was organized. Chapter 2 was published as a chapter of the book Sugarcane Fuel Ethanol Production (CASTRO, R. E. N. De *et al.*, 2019) by IntechOpen. It presents a broad understanding of sugar and bioethanol production from sugarcane in Brazil. Furthermore, it delves into the energy potential of the sugarcane industry. The main growth potential comprises the use of agricultural and industrial residues.

Chapter 3 presents the concept of the simulation platform. It was published in 2018 in the Proceedings of the 13th International Symposium on Process Systems Engineering – PSE 2018 (CASTRO *et al.*, 2018). In this platform, each unit operation in the sugarcane industry was treated as a black-box, i.e., the unit operations can be replaced, attached, or excluded, depending on the objective of the simulation. Thus, the evaluation of the process that uses, for example, the residues for the production of advanced fuels can be interconnected with the current sugarcane industry. Moreover, different technologies can be assessed by replacing one unit operation with another with a novel technology.

Chapter 4 details the mathematical equation used to simulate the sugarcane industry. Most mathematical models are in the literature; however, to the best of our knowledge, the

multiple-effect evaporation and how it behaves when it is responsible for providing steam to a batch industrial process, such as the one used in sugar crystallization, have not been published before. Therefore, Chapter 5 presents the mathematical model for the simulation of multiple-effect evaporation; it was published in the Journal of Case Studies Applied Thermal Engineering in 2022. (CASTRO; ALVES; NASCIMENTO, 2022) It dynamically simulates the multiple-effect evaporation that supplies steam to the sugar batch crystallization process.

Chapter 6 was published in 2021 in the journal Sustainable Energy and Fuels (CASTRO; ALVES; NASCIMENTO, 2021). This article simulates the use of sugarcane bagasse and straw being converted into electricity, second-generation ethanol, and biogas and then used to propel a light vehicle. Chapter 7 presents the final consideration and suggestions for future studies.

References

CASTRO, Rubens E. N. De; ALVES, Rita M. B.; HAWKES, Adam; NASCIMENTO, Claudio A. O. Open Sugarcane Process Simulation Platform. *In*: **International Symposium on Process Systems Engineering – PSE 2018**. San Diego: Elsevier B.V., 2018. p. 1819–1824. DOI: 10.1016/B978-0-444-64241-7.50298-6. Disponível em: https://linkinghub.elsevier.com/retrieve/pii/B9780444642417502986.

CASTRO, Rubens Eliseu Nicula De; ALVES, Rita Maria Brito; NASCIMENTO, Claudio Augusto Oller. Assessing the sugarcane bagasse and straw as a biofuel to propel light vehicles. **Sustainable Energy & Fuels**, *[S. l.]*, n. 5, p. 2563–2577, 2021. DOI: 10.1039/D1SE00129A. Disponível em: http://pubs.rsc.org/en/Content/ArticleLanding/2021/SE/D1SE00129A.

CASTRO, Rubens Eliseu Nicula De; ALVES, Rita Maria de Brito; NASCIMENTO, Cláudio Augusto Oller Do; GIUDICI, Reinaldo. Assessment of Sugarcane-Based Ethanol Production. *In*: BASSO, Thalita Peixoto; BASSO, Luiz Carlos (org.). **Fuel Ethanol Production from Sugarcane**. [s.l.] : IntechOpen, 2019. p. 3–22. DOI: 10.5772/intechopen.78301. Disponível em: https://www.intechopen.com/books/fuel-ethanol-production-from-sugarcane.

CASTRO, Rubens E. N.; ALVES, Rita M. B.; NASCIMENTO, Claudio A. O. Dynamic simulation of multiple-effect evaporation. **Case Studies in Thermal Engineering**, *[S. l.]*, v. 34, p. 102035, 2022. DOI: 10.1016/j.csite.2022.102035. Disponível em: https://linkinghub.elsevier.com/retrieve/pii/S2214157X22002817.

GOLDEMBERG, José; COELHO, Suani Teixeira; GUARDABASSI, Patricia. The sustainability of ethanol production from sugarcane. **Energy Policy**, *[S. l.]*, v. 36, n. 6, p. 2086–2097, 2008. DOI: 10.1016/j.enpol.2008.02.028.

OECD-FAO. **OECD-FAO Agricultural Outlook 2021-2030**. [s.l.] : OECD, 2021. DOI: 10.1787/19428846-en. Disponível em: http://dx.doi.org/10.1787/agr-outl-data-

%0Ahttp://www.fao.org/documents/card/en/c/cb5332en.

RFA RENEWABLE FUELS ASSOCIATION. **Annual Ethanol Production**. [s.d.]. Disponível em: https://ethanolrfa.org/markets-and-statistics/annual-ethanol-production. Acesso em: 20 fev. 2022.

RIBEIRO, Barbara Esteves. Beyond commonplace biofuels: Social aspects of ethanol. **Energy Policy**, *[S. l.]*, v. 57, p. 355–362, 2013. DOI: 10.1016/j.enpol.2013.02.004. Disponível em: http://dx.doi.org/10.1016/j.enpol.2013.02.004.

RODRIGUES, T. R. Entrevista: Energia Verde. **Vanzolini em foco**, São Paulo, 2008.

CHAPTER 2: ASSESSMENT OF SUGARCANE-BASED ETHANOL PRODUCTION

This chapter corresponds to a book chapter published in Fuel Ethanol Production from Sugarcane.

Rubens Eliseu Nicula de Castro, Rita Maria de Brito Alves, Cláudio Augusto Oller do Nascimento and Reinaldo Giudici. Assessment of Sugarcane-Based Ethanol Production. In: BASSO, Thalita Peixoto; BASSO, Luiz Carlos (Eds.). **Fuel Ethanol Production from Sugarcane**. [s.l.] : IntechOpen, 2019. b. p. 3–22.

Abstract

This chapter aims to explain how bio-ethanol has been drawn to become a successful alternative to partially replace petroleum as a source of liquid fuels in Brazil. A brief historical analysis about the production of bio-ethanol from sugarcane is presented. The motivation to start the production of the ethanol as biofuel in the 1970s and how the governmental policies have contributed to the ups and downs, successes, and failures of the sugarcane industry is shown. Then, the efficiency of the sector is addressed; firstly, the increasing efficiency of the agricultural sector is discussed, showing how the productivity per hectare has increased in the last decades and which improvements are further expected in a near future. Finally, the industrial process is discussed: the current efficiency in processing sugarcane to produce ethanol and the emerging technologies, not only to process sugarcane juice, but also to harness bagasse, vinasse, and sugarcane straw.

Keywords: Brazilian ethanol fuel, *Proálcool*, ethanol production, sugarcane ethanol, bio-ethanol

2.1 Introduction

The beginning of sugarcane cultivation in Brazil is related to the Portuguese occupation during the colonial period. Sugarcane crop met ideal soil and climate conditions, and it was used by the Portuguese to establish their settlement in Brazil. With the production of sugar, alcoholic beverages were produced by the alcoholic fermentation of sucrose. The first studies on ethanol, as a fuel for internal combustion vehicles, started in the 1920s (OLIVEIRA, 1937). The characteristics of ethanol (liquid fuel, high-energy density, and relatively safe handling) made it an important substitute for liquid fuel from petroleum in the Brazilian energetic

matrix. In fact, the world overwhelming dominance of gasoline, diesel, and jet fuel for transportation clearly shows the preference for liquid fuels due to their high-energy density. Except for the ethanol, most of the liquid fuels in the world are petroleum based. As petroleum is not renewable, in the long term, it must be substituted by other kind of energy. Aside from that, the use of fossil energy results in the releasing of greenhouse gas emission, which contributes for global warming. Hence, society in general is looking for alternatives to avoid global warming and thus replace petroleum. Biomass, like the sugarcane, clearly represents a sustainable and low-cost resource that can be converted into liquid fuels on a large scale to have a meaningful impact on petroleum use.

2.2 Why has bio-ethanol become a successful alternative to partially replace petroleum fuels? A short history

The beginning of the development of the ethanol fuel in Brazil is related to the petroleum shortage in Brazilian territory and the worldwide oil crisis. Brazil had few oil wells in 1970s, and the country was extremely vulnerable to international oil crisis. In 1973, during the first oil crisis, prices increased by 400%, which greatly affected the Brazilian economy in this way, and the Brazilian government began to seek an alternative to reduce its international dependence on oil. At that time, anhydrous ethanol, produced from sugarcane, had already been mixed to gasoline at a ratio of 5%, since 1931. In 1975, government created the Brazilian ethanol program, *Proálcool*, which involved many economical sectors to develop bio-ethanol as fuel to replace gasoline (BRAZIL, 1975). This program had massive governmental funds to develop feedstock and industry. In 1979, during the second oil crisis, Brazil presented the first ethanol fuel-powered car. At that time, Brazil had active state intervention over the price and the production of ethanol (BRAZIL, 1979), which dictated the amount of sugar and ethanol to be produced. The ethanol price paid to the producers was a function of the sugar price. The price of ethanol and gasoline was established by the government at the fuel station. Therefore, the lower price of ethanol compared to gasoline led the population to choose ethanol-powered car instead of gasoline-powered one. As shown in Figure 1, the sales of ethanol cars skyrocketed, and in 1984, about 76% of the sales of cars using Otto cycle engines were ethanol fuel-based. At that time, most fuel stations in Brazil could offer ethanol as fuel.

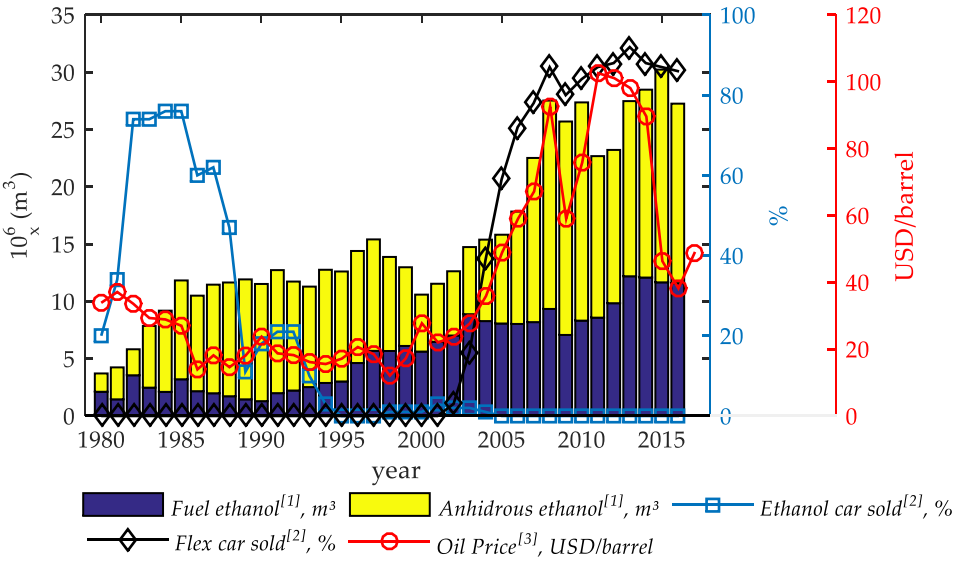

Figure 1 - Fuel and anhydrous ethanol production; ethanol-powered car and flex-fuel car sold in Brazil; and the price of the oil barrel

Source: [1] UNICA União da Indústria de Cana de Açúcar (2017); [2] ANFAVEA Associação Nacional dos Fabricantes de Veículos; Automotores; *[3] eia U. S. Energy Information Administration*

At this point, it is worth defining "ethanol fuel" compared to anhydrous ethanol. "Ethanol fuel" is also known as "hydrous ethanol," and it is basically composed of ethanol (92.5–94.6%wt) and water. Ethanol fuel is used straightly into car engines without any blend. Anhydrous ethanol consists of at most 0.7% water by weight, and it has been used mixed with gasoline in different blend levels. Figure 2 shows the fraction of anhydrous ethanol mixed with gasoline over the years. Anhydrous ethanol is also used as anti-knock agent, substituting the additive added to gasoline to avoid getting ignited early before spark occurs. Many countries still use methyl tert-butyl ether (MTBE) as a gasoline additive instead of ethanol, despite the environmental and health concerns. In the United States, MTBE has been replaced by corn ethanol since 2005 (EPA, [*s. d.*]). In Europe, part of the MTBE has been substituted by ethyl-tertiary-butyl-ether (ETBE) which is an additive obtained by the reaction of isobutene with ethanol (THE EUROPEAN FUEL OXYGENATES ASSOCIATION, [*s. d.*]). In Europe, the amount of ETBE used instead of MTBE is dependent on the price of ethanol.

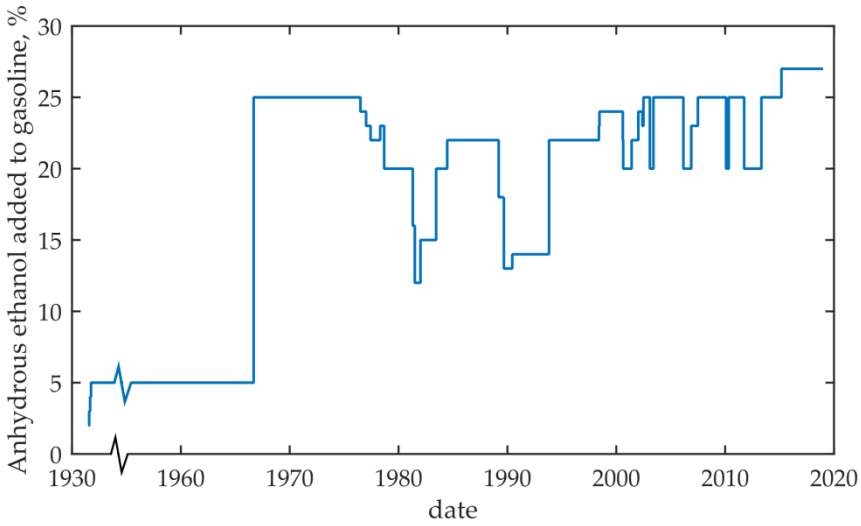

Figure 2 - Fraciton of anhydrous ethanol added to gasoline.
Source: MME Brazilian Ministry of Mines and Energy.

In 1985, after government system changed to democracy, the congress changed the rules of public policy concerning ethanol to include stakeholders on the government decision. As a result, the government moved away from the sector and the bio-ethanol fuel development faced more challenges to overcome. Firstly, the oil price decreased and ethanol became economically noncompetitive compared to gasoline. Oil should cost more than U$ 45.00/barrel in order to let sugarcane ethanol to be competitive (RODRIGUES, 2008). Then, in 1990, the government suspended the quote requirement on the mill to produce ethanol (BRAZIL, 1965, 1990). In 1996, the price control on the fuel sector ended (BRAZIL - MINISTÉRIO DA FAZENDA, 1996). In 1999, government completely deregulated the sugarcane sector (ZILBERMAN; MORAES, 2013). As a result, the ethanol consumption stopped rising, and the ethanol fuel sector suffered without government regulations and incentives.

Besides the end of the many subsidies, ethanol car technology had to deal with lack of consumer confidence, and so the sales of ethanol fuel-based car decreased. In 1984, ethanol car was still under development and, at that time, many problems were still unsolved such as the engine cold start. In 1989, due to the sugar price raising and the low oil price, sugarcane mills started to produce more sugar than ethanol. This resulted in a shortage of ethanol fuel, which led ethanol car users to stop using it. Besides, the ethanol engine, due to technical reasons, could not be easily converted to gasoline engine. For this reason, as shown in Figure 1, the ethanol car sales dropped from 76% to about 11% in Brazil, and 6 years later, no car manufacturer had ethanol fuel cars in its production lines. From 1995 to 2003, the ethanol demand was basically to supply fuel to the ethanol cars which had been sold before.

By 2003, due to the rising of oil price, ethanol fuel regained its competitiveness. At this time, as a consequence of the ethanol production/demand occurred after 1985, automakers started manufacturing cars using flex fuel technology and, as a result, the demand for ethanol as fuel rose again. Due to the flex technology, the customers can decide whether to fuel their cars with ethanol or gasoline. So, there were no more customers concerns about purchasing ethanol-powered cars. Hence, it became a self-regulating market; for instance, during the sugarcane crop season, the ethanol fuel price decreases, which motivates the preferential use of ethanol instead of gasoline. By analogy, when the stock of ethanol fuel is low, the price of ethanol would rise and it could be preferable for customers to use gasoline instead. This also corrected the problems related to the possibility of ethanol shortage due to climate changes that would affect the sugarcane crop and the amount of sugarcane diverted to produce sugar instead of ethanol. Consequently, the flex technology seems to have solved most of the problems related to the use of ethanol as fuel.

Flex-fuel technology consists in adjusting the engine to operate using both kinds of fuel, ethanol or gasoline, and their blend in any concentration. In an Otto cycle engine, each fuel has different operation characteristics such as air/fuel ratio, compression ratio, and ignition timing (COSTA; SODRÉ, 2011). The air/fuel ratio issue has been solved by measuring the oxygen content of the exhaust gas by the lambda sensor, which supplies the necessary information for optimal air/fuel mixture to the engine control unit. Electronic ignition timing controller adjusts the ignition time for maximum torque and fuel conversion efficiency (WANG *et al.*, 2000). However, the compression ratio, which is the ratio of the volume of the combustion chamber from its largest to its smallest capacity, cannot be easily changed in an engine. Ethanol engine requires a higher compression ratio than the gasoline one; thereby, the commercial flex-fuel car has an intermediate compression ratio, which is intermediate to the ideal one for both fuels. Automakers have worked in variable compression ratio engines, which would result in an increment of engine efficiency (LARSEN, 1991).

Nowadays, most of the cars sold in Brazil are flex-fuel, and ethanol is easily found in every fuel station; thus, the customers are able to choose which fuel they want to use. It is worth noting that most Brazilian customers do not choose to use ethanol because it is environmentally friendly, but due to economic reasons. A survey carried out by the Brazilian Sugarcane Industry Association (UNICA) (FABIANA BATISTA, 2013) shows that Brazilian consumers in general are not willing to pay more for ethanol than for gasoline even though

the majority recognize its environmental benefits. Even when ethanol has the same cost per driving kilometer (about 70% of the price of gasoline), 55% of the consumers choose to fuel the car with gasoline due to its higher autonomy. This behavior may be explained by "The Tragedy of the Commons" (HARDIN, 1968) in which the rational man finds that his share of the cost of the CO_2 he discharges into the commons is less than the cost of not releasing it individually. Consequently, the majority of the consumers choose the fuel taking into account only their own benefits. This means that ethanol can survive as an alternative fuel only if it is economically competitive when compared to gasoline or by law regulations.

Environmental and social concerns also have a beneficial impact on the fuel ethanol program: pressures from nongovernmental organizations (NGO) and the United Nations (UN) about reduction of greenhouse gas emissions (GHGs), and some civil society organizations about the social impact of ethanol supply chain on the society. One action taken to support the claim for reducing GHG was the creation of a tax on the nonrenewable fuel (BRAZIL, 2001), which aims to support environmental programs and natural disasters caused by GHG. This is based on the "beneficiary pays principle," whereby when purchasing fossil fuel, the beneficiaries should pay the bear costs on the environment, which are believed to contribute to climate change. This seems suitable; however, it is very difficult to precisely evaluate the impact on the environment. Moreover, in 2018, the Brazilian government created the *RenovaBio* (BRAZIL. MINISTÉRIO DE MINAS E ENERGIA., 2018)—a national biofuel policy to set rules to allow sustainable expansion of the Brazilian biofuel market. In fact, nowadays, ethanol supply chain is responsible for 950,000 direct jobs and 70,000 farmers (UNICA; CEISE, 2016) in the country. For each direct job, 2.39 indirect ones (MONTAGNHANI *et al.*, 2009) are estimated, resulting in over 2.4 million jobs. For this reason, the ethanol fuel environmental and social benefits cannot be left at the mercy of the variations in petroleum price.

Besides its use as fuel, ethanol is used as a raw material to produce biopolyethylene. Polyethylene is one of the most popular plastics in the world. It is a polymer of ethylene and consists of a carbon backbone chain with pendant hydrogen atoms. Biopolyethylene is a polyethylene made from ethanol. The process consists in dehydrating ethanol to obtain ethylene prior to polymerization. The properties of this bioplastic are identical to the fossil-fuel-based polymer. The main advantage of the polyethylene made from ethanol is that it captures and fixes CO_2 from the atmosphere.

Through this brief ethanol history, it is possible to infer that biofuel ethanol has undergone two different expansion phases: the first one is the *Proálcool* policy and the second one is the flex-fuel car (concerning ethanol as liquid fuel). In these two expansion phases, the main claim was not the environmental one but an alternative fuel to the high price of petroleum. However, due to current global warming concerns, the world is looking for a renewable fuel to replace petroleum and reduce emissions. A number of alternatives are under development, and the question that arises is if the bio-ethanol is going to be "the fuel." In case of a positive answer, one may expect a new expansion phase in the ethanol production sector. Further, in this new expansion phase, not only an alternative fuel is expected, but also a fully environmentally friendly one. Thus, the process might be highly efficient in all steps of the production chain, from the crop to its final use. Therefore, the efficiency of the production of ethanol and some opportunities to improve the efficiency will be addressed subsequently in this chapter.

2.3 Efficiency of the sugarcane ethanol production and what is expected in a near future

Since the beginning of the ethanol fuel program in Brazil, an improvement in all production chain has been observed. With the emerging technologies, new improvements are expected. Hence, in this section, the recent enhancements in productivity and efficiency of the sector and what is expected in a near future are analyzed.

2.3.1 Sugarcane crop

During the last decade, the principal change in crop management was the mechanization. One of the main reason for mechanizing the sugarcane crop is environmental protection. The traditional harvest was done manually and the sugarcane leaves had to be burned in the field. The consequence was high particle and CO_2 emissions, which led the Brazilian legislation to prohibit the burning of sugarcane leaves in the field (BRAZIL, 1998). This provided an opportunity to the sector to use this leaves (straw) as an additional feedstock to the ethanol process, producing electricity or second-generation ethanol. Yet this has also increased the amount of pesticides needed to control sugarcane bugs and diseases (MATSUOKA; MACCHERONI, 2015; PROCÓPIO *et al.*, 2015) that are kept in the field for the next crop. It is important to mention that sugarcane is a semi-perennial crop, which means

that the same plant may be harvested (without uprooting the plant) and re-grown for up to 5 years. In addition, mechanical harvest and crop have reduced the production cost; however, the amount of dirt brought with the cane to the refinery has increased, thus affecting the industrial process (AHMED; ALAM-ELDIN, 2015).

The productivity in Brazil is uneven concerning the region of the country, for example, in the 2016/2017 crop, the average productivity in the south, southeast, and central regions was 75.3 tonne/ha while in the north and northeast it was 48.6 tonne/ha (CONAB, 2017a). In addition, some regions in Brazil, such as the southeast, can reach an avarange production yield higher than 100 tonne/ha (DIAS; SENTELHAS, 2017). Nowadays, in a good climate condition scenario, a national average productivity of at least 80 tonne/ha is expected (NYKO *et al.*, 2013). The average sugarcane productivity and planted area have increased since 1980. There was a rapid acceleration in productivity growth in the 1980s, which is mainly due to the investments from the *Proálcool* program. Figure 3 shows the productivity and planted area from 2005 to 2015 (CONAB, 2017a). Nyko (2013) studied the recent drop in the sugarcane productivity (2010/11 harvest) and concluded that mechanization of sugarcane planting and harvesting were the main cause, besides climate change and the lower investment in the agricultural field due to the lower price of sugar and alcohol in this crop season. In fact, mechanization is a relatively new technology for some industries in Brazil, and they might have to adapt to the mechanical crop management and a learning curve is required. In addition, some researches in genetic-modified sugarcane have been carried out to increase the yield, and pest and disease resistance (ARRUDA, 2012). Consequently, the average productivity is expected to increase in the near future.

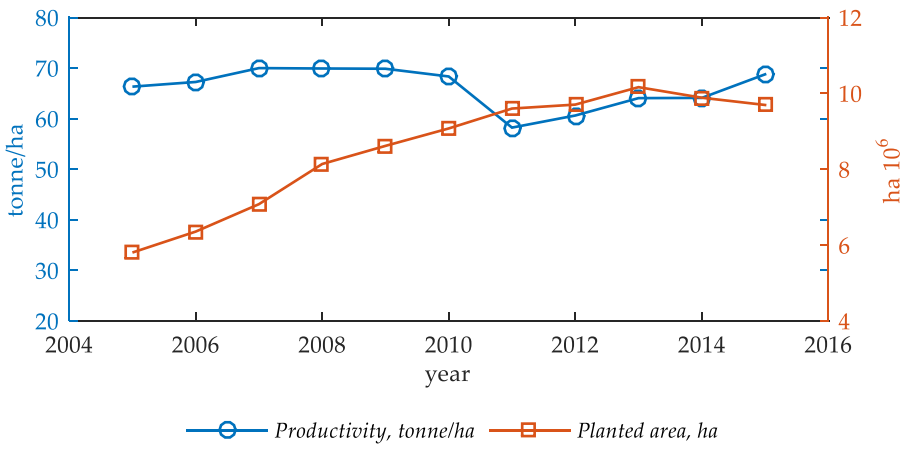

Figure 3 - Productivity of sugarcane and planted area
Source: UNICA União da Indústria de Cana de Açúcar

2.3.2 Sugarcane transportation

Transportation plays a crucial role in the cost of sugarcane production, owing to the multiple transport facilities and time-consuming activities involved in the delivery process. For instance, the total average cost of sugarcane production in São Paulo, in 2016/2017, was R$ 49.56 (U$ 14.57) per tonne of sugarcane (CONAB, 2017b). In order to evaluate how much the delivery represents on the total cost, Françoso et al. (FRANÇOSO *et al.*, 2017) studied two cities in the same state and in the same crop season, and the cost of cutting, loading, and transportation of sugarcane from the farm to the mill gate 25-km away varied from R$ 26.77 (U$ 7.87) to R$ 37.25 (U$ 10.96) which represents 54–75% of the total production cost, respectively. The great variation in the transportation costs of sugarcane is due to the region topography, quality of roads, and technology employed in the transportation. So, the role of sugarcane transportation on the cost of bio-ethanol cannot be overlooked.

The most economical way of transporting sugarcane from field to the industry is the two semitrailers attached to a tractor unit. The distance from the farm to the sugar mill is about 25 km. Different ways to transport sugar have been tested, from railroad, rivers, and road (HUGOT, 1960). Until 2017, the largest truck licensed was nine axles with the total length of 30 m and a load of 74 tonne, which was the most economical way of bringing sugarcane from the field to the industry (BRASSOLATTI- *et al.*, 2014). This kind of transport allows drivers to disconnect the tractor from the full trailer on arrival in the mill and then connect to an empty trailer and get back to the field without waiting to unload. As from 2017, the department responsible for monitoring the road traffic has authorized 11 axles, two semi-trailers attached to a tractor unit with the same length, and a total load of 91 tonne (BRAZIL, 2016). To the best of our knowledge, there are no studies on the viability of this transport mode; however, this might be the most efficient transport mode since this is a claim made by sugarcane producers.

2.3.3 Cane reception preparation and extraction

The farmers are rewarded according to the quality of the sugarcane supplied to the industry. When the sugarcane arrives at the mill by a truck, it is weighed, and then the load is drilled in order to collect a sample. The quality of the sugarcane undergoes standardized analysis of the sample. The responsible for the standard is *Consecana* and *ABNT NBR 16271*.

The payment is made in accordance with a coefficient called “total recoverable sugar,” which is proportional to the sugarcane sucrose content. With the recent use of bagasse to produce electricity and the possibility to produce second-generation ethanol, the possibility of rewarding the producer for the amount of fiber in the sugarcane is under discussion by the agricultural and industrial sectors (NOVACANA.COM, 2016). Besides, new varieties, aiming to produce more fiber than sugar, have been developed by BioVertix®. Consequently, the sugarcane payment is expected to soon take into account the sugarcane fiber in addition to the amount of sugar.

An appropriate sampling method is fundamental to correctly evaluate the shipment. The collection of samples is usually done by drilling the shipment with mechanical oblique probe samplers. This kind of sampler was introduced in 2007 and has undoubted advantages over the method formerly used because it allows the sample to be taken from the top to the bottom of the truck load. Before the oblique probe, sugarcane was sampled using a horizontal probe or randomly samples were taken at three different points of the shipments.

Mechanization has increased the level of dirt brought with the sugarcane to the industrial process, so a cleaning process has become necessary. When sugarcane was harvested manually, it was possible to wash it before its being forward to an industrial-cutting shredder and milling process. However, because of mechanization, sugarcane arrived at the industry in small stalks since the harvester already cut the sugarcane. Sugarcane in small pieces cannot be washed due to the fact that a lot of sugar would be lost by the stalk-cutting edge. For this reason, a dry-cleaning technology has been adopted by many industries to avoid dirt from entering the industrial process. Increasing 1 kg of dirt per 100 kg of sugarcane is expected to a decrease in the sugar recovery at the industrial process by 0.1% (AHMED; ALAM-ELDIN, 2015). The loss of sugar occurs with bagasse and filter cake during the sugar juice treatment step. However, the dry-cleaning system consumes about 0.5–1.0 kW per tonne of cane. Because electricity and sugar are products sold by the refinery, there is a feasible balance between profit and loss, that is, the cost of the electricity used to clean the sugarcane should be lower than the cost of the sugar lost due to the dirt. In fact, as shown by some suppliers (EMPRAL; SERMATEC; ZANINI, [*s. d.*]), the dry cleaning system would be feasible when the sugarcane leaves (straw) are intentionally brought with the sugarcane to be burnt in the boiler. In this case, straw is easily collected with cane by lowering the speed of the harvester clean blower. Thus, the drycleaning process would separate straw from stalks

before the extraction process and then would mix the straw and bagasse after milling. In fact, this is not a consolidated technology, since some industries prefer to harvest the straw on the field and bring it separately. Thus, the implementation of the sugarcane dry cleaner method will depend on the manner of straw handling.

The next process applied to the sugarcane is the extraction, which is done by the mill or diffuser. The aim is to separate fiber, a solid stream, from sugar in a liquid stream. In this process, sugarcane is first reduced into small pieces and the sugar-bearing cells are ruptured to facilitate the subsequent extraction process. This is basically a mechanical process whereby size reduction is generally achieved through the use of rotating knives and swing hammer shredder in the cane-conveying system. In the case of billeted cane, mechanically harvested, it can be fed directly into a shredder without any additional cutting. For cane juice extraction, there are many studies comparing milling and diffuser (HUGOT, 1960; REIN, 2007, 1995). The main advantage of a diffuser over mill is the greater extraction of sugar; however, a diffuser uses more imbibition water and steam than a mill. As a result, there is a dilemma to the industrials: to increase sugar extraction, more thermal energy is spent. In Brazil, the preference has been for the use of mills, which consists of a set of four to six mill units. A new extraction technology called “Hydrodynamic Extraction” or “Rivière Juice Extractor” is under development and aims to achieve the same level of diffuser extraction using less imbibition water with a lower cost of installation and maintenance when compared to both technologies (WALSH, 1998); however, to the best of our knowledge, there is no commercial plant using this technology.

Sugarcane milling did not change much during the last two decades, except for the driving system. Two driving systems are the mostly used in Brazil: steam turbine and electric motor. Even when an electric motor is used, the electricity is produced using a steam turbo-generator, that is, in both cases, the primary energy to drive the extraction process is the bagasse, which is burned in a boiler to produce steam. The driving system with steam turbine is the most widely used, mainly in old industries. This system consists of a low-efficiency steam turbine working around 22 bar and 350°C admission, and 2.5 bar exhaust, so, in this system, steam energy is converted into a mechanical energy to the mill. The electric drive system consist of an electric motor attached to each roll of the mill unit. Even with the double transformation of energy, the overall efficiency of the electric drive is higher than the work done by a singlestage turbine. These become an issue for the sugar mill, since the surplus

electricity becomes a profitable product for the mills. As from 2002 when the government has regulated the commercialization of electricity by the private sector using biomass (BRAZIL, 2002), many sugar mills have invested in higher-pressure boilers (65–100 bar) and high-efficiency cogeneration systems.

2.3.4 Juice treatment

After being milled, the juice contains several impurities, which must be removed prior to fermentation or concentration. These impurities are removed using a set of unit operations, which basically consist of heating, adjusting the pH, settling the precipitate formed in the body juice, and filtering

Only small changes on these processes were adopted during the last decades. In the heating, most industries prefer vertical shell-and-tube steam heaters. Despite the higher overall heat transfer coefficient in the horizontal one, the vertical one is easier to clean. The extracted sugarcane juice has a pH of about 5.3, and needs to be adjusted to 7 before clarification. For this, lime Ca(OH) is added, which is the most widespread process used. For refineries that produce sugar in addition to ethanol, processes such as sulfitation, phosphatation, and carbonation (REIN, 2007) are also used, aiming to lower the color and turbidity. After the pH adjustment, the juice is sent to a clarifier to settle the insoluble part of the juice. Before the use of chemical products (flocculants and polymer) and instruments to control the flow and dosing, the most popular installation used multi-tray clarifiers. The main disadvantage of multi-tray is the retention time of about 3 h. Single-tray clarifiers, known as “rapid clarifiers,” became possible with the development of chemicals that promotes the mud coagulation and settling. The retention time in this case is about 1 h. The main advantages of the rapid clarifiers over the multi-tray ones are the lower installation costs, and the small retention time, which reduces the degradation of sugars (HUGOT, 1960). There are not many research works carried out recently about juice treatment, and consequently, great changes in this process are not expected in a near future.

2.3.5 Juice concentration

Ethanol can be produced in an autonomous distillery, producing only ethanol, or in an attached distillery, which produces sugar and ethanol. In the second case, ethanol can be

produced only from molasses, a residue from the sugar production process, or a mixture of molasses and juice, depending on the amount of juice diverted to produce ethanol. When sugar is produced, the juice destined to the sugar process must be concentrated to achieve a suitable brix to start the crystallization process at about 60% sucrose by weight. This concentration is obtained using multiple-effect evaporators (MEEs), which reduces the required steam to concentrate the juice, since each effect produces lower-pressure steam, which is used in the next effect to evaporate more water and so on. In this way, only the first-effect evaporator uses the exhaust steam from turbines. Saving the exhaust steam is crucial for industries that have condensation turbine installed or for refineries that want to save bagasse for other purposes, such as second-generation ethanol or just selling bagasse as a product.

When sugar and ethanol are produced in a refinery, there is a synergistic effect that reduces the total consumption of steam. Since large amount of water must be taken off from the juice in order to concentrate it in the crystallization process, this water is withdrawn as steam in an MEE. This steam from MEE is used in the ethanol process. In this manner, steam from MEE replaces the necessity of using exhaust steam. Combining ethanol and sugar production, results in an energy efficient refinery.

2.3.6 Fermentation

Alcoholic fermentation is a biological process, which converts sugars such as glucose, fructose, and sucrose into cellular energy, producing ethanol and carbon dioxide as a side effect. The overall chemical reaction for alcoholic fermentation is as follows:

$$\underset{\text{sucrose}}{C_{12}H_{22}O_{11}} + H_2O + \text{enzyme} \rightarrow \underset{\text{fructose and glucose}}{2\,C_6H_{12}O_6} \rightarrow \underset{\text{ethanol}}{4\,C_2H_5OH} + 4\,CO_2$$

Sucrose is a dimer of glucose and fructose molecules. In the first step of alcoholic fermentation, the enzyme invertase cleaves the glycolic linkage between the glucose and fructose molecules. When the fermentation finishes, the fermented liquor is centrifuged to remove east (*Saccharomyces cerevisiae*), which is recycled to fermentation. The product from the centrifugation (a stream with about 8°GL ethanol content) is sent to the distillation process.

There are two types of processes for alcoholic fermentation commonly used to produce ethanol. The majority of the sugar mills use a fed-batch fermentation process. The continuous process is also used by some industries; however, despite the lower installation cost, continuous fermentation results in lower efficiency in the production of ethanol. The lower efficiency is a result of bacterial contamination since, in a continuous process, the fermenter cannot be as frequently cleaned as in a fed-batch, in which cleaning can be carried out after each batch.

The main disadvantage of the fed-batch process is related to the large size of the fermenters. Many technologies are under development to reduce this size. There are many problems in the operation of such large equipment: high cost of installation, difficulty to control parameters, such as contamination, mixing, and temperature, which can cause temperature gradients and dead zones inside the fermenter. To reduce these problems, the total volume of broth under process must be reduced. Therefore, the proposed technologies aim to increase the concentration of reactants and products. Removing ethanol during the fermentation process is one possibility, since a high concentration of ethanol is toxic to yeast. There are some studies of pervaporation (GAYKAWAD *et al.*, 2013) and stripping (HASHI; THIBAULT; TEZEL, 2010) to take ethanol off the fermentation broth during the ethanol fermentation. The high cost of pervaporation membranes and the difficulty in recovering ethanol from CO_2 make this technology unfeasible nowadays. Reducing the temperature of the fermentation broth using a chiller is also an option under development, and there are some commercial-scale units (PROCKNOR, 2015). At a lower temperature, the yeast would resist a higher concentration of ethanol, but reducing the temperature would also reduce the reaction rate. By now, the best available technology continues to be the fed-batch cooled by cooling towers.

2.3.7 Downstream processing

The recent development in downstream process did not aim to improve the ethanol recovery efficiency but to save the energy demand by the process. Downstream consists of the separation of ethanol from the other components in the fermented wine; the first step is the centrifugation of wine, which recovers yeast to the next fermentation fed-batch. There are two main components at the centrifuged wine: water and ethanol. Fuel ethanol also called

“hydrous ethanol” (ethanol 92.5–94.6 wt%) is obtained by distillation. Due to the azeotropic point in the mixture ethanol-water, anhydrous ethanol cannot be obtained using a common distillation process. Anhydrous ethanol (99.3 wt%) must be produced in order to be used in a mixture with gasoline. There are two common dehydration systems used in Brazil: azeotropic distillation with cyclohexane or monoethyleneglycol, and, more recently, absorption on molecular sieves. The main advantage of using molecular sieves is that steam consumption is about one-third of those in the azeotropic distillation. Pervaporation is a process that could significantly reduce the energy demand; however, the high cost of membranes makes it unfeasible to be used in a commercial scale.

2.3.8 Vinasse and biogas

Vinasse is the final by-product of the ethanol distillation and is the main effluent of the ethanol process. About 12 liters of vinasse are produced per liter of hydrous ethanol. Most industries use the vinasse without any treatment as a fertilizer and, it is simultaneously used for irrigation due to its high amount of water (fertigation). The vinasse produced in a distillery is a stream composed basically of water, organic matter, and inorganic salts. Therefore, there are many possibilities to utilize this vinasse: as biogas obtained by conversion of the organic matter into gas, and as fertilizer through using the inorganic salts (phosphorus, potassium, and nitrogen) to partially replace synthetic fertilizers derived from the petroleum industry.

Biogas has a great potential opportunity for using the vinasse. Many studies have been carried out about the bio-digestion of vinasse (BERNAL *et al.*, 2017; LONGATI; CAVALETT; CRUZ, 2017; MORAES; ZAIAT; BONOMI, 2015). Biogas is an easy to handle fuel since it can be transported in high-pressure cylinders, or by pipeline, and can fuel farm machinery and trucks to partially replace diesel (LANDIRENZO, [*s. d.*]). Biogas can also be obtained from sugarcane trash (bagasse and straw) (KEERTHANA; KRISHNAVENI, 2016) in a bio-digester blended with vinasse. This is also an opportunity to the use of bagasse, that is, bagasse, as well as straw, can be converted into biogas instead of producing electricity or 2G ethanol. There are also many sugar mills close to the gas pipeline network in Brazil, which would raise the feasibility of implementing a biogas facility. Besides the high cost of installation, a great challenge to implementing biogas facilities is to deal with an unstable vinasse supply. Vinasse is not

produced continuously, since industry interrupts its operation relatively frequently due to the rain, which stops the harvest, or due to the maintenance or the braking of equipment.

Another possibility is to concentrate vinasse and to recover water to be used in the process. In this case, the concentrated vinasse can be transported to longer distances to be used as liquid fertilizer. Concentrated vinasse can also be burned into the boiler; in this case, the higher the concentration, the higher its net calorific value. The main disadvantage in this process is the steam demand to concentrate vinasse.

After biodigestion, water can be withdrawn from vinasse using commercial technologies such as evaporator or ultra-filtration membrane. Reducing the use of water has a positive environmental impact, but the cost of these processes may be higher than the intake of water from natural sources (mainly rivers). So, only few refineries in Brazil are withdrawn water from vinasse to be used in the process.

2.3.9 Combined heat and power

What makes ethanol from sugarcane superior to that from other feedstocks (e.g., corn) is the bagasse that comes with the sugarcane. First-generation ethanol processes from sugarcane have a positive energetic balance, which means that it is not only self-sufficient on energy, but it can export the surplus energy usually as electricity. Using the combined heat and power (CHP) process is the most efficient way to produce electricity. In the CHP, high-pressure steam (between 65 and 100 bar) is expanded in turbines coupled with electric generators, and the exhaust steam from the turbines is used as thermal energy for the process. A high-efficient process, that is, a process which consumes small amount of thermal energy, results in surplus bagasse that can be used as feedstock to another process, such as second-generation ethanol, or to produce surplus steam—the steam produced by the boiler and not condensed in the process. The surplus steam can be expanded in condensation steam turbines to allow maximizing the electricity production.

The condensation turbine used to produce electricity with the steam competes with the cellulosic ethanol. The condensation turbine cannot be classified as CHP, since only power is produced and the exhaust steam is condensed by cooling water, that is, heat is not used in the process. Despite the fact that it maximizes the production of electricity, an energetic analysis shows that the larger enthalpy jump occurs in the condenser and not in the turbo-

generator expansion. Thus, the energy to condense the steam is released to the surrounding by the cooling tower.

Sugarcane bagasse has become a valuable product for sugarcane refineries, and it is really an important source of energy for the Brazilian economy. Before the possibility of exporting electricity to the grid (BRAZIL, 2002), most sugarcane mills had low pressure and inefficient boiler and turbo-generator (about 22 bar 350°C). This allows the refinery to be self-sufficient in electricity, however, without the possibility to export to the grid. Some sugarcane mills are still running using this old technology. High-pressure and high-efficiency boiler and turbines allow the refinery to export electricity. For instance, in a scenario in which a refinery has a higher-efficiency boiler, counter-pressure and condensation turbine, and electrified mill, it is possible to export about 79.7 kW·h per tonne of sugarcane. The parameter and efficiency of this scenario are shown in Table 1. To verify the potential of the bagasse in Brazil, in 2016, the country produced 666.8 million tonne of sugarcane (UNICA, [*s. d.*]) and in the same year produced 35,236 GW·h of electricity from sugarcane bagasse (MINISTÉRIO DE MINAS E ENERGIA, 2017). If every sugar mill was prepared to export electricity as described in this scenario, this number could have been 53,135 GW·h. Further, considering the possibility of bringing 50% of the sugarcane straw (leaves and tips) which yields about 140 kg per tonne of sugarcane (15% humidity) (LANDELL; SCARPARI; XAVIER, 2013), it would be possible to export 135,470 GW·h per year. For an idea of the order of magnitude, Itaipu, the biggest hydroelectric power plant in Brazil, in the same year, produced 103,098 GW·h.

Table 1 - Parameters used to obtain the electricity production from sugarcane bagasse

Parameter	Value
Bagasse produced per kg of sugarcane	0.276 kg
Bagasse losses due to degradation, startup boiler and to surrounding	5 %
Net calorific value of bagasse	7,300 kJ/kg
Boiler temperature	520 °C
Boiler pressure	68 bar
Boiler efficiency	85 %
Counter-pressure Turbo-generator efficiency	83.5 %
Condensation-pressure Turbo-generator efficiency	78.3 %
Steam consumption in the first generation process per kg of sugarcane	0.4 kg
Electricity consumption per tonne of sugarcane	32 kW
Sugarcane straw brought with sugarcane per kg of sugarcane	0.140 kg
Net calorific value of sugarcane straw	12,900 kJ/kg

2.3.10 Second-generation ethanol

The conventional ethanol production utilizes a fermentation process to convert sugars, such as starch, sucrose, glucose, and fructose, into ethanol. Second-generation biofuels, also commonly known as advanced biofuels, utilize agricultural residues or other feedstock that cannot be straightly used as food for humans. Cellulose is an important structural material for plants (along with lignin), and it is made up of many repeating sugar units. These repeating sugar units can be broken down by various processes into the component sugars, which can finely be fermented into ethanol.

Many investments on the development of ethanol from cellulosic material have been made, and some industrial-scale plants have been built; however, it has been taken longer than expected for cellulosic ethanol to succeed. In the United States, for instance, there are at least four commercial plants (DuPont Cellulosic Ethanol, Poet Project Liberty, Abengoa Bioenergy Biomass, Alliance Bio-Products INEOS) with an installed capacity of 121, 88, 110, and 35 million liters per year, respectively. In Brazil, there are two commercial plants, Granbio and Raizen, with an installed capacity of 82 and 40 million liters per year, respectively. In addition, in Italy, the first cellulosic plant, Crescentino, a Mossi & Ghisolfi group company, has an installed capacity of 31 million liters per year. Most of them started their operation in 2014, but not all has been well: in 2017, DuPont decided to close its plant and announced that it will sell the company's ethanol facility in Nevada, Iowa. Abengoa announced bankruptcy and financial restructuring in 2016 and, in the same year, the cellulosic biofuel plant was bought by Sinatra-Bio. In the end of 2017, Crescentino also applied for *concordato preventivo* in accordance to local bankruptcy Law. Granbio, in 2016, stopped producing ethanol and it is only burning bagasse to produce electricity. In January 2018, Frankens Energy LLC bought INEOS cellulosic plant in Florida, which had been closed at the end of 2016 (TEXASENERGYREPORT.COM, 2018). Conversely, Poet announced in 2017, on its website press release, the achievement of the major breakthrough in cellulosic biofuels production and its intention to build an onsite enzyme manufacturing facility to directly pipe DSM enzymes into the process. Also, Ek Laboratories, Inc., a subsidiary of Alliance BioEnergy and owner of the CTS® patent whose process makes the pretreatment without using enzymes, started the operation of a demonstration plant processing 2.5 tonne/day, in 2015 (ALLIANCE BIOENERGY, [*s. d.*]). In fact, by 2018, the cellulosic ethanol process has not been shown to be completely

commercially feasible yet, but it has still a great potential to convert low-value feedstocks for increasing the production of biofuel.

2.3.11 Second-generation ethanol versus CHP

Surplus bagasse can be used to produce more electricity or second-generation ethanol. Both fuels can be used in light vehicles. For instance, take two commercial cars where car “A” being sold in the USA and uses electricity and car “B” being sold in Brazil and using a flex-fuel engine (it can use ethanol or gasoline). Knowing that surplus bagasse can be converted into electricity or second-generation ethanol, it is possible to draw two hypothetical scenarios where scenario 1 consists in a refinery processing 1 tonne of sugarcane to produce ethanol in the first-generation process and electricity using a condensation turbine as described in Table 1, and scenario 2, in which the same 1 tonne of sugarcane is used to produce second-generation ethanol from surplus bagasse besides first-generation ethanol. The parameters and efficiency adopted for second-generation ethanol is described in Table 2. Table 3 compares both scenarios side by side to obtain the distance driven in each scenario.

Looking through these results, it would be possible to infer that, considering these parameters and efficiency, it is better to produce electricity instead of ethanol since the distance driven in scenario 1 is higher than in scenario 2. However, this is not a conclusive result since to reach a reliable best scenario, studies such as live cycle analysis, return on investment, energy storage method, concentrated versus dispersed emissions, autonomy, and the preferable fuel by customers are needed.

Table 2 - Parameters used to obtain the consumption rating of two vehicles

Parameter and efficiency adopted	2nd generation ethanol plant
Steam consumed per tonne of bagasse at 2nd generation process.	451 kg[1]
Electricity consumed per tonne of bagasse at 2nd generation process.	155 kW·h[1]
Lignin per kg of bagasse (dry basis).	0.264 kg[2]
Glucan group per kg of bagasse (dry basis).	0.405 kg[2]
Xylan group per kg of bagasse (dry basis).	0.197 kg[2]
Net calorific value of lignin (35% moisture).	12,671.8 kJ/kg[3]
Pretreatment efficiency.	90 %
Sucrose and Glucose fermentation efficiency.	90 %
Xilose fermentation efficiency.	80 %
Distillation efficiency.	97 %

[1] (HUMBIRD *et al.*, 2011); [2] (Ethanol production from enzymatic hydrolysis of sugarcane bagasse pretreated with lime and alkaline hydrogen peroxideRABELO *et al.*, 2011); [3](MANSOURI; SALVADÓ, 2006)

Table 3 - Parameters used to obtain the consumption rating of two vehicles

Parameter \ Scenario	1st scenario	2nd scenario
Surplus electricity	79.7 kW·h	38 kW·h
Ethanol	90 L	104.3 L
City consumption ratings car “A”	6.20 km/kW·h	
Highway consumption ratings car “A”	4.90 km/kW·h	
City consumption ratings car “B”	8.34 km/L	
Highway consumption ratings car “B”	9.9 km/L	
Driven distance in city using car “A”	494 km	237 km
Driven distance in highway using car “A”	390 km	186 km
Driven distance in city using car “B”	750 km	870 km
Driven distance in highway using car “B”	891 km	1072 km
Total driven distance in a city	1245 km	1107 km
Total driven distance in highway	1281 km	1258 km

2.4 Conclusion

A new era with a clean worldwide energy matrix is expected nowadays. Ethanol has been shown to be a fuel with great potential to meet this world’s aspirations. In this new phase, the fuel needs to be recognized by its environmental benefits and not only by the energy that it contains. Consequently, it has to be rewarded according to the benefits it brings to society. For this, in recent years, the sugarcane industry has positioned itself not only as a food industry but also as an energy industry. Having a look into the sugarcane feedstock, bringing a different viewpoint, one could say that it produces three different kinds of energy: sugar-energy for human beings; ethanol-energy for transportation; and electricity-energy for

a variety of uses. As an energy company, the process itself cannot be energetically wasteful. So, recent improvements in the process have aimed to maximize its efficiency; meaning that using less energy in the process itself results in more energy left to be sold as a product. However, many questions, such as the destination of the use of straw, bagasse, and vinasse, are still unanswered and will depend on the next technology improvement. This new era will result in increasing the demand for ethanol, which must be met not only by the increase in the production but also in the productivity and efficiency. Nevertheless, many technologies, with notorious performances, are not applied to the production of ethanol nowadays because of their low feasibility. They would become feasible, however, if ethanol was rewarded for its environmental benefits.

Acknowledgments

The authors kindly acknowledge FAPESP (Fundação de Amparo à Pesquisa do Estado de São Paulo) process number 2015/50684-9 for its financial support.

References

AHMED, Adam E.; ALAM-ELDIN, Amna O. M. An assessment of mechanical vs manual harvesting of the sugarcane in Sudan – The case of Sennar Sugar Factory. **Journal of the Saudi Society of Agricultural Sciences**, [s. l.], v. 14, n. 2, p. 160–166, 2015.

ALLIANCE BIOENERGY. **Ek Labs | Alliance BioEnergy**. [s.d.]. Disponível em: <http://www.alliancebioe.com/subsidiaries/ekl/>. Acesso em: 18 mar. 2018.

ARRUDA, Paulo. Genetically modified sugarcane for bioenergy generation. **Current Opinion in Biotechnology**, [s. l.], v. 23, n. 3, p. 315–322, 2012. Disponível em: <https://www.sciencedirect.com/science/article/pii/S0958166911007087>. Acesso em: 17 abr. 2018.

BERNAL, Andressa Picionieri et al. Vinasse biogas for energy generation in Brazil: An assessment of economic feasibility, energy potential and avoided CO2 emissions. **Journal of Cleaner Production**, [s. l.], v. 151, p. 260–271, 2017. Disponível em: <https://www.sciencedirect.com/science/article/pii/S0959652617304997>. Acesso em: 21 mar. 2018.

BRASSOLATTI-, Tatiane Fernandes Zambrano et al. Estudo de viabilidade da mudança do transporte de cana-de-açúcar de treminhão para rodotrem. In: 7º ECAECO 2014, Ponta Porã - MS. **Anais**... Ponta Porã - MS Disponível em: <https://anaisonline.uems.br/index.php/ecaeco/article/download/2803/2873>

BRAZIL. MINISTÉRIO DE MINAS E ENERGIA. **Ordinance n. 103, de 22 de março de 2018**Diário Oficial, , 2018. Disponível em: <http://www.lex.com.br/legis_27629166_PORTARIA_N_103_DE_22_DE_MARCO_DE_2018.aspx>. Acesso em: 26 mar. 2018.

BRAZIL. **Law n. 4.870, de 1 de dezembro de 1965. Dispõe sôbre a produção açucareira, a receita do Instituto do Açúcar e do Álcool e sua aplicação, e dá outras providências.**Diário Oficial, , 1965. Disponível em: <http://www.planalto.gov.br/ccivil_03/leis/l4870.htm>. Acesso em: 12 mar. 2018.

BRAZIL. **Decree n. 76593 de 14 de novembro de 1975. Institui o Programa Nacional do Álcool e dá outras Providências.**Diário Oficial, , 1975. Disponível em: <http://legis.senado.gov.br/legislacao/ListaTextoSigen.action?norma=499233&id=14242670&idBinario=15706117&mime=application/rtf>. Acesso em: 7 mar. 2018.

BRAZIL. **Decree n. 83700 de 05de julho de 1979. Dispõe sobre a execução do Programa Nacional do Álcool, cria o Conselho Nacional do Álcool - CNAL, a Comissão Executiva Nacional do Álcool - CENAL, e dá outras Providências.**Diário Oficial, , 1979. Disponível em: <http://legis.senado.gov.br/legislacao/ListaTextoSigen.action?norma=506340&id=14330511&idBinario=15706194&mime=application/rtf>. Acesso em: 7 mar. 2018.

BRAZIL. **Decree n. 99.240, de 7 de maio de 1990. Dispõe sobre a extinção de autarquias e fundações públicas, e dá outras providências.**Diário Oficial, , 1990. Disponível em: <http://www.planalto.gov.br/ccivil_03/decreto/1990-1994/D99240.htm>. Acesso em: 12 mar. 2018.

BRAZIL. **Decree n. 2.661 de 8 de julho de 1998. Regulamenta o parágrafo único do art. 27 da Lei nº 4.771, de 15 de setembro de 1965 (código florestal), mediante o estabelecimento de normas de precaução relativas ao emprego do fogo em práticas agropastoris e flores**Diário Oficial, , 1998. Disponível em: <http://www.planalto.gov.br/ccivil_03/decreto/d2661.htm>. Acesso em: 8 mar. 2018.

BRAZIL. **Law n. 10.336, de 19 de dezembro de 2001. Institui Contribuição de Intervenção no Domínio Econômico incidente sobre a importação e a comercialização de petróleo e seus derivados, gás natural e seus derivados, e álcool etílico combustível (Cide), e dá outr**Diário Oficial, , 2001. Disponível em: <http://www.planalto.gov.br/ccivil_03/Leis/LEIS_2001/L10336.htm>. Acesso em: 10 mar. 2018.

BRAZIL. **Law n. 10.438, de 26 de abril de 2002. Dispõe sobre a expansão da oferta de energia elétrica emergencial, recomposição tarifária extraordinária, cria o Programa de Incentivo às Fontes Alternativas de Energia Elétrica (Proinfa), a Conta de Desenvolvimento**Diário Oficial, , 2002. Disponível em: <http://www.planalto.gov.br/ccivil_03/Leis/2002/L10438.htm>. Acesso em: 13 mar. 2018.

BRAZIL. **Resolution n. 640, de 14 de dezembro de 2016. Altera a Resolução CONTRAN nº 211, de 13 de novembro de 2006, que estabelece requisitos necessários para circulação de Combinações de Veículos de Carga (CVC).**Diário Oficial, , 2016. Disponível em: <http://www.denatran.gov.br/images/Resolucoes/Resolucao6402016.pdf>. Acesso em: 12

mar. 2018.

BRAZIL - MINISTÉRIO DA FAZENDA. **Ordinance n. 0059, de 29 de março de 1996. Resolve: Liberar os preços da gasolina automotiva e do álcool hidratado para fins carburante, inclusive dos aditivados, nas unidades de comércio atacadista ou varejista.**Diário Oficial, , 1996. Disponível em: <http://webcache.googleusercontent.com/search?q=cache:vs07gSt3f8EJ:www.mpsp.mp.br/portal/page/portal/cao_consumidor/legislacao/leg_combustiveis_derivados/leg_comb_postos_combustiveis/Port59-96-MF.doc+&cd=1&hl=pt-BR&ct=clnk&gl=br>. Acesso em: 7 mar. 2018.

CONAB - COMPANHIA NACIONAL DE ABASTECIMENTO. **Safra Brasileira de Cana de Açúcar**. [s.d.]. Disponível em: <https://www.conab.gov.br/index.php/info-agro/safras/cana>. Acesso em: 19 mar. 2018a.

CONAB - COMPANHIA NACIONAL DE ABASTECIMENTO. **Custos de Produção - Cultura Semi-perene**. [s.l: s.n.]. Disponível em: <http://www.conab.gov.br/conteudos.php?a=1558&t=2>. Acesso em: 10 mar. 2018b.

COSTA, Rodrigo C.; SODRÉ, José R. Compression ratio effects on an ethanol/gasoline fuelled engine performance. **Applied Thermal Engineering**, [s. l.], v. 31, n. 2–3, p. 278–283, 2011. Disponível em: <http://dx.doi.org/10.1016/j.applthermaleng.2010.09.007>

DIAS, Henrique Boriolo; SENTELHAS, Paulo Cesar. Evaluation of three sugarcane simulation models and their ensemble for yield estimation in commercially managed fields. **Field Crops Research**, [s. l.], v. 213, n. August, p. 174–185, 2017. Disponível em: <http://dx.doi.org/10.1016/j.fcr.2017.07.022>

EMPRAL; SERMATEC; ZANINI. **Solução para limpeza de cana a seco e aproveitamento da palha**. [s.d.]. Disponível em: <http://sermatec.com.br/media/uploads/produtos_arquivo/limpeza-a-seco_sermatec-zanini_empral.pdf>. Acesso em: 13 mar. 2018.

EPA, US. **Overview | Methyl Tertiary Butyl Ether (MTBE) | US EPA**. [s.d.]. Disponível em: <https://archive.epa.gov/mtbe/web/html/faq.html>. Acesso em: 24 mar. 2018.

FABIANA BATISTA. **Para o etanol, preço ainda é quase tudo**. 2013. Disponível em: <https://www.novacana.com/n/etanol/mercado/para-etanol-preco-ainda-quase-tudo-221113/>. Acesso em: 7 mar. 2018.

FRANÇOSO, Renato Frias et al. Relação do custo de transporte da cana-de-açúcar em função da distância. **Revista IPecege**, [s. l.], v. 3, n. 1, p. 100–105, 2017. Disponível em: <https://revista.ipecege.org.br/Revista/article/view/123>. Acesso em: 22 ago. 2020.

GAYKAWAD, Sushil S. et al. Pervaporation of ethanol from lignocellulosic fermentation broth. **Bioresource Technology**, [s. l.], v. 129, p. 469–476, 2013. Disponível em: <http://dx.doi.org/10.1016/j.biortech.2012.11.104>

HARDIN, G. The tragedy of the commons. The population problem has no technical solution;

it requires a fundamental extension in morality. **Science (New York, N.Y.)**, [s. l.], v. 162, n. 3859, p. 1243–8, 1968. Disponível em: <http://www.ncbi.nlm.nih.gov/pubmed/5699198>. Acesso em: 10 mar. 2018.

HASHI, M.; THIBAULT, J.; TEZEL, F. H. Recovery of ethanol from carbon dioxide stripped vapor mixture: Adsorption prediction and modeling. **Industrial and Engineering Chemistry Research**, [s. l.], v. 49, n. 18, p. 8733–8740, 2010.

HUGOT, E. **Handbook of Cane Sugar Engineering**. 3. ed. [s.l.] : Elsevier, 1960. Disponível em: <https://linkinghub.elsevier.com/retrieve/pii/C20130124373>

HUMBIRD, D. et al. **Process Design and Economics for Biochemical Conversion of Lignocellulosic Biomass to Ethanol**. Colorado. Disponível em: <https://www.nrel.gov/research/publications.html>.

KEERTHANA, T.; KRISHNAVENI, A. Biogas Production From Sugarcane Bagasse in Co-Digestion with Vegetable Waste. **International Journal of Latest Engineering Research and Applications**, [s. l.], v. 01, n. 03, p. 2455–7137, 2016. Disponível em: <www.ijlera.com>. Acesso em: 21 mar. 2018.

LANDELL, Mga; SCARPARI, Ms; XAVIER, Ma. Residual biomass potential of commercial and pre-commercial sugarcane cultivars. **Scientia …**, [s. l.], v. 70, n. 5, p. 299–304, 2013. Disponível em: <http://www.scielo.br/scielo.php?pid=S0103-90162013000500003&script=sci_arttext>

LANDIRENZO. **Diesel + Methane Conversion**. [s.d.]. Disponível em: <https://landirenzo.com/sites/default/files/gamma-ddf-en.pdf>. Acesso em: 21 mar. 2018.

LARSEN, GREGORY J. **Reciprocating piston engine with a varying compression ratio**, patent US5025757, 1991.

LONGATI, Andreza A.; CAVALETT, Otávio; CRUZ, Antonio J. G. Life Cycle Assessment of vinasse biogas production in sugarcane biorefineries. In: **Computer Aided Chemical Engineering**. [s.l.] : Elsevier, 2017. v. 40p. 2017–2022.

MANSOURI, Nour Eddine El; SALVADÓ, Joan. Structural characterization of technical lignins for the production of adhesives: Application to lignosulfonate, kraft, soda-anthraquinone, organosolv and ethanol process lignins. **Industrial Crops and Products**, [s. l.], v. 24, n. 1, p. 8–16, 2006.

MATSUOKA, Sizuo; MACCHERONI, Walter. Disease Management. In: **Sugarcane**. [s.l.] : Elsevier, 2015. p. 115–132.

MINISTÉRIO DE MINAS E ENERGIA. **Balanço Energético Nacional**. [s.l: s.n.]. Disponível em: <http://www.epe.gov.br>.

MONTAGNHANI, Bruno Astolphi et al. O Papel da Agroindústria Canavieira na Geração de Empregos e no Desenvolvimento Local: o caso da usina mundial no município de Mirandópolis, Estado de São Paulo. **Informações Econômicas**, [s. l.], v. 3912, p. 26–38, 2009. Disponível em: <http://www.iea.sp.gov.br/ftpiea/publicacoes/ie/2009/tec3-1209.pdf>.

Acesso em: 26 mar. 2018.

MORAES, Bruna S.; ZAIAT, Marcelo; BONOMI, Antonio. Anaerobic digestion of vinasse from sugarcane ethanol production in Brazil: Challenges and perspectives. **Renewable and Sustainable Energy Reviews**, [s. l.], v. 44, p. 888–903, 2015. Disponível em: <http://dx.doi.org/10.1016/j.rser.2015.01.023>

NOVACANA.COM. **Bagaço da cana pode ser o décimo produto a fazer parte do Consecana**. 2016. Disponível em: <https://www.novacana.com/n/cana/mercado/bagaco-cana-produto-consecana-070116/>. Acesso em: 13 mar. 2018.

NYKO, Diego et al. **A evolução das tecnologias agrícolas do setor sucroenergético: estagnação passageira ou crise estrutural?BNDES**. [s.l: s.n.]. Disponível em: <https://web.bndes.gov.br/bib/jspui/bitstream/1408/1503/1/A mar37_10_A evolução das tecnologias agrícolas do setor_P.pdf>.

OLIVEIRA, Eduardo Sabino De. **Alcool Motor e Motores a Explosao**. [s.l.] : Instituto de Thechnologia, 1937.

PROCKNOR, Celso. Vinhaça: Concentração X Redução do Volume. **Stab**, [s. l.], v. 1, p. 3–7, 2015.

PROCÓPIO, Sérgio de Oliveira et al. Weed Management. In: SANTOS, Fernando; BORÉM, Aluízio; CALDAS, Celso (Eds.). **Sugarcane**. [s.l.] : Elsevier, 2015. p. 133–159.

RABELO, S. C. et al. Ethanol production from enzymatic hydrolysis of sugarcane bagasse pretreated with lime and alkaline hydrogen peroxide. **Biomass and Bioenergy**, [s. l.], v. 35, n. 7, p. 2600–2607, 2011. Disponível em: <http://dx.doi.org/10.1016/j.biombioe.2011.02.042>

REIN, P. W. A Comparison of Cane Diffusion and Milling. In: PROCEEDINGS OF THE SOUTH AFRICAN SUGAR TECHNOLOGY ASSOCIATION 1995, **Anais**... [s.l: s.n.]

REIN, Peter. **Cane Sugar Engineering**. Berlin: Bartens, 2007.

RODRIGUES, T. R. Entrevista: Energia Verde. **Vanzolini em foco**, [s. l.], [s.d.].

TEXASENERGYREPORT.COM. **Texas Energy Investor New Owner of Southeast Florida Biofuel Plant: Report – TheTexasEnergyReport.com**. 2018. Disponível em: <https://texasenergyreport.com/blog/2018/01/25/texas-energy-investor-new-owner-of-southeast-florida-biofuel-plant-report/>. Acesso em: 17 mar. 2018.

THE EUROPEAN FUEL OXYGENATES ASSOCIATION. **EFOA - Home - EFOA**. [s.d.]. Disponível em: <http://www.efoa.eu/en/home-99.aspx>. Acesso em: 25 mar. 2018.

UNICA. **UNICADATA - União da Indústria de Cana-de-Açúcar - Histórico de produção e moagem por produto**. [s.d.]. Disponível em: <http://www.unicadata.com.br/>. Acesso em: 16 abr. 2018.

UNICA; CEISE. **Setor Sucroenergético no Brasil uma Visão para 2030**. [s.l: s.n.]. Disponível em: <http://www.mme.gov.br/documents/10584/7948692/UNICA-

CEISE_Setor+Sucroenergético+no+Brasil_Uma+Visão+para+2030.pdf/80da9580-60c7-4f53-afaf-030ad01f3ebf;jsessionid=AC802B166C93389BED1AB445EAB7CD10.srv155>. Acesso em: 26 mar. 2018.

WALSH, G. H. The Riviere Juice Extractor : a New Approach To the Extraction of Juice From Cane. In: PROCEEDINGS OF THE SOUTH AFRICAN SUGAR TECHNOLOGISTS ASSOCIATION 1998, **Anais**... [s.l: s.n.]

WANG, W. et al. Fuzzy ignition timing control for a spark ignition engine. **Proceedings of the Institution of Mechanical Engineers, Part D: Journal of Automobile Engineering**, [s. l.], v. 214, n. 3, p. 297–306, 2000.

ZILBERMAN, David; MORAES, Márcia Azanha Ferraz Dias De. **Natural Resource Management and Policy**. [s.l.] : Springer Cham Heidelberg New York Dordrech London, 2013. Disponível em: <http://www.springer.com/series/6360>

CHAPTER 3: OPEN SUGARCANE PROCESS SIMULATION PLATFORM

This chapter corresponds to an article presented and published as a book chapter in the proceedings of the International Symposium on Process Systems Engineering – PSE 2018.

Rubens E. N. de Castro, Rita M. B. Alves, Adam Hawkes, Claudio A. O. Nascimento Open Sugarcane Process Simulation Platform. **In: International Symposium on Process Systems Engineering – PSE 2018**. San Diego: Elsevier B.V., 2018. p. 1819–1824.

Abstract

Software tools for process simulation and optimization have increasingly been used in industry to design and operate complex, highly interconnected plants. This allows the design of industrial plants to be profitable and to meet quality, safety, environmental and other standards. The aim of this work is to create a platform to simulate the industrial sugarcane first-generation process. Brazilian sugarcane industry is a well-known process with many parameters available from industrial and literature data. The current first-generation process seems to have reached the state of art and no great improvements seams to emerge nowadays. However, engineering research has dedicated great efforts recently to improve efficiency through the use of industrial and agricultural residues. Most of these studies are related to the use of lignocellulosic material and vinasse. In this context, an easy and simple platform has been developed to provide reliable outputs that could provide data for the studies of viability, social and environmental impacts when additional processes are interconnected to the first generation plant. The model has been validated using industrial data in order to attain the most realistic outputs.

Keywords: Sugarcane, biofuel, process simulation.

3.1 Introduction

In Brazilian sugarcane industries, several studies have been carried out as an attempt to use agricultural residues such as straw (DIAS *et al.*, 2012) or industrial residues such as vinasse (LONGATI; CAVALETT; CRUZ, 2017) and bagasse (FURLAN *et al.*, 2012) to sum up with new co-products or improve the whole sector more efficiently (JUNQUEIRA; BONOMI, 2011). These new processes can be understood as an interconnected plant to the current first generation process where materials and utilities are shared (FONSECA; COSTA; CRUZ, 2017). Indeed, there is a synergetic interaction between the new and the main process which could

result in better overall energy balance(FURLAN *et al.*, 2012). The objective of this work is to develop a model for quantitative simulation of a feasible ethanol and sugar conversion process that uses these residues as raw materials and is interconnected to the first generation process.

3.2 Process Overview

The development of this computational platform follows the process configuration presented in Figure 4, which is a typical sugarcane mill. Each step represents an area at the sugar mill industry and each area has a number of unit operation processes. In Figure 4, "cane reception and extraction" is the process where the sugarcane feed is reduced into small pieces and the sugar bearing cells is ruptured to facilitate the subsequent extraction process. The size reduction is generally achieved through the use of rotating knives and swing hammer shredder in the cane conveying system. In the case of billeted cane, mechanically harvested, sugarcane can be fed directly into a shredder without any knifing. For sugarcane juice extraction, two systems are used: milling tandem or diffuser. In Brazil, the preference has been for the mill extraction process which consists of a set of four to six mills. This step produces two streams: bagasse and juice.

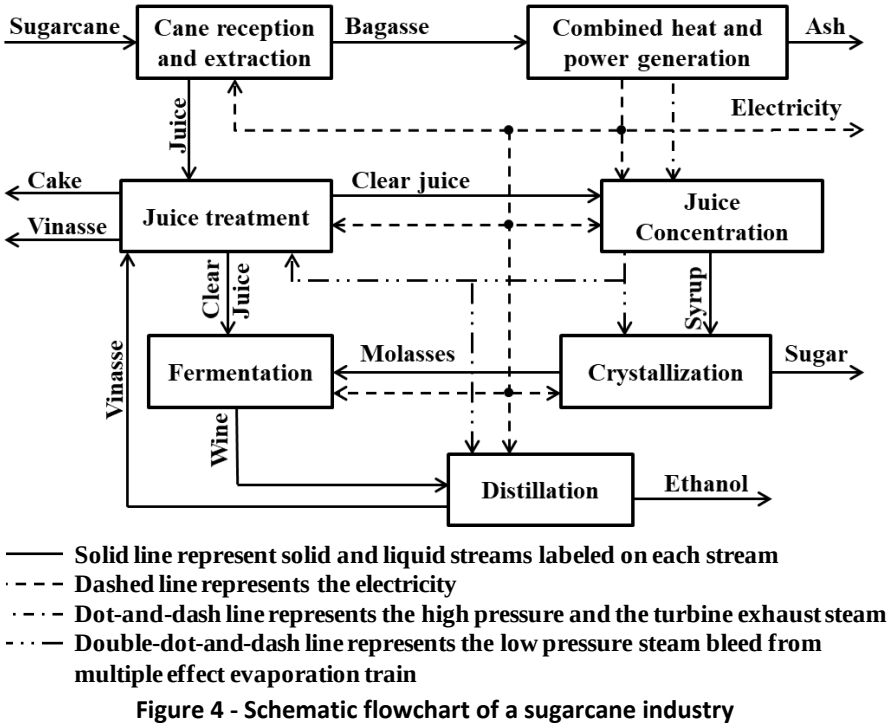

Figure 4 - Schematic flowchart of a sugarcane industry

Juice after mill contains several impurities which must be removed prior to fermentation or concentration. This process takes place in the juice treatment area where these impurities are removed using a set of unit operations which basically consist of heating, pH adjusting, settling the precipitate formed in the body juice, and filtering.

Clear juice must be concentrated to achieve a suitable brix to start the crystallization process, about 60 % (w/w) sucrose. This concentration is obtained using multiple-effect evaporators, which use the exhaust steam from the turbines and produce lower pressure steam used as utility in the process.

Concentrated juice, called syrup, is further concentrated in a vacuum boiling pan until it becomes supersaturated. Finely ground sugar crystals suspended in alcohol are introduced into the vacuum pan as seed crystals around which sucrose is deposited. These crystals then grow until they are ready to be discharged. Maximum recovery of sucrose by crystallization cannot be achieved in one step. Various crystallization schemes can be employed. In Brazil, two-boiling scheme is the most used, because it is not necessary to completely exhaust molasses since ethanol is produced using it.

Broth for alcoholic fermentation is a mixture containing molasses and clear juice. This mixture uses a biological process that converts sugars such as glucose, fructose, and sucrose into cellular energy, producing ethanol and carbon dioxide as a side-effect. The overall chemical reaction for alcoholic fermentation is:

$$C_{12}H_{22}O_{11} + H_2O + enzyme \rightarrow 2\ C_6H_{12}O_6 \rightarrow 4\ C_2H_5OH + 4\ CO_2$$

In the first step of alcoholic fermentation, the enzyme invertase cleaves the glycolic linkage between the glucose and fructose molecules. This process usually takes place in a fed-batch fermentation process. When fermentation finishes the fermented wine is centrifuged to remove yeast (*Saccharomyces cerevisiae*) which is recycled to the next fed-batch while wine with an ethanol content of about 8 °GL is sent to the next process.

Ethanol is recovered from wine in the distillation process. Fuel ethanol or hydrous ethanol 93 wt% is produced by a simple distillation process while anhydrous ethanol 99.3 wt%, for mixing with gasoline, is produced by azeotropic distillation with cyclohexane or monoethyleneglycol or by absorption on molecular sieves. Vinasse rich in nutrients is used in the fertigation of the sugarcane fields.

Sugarcane bagasse is burnt in the boiler, producing steam that is expanded in turbines coupled with electric generators. Steam exhaust from the turbines is used as thermal energy in the evaporation area. The surplus steam (not consumed in the process) is used in condensing steam turbines to maximize the electricity production. Therefore sugarcane mill is self-sufficient in electricity and can sell the surplus to the grid.

3.3 Model

The model-based simulation framework involved two main parts: (1) mass and energy balances; (2) constitutive equations. The in-house model was implemented in Matlab®.

Sugarcane, biomass feedstock for the first generation process, can be represented by 3 main parts: (1) the insoluble part includes fibrous and other insoluble materials like soil, which in this text is called 'Fibre'; (2) water which is about 70 % of the total sugarcane; and (3) soluble solids like sucrose, other sugars, some proteins, some salts, etc., which is usually called 'Brix'. Consequently, mass balance is applied for the three parts (Eqs 1 to 3).

$$\sum_{i=1}^{n} Fibre_{in} - \sum_{i=1}^{n} Fibre_{out} = 0 \qquad (3.1)$$

$$\sum_{i=1}^{n} Brix_{in} - \sum_{i=1}^{n} Brix_{out} = 0 \qquad (3.2)$$

$$\sum_{i=1}^{n} Flow_{in} - \sum_{i=1}^{n} Flow_{out} = 0 \qquad (3.3)$$

For the energy balance, Eq. 3.4, thermodynamic properties of water were obtained adjoining packages from IPAWS. Specific heat of juice is given by Eq. 3.5 (HUGOT, 1960) and specific heat of fibre is given by Eq. 3.6 adapted from Hatakeyama et al (1982)

The parameters for the constitutive equations come from industrial or literature data, or from equipment modelling (REIN, 2007). This equation and its parameters depend on the type of operation, for example, overall coefficient and area are the needed parameters for

heat exchangers; mud concentration is the parameter for the juice clarification process, and so on.

$$\sum_{i-stream}^{n-stream} (Flow_i \cdot cp_i \cdot T_i)_{in} - \sum_{i-stream}^{n-stream} (Flow_i \cdot cp_i \cdot T_i)_{out} = 0 \qquad (3.4)$$

$$cp_j = \left(1 - \left(0.6 - 0.0018 \cdot T + 0.08 \cdot (1 - P)\right) \cdot Brix\right) \cdot 4.187 \qquad (3.5)$$

$$cp_b = 1.364 + 5.06 \cdot 10^{-3} \cdot (T - 76.85) \qquad (3.6)$$

The model is then comprised by three independent equations from mass balance that are obtained: Fibre balance, Brix balance, overall balance or water balance; and the energy balance. Consequently, the number of parameters and constitutive equations depends on the number of unknown variables. Usually, feed stream is known and the outflow is unknown, consequently, the number of parametric equations needed will depend on the number of streams out of the 'unit operation'.

This platform aims to allow the user to customize the configuration in many ways one requires. Consequently, this model deals with each unit operation as a separate algorithm. Figure 5 shows an example of one unit operation.

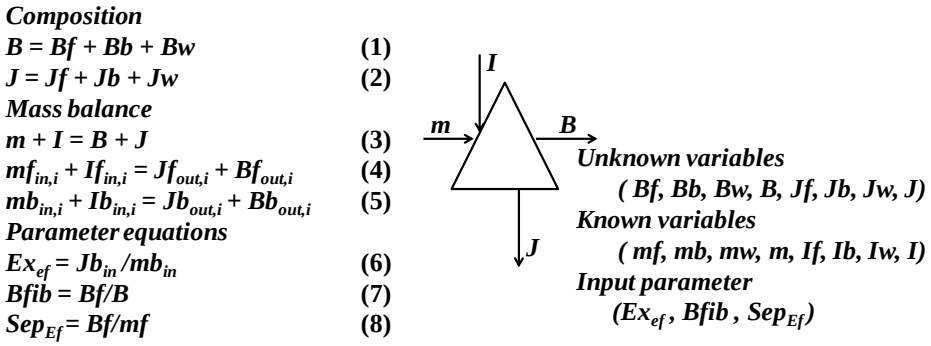

Figure 5 - Schematic flowchart of a sugarcane industry

Therefore, one script is used to represent a unit operation, and another one is used to call a given unit operation by identifying recycling loops to solve each area individually as shown in Figure 6. The result from one unit operation becomes the input for the next unit operation.

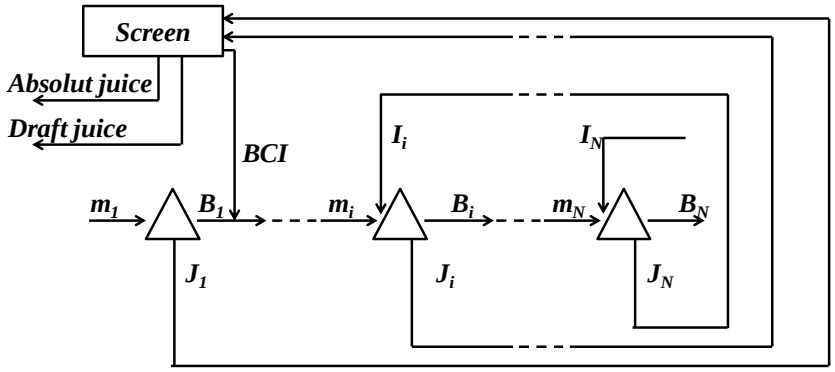

Figure 6 - Schematic flowchart of a sugarcane industry

Flowsheet analysis or simulation is complicated because the mass and energy balances are tightly coupled between different unit operations and consequently between areas. This problem was stated in a standard form of a "Direct Substitution Method", which uses a fixed point relation $x^{k+1} = g(x^k)$ (BIEGLER; GROSSMANN; WESTERBERG, 1997), where x is for instance the stream flow rate and $g(x)$ is the corresponding algorithm to calculate this stream and x_0 is the initial guess. The convergence of this method depends on the relation:

$$|\lambda| = \frac{|x^{k+1} - x^k|}{|x^k - x^{k-1}|} \qquad (3.7)$$

Where $|\lambda|^{max}$ is the Euclidean norm and a necessary and sufficient condition for convergence is that $|\lambda|^{max} < 1$. The fixed point methods developed for recycling convergence are strongly influenced by the structure of the flowsheet and the choice of the tear streams. The algorithm proposed by Biegler et al. (1997) was used to find the partitions and precedence ordering of resolution.

3.4 Results

Figure 7 shows the synergetic effect of producing sugar and ethanol simultaneously and Table 4 shows the specifications and operating conditions used in this simulation. When both sugar and ethanol are produced, the steam consumption in first-generation process is reduced while surplus power generation increase against the industrial mix. Industrial mix is the step to decide which product is going to be produced using the sucrose from juice: ethanol or sugar. In this configuration, steam from the first effect of the multiple effect evaporation train is bled and directly injected into a distillation column. It is observed that when about 60 % of cane is used to produce sugar, the steam consumption is the lowest and consequently

the energy production is the highest. This occurs because a great amount of water has to be taken off the sugar juice in order to concentrate it for the crystallization process and the water withdrawn as steam from the sugar juice is used in the distillation process. For higher sugar production, the steam used to concentrate the juice is predominant; while for a lower sugar production, distillation it is major responsible for the overall heat consumption and it is necessary to concentrate ethanol juice using one effect evaporator which increases the overall steam consumption when compared to multiple-effect evaporation.

Table 4 - Specifications and operations conditions used in this simulation

Sugarcane	1000 t/h
Fibre % Cane	13.0%
Sucrose wt%	15.0%
Bagasse	265 t/h
Extraction efficiency	97.7
Boiler steam pressure and temperature	67 bar / 520°C
Boiler efficiency	79%
Back pressures turbine overall efficiency	82%
Condensation turbine overall efficiency	73%

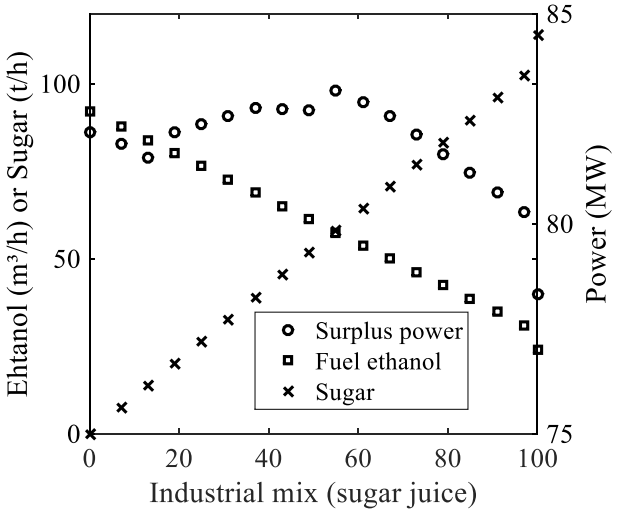

Figure 7 - Ethanol Sugar and Power production

It is important to say that, in this scenario, even when the whole sugarcane juice stream is sent to the sugar process, ethanol is still being produced using molasses. Nevertheless, the behavior shown in Figure 7 is valid for this configuration and operation streams.

3.5 Conclusion

A typical sugar and ethanol process has been presented. Assumptions and results of the simulation have been carefully validated using industrial data to reflect the reality. Consequently a platform simulation has been developed to provide reliable outputs that could provide data for studies of technical and economic viability and social and environmental impacts when any new process is interconnected to the first generation plant, by sharing materials, utilities and products. Research will continue using agricultural residues (straw) or industrial residues (vinasse and bagasse) to sum up with new co-products or improve the whole sector more efficiently.

Acknowledgments

The authors kindly acknowledge FAPESP (Fundação de Amparo à Pesquisa do Estado de São Paulo) process number 2015/50684-9 for its financial support.

References

BIEGLER, L. T.; GROSSMANN, I. E.; WESTERBERG, A. W. **Systematic Methods of Chemical Process Design**. 1. ed. Pittsburgh: Prentice Hall, 1997.

DIAS, M. O. S. *et al.* Improving second generation ethanol production through optimization of first generation production process from sugarcane. **Energy**, [*s. l.*], v. 43, n. 1, p. 246–252, 2012. Disponível em: http://dx.doi.org/10.1016/j.energy.2012.04.034.

FONSECA, G. C.; COSTA, C. B. B.; CRUZ, A. J. G. Superstructural economic optimization of sugarcane bagasse exploitation in an ethanol distillery connected to Rankine cycle, BIGCC system and second generation ethanol process. *In*: COMPUTER AIDED CHEMICAL ENGINEERING. [*S. l.*]: Elsevier B.V., 2017. v. 40, p. 889–894.

FURLAN, F. F. *et al.* Assessing the production of first and second generation bioethanol from sugarcane through the integration of global optimization and process detailed modeling. **Computers and Chemical Engineering**, [*s. l.*], v. 43, p. 1–9, 2012.

HATAKEYAMA, T.; NAKAMURA, K.; HATAKEYAMA, H. Studies on heat capacity of cellulose and lignin by differential scanning calorimetry. **Polymer**, [*s. l.*], v. 23, n. 12, p. 1801–1804, 1982.

HUGOT, E. **Handbook of Cane Sugar Engineering**. 3. ed. [*S. l.*]: Elsevier, 1960. *E-book*. Disponível em: https://linkinghub.elsevier.com/retrieve/pii/C20130124373.

JUNQUEIRA, T. L.; BONOMI, A. Simulation and Evaluation of Autonomous and Annexed Sugarcane Distilleries. **Chemical Engineering Transactions**, [*s. l.*], v. 25, p. 941–946, 2011.

LONGATI, A. A.; CAVALETT, O.; CRUZ, A. J. G. Life Cycle Assessment of vinasse biogas production in sugarcane biorefineries. *In*: COMPUTER AIDED CHEMICAL ENGINEERING. [*S. l.*]: Elsevier, 2017. v. 40, p. 2017–2022. Disponível em: https://www.sciencedirect.com/science/article/pii/B978044463965350338X. Acesso em: 21 dez. 2017.

REIN, P. **Cane Sugar Engineering**. Berlin: Bartens, 2007.

CHAPTER 4: REPORT: SUGARCANE PROCESS SIMULATION PLATFORM

This chapter is a report on the mathematical model used to simulate the sugarcane industry. The mathematical model and the parameters used to simulate the production of first-generation ethanol, sugar, and electricity production are presented.

4.1 Introduction

In almost all industrial processes, the product passes through several interconnected processing units. These processing units vary from one industry to another; i.e., different technologies can be used to provide the same service; for example, fluidized-bed boiler versus bottom ash conveyor boilers, fed-batch versus continuous fermentation, belt-press filter versus rotary-drum filter, etc. Therefore, it is logical to divide a mathematical model into parts, each of which is a processing unit. Thus, to generate the model of a complex industrial plant, the processing units are connected. Processing units are grouped to represent a processing area, and a refinery is an assembly of areas. The parameters for solving these mathematical models are either from the literature or industry, to reflect the current Brazilian sugarcane process.

Many sugarcane mill simulation platforms have been developed (CHIAPPETA; NASCIMENTO, 1989; CHIAPPETTA; GIUDICI; NASCIMENTO, 1986) in many types of software, such as Aspen Plus (CHANDEL *et al.*, 2014; IGLESIAS, 2009), EMSO (FURLAN *et al.*, 2012), and SysCAD (THAVAL, 2012). The algorithm of this platform has been developed in Matlab because of its widespread use in academic research.

Here, each unit operation of a typical Brazilian sugarmill industry is described and their interconneticon is explanined. This chapter is organized into 18 sections; the first begins with this introduction. Next, the properties and thermodynamic models are described. The third section (Section 4.3) details the model used in some general unit operations. A general unit operation is used in more than one area, such as pumping, solid conveyance, and vapor condenser. In Sections 4.4 to 4.16, the areas and each specific unit operation in each area are presented; a specific unit operation is the one used only in one area; they are detailed in each area section. Each of these sections also shows how electricity consumption is calculated. In some areas, a convergence algorithm was applied to solve some recycling streams within the area. After solving each area, a convergence algorithm is applied to solve the recycling streams

between areas, as shown in Section 4.17. Section 4.18 shows the conclusion and provides some recommendations for future research.

4.2 Thermodynamic properties:

Herein the equations used to obtain the thermodynamic properties of components and mixtures are presented. They are water, sugary solutions, fiber, and ethanol. It was considered that sugarcane is a mixture of water, fiber, and soluble solids (Brix). Fiber comprises all nonsoluble components. Soluble solids, namely Brix, comprise the soluble solids; Brix is divided into sucrose and other solids; the term purity is defined as the ratio between the sucrose and the soluble solids.

4.2.1 Water

Thermodynamic properties of water and steam were obtained adjoining packages from the International Association for the Properties of Water and Steam, IAPWS IF - 97. The quality or range of the data is available in their release guidelines on their website (IAPWS, [*s. d.*]). The correlation written for Matlab use was created by Holmgren and is available online (HOLMGREN, [*s. d.*]).

4.2.2 Sugary solutions

Juice, syrup, and molasse are a mixture of water, sucrose, and other soluble solids; massecuite and magma are also of the same mixture type; however, part of the sucrose is crystallized. Hence, when sucrose is in crystal form, a different equation for the property is used.

4.2.2.1 Juice specific gravity

The specific gravity of juice, syrup, and molasse is given by Equation (4.1), which is obtained by the polynomial regression of the data shown in Table 5, as shown in Figure 8, which has been taken from Hugot (1960, p. 500)

$$SG = 1 + 0.316 \cdot Brix + 0.425 \cdot Brix^2 - 0.251 \cdot Brix^3 \qquad (4.1)$$

where:

Brix is the ratio between soluble solids and juice, *kg of solids/kg of solution.*

Table 5 - Specific Gravity for sugarcane juice

Brix %	SG
0	1.00
10	1.04
20	1.08
30	1.13
40	1.18
50	1.23
60	1.29
70	1.35
90	1.47

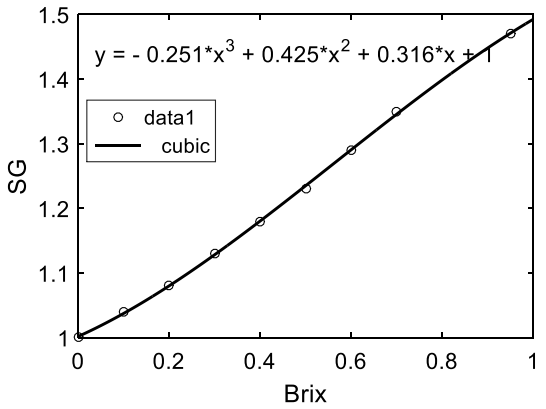

Figure 8 - Specific Gravity correlation for sugarcane juice

4.2.2.2 Juice specific heat

The specific heat of juice, syrup, and molasse is given by Equation (4.2) from Hugot (1960, p. 449) which takes into account the temperature and purity of the juice:

$$cp = \{1 - [0.6 - 0.0018 \cdot T + 0.08 \cdot (1 - P)] \cdot Brix) \cdot 4.1868\} \qquad (4.2)$$

where:

cp is the specific heat capacity, *kJ/(kg·K);*

Brix is the ratio between soluble solids and juice, *kg of solids/kg of solution;*

P is the purity of the juice, *kg of sucrose/kg of solids*;

T is the temperature of the juice, *°C*.

4.2.2.3 Juice viscosity

The viscosity of juice, syrup, and molasse is obtained using the empirical equation (Equation 4.3) from Astolfi (2011)

$$\mu = 0.14 \cdot 10^{-10} \cdot exp\left(\frac{44912.9}{8.31 \cdot (T+273.15)}\right) \quad (4.3)$$

where:

μ is the viscosity, $Pa \cdot s$;

T is the juice temperature, $°C$.

4.2.2.4 Massecuite density

The density of massecuite and magma is obtained using Equation (4.4). This equation considers the density of sugar crystal as 1587.9 kg/m³ and the density of mother liquor as 1470 kg / m³.

$$\rho = 1587.9 \cdot \gamma + 1470 \cdot (1-\gamma) \quad (4.4)$$

where:

ρ is the density, kg/m^3;

γ is the crystal ratio in the product.

4.2.2.5 Massecuite specific heat

Equation (4.5) (HUGOT, 1960, p. 628) provides the specific heat of a mixture of sucrose solution and crystals, such as massecuite and magma.

$$cp = \left(1 - 0.1\left(6 + \frac{10 \cdot \gamma}{6}\right) Brix\right) \cdot 4.1868 \quad (4.5)$$

Where:

γ is the crystal ratio;

cp is the specific heat capacity, $kJ/(kg \cdot K)$;

$Brix$ is the ratio between soluble solids and juice, $kg\ of\ solids/kg\ of\ solution$.

4.2.2.6 Juice boiling point elevation

As the concentration of dissolved solids increases, the boiling temperature of the juice increases above the temperature of saturated vapor at the same pressure. The degree of boiling point elevation is determined as a function of the concentration of soluble solids (*Brix*) by the Equation (4.6) (REIN, 2007, p. 271):

$$T = T_{sat,w} + \frac{2 \cdot Brix}{1 - Brix} \qquad (4.6)$$

Where:

T is the boiling point temperature, °C ;

$T_{sat,w}$ is the water saturation temperature, °C ;

Brix is the ratio between soluble solids and juice, *kg of solids/kg of solution.*

4.2.3 Fiber

The specific heat of the fiber is given by Equation (4.7) adapted from Hatakeyama et al. (1982).

$$cp = 1{,}364 + 5.06 \cdot 10^{-3}(T - 76.85) \qquad (4.7)$$

Where:

cp is the specific heat capacity, *kJ/(kg·K);*

T is the temperature, *°C.*

4.2.4 Ethanol

The properties of ethanol and alcoholic solutions required in this simulation platform are vapor pressure, specific heat capacity, and equilibrium of ethanol/water.

4.2.4.1 Vapor pressure

The ethanol vapor pressure is obtained using the Antoine equation, which relates the vapor pressure to temperature using three fitted parameters, A, B, and C.

$$ln\, P_{sat} = A - \frac{B}{T - C} \qquad (4.8)$$

Where:

P_{sat} is the vapor pressure of ethanol, *kPa;*

T is the temperature, *°C;*

A, B, and C are the coefficients of the Antoine equation *16.8958*, *3795.17,* and *230.918,* respectively, valid for the temperature range between *3 °C to 96 °C* (PATIENCE, 2013, p. 127).

4.2.4.2 Specific heat capacity

The specific heat capacity of pure ethanol was adapted from Pederson et al. (1975) and is given by Equations (4.9) and (4.10) according to the temperature range.

$$cp = 2.1389 + 0.01167 \cdot T \quad (range\ T = 25°C\ to\ 75°C) \qquad (4.9)$$

$$cp = 2.27636 + 0.007779 \cdot T + 0.000041 \cdot T^2 \quad (range\ T = -99°C\ to\ 25°C) \qquad (4.10)$$

Where:

T is the temperature, *°C;*

cp is the specific heat capacity *kJ/(kg·K).*

4.2.4.3 Ethanol/water equilibrium

Alcoholic fluids (such as fermented wine) were considered to be composed only of ethanol and water, i.e., neglecting other molecules. The equilibrium of ethanol and water is represented by Equation (4.11) which takes into account the activity coefficient; the gas phase was considered as an ideal gas.

$$y_i = \frac{x_i \cdot \gamma_i \cdot P_{sat,i}}{P} \qquad (4.11)$$

Where:

y_i is the mole fraction of the component *'i'* in the vapor phase;

x_i is the mole fraction of the component *'i'* in the liquid phase;

P is the pressure (bar);

$P_{sat,i}$ is the vapor pressure of the component 'i' (bar);

γ_i is the activity coefficient of the component *'i'* obtained by the UNIQUAC method according to Equations (4.12 - 4.23).

$$\ln \gamma_1 = \ln\left(\frac{\phi_1}{x_1}\right) + \frac{z}{2}\cdot q_1 \cdot \ln\left(\frac{\theta_1}{\phi_1}\right) + \phi_2\left(\ell_1 - \frac{r_1}{r_2}\ell_2\right) - q'_1 \cdot \ln(\theta_1' + \theta_2' \cdot \tau_{21}) + \\ + \theta_2' \cdot q'_1 \cdot \left(\frac{\tau_{21}}{\theta_1' + \theta_2' \cdot \tau_{21}} - \frac{\tau_{12}}{\theta_2' + \theta_1' \cdot \tau_{12}}\right) \qquad (4.12)$$

$$\ln \gamma_2 = \ln\left(\frac{\phi_2}{x_2}\right) + \frac{z}{2}\cdot q_2 \cdot \ln\left(\frac{\theta_2}{\phi_2}\right) + \phi_1\left(\ell_2 - \frac{r_2}{r_1}\ell_1\right) - - q'_2 \cdot \ln(\theta_2' + \theta_1' \cdot \tau_{12}) + \\ + \theta_1' \cdot q'_2 \cdot \left(\frac{\tau_{12}}{\theta_2' + \theta_1' \cdot \tau_{12}} - \frac{\tau_{21}}{\theta_1' + \theta_2' \cdot \tau_{21}}\right) \qquad (4.13)$$

$$\phi_1 = \frac{x_1 \cdot r_1}{x_1 \cdot r_1 + x_2 \cdot r_2} \qquad (4.14)$$

$$\phi_2 = \frac{x_2 \cdot r_2}{x_1 \cdot r_1 + x_2 \cdot r_2} \qquad (4.15)$$

$$\ell_1 = \frac{z}{2}\cdot(r_1 - q_1) - (r_1 - 1) \qquad (4.16)$$

$$\ell_2 = \frac{z}{2}\cdot(r_2 - q_2) - (r_2 - 1) \qquad (4.17)$$

$$\theta_1 = \frac{x_1 \cdot q_1}{x_1 \cdot q_1 + x_2 \cdot q_2} \qquad (4.18)$$

$$\theta_2 = \frac{x_2 \cdot q_2}{x_1 \cdot q_1 + x_2 \cdot q_2} \qquad (4.19)$$

$$\theta_1' = \frac{x_1 \cdot q'_1}{x_1 \cdot q'_1 + x_2 \cdot q'_2} \qquad (4.20)$$

$$\theta_2' = \frac{x_2 \cdot q'_2}{x_1 \cdot q'_1 + x_2 \cdot q'_2} \qquad (4.21)$$

$$ln(\tau_{21}) = -\frac{\Delta u_{21}}{R \cdot T} \qquad (4.22)$$

$$ln(\tau_{12}) = -\frac{\Delta u_{12}}{R \cdot T} \qquad (4.23)$$

Where the subindex *'1'* means ethanol and *'2'* means water. The parameters used in the above equations are from Poling et al. (2004-) presented in Table 6.

Table 6 - Uniquac parameters

Parameter	Value
r_1	2.1055
r_2	0.9200
q_1	1.9720
q_2	1.4000
q'_1	0.92
q'_2	1,00
Δu_{12}	1525 J/mol
Δu_{21}	1000 J/mol

4.3 General unit operation

Some unit operations may be used many times in different areas. Their mathematical model is presented in this section. Most of these operations are not directly related to the main process that converts the feedstock into products, i.e. they are auxiliary to the main process, such as pumping, conveyor, and condenser.

4.3.1 Centrifugal Pump

The centrifugal pump is modeled to obtain the electrical power consumption. Equation (4.24) relates the mass flow rate and pressure to energy consumption.

$$ElPower = \frac{H \cdot g \cdot Q}{3600 \cdot \eta} \qquad (4.24)$$

Where:

$ElPower$ is the electric power consumption, kW;

g is gravity constant, $9.81 m/s^2$;

Q is the mass flow rate, ton/h;

H is the pump head in, m;

η is the pump efficiency.

4.3.2 Vacuum pump

Vacuum pumps are modeled to obtain the electrical power consumption and the water consumption of the seal. The power consumption of the liquid-ring vacuum pumps is obtained using Equation (4.25). (HEI STANDARDS, 2016)

$$ElPower = 21.4 \cdot \left(\frac{m}{P}\right)^{0.924} \quad (4.25)$$

Where:

$ElPower$ is the electric power consumption, kW;

m is the airflow rate, kg/h;

P is the absolute operating pressure of the system, $mmHg$.

The water consumption of the seal is obtained using Equation (4.26). The Nash vacuum pump operation manual (NASH, 2017) shows a linear relationship between water and airflow rate; Equation (4.26) is a linear regression of these data values.

$$SealWater = 0.0095 \cdot m \quad (4.26)$$

Where:

$SealWater$ is the water flow rate, $tonne/h$;

m is the airflow rate, kg/h.

4.3.3 Rubber belt conveyor

Rubber belt conveyors are modeled to obtain the electrical power consumption. The power absorbed by the rubber belt conveyor is obtained by Equation (4.27) (FAÇO, 1995), which consists of calculating four terms (Fv, Fg, $N1$, and Nh) as described hereafter.

$$ElPower = (Fv + Fg) \cdot u + (N1 + Nh) \quad (4.27)$$

Where:

Fv is the force necessary to move the empty belt and is given by Equation (4.28);

$$Fv = 2 \cdot w + 0.008203 \cdot L - 0.5705 \quad (4.28)$$

Fg is the force necessary to overcome friction to the sidewall and is given by Equation (4.29);

$$Fg = 0.1385 \cdot L - 0.2133 \quad (4.29)$$

$N1$ is the power to overcome friction caused by the material conveyed with the rolls and is given by Equation (4.30);

$$N1 = C \cdot \frac{0.1302}{100} \cdot L^{0.5797} \quad (4.30)$$

Nh is the power to move the material at height h and it is given by Equation (4.31);

$$Nh = \frac{1000 \cdot C \cdot g \cdot h}{3600} \quad (4.31)$$

w is the width of the conveyor, m;
L is the length of the conveyor, m;
h is the height difference (inlet to outlet) of the conveyor, m;
C is the load, ton/h;
u is the speed of the conveyor, m/s;
g is the gravity constant, $9.81\ m^2/s$;
$ElPower$ is the electric power consumption, kW.

4.3.4 Barometric condenser

Barometric condensers are modeled to obtain the cooling water flow rate necessary to condense the steam. The condenser is responsible for maintaining the vacuum pressure in the last evaporation effect of multiple-effect evaporation, or inside the vacuum pan of the sugar crystalization. The water rate is obtained from the energy and mass balances around the condenser, as shown schematically in Figure 9. Equation (4.32) is the energy balance, Equation (4.33) is the mass balance, and Equation (4.34) is the parametric equation. The parameter in this equation is the ‘Approach', which is the temperature difference between

steam and the return cooling water (Hot Water). This parameter depends on the internal construction design such as baffles and nozzles; thus, it is usually given by the supplier or the device designer. A typical approach value of a well-designed barometric condenser is between 10 and 20 ° C.

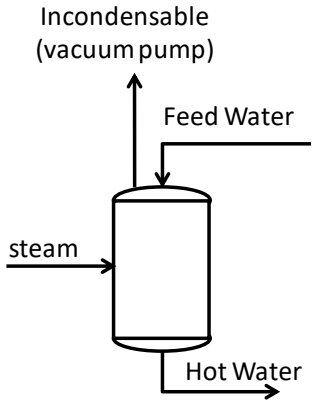

Figure 9 - Schematic flow diagram of a condenser

$$m_v \cdot h_v + m_{w,in} \cdot cp \cdot T_{in} = m_{w,out} \cdot cp \cdot T_{out} \qquad (4.32)$$

$$m_v + m_w = m_{w,out} \qquad (4.33)$$

$$Approach = T_v - T_{out} \qquad (4.34)$$

where:

m_v is the flow rate of steam, t/h;

H_v is the enthalpy of steam, kJ/kg;

$m_{w,in}$ is the flow rate of the feed cooling water, t/h;

$m_{w,out}$ is the flow rate of the returning cooling water, t/h;

cp is the specific heat capacity, $kJ/(kg \cdot K)$;

T_{in} is the temperature of the feed cooling water, $°C$;

T_{out} is the temperature of the return cooling water, $°C$;

T_v is the steam temperature, $°C$.

4.4 Cane reception and preparation

This is the process in which sugarcane is fed into the industrial process; in addition, sugarcane is prepared for the extraction process by reducing it into small pieces and rupturing the sugar-bearing cells to facilitate the extraction of the juice. Size reduction is generally achieved by using rotating-knife choppers and swing-hammer shredders on the steel slat conveyor. In the case of mechanically harvested, the billeted cane can be fed into a shredder without any knifing. The preparation performance is measured by the “preparation index”. Unfortunately, measuring the degree of cane preparation is difficult and existing methods are not always reliable (REIN, 2007, p. 81).

The aim of modeling this area is to obtain the power consumption of each device. Cane preparation devices can use more than 25% of total industrial power requirements (REIN, 2007, p. 79). A simple arrangement frequently used by Brazilian industries is shown in Figure 10. It comprises a knife type COP-8 and a light-duty shredder type COP-5. This configuration yields a preparation index of about 85 %, which is quite suitable for milling. Different configurations allow the industry to obtain different preparation indexes with different power consumption. The required preparation index depends on the extraction step, which can be milling or diffuser: the diffuser requires a higher preparation index. The results, shown in this work, focus on the configuration described in Figure 10; thus, the mathematical model is divided into 5 steps. They are the feeder table, steel slat conveyor, rubber belt conveyor, shredder, and knifing. The following subsections will describe the mathematical model and the parameters used in each step.

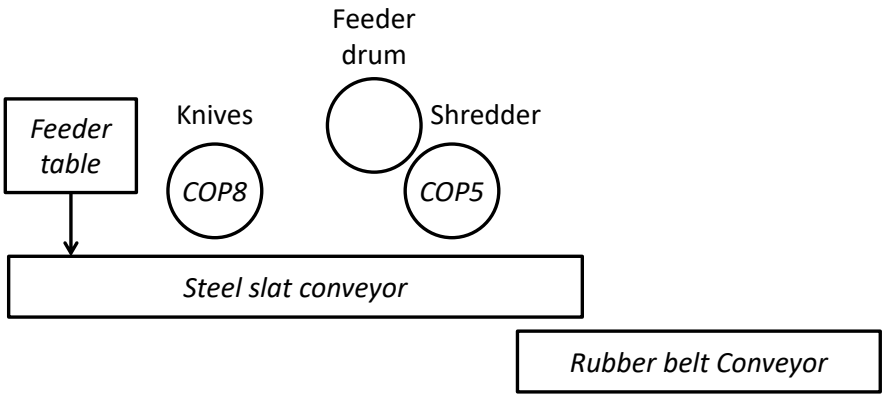

Figure 10 - Schematic sugarcane preparation and conveyor system for a mil extraction process

4.4.1 Feeder table

The cane is discharged from large vehicles into an elevated feed conveyor, namely, 'Feeder table'. A commonly used system, particularly with cane truck vehicles, involves lifting the truck trailer on a feeder table using a crane. The power duty requirement is typically 0.4 to $0.6\ kW.h$ per tonne of cane (REIN, 2007, p. 66).

4.4.2 Steel Slat

The mean power absorbed by the steel slat cane carrier consists of two terms: The power necessary to overcome friction; and the power necessary to carry the cane and the chain (HUGOT, 1960, p. 24). The necessary chain pull force can be calculated from the mass of the chain plus the mass of the material being conveyed and from the frictional forces as shown by Equation (4.35) (REIN, 2007, p. 72). Thus, the power required can be calculated from the speed and force as shown by Equation (4.36).

$$F = \frac{g \cdot (m_{cane} + m_{chain}) \cdot (L \cdot \mu + h)}{1000} \qquad (4.35)$$

$$Power = F \cdot u \qquad (4.36)$$

Where:

F is the force, kN;

$Power$ is the power, kW;

g is the gravity constant adopted $9.81\ m^2/s$;

m_{cane} is the mass of cane per meter of chain, kg/m, obtained using Equation (4.37);

$$m_{cane} = d \cdot w \cdot h \qquad (4.37)$$

m_{chain} is the mass of the chain plus the mass of the slats, kg/m, obtained using Equation (4.38).;

$$m_{chain} = 2 \cdot (120 \cdot 2 + w \cdot 120) \quad (4.38)$$

w is the width of the chain the same width of the first mill tandem, m;

L is the chain length adopted 45 m, for the results shown in this report, m;

μ is the friction coefficient between 0.15 and 0.30;

h is the average height of the cane on the conveyor, m;

u is the chain speed, m/s calculated according to the sugarcane flow rate in Equation (4.39);

$$u = \frac{1000_x Cane}{3600_x w_x h_x d} \quad (4.39)$$

d is the density of billeted cane in conveyor about $350\ kg/m^3$;

$Cane$ is the amount of sugarcane processed, t/h.

4.4.3 Rubber belt conveyor

The power requirement for the rubber belt conveyor is calculated as described in Section 4.3.3

4.4.4 Shredder and knifing

To obtain the power consumption, this model uses a specific power consumption in kW per tonne of fiber for each device, as shown in Table 7. These specific power consumptions were obtained from different sugarcane mills. Many equipment configurations are possible (HUGOT, 1960, p. 73; REIN, 2007, p. 75). Table 7 also shows some other types of equipment used in cane preparation and their specific power consumption.

Table 7 - Power consumption in cane preparation

	Power consumption (kW/tfh)				
	Type	Cosan*	Dedini*	CTC*	**
Leveler	COP-8	15	16	14	-
	COP-9	15	16	14	-
	FOL	14	13	-	-
	SD-3	14	10	14	-
Knives	COP-8	28	28	28	25.76
	COP-9	28	28	28	-
	FOL	28	24	-	-
	SD-3	24	20	24	-
Feeder	FOL	20	13	-	-
	SD-3	20	10	20	20
Shredder	DH-1	44	36	44	-
	TONGAAT	44	40	44	-
	MAXCELL	44	44	44	-
	FIVES-LILLE	68	-	68	-
	COP-5	28	26	28	22.69
	COP-6	28	26	28	-

Source: * (DELFINI, 2013) ** industrial data

4.4.5 Others power requirements

The electric power is also consumed by small devices such as the cleaning water pump, instruments, electric panels, lubrication systems, illumination systems, etc. These devices slightly change the overall energy duty in this area, and this energy is considered using the specific parameter of 0.01 kW per tonne of cane.

4.5 Extraction

This is the area in which the juice is extracted from sugarcane. The aim is to separate fiber, in the solid fraction, from sugars in the liquid fraction. Thus, in this area the flow rate and composition of juice and bagasse are obtained as a function of the sugarcane fed. Additionally, the power required for the extraction process is calculated.

The extraction process is typically carried out by the mill or diffuser; for sugarcane juice extraction, there are many studies comparing milling and diffuser (HUGOT, 1960; REIN, 2007, 1995). Milling tandem extraction allows the industry to separate absolute juice from draft juice. The absolute juice extracted in the first mill stages has characteristics that are more

appropriate for sugar production, while the mixed juice, extracted in the following stages, has a higher concentration of other substances present in the cane cell wall, such as pentoses, polysaccharides, phenols, colorants, etc. It can be used for ethanol production without hindering fermentation. In addition, part of such contaminant substances, such as starch and dextrose, can be converted into ethanol. (REIN, 2007). The diffuser, instead of producing two streams (absolute and draft juice), produces a single stream, named as mixed juice. The positive point of the diffuser is the extraction efficiency, which is 2 to 3% higher than the milling (MODESTO; ENSINAS; NEBRA, 2005). The drawbacks are the higher cost, the higher moisture in bagasse, and the higher water imbibition.

In Brazil, the preference has been for the use of mills, which consist of a set of four to six mill units. A new extraction technology called 'Hydrodynamic Extraction' or 'Rivière Juice Extractor' is being developed and aims to achieve the same level of diffuser extraction using less imbibition water with a lower installation and maintenance cost compared to both technologies (WALSH, 1998). However, to our knowledge, there is no commercial plant using this technology. In this work, only the milling process has been modeled.

The mathematical model is divided into four main steps: milling, screening, pumping, and conveying. These steps are interconnected, as shown in Figure 11. The recycling flow rate is calculated using the fixed-point interaction method, in which the first guess of the recycling flow is zero. The following sections describe the mathematical model and the parameters used in each step. The results of this simulation are the flow rate of juice and bagasse; the concentrations of sugar and solids; the amount of water used for imbibition; and the power required to extract the juice. Sugarcane flow is the input variable.

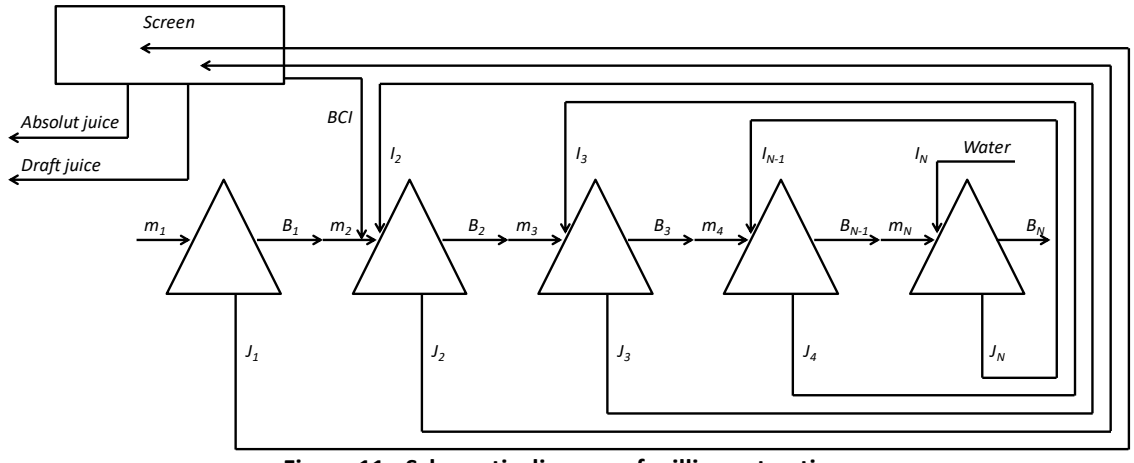

Figure 11 - Schematic diagram of milling extraction

4.5.1 Mil Tandem

Each mill tandem is modeled to obtain the output streams, bagasse and juice, as a function of the feed streams, which can be bagasse from the previous tandem or sugarcane for the first one. Additionally, the power consumed by the milling process is calculated.

4.5.1.1 Mass and energy balance

Figure 12 shows the streams from a single-mill tandem. The model used in each mill is based on the overall mass balance as described in Equation (4.40). Since sugarcane can be divided into three main parts, which are water, soluble solids and fiber, each stream composition are described by Equations (4.41 – 4.44); the mass balance around each component for each stream is obtained by Equations (4.45 – 4.47). The solid stream from the i-th tandem becomes the feed stream to the tandem i+1 as shown by Equation (4.48); the liquid stream from the i-th tandem becomes the imbibition stream in the tandem i-1 (Equation 4.49).

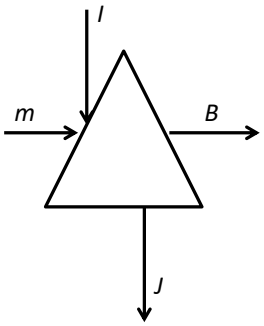

Figure 12 - Schematic diagram of the mass inlet and outlet milling unit tandem

$$m_i + I_i = J_i + B_i \qquad i=1...n \qquad (4.40)$$

$$m_i = m_i \cdot f_i + m_i \cdot b_i + m_i \cdot w_i \qquad i=1...n \qquad (4.41)$$

$$I_i = I_i \cdot f_i + I_i \cdot b_i + I_i \cdot w_i \qquad i=1...n \qquad (4.42)$$

$$J_i = J_i \cdot f_i + J_i \cdot b_i + J_i \cdot w_i \qquad i=1...n \qquad (4.43)$$

$$B_i = B_i \cdot f_i + B_i \cdot b_i + B_i \cdot w_i \qquad i=1...n \qquad (4.44)$$

$$m_i \cdot f_i + I_i \cdot f_i = J_i \cdot f_i + B_i \cdot f_i \qquad i=1...n \qquad (4.45)$$

$$m_i \cdot b_i + I_i \cdot b_i = J_i \cdot b_i + B_i \cdot b_i \qquad i=1...n \qquad (4.46)$$

$$m_i \cdot w_i + I_i \cdot w_i = J_i \cdot w_i + B_i \cdot w_i \qquad i=1...n \qquad (4.47)$$

$$m_{i+1} = B_i \qquad i=1...n-1 \qquad (4.48)$$

$$I_{i-1} = J_i \qquad i=3...n \qquad (4.49)$$

Where:

m is the mass that enters into the ith tandem, *tonne/h;*

I is the imbibition of water or juice in the ith tandem, *tonne/h;*

J is the juice extracted from the ith tandem, *tonne/h;*

B is the bagasse leaving the ith tandem, *tonne/h;*

f is the fiber content in the stream, *kg of fiber/kg;*

b is the brix content in the stream, *kg of soluble solids/kg;*

w is the water content in the stream*; kg of water/kg;*

fiber is the sugarcane fiber, *tonne/h*.

To solve this set of equations, the sugarcane flow rate, m_1, and its composition, f_1, b_1, and w_1, are known, as well as the imbibition of water, I_n. Additionally, three parametric equations were added based on the following parameters: Fiber ratio in Bagasse, *Bfib*; Extraction Efficiency Ex_{ef}; Separation Efficiency Sep_{Ef} as given by Equations (4.50–4.52).

$$Bfib_i = \frac{B_i \cdot f_i}{B_i} \qquad (4.50)$$

$$Ex_{ef,i} = \frac{J_i \cdot b_i}{m \cdot b_i} \qquad (4.51)$$

$$Sep_{Ef,\,i} = \frac{B_i \cdot f_i}{m_i \cdot f_i} \qquad (4.52)$$

Bfib is the ratio between insoluble material and Bagasse. Bagasse, after being subjected to a high-pressure squeeze, possesses a liquid fraction that is composed of water and brix (soluble solids). The amount of moisture in bagasse depends on the pressure applied by the roll to the sugarcane, where the higher the pressure, the lower the moisture. Data for the fiber bagasse parameter (Bfib) are shown in Table 8 derived from information provided by various sugar factories and published by the authors cited at the top of the table.

Table 8 – Ratio of fiber to bagasse (*Bfib*)

Bfib	(KENT, 2001)	(REIN, 2007)	(WIENESE, 1990)
1-st mill	0.30	0.3221	0.2971 - 0.3882
2-nd mill	0.36	0.3400	0.3008 - 0.4205
3-rd mill	0.41	0.3961	0.3046 - 0.4529
4-th mill	0.44	0.4358	0.3558 - 0.4852
5-th mill	0.47	0.4781	0.3504 - 0.5122
6-th mill	-	-	0.3774 - 0.6200
7-th mill	-	-	0.4800 - 0.4991

The extraction efficiency (Ex_{ef}) is the ratio of the soluble material (brix) between the juice and the brix in the inlet stream. Kent (2001) and Thaval (2012) used a similar parameter, however, named the 'imbibition coefficient'. Table 9 shows the coefficient values. A value greater than 1 means that the concentration of dissolved solids in the extracted juice is greater than the concentration of dissolved solids in the liquid part of the bagasse.

Table 9 – Ratio of brix between the juice and the inlet stream (Ex_{ef})

Extraction efficiency Ex_{ef}		
	(THAVAL, 2012)	(REIN, 2007)
1-st mill	1.04	0.10372
2-nd mill	0.87	0.9000
3-rd mill	0.67	0.8485
4-th mill	0.57	0.7561
5-th mill	0.57	0.6500

Separation efficiency (Sep_{Ef}) is the ratio of insoluble material between bagasse and the feed stream. During the milling process, the insoluble part (fiber) is separated from the liquid part (water and brix) by the backplate. However, part of the fiber leaves the mill tandem mixed with the juice (liquid part). Table 10 shows the parameters published by the authors cited at the top of the table.

Table 10 - The ratio of fiber between bagasse and the fed stream

Separation efficiency		
$SepEF$	(THAVAL, 2012)	(REIN, 2007)
1-st mill	0.918	0.8950
2-nd mill	0.9112	0.8950
3-rd mill	0.948	0.8950
4-th mill	0.9541	0.8950
5-th mill	0.9566	0.8950

Purity is the ratio between sucrose and soluble solids, as shown in Equation (4.53). The purity of the extracted juice is different from that of sugarcane. The extraction of sucrose is determined using an empirical equation proposed by Lionnet (1981), which correlates sucrose extraction from brix extraction based on juice purity and sugarcane purity. This equation was then published comprehensively by Wienese (1990) and is given by Equation (4.54).

$$Purity = \frac{sucrose}{soluble\ solids\ or\ brix} \qquad (4.53)$$

$$Sucrose\ extraction = \sqrt{1919 + 187.6 \cdot BrixExtraction} - \sqrt{1919} \qquad (4.54)$$

In terms of the variables adopted in this model the equation becomes Equation (4.55).

$$\frac{Sucrose\ out}{Sucrose\ in} = \sqrt{1919 + 187.6 \, x \, \frac{J_i \cdot b_i}{m_i \cdot b_i + I_i \cdot b_i}} - \sqrt{1919} \qquad (4.55)$$

Lionnet also fitted the correlation from Equation (4.55) to describe sucrose extraction for different milling tandem manufacturers given by Equations (4.56) and (4.57).

$$Sucrose\ extraction = \sqrt{871 + 159.49 \, x \, BrixExtraction} - \sqrt{871} \qquad (4.56)$$

$$Sucrose\ extraction = \sqrt{1080 + 166.39 \, x \, BrixExtraction} - \sqrt{1080} \qquad (4.57)$$

The same correlation was tested using industrial data from a Brazilian sugar mill tandem, and the parameters were then adjusted according to Equation (4.58), which was used in this work.

$$Sucrose\ extraction = \sqrt{623 + 234{,}44 \, x \, BrixExtraction} - \sqrt{623} \qquad (4.58)$$

The temperature of the juice and bagasse is determined using the energy balance based on the flow chart shown schematically in Figure 12 and calculated using Equation (4.59). The specific heat capacity of each component is described in Section 4.2.

$$Em_{in,i} + EI_{in,i} = EJ_{out,i} + EB_{out,i} - E_{loss} \qquad (4.59)$$

Where:

$Em_{in,i}$ is the enthalpy of sugarcane or bagasse entering the tandem "i", *kJ;*

$EI_{in,i}$ is the enthalpy of water or juice imbibition entering the tandem "i", *kJ;*

$EJ_{out,i}$ is the enthalpy of the juice extracted from the tandem "i", *kJ;*

$EB_{out,i}$ is the enthalpy of the bagasse leaving the tandem "i", *kJ;*

E_{loss} is the energy lost as heat to surrounding "i" , *kJ.*

The term E_{loss}, given in Equation (4.60), is the energy released to the surrounding. It is used to adjust the temperature of bagasse and juice measured on-site. However, a slight loss is observed, sometimes rather difficult to detect, and often negligible. The results of the simulation in this work have considered that λ is 0.01%.

$$E_{loss} = \lambda \cdot (Em_{in,i} + EI_{in,i}) \qquad (4.60)$$

Where:

λ is the ratio of between the energy lost to the surrounding and the fed stream energy.

The imbibition consists of adding water before the last mill and returning the juice obtained from the last mill as imbibitions before the second-last mill, then the juice from the latter mill before the next proceeding, and so on, as shown in Figure 13. There is no imbibition in the first mill. The juice from the second mill (draft juice) and the first mill (absolute juice) go to the next process step. Figure 13 shows a set of five tandems as an example.

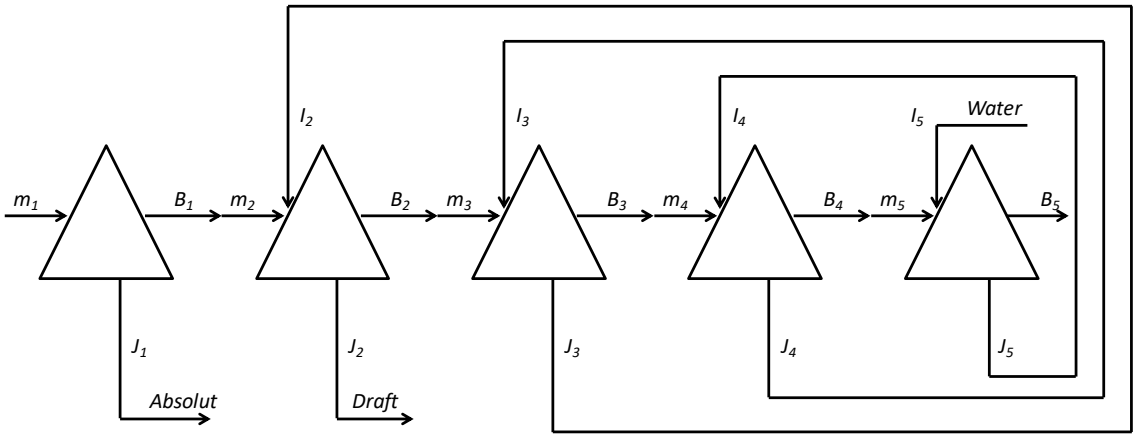

Figure 13 - Schematic diagram of milling train

The flow rate of water imbibition is calculated using the parametric equation in which Ir is the ratio of water to fiber (Equation 4.61). This parameter ranges from 250 to $280\ \%$ on fiber (REIN, 2007, p. 130).

$$I_n = Ir \cdot fiber \qquad (4.61)$$

Where:

I_n is the water flow rate used for mill imbibition, $tonne/h$;

Ir is the water imbibition ratio to fiber;

$fiber$ is the sugarcane fiber, $tonne/h$.

4.5.1.2 Power

The power absorbed by a milling process depends on many aspects (REIN, 2007, p. 139), such as crushing rate, mill speed, mill configuration, friction loss power, and mill feed device. The first and last mills usually absorb a power in the order of 10 to 13 kW per tonne of fiber, and the intermediate mills are in the range of 8 to 11 kW per tonne of fiber. Various methods have been proposed to calculate the milling power consumption; some are complex and contain several parameters that are not easy to determine. (HUGOT, 1960, p. 229) In this work, a simplified equation given by Equation (4.62) is used (HUGOT, 1960, p. 234; REIN, 2007, p. 119).

$$Power = k \cdot F \cdot n \cdot D \qquad (4.62)$$

Where:

$Power$ is the power absorbed by the mill in kW;

k is a proportionality factor 0.149 for first and 0.134 for further mill tandem (CASTRO; ANDRADE, 2007);

n is the rotation speed, s-1;

D is the roll diameter, inch;

F is the hydraulic force, kgf ;

The hydraulic force, F, is given by Equation (4.63).

$$F = P \cdot S \qquad (4.63)$$

Where:

P is the pressure, kgf/cm^2. Table 11 shows some typical pressure values (CASTRO; ANDRADE, 2007);

S is the area, cm^2;

The area is calculated using Equation (4.64).

$$S = \frac{\alpha}{360} \cdot \pi \cdot D^2 \cdot L \qquad (4.64)$$

Where:

D is the diameter of the roll, *cm;*

L is the length of the roll, *cm;*

α is the angle shown inFigure 14; it is about 72°.

Table 11 - Mill gearing

Tandem	P Pressure on roll kgf/cm²	η Electric drive overall efficiency	η Turbine drive overall efficiency
1-st	250	72% - 92%	51%
2-nd	210	72% - 92%	51%
3-rd	220	72% - 92%	51%
4-th	230	72% - 92%	51%
5-th	240	72% - 92%	51%
6-th	250	72% - 92%	51%

Adapted from Hugot (1960, p. 174)

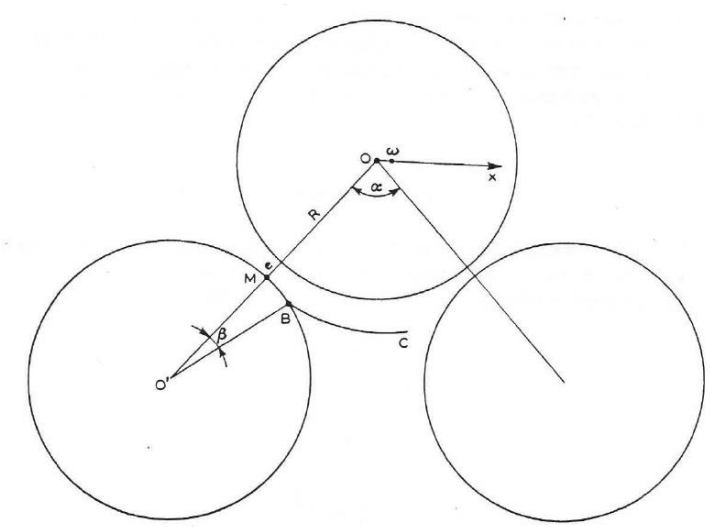

Figure 14 - Mill roll showing wedges for adjustment of rollers
Source: Hugot (1960, p. 218)

In a mill driven by an electric motor, the electric power consumption is calculated using Equation (4.65). Table 11 also shows the typical efficiency (η) for electric motors (REIN, 2007, p. 122).

$$ElPower = \frac{Power}{\eta} \qquad (4.65)$$

In a mill driven by a steam turbine, the steam consumption is calculated using Equation (4.66). Table 11 also shows the typical efficiency (η) for turbines (REIN, 2007, p. 122).

$$Q = \frac{Power}{(H_{vap,in} - H_{vap,out}) \cdot \eta} \qquad (4.66)$$

Where:

$ElPower$ is the electric power used to drive the mill, kW;

H is the enthalpy of steam in and out of the turbine, kJ/kg;

Q is the steam flow to drive the turbine, kg/s;

η is the overall efficiency.

The mill rotation (n) is calculated using Equation (4.67), which is given by Hugot (1986, p. 191). The extraction efficiency depends on the rotation of the mill, the diameter, and the length of the roll. Thus, for a tandem mill, the extraction efficiency varies with the amount of entering material. For technical reasons, the rotation speed shall be less than $7\ rpm$.

$$C = \frac{47.12 \cdot D^2 \cdot L \cdot n}{\frac{0.97}{0.52} - 1.75 \cdot f} \qquad (4.67)$$

Where:

C is the mill capacity (sugarcane flow rate), t/h;

D is the roll diameter, m;

L is the roll length, m;

n is the rotation speed, rpm;

f is the fiber ratio in cane.

4.5.2 Drag conveyor

Drag conveyors are intermediate carriers that move the bagasse from one mill to the next mill feed duct, namely ‘Chute Donelly’, as shown in Figure 15. The aim of modeling this operation is to obtain the power necessary to convey the bagasse given by Equations (4.68 – 4.72).

$$ElPower = F \cdot u \tag{4.68}$$

$$u = \frac{B}{3600 \cdot w \cdot d \cdot hbed} \tag{4.69}$$

$$F = \frac{g \cdot (m_{cane} + m_{chain}) \cdot (L \cdot m + h)}{1000} \tag{4.70}$$

$$m_{chain} = SPW \cdot w \cdot 2 \tag{4.71}$$

$$m_{bagasse} = \frac{B}{3600 \cdot u} \tag{4.72}$$

Where:

u is the conveyor speed, m/s;

B is the mass flow rate of bagasse, $tonne/h$;

d is the density of bagasse, $0.15\ t/m^3$;

w is the width of the conveyor, m (the same width of the mill);

$hbed$ is the estimated height of the bagasse bed, typically $0.4\ m$;

F is the force to move the chain and bagasse, kN;

L is the length of the conveyor, m;

h is the height of the conveyor m;

μ is the friction factor;

m_{chain} is the mass of the chain per meter long, kg/m;

SPW is the specific weight of the chain, typically $25\ Kg/m^2$;

$m_{bagasse}$ is the mass of bagasse per meter long of conveyor, kg/m.

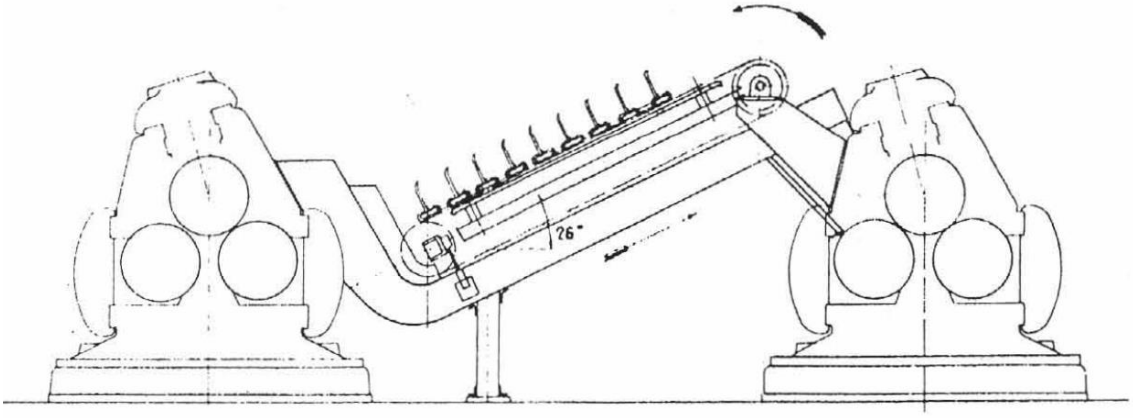

Figure 15 - Schematic drag conveyor intermediate carrier
Source: Hugot (1960, p. 218)

4.5.3 Screen

The juice from the first and second tandems is then transferred to a screen to remove the large-size fiber. As shown in Figure 16, the solid stream named Bagacillo (BCI_{out}) returns to the second tandem mill. The aim is to obtain the fiber content in the absolute juice, the filtered juice, and the Bagacilo as a function of the fed juice. The power absorbed by the screen is also calculated.

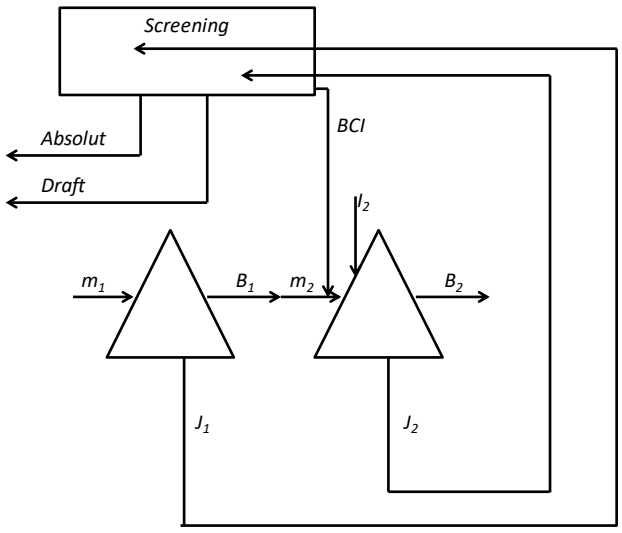

Figure 16 - Schematic flow diagram of a Juice screen process

4.5.3.1 Mass balance

The fiber content in the Bagacillo (fib) ranges between 8 and 12% (KENT, 2001), and the screen separation efficiency is approximately $92{,}3\%$ (THAVAL, 2012). This parameter may depend on the screen mesh aperture. Industrial data (REIN, 2007, p. 191) show that about 36% of the dirt in the cane is washed into the juice and, consequently, the amount of fiber in

the juice stream is given by Equation (4.73). Then, the mass balance equation around the screen is used to determine the juice and Bagacilo flow rate, and the fiber content in each stream according to Equations (4.74–4.77).

$$Jf_{out} = 0.36 \; _x \, Dirt_{cane} \qquad (4.73)$$

$$J_{in} = J_{out} + BCI_{out} \qquad (4.74)$$

$$J_{in} \cdot f = J_{out} \cdot f + BCI_{out} \cdot f \qquad (4.75)$$

$$EfSc = Jf_{in} \, / \, BCIf_{out} \qquad (4.76)$$

$$fib = BCIf_{out} \, / \, BCI \qquad (4.77)$$

Where:

J_{in} is the juice that enters the screening, *tonne/h*; (can be J_1 or J_2 see Figure 16)

f is the fiber content in the stream, *kg of fiber/kg;*

J_{out} is the screened juice, *tonne/h* (absolute or draft);

BCI_{out} is the fiber-rich stream, *tonne/h*;

4.5.3.2 Power

These screen systems typically have the following characteristics: *1.6 m* diameter, up to *4.5 m* lengths, and *0.5 mm* screen aperture for an industry that processes about *500 tonne/h* of cane (REIN, 2007, p. 191). The electric power consumed per device with these characteristics is 7.25 kW. Additionally, the electric power consumed in the screening process is the pumping of the raw juice, as given by Equation (4.24) described in Section 4.3.1.

4.6 Juice separation

This is the area in which the juice from the extraction area is separated into two streams: ethanol juice and/or sugar juice. As aforementioned, the milling extraction process allows the separation of the absolute juice from the draft juice. The aim of this area is to define whether the absolute juice is separated from the draft juice, and the amount of juice diverted to produce sugar or ethanol as shown in Figure 17. If the absolute juice is not separated from the draft juice, the juice becomes the mixed juice, which is the sum of the absolute and the draft juice. This model uses a discrete decision variable "*juice separation*" as follows:

$$JuiceSeparation = \begin{matrix} 1 => yes \\ 0 => no \end{matrix} \qquad (78)$$

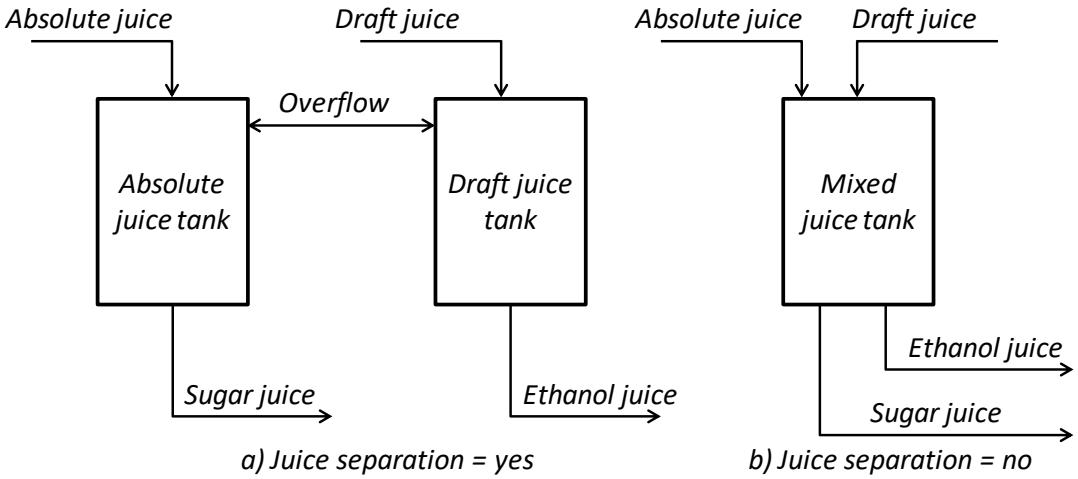

Figure 17 - Juice separation scheme

The decision to produce sugar or ethanol is made using the input variable *Mix*. This consists of a variable in which the extracted sucrose is diverted to produce ethanol or sugar and is given by Equation (4.79). *Mix* is a variable ranging from *0* to *1,* where *0* means that there is only ethanol and *1* means that there is only sugar juice. Based on this variable, the ethanol juice and the sugar juice stream are obtained as shown by Equations (4.80 – 4.82).

$$Mix = \frac{Sucrose\ in\ sugar\ juice\ stream}{Total\ extracted\ sucrose} = \frac{P \cdot Brix}{(P \cdot Brix)_{total}} \qquad (4.79)$$

$$SugarJuice = \frac{Mix\ (AbsJuice \cdot P \cdot Brix + DraftJuice \cdot P \cdot Brix)}{(P \cdot Brix)_{total}} \cdot JuiceSeparation + \frac{Mix\ (AbsJuice + DraftJuice)}{(P \cdot Brix)_{total}} \cdot (1 - JuiceSeparation) \quad (4.80)$$

$$Overflow = AbsJuice - SugarJuice \quad (4.81)$$

$$EthanolJuice = AbsJuice + DraftJuice - SugarJuice \quad (4.82)$$

Where:

P is the juice purity, *kg of sucrose/ kg of solids*;

Brix is the concentration of soluble solids, *kg of solids/kg of solution.*

4.7 Regenerative Heat Exchange

A regenerative heat exchanger, or more commonly a regenerator, is a type of heat exchanger where heat from a hot fluid is transferred to a cold fluid. To accomplish this, the hot fluid is brought into contact with the cold fluid in a counterflow plate heat exchanger. Figure 18 summarizes this process.

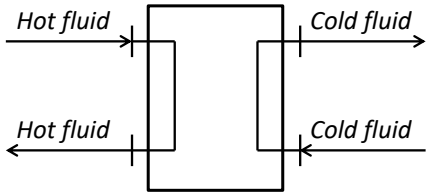

Figure 18 - Regenerative heat exchange scheme

4.7.1 Mass and energy balance

The model that describes this process is given by Equations (4.83 – 4.87). The model consists of specifying the overall heat transfer coefficient U and the area·A, then obtaining the temperature of the hot and cold fluid that leaves the device and the total heat exchanged Q.

$$\delta = m_{cold} \cdot cp_{cold} \cdot m_{hot} \cdot cp_{hot} \quad (4.83)$$

$$\varepsilon = exp\left(\frac{U \cdot A}{m_{cold} \cdot cp_{cold}} - \frac{U \cdot A}{m_{cold} \cdot cp_{cold}}\right) \quad (4.84)$$

$$Q = \frac{\delta \cdot (\varepsilon - 1)\ (T_{in,hot} - T_{in,cold})}{\varepsilon \cdot m_{cold}\ cp_{cold} - m_{hot} \cdot cp_{hot}} \quad (4.85)$$

$$T_{out,\ hot} = T_{in,hot} - \frac{Q}{m_{hot} \cdot cp_{hot}} \quad (4.86)$$

$$T_{out,\ cold} = T_{in,cold} + \frac{Q}{m_{cold} \cdot cp_{cold}} \quad (4.87)$$

Where:

m_{fluid} is the fluid flow rate, hot or cold, $tonne/h$;

$T_{out,fluid}$ is the temperature of the fluid, hot or cold, leaving the regenerator, ^{o}C;

$T_{in,fluid}$ is the temperature of the fluid, hot or cold, entering to the regenerator, ^{o}C;

cp_{fluid} is the specific heat capacity of the fluid, $kJ/(kg \cdot K)$ (see Section 4.2.2.2);

Q is the total heat exchanged, kJ;

U is the overall heat transfer co-efficient, $kJ/(m^2 \cdot K)$;

A is the area of the heat exchange, m^2.

ε is the parameter used in Equation (4.85) obtained using Equation (4.84);

δ is the parameter used in Equation (4.85) obtained using Equation (4.83), $(kJ/(K \cdot h))^2$.

4.7.2 Power

The electric power consumed in this step is due to the pumping of the hot and cold fluid through the plate heat exchange; a pressure drop of 10-meters is adopted for each fluid. Thus, the electrical power consumption is calculated as described in Section 4.3.1.

4.8 Juice treatment

This is the area in which the juice is sterilized by heating and insoluble impurities are removed. This area is to obtain the flow rate of clear juice, filter cake, and flashed steam as a function of the raw juice and also to calculate the amount of steam, water, sulfur, and lime consumed. The juice treatment area consists of a set of unit operations such as the one shown in Figure 19 to Figure 21. Besides these three examples, many configurations are possible. In the case of a single juice treatment, depicted in Figure 19, only one product is produced: sugar or ethanol. In the case where sugar and ethanol are produced simultaneously, the treatment scheme is shown in Figure 20. In the case where both are produced and the amount of steam bled from the sugar juice evaporation is not enough to handle the steam demand of the process; it is necessary to also evaporate the ethanol juice; consequently, it is necessary to reheat (heater 5) the clear juice ethanol before entering the evaporation area as shown in Figure 21.

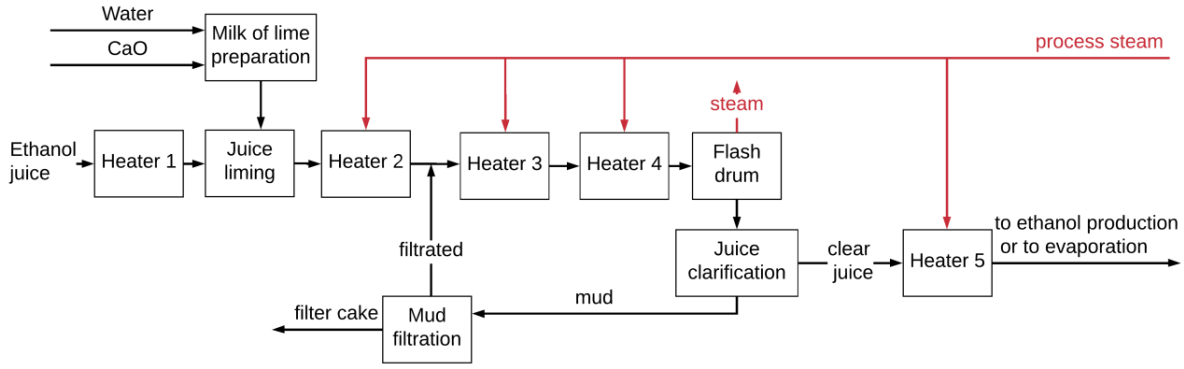

Figure 19 - Single juice treatment scheme (only ethanol is produced)

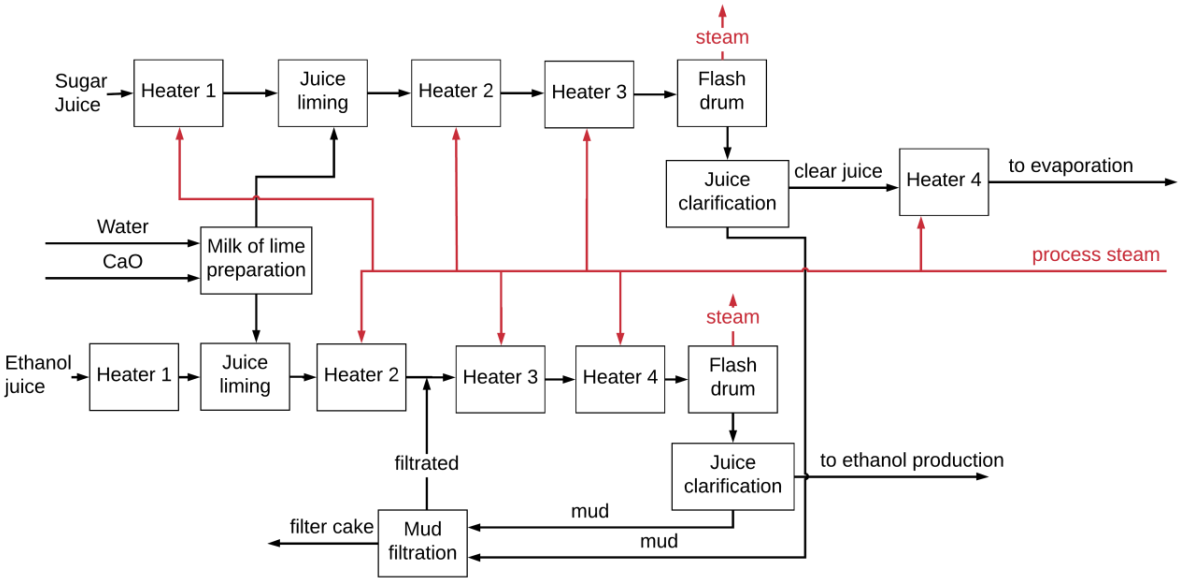

Figure 20 - Double juice treatment scheme without evaporation of ethanol juice

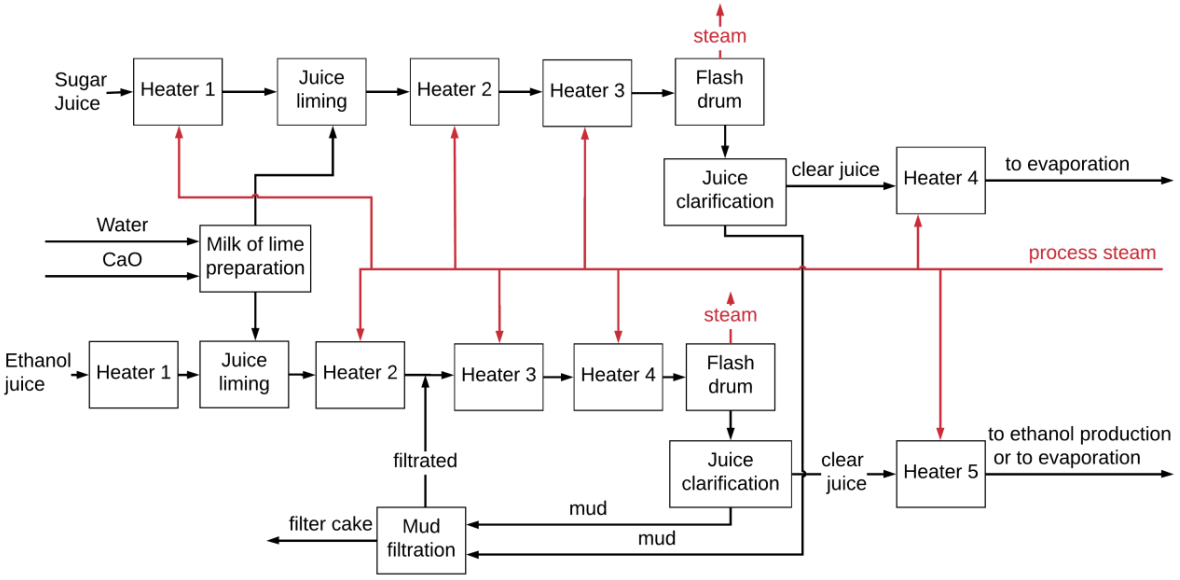

Figure 21 - Double juice treatment scheme

The recycling flow rate is calculated using the fixed-point interaction method, in which the first guess of the recycling flow is zero. The mathematical model is divided into six different steps. They are sulphitation, heating, clarification, filtration, liming, and flashing. The next sections describe the mathematical model and the parameters used in each step.

4.8.1 Sulfitation

Sulfitation is an auxiliary process to liming. The main reason for adding sulfite to the juice is to reduce the color of the sugar produced. It also helps to eliminate ferric slats that

have been formed by friction with the mill rolls or the iron scale detached from tanks and pipes (HUGOT, 1960, p. 407). Sulfur dioxide is a gas resulting from sulfur combustion. It is prepared from sulfur in an air-excess heating furnace. Contact with juice takes place in a column where juice descends returning to the tank while gas flows countercurrent.

4.8.1.1 Mass balance

Sulfur consumption is about 0.3 to 0.45 kg per tonne of sugarcane, which makes no difference in the overall juice flow rate, and therefore is neglected in the mass balance of the juice stream. However, it is considered to calculate the cost and greenhouse gas emission.

4.8.1.2 Power

The electricity demand in this process is mainly because the juice is pumped to the top of the sulfitation column. Consequently, the electrical power consumption is calculated as described in Section 4.3.1.

4.8.2 Liming and milk of lime preparation

Sugarcane juice has a pH of about 5.3 (REIN, 2007, p. 220), which is quite acidic. Consequently, before clarification, lime is used to adjust the pH to 7. The lime treatment forms a heavy precipitate of complex composition, part lighter and part heavier than the juice, which contains insoluble lime salts, coagulated albumin, and varying proportions of fats, waxes, and gums. The lime, $Ca(OH)_2$, is used in the form of milk of lime dosed into the juice pipe line as shown schematically in Figure 22. This model aims to obtain the amount of water and calcium added to the juice stream.

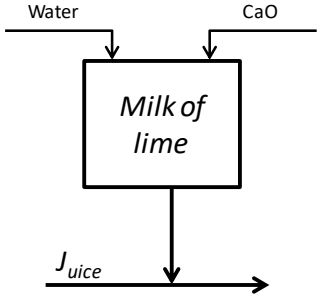

Figure 22 - Schematic flow diagram of a Milk of Lime preparation

4.8.2.1 Mass balance

The amount of milk of lime dosed is obtained using Equation (4.88), which uses a parameter named 'calcium saccharate concentration', which is the calcium hydroxide concentration necessary to adjust the pH to 7, by adding milk of lime to the juice. The milk of lime is obtained by mixing CaO with water. The amount of water used and the amount of milk prepared depends on the concentration of milk, $Ca(OH)_2$. Equation (4.89) calculates the amount of water. The literature recommends the use of calcium saccharate of about 0,075 g of $Ca(OH)_2$ per 100 g of juice (REIN, 2007, p. 221) at a concentration of 5 wt% $Ca(OH)_2$ in milk of lime. Therefore, Equation (4.90) provide the amount of CaO consumed by the industry.

$$Milk\ of\ lime\ (kg/h) = \frac{Calcium\ sacc.\ conc.(kg_{Ca(OH)2}/kg_{Juice})}{Milk\ of\ lime\ conc.(kg_{Ca(OH)2}/kg_{Milk})} \cdot (Juice\ (kg/h)) \quad (4.88)$$

$$Water = \frac{Ca(OH)_2}{Milk\ of\ lime\ conc.} \quad (4.89)$$

$$CaO = \frac{Milk\ of\ lime}{Milk\ of\ lime\ conc.} \quad (4.90)$$

4.8.2.2 Power

The electric power consumed in this step is due to the pumping of milk and the mixer on the tank where the reaction between lime and juice occurs. Therefore, the electrical consumption due to pumping is obtained as described in Section 4.3.1, and the power input by the mixer per unit of volume is 1.015 kW/m³. The tank volume is calculated considering a retention time of 10 minutes, which is the time necessary to promote the reaction between lime and juice.

4.8.3 Heating

The juice is heated to about 110 °C to promote the reaction between lime and juice, reduce the viscosity of the juice before clarification, and sterilize the juice from any microorganisms from the field. The heater uses saturated steam as shown schematically in Figure 23.

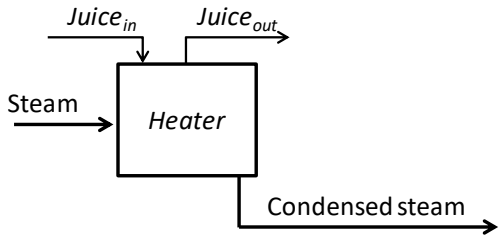

Figure 23 - Schematic flow diagram of a steam heat exchanger

4.8.3.1 Mass and energy balance

Steam from the first and second effects of the multiple-effect evaporator is used to heat the juice. The aim is to obtain the steam consumed, the temperature of the juice, and the heat exchanged as a function of the heating surface area as shown by Equations (4.91–4.93).

$$T_{out} = T_s - (T_s - T_{in}) \cdot exp\left(-\frac{As \cdot U}{m_J \cdot cp}\right) \qquad (4.91)$$

$$Q = U \cdot A \, ln\left(\frac{(T_s - T_{out}) - (T_s - T_{in})}{\frac{(T_s - T_{out})}{(T_s - T_{in})}}\right) \qquad (4.92)$$

$$m_{St} \cdot = \frac{Q}{\Delta H_{St}} \qquad (4.93)$$

Where:

m_J is the Juice flow rate, kg/h;

T_{out} is the temperature of the juice leaving heater, $°C$;

T_{in} is the temperature of the juice entering heater, $°C$;

T_s is the temperature of the steam entering heater, $°C$;

m_{St} is the steam flow rate, kg/h;

ΔH_{st} is the specific heat evaporation, kJ/kg (see Section 4.2.1);

cp_J is the specific heat capacity of juice, $kJ/(kg \cdot K)$ (see Section 4.2.2.2);

Q is the total heat, kJ;

A is the area of the heat exchange, m^2;

U is the overall heat transfer coefficient $kW/(m^2 \cdot K)$.

The heater used is a vertical shell tube. The overall heat transfer coefficient is obtained using Equation (4.94), wherein R_i R_p R_o R_F is the heat transfer resistance inside, wall, outside, and fouling, respectively. The internal resistance is obtained using the empirical equation for the Nusselt number (Equation 4.95), then the heat transfer coefficient is calculated using Equation (4.96) and the resistance, Equation (4.97). The wall pipe resistance is obtained using Equation (4.98). The outside resistance is obtained using Equations (4.99 – 4.101).

$$U = \frac{1}{R_i} + \frac{1}{R_p} + \frac{1}{R_O} + \frac{1}{R_F} \tag{4.94}$$

$$Nu_i = 0.0243 \cdot Re^{0.8} \cdot Pr^{(1/3)} \cdot \frac{\mu_{juice}}{\mu_{juiceSur}} \quad (if\ turbulent\ flow)$$

$$Nu_i = 3.66\ (if\ laminar\ flow) \tag{4.95}$$

$$h = \frac{k}{D \cdot Nu} \tag{4.96}$$

$$R_i = \frac{1}{h_i \cdot A_i} \tag{4.97}$$

$$R_p = \frac{ln\frac{D_o}{D_i}}{2 \cdot \pi \cdot k_{pipe} \cdot L} \quad (4.98)$$

$$Nu_o = \left(\frac{g \cdot \rho_L \cdot (\rho_L - \rho_V) \cdot k_L \cdot h_{fg} \cdot (1 + 0.68 \cdot cp_L \cdot (T_{sat} - T_s))}{4 \cdot \mu_L \cdot (T_{sat} - T_s) \cdot L} \right)^{1/4} \quad (4.99)$$

$$h_o = \frac{k}{D_o \cdot Nu_o} \quad (4.100)$$

$$R_o = \frac{1}{h_o \cdot A_o} \quad (4.101)$$

Where:

R_i is the inside resistance to heat transfer, K/W;

R_p is the wall resistance to heat transfer, K/W;

R_o is the outside resistance to heat transfer, K/W;

R_F is the fouling resistance to heat transfer, K/W;

Re is the Reynold number;

Pr is the Prandtl number;

μ_{juice} is the viscosity of the juice at the mean temperature, $N \cdot s/m^2$; (see Section 4.2.2.3);

$\mu_{juiceSur}$ is the viscosity of the juice at the tube surface temperature, $N \cdot s/m^2$; (see Section 4.2.2.3);

k is the juice thermal conductivity, $W/(m \cdot K)$;

h_i is the heat transfer coefficient, $W/(m^2 \cdot K)$;

D_i is the internal diameter of the tube, m;

D_o is the outer diameter of the tube, m;

k is the tube thermal conductivity, $W/(m \cdot K)$;

L is the length of the tube, m;

ρ_L is the liquid density at steam saturated temperature, kg/m^3;

ρ_V is the vapor density at steam saturated temperature, kg/m^3;

H_{fg} is the latent heat of steam, kJ/kg; (see Section 4.2.1)

μ_L is the viscosity of the water at the saturated temperature, $N{\cdot}s/m^2$; (see Section 4.2.1);

$\mu_{juiceSur}$ is the viscosity of the juice at the tube surface temperature, $N{\cdot}s/m^2$; (see Section 4.2.2.3);

k is the juice thermal conductivity, $W/(m{\cdot}K)$;

h_o is the heat transfer coefficient, $W/(m^2{\cdot}K)$;

A_o is the outer area, m^2.

4.8.3.2 Power

The electric power consumed in this step is due to the pumping of the juice through the heat exchangers. A 10-meter pressure drop is adopted for each heater. Therefore, the electrical power consumption is calculated as described in Section 4.3.1.

4.8.4 Flash

Before entering the clarifier, the superheated juice is allowed to flash to its saturation temperature. This enables any air in the juice to be removed and ensures that the juice runs at a constant temperature to the clarifier.

4.8.4.1 Mass and energy balance

The aim is to obtain the amount of flashed steam and thus the juice that feeds the clarification unit. The calculation of steam and juice is given by Equations (4.102) and (4.103), which are the energy and mass balance of the flash tank, respectively.

$$(m_J{\cdot}cp_J{\cdot}T)_{in} = m_{St}{\cdot}\Delta H_{St} + (m_J{\cdot}cp_J{\cdot}T)_{out} \qquad (4.102)$$

$$m_{J,in} = m_{St} + m_{J,out} \qquad (4.103)$$

Where:

m_J is the juice flow rate, $tonne/h$;

m_{ST} is the steam flow rate, $tonne/h$;

T_{in} is the temperature of the juice that enters the flash drum, $°C$;

T_{out} is the temperature of the juice that leaves the flash drum, $°C$ (saturation temperature at atmospheric pressure);

ΔH_{st} is the specific heat evaporation, kJ/kg (see Section 4.2.1);

cp_J is the specific heat capacity of juice $kJ/(kg \cdot K)$ (see Section 4.2.2.2).

4.8.5 Clarification

Clarifiers are settling tanks for the continuous removal of solids deposited by sedimentation. A clarifier is generally used to remove solid particulates or suspended solids from liquid for clarification or thickening. When the stream target is the supernatant, this equipment is called clarifiers, and decanters when the target is the bottom thickened stream. Concentrated impurities, discharged from the bottom of the tank, are namely sludge or mud. The aim is to calculate the flow rate of the sludge and the clear juice as a function of the feed juice. Figure 24 summarizes these streams.

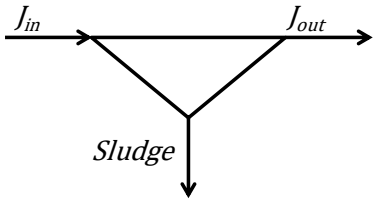

Figure 24 - Schematic flow diagram of juice decanter

4.8.5.1 Mass balance

The supernatant, known as clear juice, is drawn from the clarifier and sent to the evaporators while the sludge is filtrated. Clear juice and sludge are obtained by Equations (4.104 and 4.105). The former is the mass balance of the clarifier and the second equation is the design equation where the parameters Dirt retention efficiency and Concentration of dirt in the Sludge are used. These two parameters are available in the literature (REIN, 2007, p. 274). The concentration of dirt in the sludge is between 4.8% and 7%, and the soil retention efficiency is about 64%.

$$J_{out} = J_{in} - Sludge \qquad (4.104)$$

$$Sludge = \frac{Dirt\ retention\ efficiency\ _x\ Dirt\ in\ juice}{Concentration\ of\ dirt\ in\ Sludge} \quad (4.105)$$

Where:

J_{in} is the feed-juice flow rate, *tonne/h*;

J_{out} is the outlet-juice flow rate, *tonne/h*;

Sludge is the outlet mud flow rate, *tonne/h*.

As aforementioned, Dirt retention efficiency is a known parameter and it is defined by Equation (4.106).

$$Dirt\ retention\ efficiency = \frac{Dirt\ in\ sludge}{Dirt\ in\ juice} \quad (4.106)$$

The Concentration of dirt in mud is a known parameter and it is defined by Equation (4.107).

$$Concentration\ of\ dirt\ in\ Mud = \frac{Dirt\ in\ Mud}{Mud} \quad (4.107)$$

4.8.5.2 Power

The electric power consumed in this step is due to the pumping of the juice and sludge, and due to the sludge scraper installed on the clarifier. The sludge scraper uses a really small and is considered as described in Section 4.8.7. Therefore, the electrical demand in this step is considered to be only due to pumping (juice and mud); thus, the electrical power consumption is calculated as described in Section 4.3.1.

4.8.6 Filtration

For sludge filtration, two systems are commonly used, belt-press or vacuum filter drum. In either of these systems, the sludge is dewatered to recover sugar and the cake produced is sent to the field as a fertilizer. This platform simulates the rotary vacuum filter drum.

The rotary vacuum filter drum consists of a drum rotating in a bath of liquid to be filtrated. A fine fraction of bagasse, namely Bagacillo, is used as a filter aid. Bagacillo forms a porous layer that coats the filter drum. The drum rotates on the liquid, and the vacuum sucks the liquid phase, while the solids are retained onto the drum pre-coat surface.

4.8.6.1 Mass balance

This step aims to obtain the flow of the filtrated, cake, bagacillo, and water as a function of the sludge. The filtration process produces two streams: the filtrated, which returns to the process before clarification, and the cake, which goes to the field as a fertilizer. Figure 25 summarizes the main flows at this step.

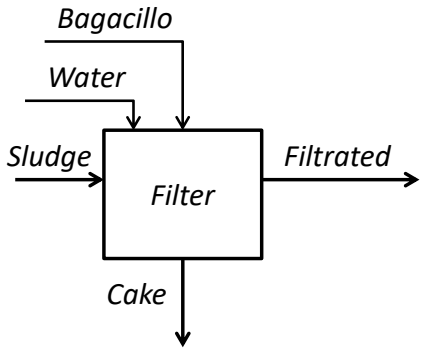

Figure 25 - schematic main flows at mud filtration

The Bagacillo added to the process is given by Equation (4.108), where the parameter *BagRatio,* according to the literature (REIN, 2007, p. 246), is between 2.5 and 3%. The cake is obtained by Equation (4.109) based on the efficiency of the filter which represents the solid retention by the filter. The literature (REIN, 2007, p. 246) shows that about 85% of the solids that enter into the process with the sludge are retained in the cake. The washing water load (*WWL*) is based on the dirt in sludge and is calculated by Equation (4.110), and, according to the literature, *WWL* ranges from 600% to 1800%. (WRIGHT; STEGGLES; STEINDL, 1997). Equation (4.111) shows the overall mass balance of the process. The amount of sucrose lost in the cake is given by empirical Equation (4.112) (WRIGHT; STEGGLES; STEINDL, 1997). The recommended filtration surface area is 100 m² per tonne of mud (WRIGHT; STEGGLES; STEINDL, 1997).

$$Bagacillo = BagRatio \cdot Sludge \quad (4.108)$$

$$Cake = FiltEff \cdot Sludge + Bagacillo \quad (4.109)$$

$$Water = DS \cdot WWL \quad (4.110)$$

$$Filtrated = Sludge - Cake + Bagacillo + Water \quad (4.111)$$

$$pol\%MS = 1.265_x MSL^{2.5} + 30.78_x WWL^{-0.25} - 12.43 \quad (4.112)$$

Where:

Sludge is the mud-flow rate, *tonne/h*;

Filtrated is the filtrated flow rate, *tonne/h*;

Bagacillo is the bagacillo flow rate, *tonne/h*;

Water is the washing water flow rate, *tonne/h*;

BagRatio is the ratio of bagacillo added to the sludge;

DS is the dirt in the sludge

FiltEff is the efficiency of the filter;

WWL is the washing water load;

Pol%MS is the sucrose content in the cake;

$MSL = \left(\frac{100_x m_{MSo}}{A}\right)$ is the mud solid loading per square meter excluding bagacillo in *tonne/(h*$_x$*100m*^{2}*)*;

$WWL = \left(\frac{100_x m_w}{A}\right)$ is the wash water load per square meter in *tonne/(h*$_x$*100m*^{2}*);*

A is the filter area m^2;

m_w is the amount of water used, *tonne/h*.

4.8.6.2 Power

This model takes into account only the electric power consumed by the centrifugal and vacuum pump. The electrical demand to move the filter drum, conveyors, and cake hopper unload is fairly small and is considered as described in Section 4.8.7. The electrical power consumed in this step due to pumping is obtained as described in Section 4.3.1. The electrical power consumption of the vacuum pump is obtained as described in Section 4.3.2. It is considered an absolute vacuum pressure of 300 mmHg and an airflow rate of 15 kg/h per square meter of filter area.

4.8.7 Power consumption

There are many electrical devices, such as lime dosing pumps, CaO dosing systems, instruments, electric panels, conveyors, illumination systems, etc. They were not individually calculated as aforementioned; for these devices, an additional $0.15\ kW$ per tonne of sugarcane milled was considered to be consumed in this area.

4.9 Multiple effect evaporation

This is the area in which the clarified juice is concentrated to produce the syrup, which has a high concentration of sucrose but is below the crystallization point. As the juice is concentrated, low-pressure steam is produced and used as heat utility in other areas, such as juice treatment, sugar crystallization, and distillery. Therefore, this area plays two roles in the industry: producing utility steam and syrup. Thus, the total thermal energy input for the whole refinery is the exhaust steam from the turbo-generator, or the boiler via a bypass valve, that enters the first-effect.

This area is to obtain the consumption of the exhaust steam and the cooling water used to produce vacuum in the last evaporation effect, and the amount of syrup and condensate produced. Figure 26 shows schematically a 5-effect multiple-effect evaporation.

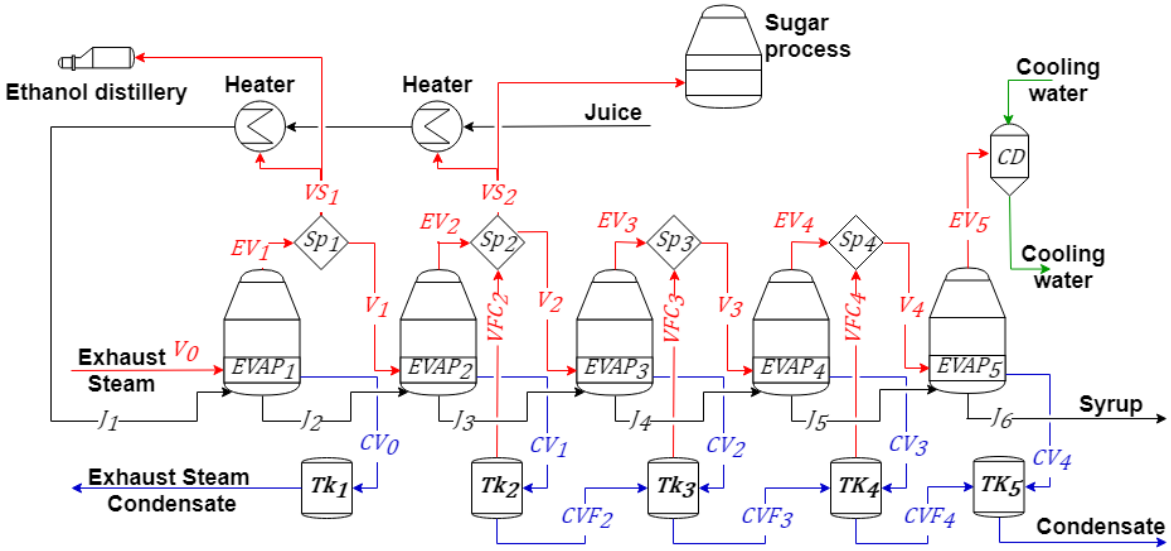

Figure 26 - Process steam flow diagram and the main consumer of thermal energy

4.9.1 Mathematical model

To the best of our knowledge, the mathematical model proposed here to solve the multiple-effect evaporation has not been published before. Therefore, an article describing the mathematical model used in the evaporation area was recently published in Case Studies in Thermal Engineering and is enclosed in Chapter 5 of this thesis.

4.9.2 Power

The electrical power consumption in this area is due to the pumping of juice, syrup, and condensate; and to the vacuum pump, which is used to remove incondensable gases. Thus, the electrical power consumption of the pumps is given as described in Section 4.3.1. The electrical power consumption to pump the cooling water for the barometric condenser is calculated as described in Section 4.3.4. The electrical power consumption of the vacuum pump is calculated as described in Section 4.3.2.

4.10 Sugar process

This is the area in which sucrose is crystallized to produce sugar. In the crystallization process, the goal is to transfer sucrose from the mother liquor to the surface of the sugar crystal. This may take many steps: crystallization must be carried out in a number of steps to reduce the sucrose content in the final molasses. The number of steps required to exhaust the

syrup to the final purity of the molasses depends on the expected purity of the molasses. Due to the fact that most Brazilian industries make alcohol using the molasse, the two boiling scheme is preferable (CASTRO, R. E. N. De *et al.*, 2019). Besides, crystalization depends on many factors, such as initial crystal size, sucrose concentration, impurities, machinery size, etc

This area is to obtain the sugar and final molasse produced, and water, steam, and seeds consumed as a function of the syrup. Figure 27 summarizes the main streams of the sugar process (considering 2 boiling pan schemes) and each unit operation. The unrecovered sucrose in the final molasses is then used to make ethanol.

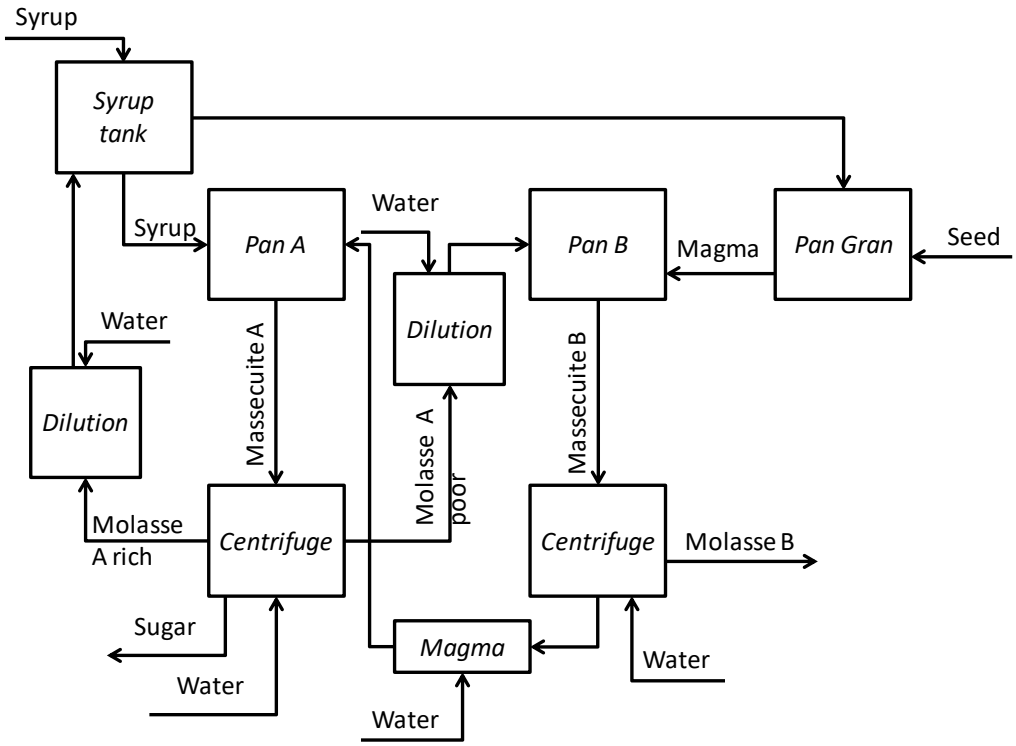

Figure 27 - Two boiling scheme sugar process

Section 4.10.1 describes a batch sugar recipe; a recipe may vary from industry to industry depending on the set of devices. The mathematical model and the parameters used in each unit operation are described in Section 4.10.2. Section 4.10.2.1 shows the set of ordinary differential equations used to simulate the vacuum pan. Depending on the information one requires from the simulation platform, it would not be useful to simulate each step of the recipe; thus, Section 4.10.2.2 describes the vacuum pan simulation considering average productions and consumptions. Apendix A shows the result of an industry operating for 72 hours. The barometric steam condenser, which is used in both sugar and evaporation processes, is described in Section 4.3.4.

4.10.1 Sugar process recipe

In a two-boiling pan scheme, the crystals start growing in crystallization B and then continue growing in crystallization A: at the end of crystallization A, the crystals reach the desired size. The syrup, which contains a higher purity of sucrose, feeds crystallization A; A-molasse, which contains a lower purity of sucrose, feeds crystallization B, while B-molasse is the exhausted molasse used to produce ethanol. The term massecuite describes the mixture of crystals, which is the solid fraction, and the mother liquor, which is the liquid fraction. The term magma describes the stream rich in crystals that provide the nuclei to initiate the growing process. Both crystallizations, A and B, occur in multiple vacuum pans. The term 'stage' is used herein when the massecuite or magma is transferred from one vacuum pan to another, while the term 'step' refers to the steps necessary to grow the crystal inside the vacuum pan. Thus, there are many steps in each stage. The flow of magma and massecuite among the vacuum pan is shown in Figure 28. The stages and steps are summarized in Table 12 for crystallization B and Table 13 for crystallization A.

Table 12 - Stages and steps for crystalization B

Stage	Step	B-pan 1	B-pan 2
1	1	A-molasse feed	
	2	Concentration	
	3	Seeding and Crystallization	
2	1	Magma transfer (cut)	Magma transfer (cut)
	2	Crystal washing	Crystal washing
	3	Crystallization	Crystallization
3	1	Magma transfer (cut)	Magma transfer (cut)
	2	Crystal washing	Crystal washing
	3	Crystallization	Crystallization
	4	Tightening	Tightening
	5	Discharging	Discharging
4	1		Magma transfer (cut)
	2		Crystal washing
	3		Crystallization
	4		Tightening
	5		Discharging
5	1		Magma transfer (cut)
	2		Crystal washing
	3		Crystallization
	4		Tightening
	5		Discharging
6	1		Magma transfer (cut)
	2		Crystal washing
	3		Crystallization
	4		Tightening
	5		Discharging

Table 13 - Stages and steps for crystalization A

Stage	Step	A-pan 3	A-pan 5	A-pan 4	A-pan 6
1	1	Magma transfer (cut)	Magma transfer (cut)		
	2	Crystal washing	Crystal washing		
	3	Crystallization	Crystallization		
2	1	Magma transfer (cut)	Magma transfer (cut)	Magma transfer (cut)	Magma transfer (cut)
	2	Crystal washing	Crystal washing	Crystal washing	Crystal washing
	3	Crystallization	Crystallization	Crystallization	Crystallization
	4	Tightening	Tightening	Tightening	Tightening
	5	Discharging	Discharging	Discharging	Discharging

In crystallization B, the crystal growth process begins in graining (stage 1). In this stage, the first step is to partially fill the vacuum pan with A-molasse. In the second step, the fluid is concentrated and the sucrose concentration must be above the solubility curve and below the labile curve. In this region, namely the metastable region, sugar crystals grow, but no new nuclei are formed. Crystallization is initiated by adding very fine seeds in form of a slurry (about 4-µm size ground sugar crystals suspended in alcohol). Adding seeds starts the third step: as sucrose leaves the mother liquor and deposits on the crystal surface, more A-molasse is added to increase the amount of sucrose in the mother liquor; then, steam is used to withdraw the water and adjust the sucrose concentration. This stage ends when the volume of the graining pan reaches its maximum level. The graining pan product is the magma that contains the crystals used to start the B-crystallization in stage 2.

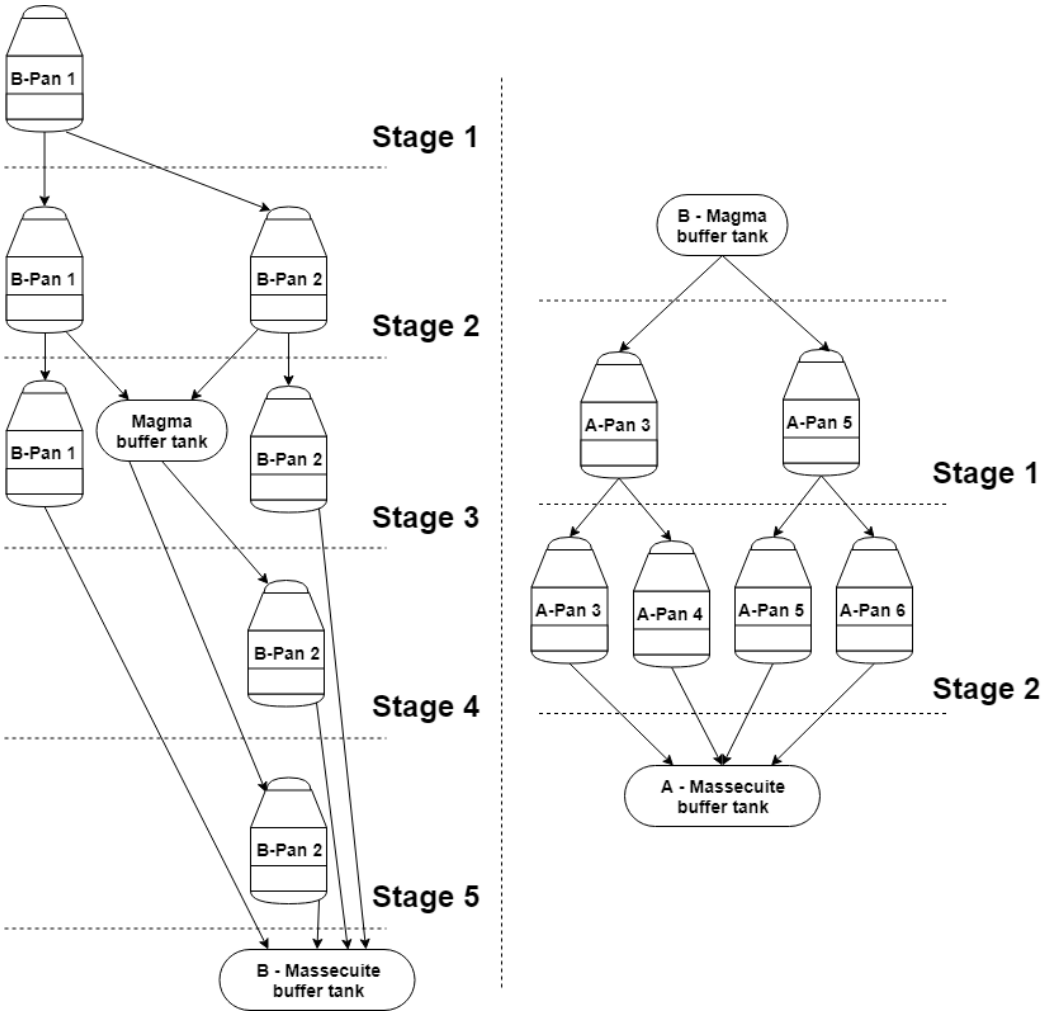

Figure 28 - Sugar crystallization stages

The amount of magma necessary to start the crystallization in each B-Pan is the volume that covers the calandria. Typically, the graining-pan produces an amount of magma to start

many B-Pans. After having the calandria filled with magma, which is the first step of stage 2, the second step of stage 2 starts, namely crystal washing. Water is added to the massecuite and then, steam is fed to evaporate the water added. This step aims to start the circulation of the massecuite by convection forces. In the third step, the sugar crystals start to grow and molasse from A-Centrifuge is added as a source of sucrose to continue the crystals growing. Steam is used during crystallization to evaporate the water from the mother liquor. As crystallization occurs, the viscosity of the massecuite increases due to the growth in the size of the crystals and the concentration of impurities. The higher the viscosity of the massecuite, the lower the heat transfer coefficient (REIN; ECHEVERRY; ACHARYA, 2004). Therefore, the steam consumption is higher at the beginning of batch crystallization and decreases as the crystal concentration increases and the concentration of mother liquor impurities increases. This stage stops when the maximum volume of the pan is reached and the magma is then partially transferred to the next vacuum pan, in a process, namely cut, to start the next stage.

Stage 3 repeats steps 1 to 3 described in stage 2. However, in stage 3, the crystals reach the desired size to be discharged and centrifuged. Thus, in step 4, namely tightening, the massecuite reaches the desired concentration of crystals, and then in step 5, the massecuite is discharged into massecuite buffer tanks. From these buffer tanks, massecuite goes to a centrifuge to separate the B-molasse from the crystals. The B-molasse is the final molasse in the two-boiling sugar production scheme and it goes to the ethanol fermentation process. The crystals from the B-centrifuges are mixed with water to produce magma for the A-pan. Stages 4, 5, and 6 repeat the steps from stage 3.

In crystallization A, the magma is the sugar produced in B and the sucrose source is the syrup from the multiple-effect evaporation. Step 1 in stage 1 of crystallization A is the magma transfer, and the amount of magma necessary to start the crystallization in each A-Pan is the volume that covers the calandria. After filling the calandria with magma, water is added to the massecuite (step 2 of stage 1), and then steam is fed to evaporate the added water. This step aims to start the circulation of the massecuite by convection forces (crystal washing). In step 3, the sugar crystals start growing and syrup from MEE is added as a source of sucrose to continue growing the crystals. Steam is used during crystallization to withdraw the water from the mother liquor in the vacuum pan. This step ends when the vacuum pan reaches its maximum level. Afterward, half of the massecuite is transferred to another vacuum pan, i.e., stage 2 and step 1. The next steps, steps 2 and 3, are the same as described in stage 1, and

then, when the vacuum pan reaches the maximum volume, before discharging the massecuite, the massecuite is tightened (step 4), then discharged (step 5).

In all the steps that involve heat transfer, the temperature of evaporation is controlled by maintaining the vacuum inside the heating chamber. The vapor, withdrawn from the product inside the vacuum pan, is conveyed through a condenser to a vacuum system composed of a water ejector and a vacuum pump.

4.10.2 Mathematical model

The sugar crystallization, which is the main step, operates discontinuously. A batch process delivers its product in discrete amounts. This means that heat, mass, temperature, concentration and other properties vary with time. Most batch processes are made up of a series of batches and semi-continuous steps. A semi-continuous step, such as centrifugation, runs continuously with periodic start-ups and shutdowns. A liquid stream from a continuous process interconnects to a batch process using buffers, i.e., storage containers.

4.10.2.1 Vacuum pan

Figure 29 shows the main streams in a vacuum pan. In a non-steady state process, the mass balance is solved using the system of ordinary differential equations, ODE, and the difference in each step is the feed stream as described above. These equations consist of an overall mass balance on the massecuite side of the vacuum pan, Equation (4.113), and on its components crystals, sucrose, impurities, and water, Equations (4.114 – 4.117), respectively The energy balance on the calandria and massecuite side is given by Equations (4.118) and (4.119), respectively. Kinetic crystallization is given by Equation (4.120) adapted from Castro (2019). The calandria pressure is regulated to maintain a preset pressure. Thus, the flow rate of the syrup, water, or A-molasse depends on the evaporation and crystallization rate (REIN, 2007, p. 397).

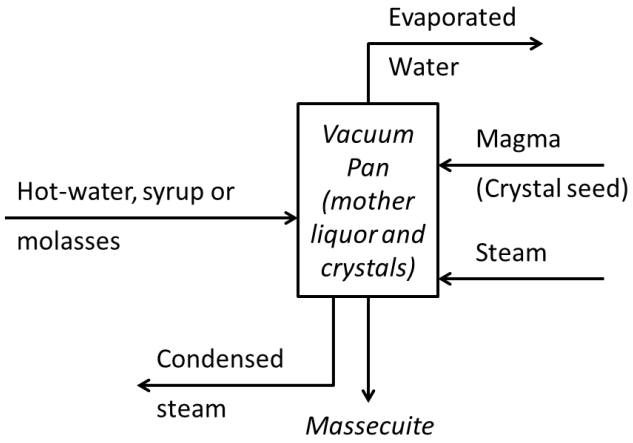

Figure 29 - Schematic diagram of a vacuum pan

$$\frac{dm_T}{dt} = F_{in} - \frac{dm_{vap\_out}}{dt} \tag{4.113}$$

$$\frac{dm_c}{dt} = K_G \cdot A_c \cdot \rho_c \tag{4.114}$$

$$\frac{dm_s}{dt} = F_{in} \cdot C_{s,in} - \left(\frac{dm_c}{m_t}\right) = F_{in} \cdot C_{s,in} - K_G \cdot A_c \cdot \rho_c \tag{4.115}$$

$$\frac{dm_I}{dt} = F_{in} \cdot C_{I,in} \tag{4.116}$$

$$\frac{dm_w}{dt} = F_{in} \cdot C_{w,in} - \frac{dm_{vap\_out}}{dt}$$
$$= F_{in} \cdot C_{w,in} - \frac{U \cdot A \cdot (T_{vap\_in} - T_{MC}) + F_{in} \cdot Cp_{in} \cdot T_{in} - F_{in} \cdot Cp_{MC} \cdot T_{MC}}{H_{vap\_out} - Cp_{MC} \cdot T_{MC}} \tag{4.117}$$

$$\frac{dm_{vap\_in}}{dt} = U \cdot A \cdot \frac{(T_{vap\_in} - T_{MC})}{\Delta H_{vap\_in}} \tag{4.118}$$

$$\frac{dm_{vap\_out}}{dt} = \frac{U \cdot A \cdot (T_{vap\_in} - T_{MC}) + F_{in} \cdot Cp_{in} \cdot T_{in} - F_{in} \cdot Cp_{MC} \cdot T_{MC}}{H_{vap\_out} - Cp_{MC} \cdot T_{MC}} \qquad (4.119)$$

$$K_G = k_G \cdot exp\left(\frac{-57000}{R(T_{MC}+273)}\right)(S-1)exp\left(-8\frac{m_I}{m_s+m_I}\left(1+2\frac{\rho_{mc}}{\rho_{crys}}\frac{m_c}{m_T}\right)\right) \qquad (4.120)$$

Where:

m_c is the mass of crystal, *kg;*

t is time, *h;*

K_G is the crystallization rate constant, *m/h;*

A is the area of crystal, m^2;

ρ is the density of the massecuite, kg/m^3;

m_s is the mass of sucrose in solution, *kg;*

m_t is the total mass of the solution, *kg;*

m_{s_sat} is the solubility of sucrose expressed as, $kg_{sucrose}/kg_{solution}$;

m_I is the mass of impurities in solution, *kg;*

m_w is the mass of water in the solution, *kg;*

R is the universal gas constant, *kJ/(kmol·K);*

E_A is the activation energy, *kJ/kmol;*

N is the number of crystals on massecuite.

4.10.2.2 Vacuum pan simulation of averages

Depending on the result desired from this simulation platform, it is convenient to use the average values in the sugar production. The simulation of averages would produce imprecise results if the process, utilities, equipment devices, pipes, etc. are to be sized. However, for example, if production from one crop season is required, using the average parameters of production and consumption provides reliable results with less computational effort.

To calculate the massecuite produced and steam consumed, the mass and energy balances are used, and the parametric equations that consider the brix of the massecuite, which is about 92% according to Equations (4.121 – 4.124).

$$MotherLiquor = Syrup + Magma \quad (4.121)$$

$$Massecuite = MotherLiquor \cdot (Brix_{massecuit} - Brix_{mother\ liquor}) \quad (4.122)$$

$$EvaporatedWater = MotherLiquor - Massecuite \quad (4.123)$$

$$Steam = \frac{MotherLiquor_x H_{Liquor} - Massecuite_x H_{Massecuite} - Evap.\ water_x H_{Massecuite}}{H_{steam} - H_{condensate}} \quad (4.124)$$

Where:

Magma is the stream with crystals that are going to grow in size during the process, *tonne/h;*

Syrup is the stream rich in sucrose added to the mother liquor, *tonne/h;*

MotherLiquor is the content in the vacuum pan syrup plus magma, *tonne/h;*

Massecuite is the product obtained after the crystallization process, *tonne/h;*

EvaporatedWater is the total water withdrawn from the *MotherLiquor, tonne/h;*

Steam is the necessary process steam to evaporate water from *MotherLiquor, tonne/h.*

Sucrose is deposited on the surface of the crystal and the crystals then grow in size until they are ready to be discharged. The degree of crystallization achieved in each stage is commonly expressed in terms of the crystal content in the massecuite. The exhaustion achieved in boiling-pan is defined by the crystal content related to the purity of the massecuite by the empirical relationship given in Equation (4.125) (Rein, 2007, p. 366).

$$Wcr = 0.78 \cdot P - 0.1 \quad (4.125)$$

Where:

Wcr is the crystal ratio content in massecuite;

P is the purity of the massecuite.

4.10.2.3 Centrifuges

After crystallization, the sugar crystals are separated from the mother liquor by centrifuging. In centrifugation, two phases can be identified. Initially, the liquid flows through the packed bed of sugar crystals. The second phase occurs once drainage is almost completed. However, some amount of liquid is retained in the bed of crystals by the surface tension and capillarity action, and thus, some water is added to remove the liquor in contact with the crystals. The washing of the sugar on the screen is necessary to whitten the sugar crystals. However, the rinse water also dissolves part of the crystal. The used quantity of water is usually in the range of 1 to 3 kg of water per 100 kg of massecuite, and each 1 kg of water can dissolve 3.54 kg of crystals (REIN, 2007, p. 432). There are two types of centrifuges: massecuite A is processed in a batch centrifuge, and massecuite B is processed in a continuous centrifuge. The aim is to obtain the sugar, molasse, and power consumed as a function of the massecuite.

4.10.2.3.1 Continuous centrifuges mass balance

To obtain the washing water, Equation (4.126) is used, in which 0.03 is the parameter that relates the washing water per amount of massecuite. To obtain the mass of dissolved crystals, Equation (4.127) is used, in which 3.54 is the parameter that relates the dissolved crystals per amount of washing water. Sugar is obtained using Equation (4.128). A continuous centrifuge produces sugar with Brix about 98%, i.e. 2% moisture. The molasses is then obtained through mass balance as shown in Equation (4.129)

$$WashingWater = 0.03 \cdot Massecuite \tag{4.126}$$

$$DissolvedCrystals = 3.54 \cdot WashingWater \tag{4.127}$$

$$Sugar = \frac{Crystal - (Dissolved\ crystals)}{Brix} \tag{4.128}$$

$$Molasses = Massecuite + Water - Sugar \quad (4.129)$$

Where:

Crystal is the amount of solid crystal in the massecuite, *tonne/h;*

WashingWater is the water used to wash the mother liquor at the surface of the crystal during the centrifugation process, *tonne/h;*

DissolvedCrystal is the amount of crystal dissolved due to the *WashingWater* added, *tonne/h;*

Sugar is the final product obtained after centrifugation composed basically of moisture crystals, *tonne/h;*

Molasses is the uncrystallized part of the massecuite without crystals but with some sucrose, *tonne/h.*

4.10.2.3.2 Electricity demand for continuous centrifuges

These machines accelerate the massecuite up to high speed without recovering any of the energy expended and also induce considerable windage. According to the literature (REIN, 2007, p. 437), the specific power usage is high and lies anywhere in the range of 3 to $10\ kW$ per tonne of massecuite. The specific power consumption of $3\ kW$ per tonne of massecuite is considered, which is in accordance with a publication from a Brazilian supplier of continuous centrifuges (MAUSA, [*s. d.*]).

4.10.2.3.3 Batch centrifuges mass balance

One difference between continuous and batch centrifuges is that two molasses can be obtained during the batch process. One is the liquid phase of the massecuite, and the other is the liquid phase of the rinsed washing process. The rinsed water from washing is mixed with the syrup and used to feed vacuum pan A. Equation (4.130) is used to obtain the washing water, in which 0.03 is the parameter that relates the washing water per massecuite. To obtain the mass of dissolved crystals Equation (4.131) is used, where 3.54 is the parameter that relates the dissolved crystals per washing water. Sugar is obtained using Equation (4.133). A batch centrifuge produces sugar with Brix of 99%, i.e. 1% moisture. The molasses is then

obtained by the mass balance in the two phases of centrifugation, as shown in Equations (4.134 and 4.135).

$$WashingWater = 0.03 \cdot Massecuite \quad (4.130)$$

$$DissolvedCrystals = 3.54 \cdot WashingWater \quad (4.131)$$

$$Crystal = Massecuite \cdot Wcr \quad (4.132)$$

$$Sugar = \frac{Crystal - DissolvedCrystals}{Brix} \quad (4.133)$$

$$Molasses1 = WashingWater + DissolvedCrystals \quad (4.134)$$

$$Molasses2 = Massecuite + Water - Molasses1 - Sugar \quad (4.135)$$

Where:

Molasses1 is the uncrystallized part of the massecuite extracted from the centrifuge without washing the crystals, typically namely, poor molasse*, tonne/h;*

Molasses2 is the liquid product obtained during the crystal washing process, typically namely, rich molasse*, tonne/h.*

4.10.2.3.4 Electricity demand for bath centrifuges

Power consumption in a batch centrifuge is strongly dependent on its parts: motor and coupling, and on the number of cycles per hour. (REIN, 2007, p. 431) In this model, the specific power consumption of $1.5\ kW$ per tonne of massecuite is considered.

4.10.2.4 Drier

Drying is the last step in sugar production. It involves the process in which excess moisture is removed from the sugar crystals after centrifugation. Three mechanisms occur in sugar drying: moisture evaporation at a rate governed by the difference in vapor pressure between the film and the surrounding air; diffusion of water molecules through the surface film, driven by the concentration gradient; crystallization of sucrose molecules in the film to the crystal surface or solidification as amorphous sugar, diluting the film and making more moisture available for removal. The sugar drier consists of an air heater with a fan and is divided into a drying portion and a cooling portion. Any practical calculation of the heat transfer in a cascade dryer is hindered by the difficulty encountered in estimating the exposed particle surface area for heat transfer (REIN, 2007, p. 477). Thus, the drying process is described by a set of empirical equations and the balance of mass and energy.

4.10.2.4.1 Mass and energy balance

Equations (4.136 – 4.142), given by Hugot (1960, p. 822), estimate the steam consumption of the process:

$$A = \frac{1.5 \cdot P \cdot h}{(H_1 - H_0)} \qquad (4.136)$$

$$V = \frac{A}{a_0 + e_0} \qquad (4.137)$$

$$q_1 = A \cdot H_0 \cdot c(T_1 - T_0) \qquad (4.138)$$

$$q_2 = P \cdot h \cdot (607 + 0.3 \cdot T_1 - T_0) \qquad (4.139)$$

$$q_3 = A \cdot H_0 \cdot c'(T_1 - T_0) \qquad (4.140)$$

$$M = 1.25 \cdot (q_1 + q_2 + q_3) \qquad (4.141)$$

$$Q = M / r \qquad (4.142)$$

Where:

A is the weight of air to be passed through the dryer, kg/h;

P is the weight of sugar to be dried, kg/h;

h is the moisture content ratio, kg/kg;

H_0 is the weight of water vapor contained in saturated air at the temperature T_0, kg/kg;

H_1 is the weight of water vapor contained in saturated air at the temperature T_1, kg/kg;

T_0 is the ambient temperature, $°C$;

T_1 is the dryer outlet temperature, $°C$;

V is the volume of air required, m^3/h;

a_0 is the density of air at T_0, kg/m^3;

e_0 is the weight of water vapor contained in saturated air at T_0, kg/m^3;

c is the specific heat of the air, $kJ/(kg \cdot K)$;

c' is the specific heat of water, $kJ/(kg \cdot K)$;

q_1 is the heat necessary to heat the weight A of air, kJ/kg;

q_2 is the heat necessary to evaporate the water contained in sugar, kJ/kg;

q_3 is the heat necessary to heat the vapor contained in the weight A of air, kJ/kg;

M is the total heat including the heat lost to the surrounding, kJ;

r is the latent heat of the steam used, kJ/kg;

Q is the steam consumption, kg/h.

4.10.2.4.2 Power

The power consumption of the fan and driver that rotates the dryer is considered to be about $2\ kW$ per tonne of dry sugar (REIN, 2007, p. 478).

4.10.2.5 Power

There are many electrical devices, such as conveyors, ball mills, magma conditioners, instruments, electric panels, illumination systems, etc. They were not individually calculated, and an additional $0.15\,kW$ per tonne of dry sugar is considered.

4.11 Ethanol process

The first generation ethanol process is a biological process that converts sugars, such as glucose, fructose, and sucrose, into cellular energy, producing ethanol and carbon dioxide as a side effect. This work simulates the fed-batch fermentation process. Figure 30 is a simplified flow diagram of the ethanol process. Each rectangle describes a unit process that will be described hereinafter. The aim is to obtain the production of ethanol and vinasse and the consumption of water, steam, sulfuric acid, cooling water, and electricity as a function of juice and molasse. In this process, the concentration of the substrate must be adjusted to a target concentration. A high concentration of sugar would produce a high concentration of ethanol, which is an inhibitory product for fermentation, and a low concentration of sugar would require large fermenters and large amounts of steam to distillate it. As the microorganism does not support high temperatures, the substrate must be cooled before entering the fermenter. Moreover, the wine must be cooled during fermentation to remove the heat produced. The yeast used in the fermentation is separated from the fermented wine using a centrifuge and then the yeast is recycled. However, to avoid bacterial infection, acid is added before reusing it, since low pH is sufficient to kill the majority of contaminating bacteria, while the yeast is left unscathed. During fermentation, the CO_2 gas strips of some ethanol from wine. To avoid losing the stripped ethanol, the exhausted gas is scrubbed, and the recovered ethanol is mixed with the centrifuged wine. The ethanol is then purified by fractional distillation.

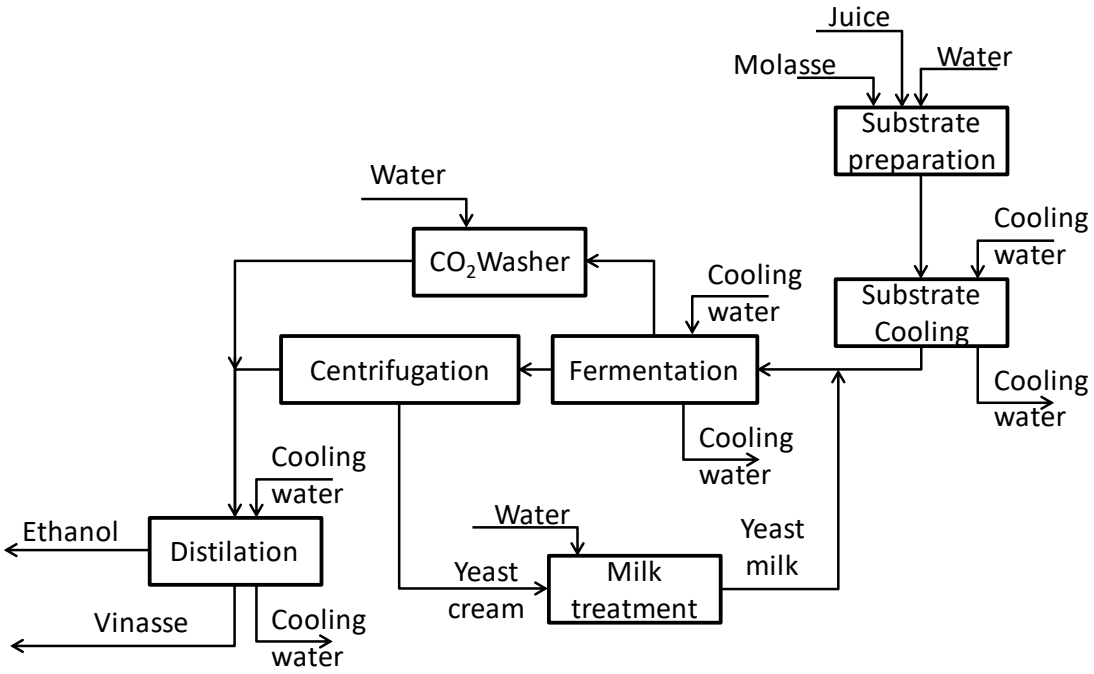

Figure 30 - Schematic diagram ethanol process

4.11.1 Broth preparation

The substrate or broth used for fermentation can be obtained from molasse, juice, or a mixture of both. The substrate requires a sugar concentration between 17-24%. The concentration is adjusted by adding water to the broth pipe line, as shown in Figure 31. To calculate the amount of water necessary for the target concentration, this model uses the mass balance of the total fermentable sugar.

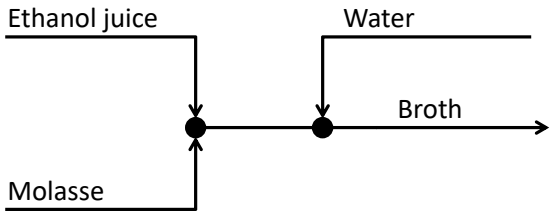

Figure 31 - Broth preparation scheme

4.11.1.1 Mass balance

This step aims to determine the amount of water necessary to adjust the broth concentration. The sugar concentrations of the juice and molasse are known, and the concentration of broth is specified. The mass balance is given by Equations (4.134 – 4.145). The fermentable sugars, ART, are glucose and fructose. The amount of ART is calculated from

the stoichiometric chemical reaction in which sucrose is converted to glucose and fructose by an enzymatic reaction, namely invertase.

$$ART = AR + Sucrose \cdot \frac{360}{342} \quad (4.143)$$

$$Broth = \frac{ART_J \cdot J + ART_M \cdot M}{ART_{Broth}} \quad (4.144)$$

$$Water = Broth - J - M \quad (4.145)$$

Where:

ART_J is the concentration of sugar (glucose and fructose) in juice;

J is the total amount of juice, *tonne/h*;

ART_M is the concentration of sugar (glucose and fructose) in molasse;

M is the total amount of molasse, *tonne/h;*

ART_{Broth} is the desired sugar ratio in must (*17% > ART > 24%);*

$Broth$ is the substrate stream to fermentation, *tonne/h;*

$Water$ is the quantity of additional water, *tonne/h.*

4.11.1.2 Power

The electric power consumed in this step is due to the pumping of clear juice, molasses, and water. Thus, it is obtained by the model described in Section 4.3.1.

4.11.2 Broth cooling

The substrate needs to be cooled before entering the fermenter. The cooling process is carried out using a counterflow plate heat exchanger (Figure 32). The cooling water from the cooling tower is used. This model aims to obtain the flow rate of the cooling water necessary to adjust the substrate to the temperature at which fermentation begins.

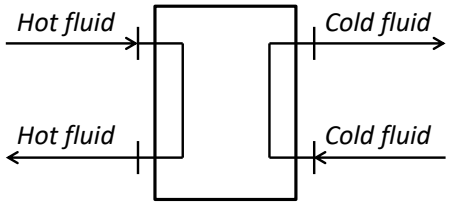

Figure 32 - Broth cooling

4.11.2.1 Mass balance

The model that describes this process is given by Equations (4.146 –4.148). These equations are solved to obtain the heat, the outlet temperature of the water, and the flow rate of the water. The overall heat coefficient and the surface area are known parameters.

$$Q = m_{sub} \cdot cp_{sub} \cdot (T_{in,sub} - T_{out,sub}) \qquad (4.146)$$

$$Q = UA \frac{(T_{in,sub} - T_{out,cold}) - (T_{out,sub} - T_{in,cold})}{Ln \frac{(T_{in,sub} - T_{out,cold})}{(T_{out,sub} - T_{in,cold})}} \qquad (4.147)$$

$$m_{cold} \cdot = \frac{Q}{cp_{cold} \cdot (T_{out,cold} - T_{in,cold})} \qquad (4.148)$$

Where:

m_{sub} is the substrate fluid flow rate, $tonne/h$;

m_{codl} is the cooling water flow rate, $tonne/h$;

T_{out} is the temperature of the fluid leaving the heat exchanger, ^{o}C;

T_{in} is the temperature of the fluid entering to the heat exchanger, ^{o}C;

cp is the specific heat capacity of the fluid, $kJ/(kg \cdot K)$ (see Section 4.2.1 and 4.2.2.2);

Q is the total heat exchanged, kJ;

U is the overall heat transfer co-efficient, $kW/(m^2 \cdot K)$;

A is the area of the heat exchange, m^2.

4.11.2.2 Power

The electric power consumed in this step is due to pumping the substrate toward the heat exchanger. A pressure drop of 10 meters is adopted for each device. Thus, the electrical power consumption of the pump is given by the model described in Section 4.3.1. The power consumption due to the pumping of cooling water is calculated in Section 4.14.1

4.11.3 Fermentation

Alcoholic fermentation is the biological process that converts 6-carbon sugars, such as glucose and fructose, to cellular energy, producing ethanol and carbon dioxide. Sucrose is a dimer of glucose and fructose molecules. In the first step of alcoholic fermentation, the enzyme invertase cleaves the glycolic linkage between the glucose and fructose molecules; The overall chemical formula for alcoholic fermentation is as follows:

$$C_{12}H_{22}O_{11} + H_2O + enzyme \rightarrow 2\ C_6H_{12}O_6$$

$$C_6H_{12}O_6 + microorganisms \rightarrow 2\ C_2H_5OH + 2\ CO_2 + heat$$

These chemical reactions are exothermic (GIUDICI; NASCIMENTO, 1984), and consequently, cooling the wine is required during fermentation. Otherwise, the wine would reach a high temperature, which would hinder the yeast. The total energy released by $1\ mol$ of glucose consumed in anaerobic fermentation is $118\ kJ/mol$ (WALTHER, 2009, p. 622). The production of ethanol is given by the mass and energy balances and the kinetic equation. Here, the fermentation process was simulated in a fed-batch reactor.

4.11.3.1 Mathematical model

The mass balance for each component is shown in Equations (4.149 – 4.151). The overall mass balance is shown in Equation (4.152), and the energy balance in Equation (4.153). The reaction rate of ethanol, CO_2, biomass production and substrate consumption are given by Equations (4.154 – 4.157), respectively. The kinetic model of Ghose-Tyagi (1979) is shown in Equation (4.158).

The terms 'E_{in}', 'E_g', 'E_{vap}', and 'E_{tc}' shown in the energy balance refer to the heat input with the feed stream, the heat released by the fermentation reaction, the heat output with the gas released and the heat withdrawn by the plate heat exchanger, respectively. The heat output with gas is due to the CO_2 produced, and the ethanol and water that are stripped with the CO_2 gas. The concentration of ethanol and water in the gas is calculated using the equilibrium ethanol/water data as described in Section 4.2.4.3. The energy by the heat of vaporization of each component is given by Equation (4.161). The heat withdrawn by the plate heat exchanger is calculated using Equations (4.162 – 4.164). Appendix B shows the result of a fed-batch fermentation process operation for 72 hours.

$$\frac{dC_{sub}}{dt} = \frac{F^{in}}{V}\left(C_{sub}^{in} - C_{sub}\right) + r_{sub} \qquad (4.149)$$

$$\frac{dC_X}{dt} = \frac{F^{in}}{V}\left(C_X^{in} - C_X\right) + r_X \qquad (4.150)$$

$$\frac{dC_{ETH}}{dt} = \frac{F^{in}}{V}\left(C_{ETH}^{in} - C_{ETH}\right) + r_{ETH} \qquad (4.151)$$

$$\frac{dV}{dt} = F^{in} - F^{out} - F^{gas} \qquad (4.152)$$

$$\frac{dT}{dt} = \frac{1}{\rho_{wine} \cdot Cp_{wine}} \cdot \left(E_{in} + E_g - E_{vap} - E_{tc}\right) \qquad (4.153)$$

$$r_{ETH} = -\mu \cdot C_X \frac{Y_{ETH/SUB}}{Y_{X/SUB}} \qquad (4.154)$$

$$r_{CO2} = r_{ETH} \cdot \frac{44}{92} \tag{4.155}$$

$$r_X = (\mu \cdot - k_D) \cdot C_X \tag{4.156}$$

$$r_{sub} = -\mu \cdot C_X \frac{1}{Y_{X/SUB}} \tag{4.157}$$

$$\mu = \frac{\mu_{max} \cdot C_{sub}}{k_s + C_{sub} + \frac{C_{sub}^2}{k_i}} \cdot \left(1 - \frac{C_{EHT}}{C^*}\right) \tag{4.158}$$

$$E_{in} = \rho^{in} \cdot Cp^{in} \cdot (T^{in} - T) \tag{4.159}$$

$$E_g = \frac{(-r_{sub}) \cdot 118}{180} \tag{4.160}$$

$$E_{vap} = r_{CO2} \cdot \left(\Delta H_{vap,CO2} + y_{w/gas} \cdot \frac{18}{44} \cdot \Delta H_{vap,w} + y_{eth/gas} \cdot \frac{46}{44} \cdot \Delta H_{eth}\right) \tag{4.161}$$

$$\varepsilon = exp\left(\frac{U \cdot A \cdot 3600}{\rho_{wine} \cdot F_q \cdot Cp_{wine}} - \frac{U \cdot A \cdot 3600}{\rho_f \cdot F_f \cdot Cp_f}\right) \tag{4.162}$$

$$\delta = F_f \cdot Cp_f \cdot F_q \cdot Cp_{wine} \tag{4.163}$$

$$E_{tc} = \frac{\delta \cdot (\varepsilon - 1) \cdot (T - T_{in,f})}{\varepsilon \cdot F_f \cdot Cp_f - F_q \cdot Cp_{wine}} \quad (4.164)$$

Where:

A is the heat transfer area, m^2;

C_{sub} is the concentration of substrate, kg/m³;

C_X is the concentration of microorganism, kg/m³;

C_{ETH} is the concentration of ethanol, kg/m³;

C^* is the constant of ethanol inhibition, kg/m³;

Cp^{in} is the specific heat capacity (the overwritten ^{in} refers to the inlet flow rate**)**, $kJ/(kg \cdot K)$;

Cp_{wine} is the wine specific heat capacity, $kJ/(kg \cdot K)$;

Cp_f is the specific heat capacity, $kJ/(kg \cdot K)$ (see Section 4.2.1);

E_{in} is the heat inlet due to inlet flow rate, $kJ/(h \cdot m^3)$;

E_g is the heat released by the fermentation reaction, $kJ/(h \cdot m^3)$;

E_{vap} is the heat output with the gas released, $kJ/(h \cdot m^3)$;

E_{tc} is the heat withdrawn by the plate heat exchanger, $kJ/(h \cdot m^3)$;

F is the volumetric flow rate (overwritten ^{in}, ^{out}, and ^{gas} is used to designate inlet, outlet, and gaseous outlet respectively), m^3/h;

F_f is the volumetric flow rate of cooling water, m^3/h;

F_q is the volumetric flow rate of recirculation wine, m^3/h;

k_D is the rate of cell death, h^{-1};

k_s is the half-velocity constant, kg/m^3;

k_i is the substrate inhibition constant, kg/m^3;

r_X is the reaction rate of microorganism production, $kg/(h \cdot m^3)$;

r_{ETH} is the reaction rate of ethanol production, $kg/(h \cdot m^3)$;

r_{sub} is the reaction rate of substrate consumption, $kg/(h \cdot m^3)$;

r_{CO2} is the reaction rate of CO_2 production, $kg/(h \cdot m^3)$;

$T_{in,f}$ is the temperature of cooling water inlet at the heat exchanger, ^oC;

T is the temperature inside the fermenter, ^oC;

t is the reaction time, h;

U is the overall heat transfer coefficient, $kW/m^2 \cdot K$;

V is the current volume of the fermenter, m^3;

$Y_{X/SUB}$ is the biomass yield;

$Y_{ETH/SUB}$ is the ethanol yield;

$y_{w/gas}$ is the mole fraction of water in the gas phase;

$y_{eth/gas}$ is the mole fraction of ethanol in the gas phase;

$\Delta H_{vap,CO2}$ is the enthalpy of vaporization of CO_2, $kJ/(kg)$;

$\Delta H_{vap,w}$ is the enthalpy of vaporization of water, $kJ/(kg)$ (see Section 4.2.1);

$\Delta H_{vap,eth}$ is the enthalpy of vaporization of ethanol, $kJ/(kg)$;

ρ_{wine} is the density of wine, kg/m^3;

ρ^{in} is the density of wine, kg/m^3 and the Overwritten in refers to the inlet flow rate;

ρ_f is the density of cooling water, kg/m^3;

μ is the specific microorganism growth rate, h^{-1} ;

μ_{max} is the maximum specific microorganism growth rate, h^{-1} ;

ε is the parameter used in Equation (4.164) obtained using Equation (4.162);

δ is the parameter used in Equation (4.164) obtained using Equation (4.163), $(m^3 \cdot kJ/(kg \cdot K \cdot h))^2$.

4.11.3.2 Power

The electric power consumed in this step is due to the pumping of the substrate, wine, and inoculum. Thus, it is obtaqined by the model described in Section 4.3.1.

4.11.4 CO_2 Scrubber

The gaseous stream produced during fermentation is scrubbed in an absorption column. Thus, most of the ethanol is absorbed by water, and the gas released into the atmosphere contains a small amount of ethanol. The liquid stream produced at the bottom of the column goes to the distillation unit. Figure 33 shows schematically the gas scrubber column.

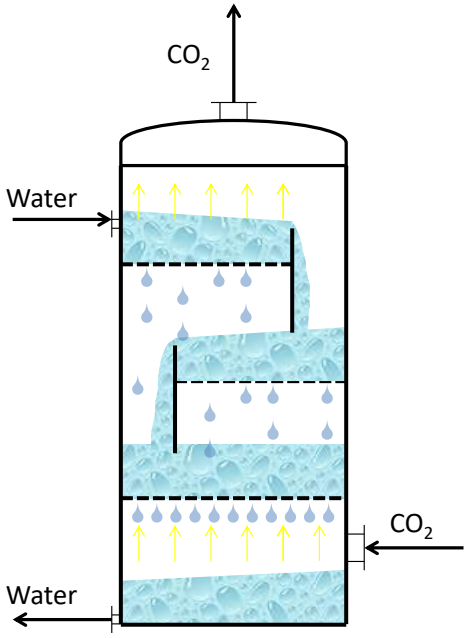

Figure 33 - Schematic diagram of CO_2 washer

4.11.4.1 Mass balance

The amount of ethanol and water recovered by the CO_2 scrubber is obtained using the equilibrium equation described in Section 4.2.4.3 and an efficiency parameter. The efficiency parameter represents how close to equilibrium the mixture is. When the ethanol is transferred from the gas to the liquid phase at each stage, the equilibrium is unlikely to happen. The efficiency will depend on the design of the equipment and accessories, such as valves or bubble caps that fill the plates. A typical efficiency value is 0.9. Thus, the mole fraction of ethanol in the liquid phase is given by Equation (4.165).

$$x_{1,j} = x_{1,j+1} + y_{1,j} \cdot Eff \qquad (4.165)$$

Where:

The index *"j"* indicates the stage of the CO_2 washer from the bottom to the top;

The index *"1"* indicates ethanol;

$X_{1,j}$ is the mole fraction of ethanol in the liquid phase at stage *"j";*

y_i is the mole fraction of ethanol in the gas phase at stage *"j";*

Eff is the efficiency of each stage.

4.11.4.2 Power

The electric power consumed in this step is due to the pumping of water to the top of the column. Thus, it is obtained by the model described in Section 4.3.1.

4.11.5 Yeast centrifuge

When fermentation ends, yeast cells are collected by centrifuging and re-used in the next fermentation cycle. This model aims to obtain the centrifuged wine and the yeast-rich stream, namely yeast cream.

4.11.5.1 Mass balance

To obtain the flow rate of the cream, C, and the wine, W_{out}, a parametric equation is used, according to Equation (4.166), in which $YL_{wt\%}$ is the parameter that relates the mass of yeast per mass of centrifuged wine, and $YC_{wt\%}$ is the parameter that relates the mass of yeast per mass of yeast cream. These parameters depend on the centrifuge device: industrial data show that the concentration of yeast in cream is about 70% by weight and the yeast in wine is about 0.5 % by weight. Equation (4.167) is the overall balance of mass.

$$Y_{wt\%} \cdot W_{in} = YL_{wt\%} \cdot W_{out} + YC_{wt\%} \cdot C \qquad (4.166)$$

$$W_{in} = W_{out} + C \qquad (4.167)$$

Where:

W_{in} is the stream that enters the centrifuge, $tonne/h$;

W_{out} is the stream that leaves the centrifuge to the distillation process, $tonne/h$;

C is the recycling yeast cream, $tonne/h$;

$Y_{wt\%}$ is the mass fraction of Yeast in feed wine stream;

$YL_{wt\%}$ is the mass fraction of yeast in wine stream to distillery;

$YC_{wt\%}$ is the mass fraction of yeast in the recycling yeast cream stream.

4.11.5.2 Power

The electric power consumed in this step is due to the centrifuge of the wine and pumping of the wine to the centrifuge. The centrifuge power consumption is estimated to be $0.32\ kW$ per tonne of processed cream (ALFA LAVAL, [*s. d.*]). The pump power consumption is given by the model described in Section 4.3.1.

4.11.6 Yeast treatment

The yeast cream produced by the centrifuge is treated with water and sulfuric acid before feeding the next batch of fermentation. After dilution and adjustment of pH, the stream is named yeast milk. The yeast milk is used to start a new fed-batch fermentation.

4.11.6.1 Mathematical model

This model computes the water and sulfuric acid necessary to dilute the cream and adjust the pH as described by Equations (4.168 – 4.170). The concentration of yeast in milk is 70% by weight. The consumption of H_2SO_4 is approximately 0.003 kg of sulfuric acid per kg of yeast milk.

$$M = \frac{C \cdot YC_{wt\%}}{YM_{wt\%}} \tag{4.168}$$

$$W = M - C \tag{4.169}$$

$$W = Ac \cdot M \tag{4.170}$$

Where:

W is the dilution water, $tonne/h$;

M is the milk of yeast, $tonne/h$;

C is the cream of yeast, $tonne/h$;

$YM_{wt\%}$ is the mass fraction of yeast in milk;

$YC_{wt\%}$ is the mass fraction of yeast in cream;

Ac is the ratio of H_2SO_4 to yeast milk, $kg_{H2SO4}/\ kg_{\text{yeast milk}}$.

4.11.6.2 Power

The electric power consumed in this step is due to the pumping of the yeast milk and the mixer on the yeast tank treatment. Thus, the electrical consumption due to pumping is obtained by the model described in Section 4.3.1. The electrical consumption due to the tank mixer is estimated to be $0.2\ kW/m^3$.

4.11.7 Distillation

Distillation is a method used to separate components on the basis of their presence in both the liquid and vapor phases, where all components exist in both phases. Separation of the components is achieved by differences in the boiling points between the species.

Figure 34 presents a simplified flow-sheet of the distillation process. In this process, the wine is preheated in the condenser E and the heat exchanger K. Then, it is fed to column A, which produces vinasse at the bottom, phlegm and second-grade ethanol at the top. Second-grade ethanol feeds column D, which is used to withdrawn gases and volatile compounds. The liquid phase of the phlegm from column D and the vapor from column A feed the rectification column (column B). Column B produces hydrated ethanol at the top and stillage at the bottom.

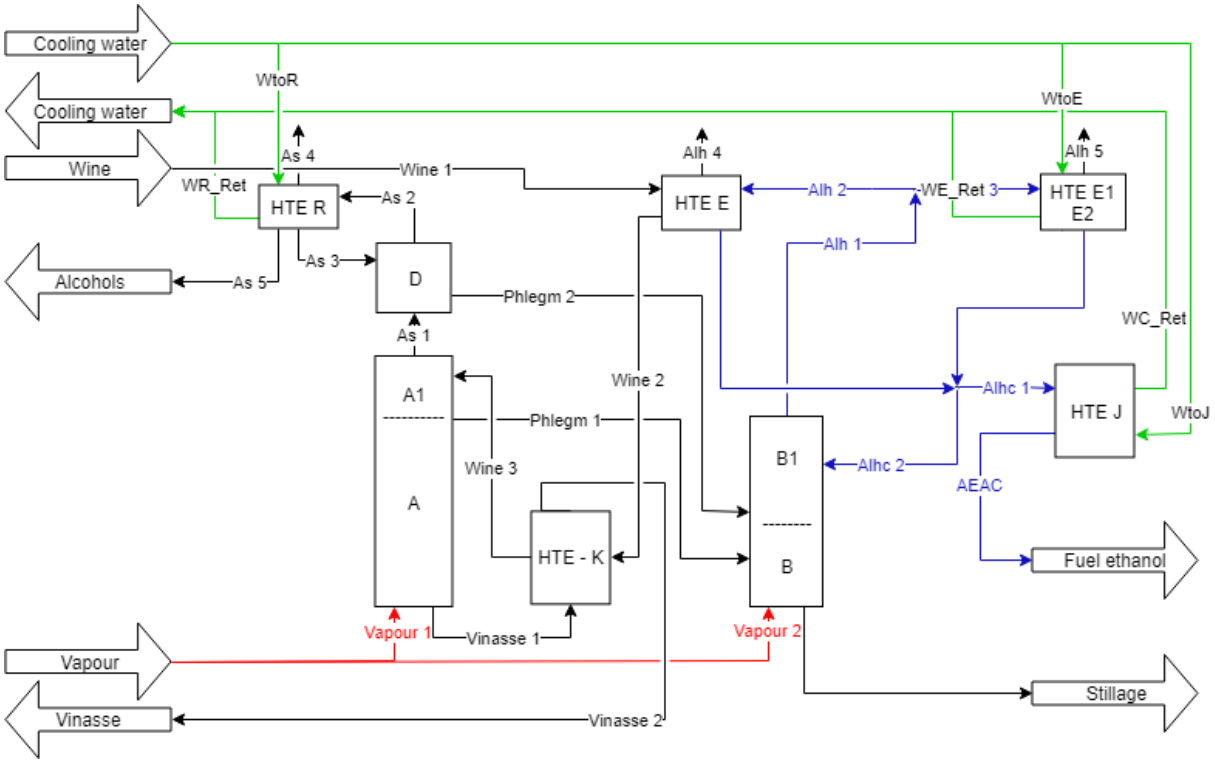

Figure 34 - Flow diagram of the ethanol distillation process

4.11.7.1 Mass and energy balance

This model aims to obtain the amount of ethanol and vinasse produced, the amount of steam consumed, and the amount of recirculation cooling water. Owing to the absence of properties data for fermented wine and seeing that the assumption that wine is composed only of ethanol and water does not represent the real distillation process, the theoretical plates and ethanol concentration at each stage of the column were not simulated. Thus, this model is based on the energy and mass balance necessary to produce the fuel ethanol. The ANP (petroleum national agency) specifies the concentration of fuel ethanol i.e. 92.5 – 93.8 INPM or 95.1 – 96 °GL. INPM is the abbreviation for wt %. Therefore, the production of fuel ethanol is obtained by Equation (4.171). The destillation efficiency is 99.5%.

$$FuelEthanol = \frac{Wine \cdot Ewt\% \cdot \eta}{INPM\_Fuel \cdot \rho} \qquad (4.171)$$

Where:

$FuelEthanol$ is the fuel ethanol flow rate, m^3/h;

$Wine$ is the wine flow rate, $tonne/h$;

$Ewt\%$ is the ethanol mass fraction in wine;

η is the distillation overall efficiency;

ρ is the ethanol specific weight adopted is $0.79\ tonne/m^3$.

Vinasse is obtained by the mass balance in the distillery. This simulation platform considers two possibilities. First, when steam is injected directly into columns A and B, vinasse is obtained by Equation (4.172). Second, if steam is not injected at the bottom of the columns, i.e., indirect steam via the use of a reboiler, vinasse is obtained by Equation (4.173).

$$Vinasse = Wine + Steam - FuelEthanol \quad (4.172)$$

$$Vinasse = Wine - FuelEthanol \quad (4.173)$$

Where:

$Vinasse$ is the vinasse flow rate, $tonne/h$;

$Steam$ is the steam flow rate to feed columns A and B, $tonne/h$.

The steam consumption flow rate in each column is obtained using parameter from industrial data as given by Equations (4.174 – 4.176). Columns C and P exist only when anhydrous ethanol is produced.

$$StDestColA = 1.8 * FuelEthanol \quad (4.174)$$

$$StDestColB = 0.8 * FuelEthanol \quad (4.175)$$

$$StDestColCP = 1.7 * FuelEthanol \quad (4.176)$$

Where:

$StDestColA$ is the steam flow rate at column A, $tonne/h$;

1.8 is the specific steam consumption at column A, $tonne/m^3_{ethanol}$;

$StDestColB$ is the steam flow rate at column B, $tonne/h$;

0.8 is the specific steam consumption in column B, $tonne/m^3_{ethanol}$;

$StDestColCP$ is the steam flow rate at columns C and P, $tonne/h$;

1.7 is the specific steam consumption at column C and P, $tonne/m^3_{ethanol}$.

The required amount of cooling water is calculated from the overall energy balance, as shown in Figure 35 and Equation (4.177). In this equation, the sub-index indicates the stream. For streams with more than one component, such as wine, the heat capacity is obtained considering each composition as an ideal mixture as shown by Equation (4.178).

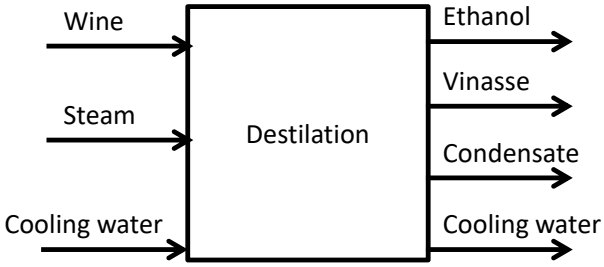

Figure 35 - Schematic diagram of distillation overall feed streams

$$m_{CoolWater} = \frac{(m \cdot cp \cdot T)_{eth.} + (m \cdot cp \cdot T)_{vin.} + (m \cdot cp \cdot T)_{cond.} - (m \cdot cp \cdot T)_{wine} - (m \cdot H)_{steam}}{(cp \cdot T_{out} - cp \cdot T_{in})_{CoolWater}} \quad (4.177)$$

$$cp_{mixture} = \Sigma\, x_i \cdot cp_i \quad (4.178)$$

Where:

m is the mass flow rate, $tonne/h$;

T is the temperature, $^{\circ}C$;

H is the enthalpy of steam, kJ/kg (obtained as described in Section 4.2);

cp is the specific heat capacity, $kJ/(kg \cdot K)$(obtained as described in Section 4.2);

x is the mass fraction of the component *"i"*.

4.11.7.2 Power

There are many electrical devices, such as wine recirculation, product transfer, electric instruments, analyzers, panels, etc. They were not individually calculated, so an additional $0.25\ kW$ per cubic meter of fuel ethanol produced is considered. This value was obtained from an industrial plant.

4.12 Combined heat and power

This is the area in which steam and electricity are produced. Part of the bagasse produced in the extraction area goes straight to the boiler and another part is stored to be burned when the mill is not milling or during the sugarcane off-season, as shown in Figure 36. When bagasse is stored, part of its calorific value is lost due to degradation mainly by yeast (DOS SANTOS *et al.*, 2011). Additionally, some amount of bagasse is lost due to rain and wind erosion in the bagasse pile. Also, part of the bagasse might be used to stop and start the boiler, which does not produce useful steam. Consequently, regarding these losses, this model considered that only 95% of the bagasse produced by the mill is available and is used to produce steam.

The aim of modeling the combined heat and power, CHP, is to obtain the production of steam and electricity, the consumption of demineralized water and bagasse, and the gas emission. The mathematical model is divided into 4 steps: the boiler, steam turbogenerator, condenser, and deaerator. These steps are interconnected, as shown in Figure 36. The recycling flow rate is calculated using the fixed-point interaction method, in which the first guess of the recycling flow is zero, i.e., low-pressure steam to the deaerator. The next sections describe the mathematical model and the parameters used in each step.

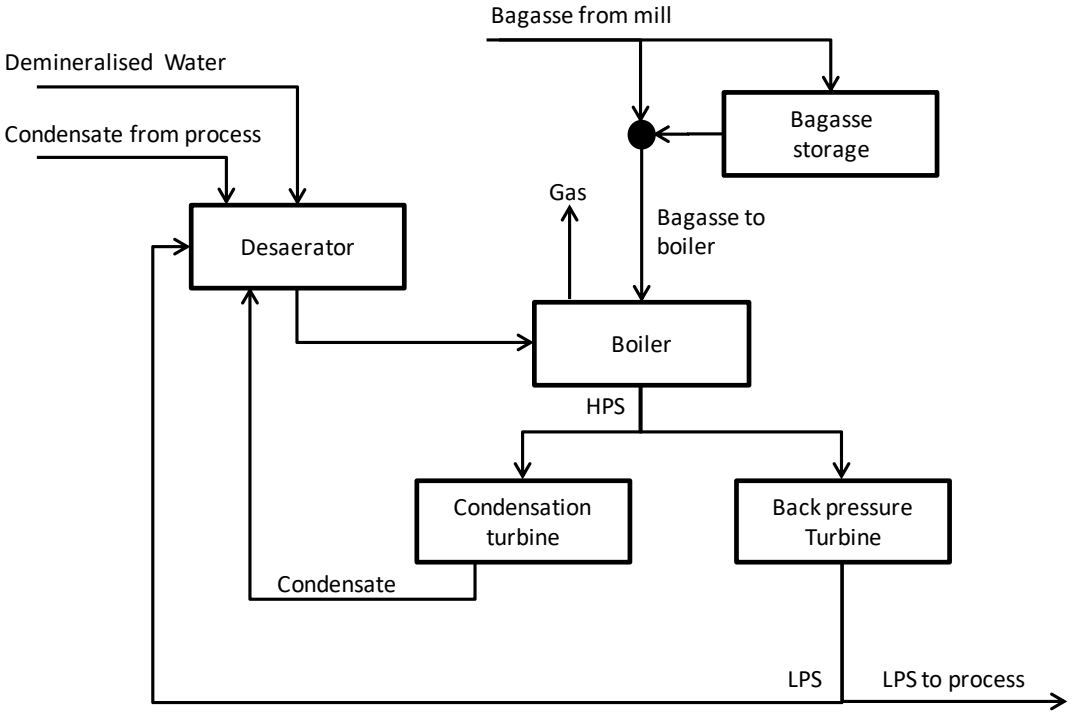

Figure 36 - Schematic diagram of bagasse circuit and high-pressure steam production

4.12.1 Boiler

A boiler or steam generator is a device used to create steam by applying heat energy to water. The fuel for a boiler in the sugarcane industry is the bagasse or another industrial or agricultural residue.

4.12.1.1 Mass and energy balance

This model aims to obtain: (1) the amount of steam produced using bagasse or other fuel, such as straw, wood chips, or lignin; and (2) the combustion gas emitted. Figure 37 summarizes the main inlet and outlet streams from a boiler. The steam produced is obtained using Equation (4.179). The condensed steam that feeds the boiler is obtained by Equation (4.180)

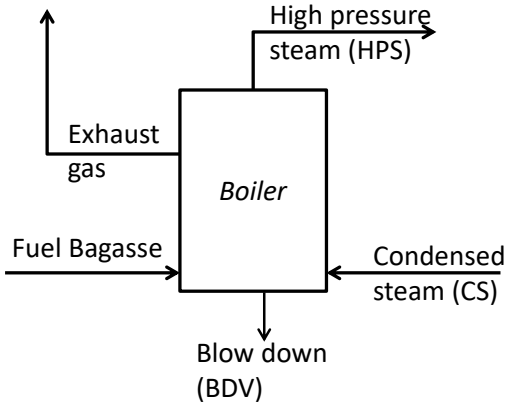

Figure 37 - Schematic diagram of a boiler

$$HPS = \frac{Fuel \cdot LHV}{H_{HPS} - H_{CS}} \cdot Fuel \qquad (4.179)$$

$$CS = \frac{HPS}{1\text{-}BDV} \qquad (4.180)$$

Where:

HPS is the high-pressure steam flow rate, $tonne/h$;

$Fuel$ is the fuel flow rate (bagasse, straw, wood-chips, and lignin), $tonne/h$;

H_{HPS} is the high-pressure steam enthalpy, kJ/kg;

H_{CS} is the condensed steam enthalpy, kJ/kg;

B_Eff is the boiler efficiency;

LHV is the fuel lower heating value or net calorific value, kJ/kg;

CS is the condensed Steam, $tonne/h$;

BDV is the boiler blowdown and other losses of condensate as a ratio of the total steam produced HPS.

The net calorific value or the lower heating value, which is the term LHV in Equation (4.179), assumes that the water formed by combustion and the moisture of the fuel remain in the vapor state. This value depends on the fuel used in the boiler. This simulation platform simulates the use of bagasse, straw, wood chips, and lignin. They can be used alone or mixed. The equations and parameters of each fuel are described as follows:

a) LHV for bagasse and straw.

The net calorific value of wet bagasse and straw is obtained using the empirical equation adapted from Hugot (1960, p. 921). The difference between bagasse and straw, when using Equation (4.181), is the moisture of each.

$$LHV = 19259 \cdot f + 16747 \cdot S - 196 \cdot D - \Delta Hw \cdot (W + 0.585 \cdot f) \qquad (4.181)$$

Where:

19259 is the calorific value of fiber, kJ/kg;

f is the of fiber to bagasse, $kg_{fiber}/kg_{bagasse}$;

16747 is the calorific value of sugar, kJ/kg;

S is the ratio of sugar to bagasse, $kg_{sucrose}/kg_{bagasse}$;

196 is the energy lost to heat the dirty, kJ/kg;

D is the ratio of dirt (such as soil) to bagasse, $kg_{dirt}/kg_{bagasse}$;

ΔHw is the enthalpy to evaporate water, kJ/kg;

W is the ratio of water to bagasse (moisture), $kg_{water}/kg_{bagasse}$;

$0.585 \cdot f$ is the water formed during the combustion.

b) LHV for wood-chips.

The net calorific value of wet wood-chips is obtained using Equation (4.182).

$$LHV = 18648 - \Delta Hw \cdot W \qquad (4.182)$$

Where:

18648 is the lower calorific value of dry wood, kJ/kg (GEBREEGZIABHER; OYEDUN; HUI, 2013);

ΔHw is the enthalpy to evaporate water, kJ/kg;

W is the ratio of water to wood-chips (moisture), $kg_{water}/kg_{bagasse.}$

c) LHV for Lignin

The net calorific value of lignin is obtained by Equation (4.183).

$$LHV = 22460\,(1-W) - \Delta Hw \cdot (9 \cdot 0.06 + W) \qquad (4.183)$$

Where

22460 is the higher heating value of lignin, kJ/kg (DOMALSKI; EVANS; JOBE JR, 1979, p. 57);

ΔHw is the enthalpy to evaporate water, kJ/kg;

W is the ratio of water to lignin (moisture), $kg_{water}/kg_{bagasse}$;

0.06 is the H_2 content in lignin that produces water due to combustion (DOMALSKI; EVANS; JOBE JR, 1979, p. 57).

The exhaustion gas is calculated from the composition of the elemental in the fuel. Biomass contains five main fuel elements: C; H_2; S; N; O_2. Table 14 shows the elements of the fuels used on a dry basis. However, it is worthy of mention that moisture and inert elements depend on many factors, such as the way biomass is handled, how long it has been in stock, the variety of the plant that originates the biomass, etc.

Table 14 – Basic elements for the bagasse wood-chips and lignin

Element	Bagasse ($kg/kg_{fuel}\,dry$)	Straw ($kg/kg_{fuel}\,dry$)	Wood-chips ($kg/kg_{fuel}\,dry$)	Lignin ($kg/kg_{fuel}\,dry$)
C	0.465	0.465	0.500	0.60
H_2	0.070	0.070	0.060	0.06
O_2	0.465	0.465	0.430	0.34
S	0	0	0.005	0
N	0	0	0.005	0
Moisture	0.5034 [(a)]	0.15 [(a)]	0.35 [(b)]	0.85 [(c)]
Inert	0.044 [(a)]	0.015 [(a)]	0.015 [(b)]	0.015 [(c)]

(a) Input from from extraction area, (b) (DEMIRBAS, 2017) (c)(DIOGO JOSÉ HORST, 2013; ROCHA *et al.*, 2015).

The combustion gas is composed of CO_2, H_2O, SO_2, N_2, O_2, NO_x, and CH_4. Although NO_x and CH_4 are not the most abundant species in the flue gas, they are significant due to the environmental impact and are calculated using the emission factor summarized in Table 15.

Table 15 - Emission factor and unreacted carbon

Element	Bagasse, (kg/kg_{fuel})	Straw , (kg/kg_{fuel})	Wood-chips (kg/kg_{fuel})	Lignin (kg/kg_{fuel})
$g\ (C)^{(a)}$	0.015	0.015	0.015	0.015
$h\ (CO)^{(a)}$	0.005	0.015	0.005	0.0
$i\ (CH_4)^{(a)}$	0.0	0.0	0	0.0000216
$m\ (NOx)^{(b)}$	0.0006	0.0	0	0.0009
$PM^{(a)}$	0.0078	0.0078	0.0078	0.0

Source [(a)] (CORTEZ; GÓMEZ, 1998) [(b)] (U.S. ENVIRONMENTAL PROTECTION AGENCY, 1993)

A completed combustion reaction means that all carbon has become CO_2. The incomplete combustion reaction results in unburned carbon and CO. The incomplete combustion reaction is given by the following chemical equation.

$$[a\,C + b\,H_2 + c\,O_2 + d\,S + e\,N + Moisture + Inert] + \alpha[0.766\,N_2 + 0.206\,O_2 + 0.009\,Ar + 0.019\,H_2O]$$
$$\rightarrow [g\,C + h\,CO + i\,CH4 + j\,CO_2 + k\,H_2O + l\,SO_2 + m\,NOx + nN_2 + o\,Ar + p\,O_2 + Ash]$$

The excess of air is obtained according to Equations (4.184 and 4.185). The chemical coefficients *g, h,* and *i* are the parameters in which the incompleteness of the reaction is given in Table 15. The chemical reaction coefficients of the products *j, k, l, m, n, o,* and *p* are obtained according to Equations (4.186 – 4.191).

$$\alpha = \frac{StoicO2 \cdot Excess}{0.206} \tag{4.184}$$

$$StoicO2 = a\frac{MM_{O_2}}{MM_C} + b\frac{MM_{O_2}}{2 \cdot MM_{H(;^2)}} + d\frac{MM_{O_2}}{MM_{SO_2}} - c; \tag{4.185}$$

$$j = (a - g - h - i)\frac{MM_{CO_2}}{MM_C} \quad (4.186)$$

$$k = f + b\,\frac{MM_{H_2O}}{MM_{H_2}} \quad (4.187)$$

$$l = d\,\frac{MM_{SO_2}}{MM_S} \quad (4.188)$$

$$n = \alpha \cdot 0.766 + e\frac{MM_{N_2}}{MM_N} - m\,\frac{MM_{N_2}}{MM_{NO_x}} \quad (4.189)$$

$$p = \alpha \cdot 0.206 + f - j\frac{MM_{O_2}}{MM_{CO_2}} - (k - f - \alpha \cdot 0.019)\frac{MM_{O_2}}{2 \cdot MM_{H_2O}} - l\frac{MM_{O_2}}{MM_{SO_2}} - m\frac{MM_{O_2}}{MM_{NO_x}} \quad (4.190)$$

$$o = \alpha \cdot 0.009 \quad (4.191)$$

Where

a is the ratio of carbon, C, to fuel in dry basis, kg/kg_{fuel};

b is the ratio of hydrogen, H_2, to fuel in dry basis, kg/kg_{fuel};

c is the ratio of oxygen, O_2, to fuel in dry basis, kg/kg_{fuel};

d is the ratio of sulfur, S, to fuel in dry basis, kg/kg_{fuel};

e is the ratio of nitrogen, N, to fuel in dry basis, kg/kg_{fuel};

f is the ratio of water, $Moiture$, to fuel in dry basis, kg/kg_{fuel};

Inert refers to the inert material such as soil, kg/kg_{fuel};

α is the combustion air-fuel ratio, kg/kg_{fuel} ;

StoicO2 is the stoichiometric oxygen necessary to complete the reaction;

Excess is the excess air added to the combustion *(1.15 to 1.30)* ;

j,k,I,n,o, and p are the parameters used to obtain the composition of the gas form from the combustion reactions kg/kg_{fuel} .

Each component in the combustion gas is obtained by Equations (4.192 – 4.200). Gas emission is the sum of the components and is given by Equation (4.201). Ash is obtained by the mass balance according to Equation (4.202). In this model, all inert material entering the boiler is considered to become ash, as well as unburned carbon that has not been released as particulate matter.

$$CO = h \cdot fuel \qquad (4.192)$$

$$CO_2 = j \cdot fuel \qquad (4.193)$$

$$H_2O = k \cdot fuel \qquad (4.194)$$

$$SO_2 = l \cdot fuel \qquad (4.195)$$

$$NO_x = m \cdot fuel \qquad (4.196)$$

$$N_2 = n \cdot fuel \qquad (4.197)$$

$$Ar = o \cdot fuel \qquad (4.198)$$

$$O_2 = p \cdot fuel \qquad (4.199)$$

$$PM = PM \cdot fuel \tag{4.200}$$

$$G = CO + CO_2 + H_2O + SO_2 + NO_x + N_2 + Ar + O_2 + PM \tag{4.201}$$

$$Ash = Inert + C - PM \tag{4.202}$$

Where:

CO, CO_2, H_2O, etc. are the flow rate of the respective molecules, *tonne/h*;

G is the total gas flow rate, *tonne/h*;

Ash is the ash flor rate, *tonne/h*.

4.12.1.2 Power

There are many electrical devices in this area, such as fans, feed conveyors, ash conveyors, etc. They were not calculated individually, and the boiler is considered to consume $7.0\ kW$ per tonne of steam.

4.12.2 Steam turbine generator

The high-pressure steam produced in the boiler is used to rotate the blades of a turbine to create mechanical (or rotational) energy. This rotational energy caused by the high-pressure steam turbine is used to generate electricity from an attached generator.

4.12.2.1 Mass and energy balance

Defining an ideal turbine provides a basis for analyzing turbine performance. An ideal turbine performs the maximum amount of work theoretically possible. An actual turbine produces less work due to blade friction and other losses. The isentropic efficiency of a turbine is defined as an ideal turbine that operates at constant entropy. Therefore, the efficiency of the turbine is defined as the ratio of the actual work done by the turbine to the work that would be done by the turbine if it were an ideal turbine according to Equation (4.203).

$$\eta_{turb} = \frac{W_{actual}}{W_{ideal}} = \frac{H_{in} - H_{out,actual}}{(H_{in} - H_{out,ideal})} \quad (4.203)$$

Besides turbine efficiency, the electricity produced should take into account the gear and generator efficiency. Consequently, the electricity produced is obtained by Equation (4.204).

$$Elec = \frac{\eta_{gen} \cdot \eta_{red} \cdot \eta_{turb} \cdot HPS \cdot (H_{in} - H_{out})}{3600} \quad (4.204)$$

Where:

$Elec$ is the electricity produced, MW;

η_{gen} is the generator efficiency;

η_{red} is the gear efficiency;

HPS is the steam-feed stream flow rate, $tonne/h$;

H_{in} is the inlet steam enthalpy, kJ/kg;

H_{out} is the outlet steam enthalpy, kJ/kg;

4.12.2.2 Water utility

A turbine also requires water to cool the gear oil and bearing. This amount of water is given by the specific consumption of $5420\ kg$ of cooling water per MW.

4.12.3 Condenser

A condensation turbine requires a condenser attached to the exhaustion steam nozzle. This allows the steam to exhaust the turbine under a vacuum. When the exhaust steam from a turbine is above atmospheric pressure, the turbine is a ‘backpressure turbine’ and when it is below atmospheric pressure, it is a ‘condensation turbine’.

4.12.3.1 Mass and energy balance

This model aims to obtain the cooling water used to condense the steam, which is obtained by the energy balance according to Equation (4.205).

$$m_{cool} = \frac{LPS \cdot (H_{LPS} - H_{cs})}{cp \cdot T_{w,in} - cp \cdot T_{w,out}} \quad (4.205)$$

Where

m_{cool} is the cooling water flow rate, *tonne/h*;

LPS is the exhaust steam flow rate, *tonne/h*;

H_{LPS} is the enthalpy of the exhaust steam, *kJ/kg;*

H_{cs} is the enthalpy of the condensate, *kJ/kg;*

cp is the specific heat capacity of the cooling water, kJ/(kg·K);

$T_{w,in}$ is the feed water temperature, *°C;*

$T_{w,out}$ is the returning water temperature, *°C.*

4.12.3.2 Power

The electricity consumption in this step is due to the pumping of the condensate from the condensation turbine to the deaerator. Thus, it is obtained by the model described in Section 4.3.1. The power consumption due to the pumping of cooling water is calculated in Section 4.14.1

4.12.4 Deaerator

The deaerator is used to remove the non-condensable gases (oxygen and free carbon dioxide) from the make-up water used to feed the boiler. This is done by heating the feed stream to 120 °C and then letting it flash. The deaerator also serves as a buffer tank to feed the boiler, which under no circumstances can be interrupted. This model aims to obtain the vapor used to heat the condensate and demineralized water. The main streams involved in this process are shown in Figure 38.

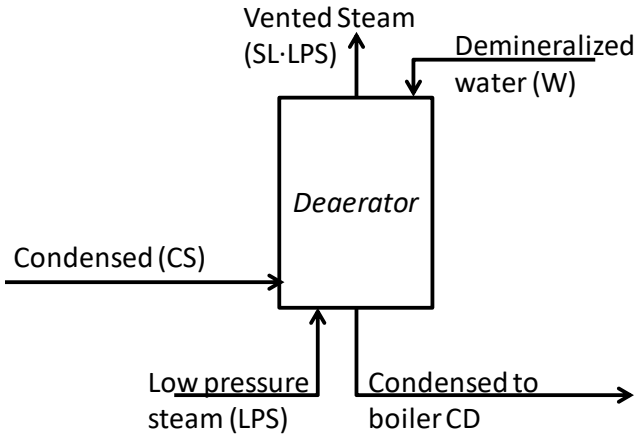

Figure 38 - Schematic diagram of a deaerator

4.12.4.1 Mass and energy balance

The make-up water and the steam are obtained by the mass and energy balance shown in Equations (4.206 and 4.207), respectively.

$$W = CD + SL \cdot LPS - CS - LPS \qquad (4.206)$$

$$LPS = \frac{\Sigma(CS \cdot H_{CS}) + W \cdot H_w}{H_{LPS} \cdot SL} \qquad (4.207)$$

Where

LPS is the low-pressure steam used at the deaerator, $tonne/h$;

H_{LPS} is the low-pressure steam enthalpy, kJ/kg;

CS is the feed condensate, $tonne/h$;

CD is the condensate pumped to the boiler, $tonne/h$;

H_{CS} is the condensate steam enthalpy, kJ/kg;

W is the make-up water, $tonne/h$;

H_w is the make-up water enthalpy, kJ/kg;

SL is the steam vented to the atmosphere, kg_{Steam}/kg_{LPS}.

4.12.4.2 Power

The electricity consumption in this step is due to pump the condensate to feed the boiler at high pressure. Consequently, the electrical power consumption in this area is given by the model described in Section 4.3.1.

4.13 Combustion gas treatment

This is the area in which the boiler combustion gas is wetly scrubbed to remove soot particles. The aim of modeling the combustion gas treatment is to obtain the required make-up water, the composition and amount of flue gas emitted and the cake, which contains the ash. The mathematical model is divided into 4 steps: wet scrubber, liming, milk of lime preparation, clarification, and filtration. These steps are interconnected by the scrubbing fluid, which is treated and recirculates in a closed circuit, as shown in Figure 39. The recycling flow rate is calculated using the fixed-point interaction method, in which the first guess of the recycling flow (filtrated) is zero. The next subsections describe the mathematical model and the parameters used in each step.

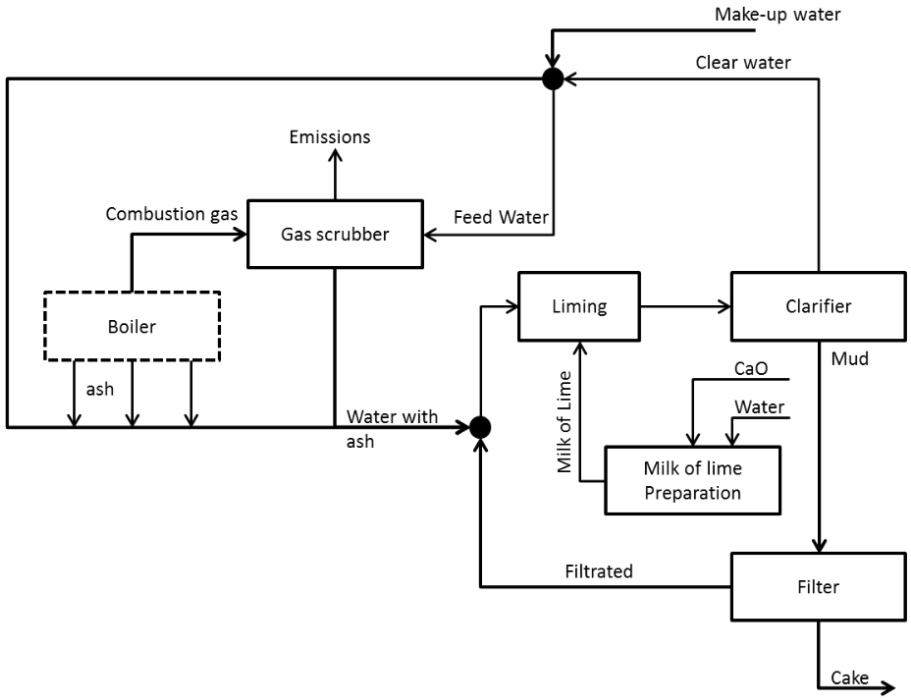

Figure 39 - Schematic flow diagram of combustion gas treatment

4.13.1 Boiler gas wet scrubber

Scrubber systems are a type of air pollution control device used to remove particulate matter from chimney exhaust. It uses water to remove unwanted pollutants from a flue. There are many types of gas scrubber, and probably the simplest is the spray tower, as shown schematically in Figure 40.

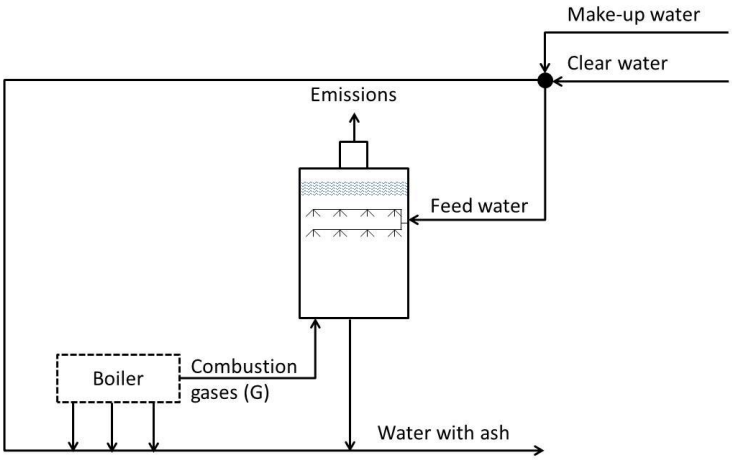

Figure 40 - schematic flow in a spray type tower gas scrubber

4.13.1.1 Mass balance

This model aims to determine the gas emissions, the amount of water used to scrub this gas, the water with ash, and the make-up water. Mass balance and an efficiency parameter as shown in Equations (4.208 – 4.211) are used. Also, 0.17 kg of water per kg of gas is considered (PIMENTEL *et al.*, 2004). The removal efficiencies for a spray tower can be as high as 90% for particles larger than 5 µm. The removal efficiencies for particles of 3 to 5 µm diameter range from 60 to 80%. Below 3 µm, removal efficiencies drop to less than 50% (MUSSATTI; HEMMER, 2002).

$$Emission = Gas - (PM)\cdot(1-\eta) \qquad (4.208)$$

$$FeedWater = WG\cdot gas \qquad (4.209)$$

$$WaterWithAsh = FeedWater + PM\cdot\eta \qquad (4.210)$$

$$MakeUpWater = FeedWater - ClearWater \quad (4.211)$$

Where:

Emission is the final gas emissions, *tonne/h*;

Gas is the combustion gas from the boiler, *tonne/h*;

PM is the particulate emission, *tonne/h*;

η is the soot particles remove efficiency;

FeedWater is the feed-water flow rate, *tonne/h*;

WG is the specific ratio of water to gas, *kg of water / kg of gas*;

WaterWithAsh is the returning water to the water treatment plant, *tonne/h.*

4.13.2 Liming and milk of lime preparation

The water with ash from the previous unit operation feeds a clarifier. However, before clarification, lime is used to adjust the pH to about 7. Usually, a pH analyzer and an automatic dosing system are used to control the milk of lime dosed. In this work, a parameter based on average industrial consumption is used.

4.13.2.1 Mass balance

This model aims to obtain the amount of water and calcium added to the recirculation stream, which is done by dosing milk of lime. The amount of milk of lime dosed is obtained using Equation (4.212), which uses a parameter called '*Calcium concentration*' given in *kg* of $Ca(OH)_2$ per *kg* of water; the average consumption of a typical industry is $7.05 \cdot 10^{-4} kg/kg$. This is the concentration of calcium hydroxide necessary to achieve a pH equal to 7 by mixing milk of lime into the stream. The milk of lime is obtained by mixing *CaO* with water; the amount of water used and the milk consumed depend on the concentration of milk, typically 0.05 *kg* of $Ca(OH)_2$ per *kg* of water, and $Ca(OH)_2$, which is given by Equation (4.213).

$$Milk\ of\ lime\ (kg/h) = \frac{Calcium\ concentration}{Milk\ of\ lime\ concentration} \cdot (waterWithAsh\ (kg/h)) \quad (4.212)$$

$$Water = \frac{Ca(OH)_2}{Milk\ of\ lime\ concentration} \qquad (4.213)$$

4.13.2.2 Power

The electricity consumed at this stage is the result of pumping milk and the mixer on the tank where the reaction between ash and lime occurs. Thus, the electrical consumption due to pumping is obtained by the model described in Section 4.3.1. The mixer uses a specific power of $1.015\ kW/m^3$.

4.13.3 Clarification

Clarifiers are settling tanks for the continuous removal of solids deposited by sedimentation. A clarifier is generally used to remove solid particulates or suspended solids from liquid for clarification or thickening. The water with ash is sent to a clarifier, which allows settling of the suspended solids. As shown in Figure 41, the supernatant is drawn from the clarifier and pumped back to the gas scrubber in a closed circuit, and the sludge is sent to filtration for dewatering.

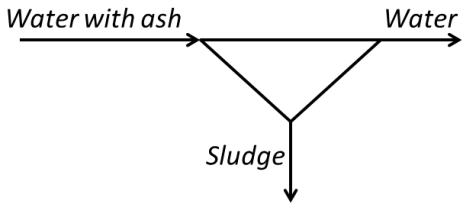

Figure 41 - Schematic flow diagram of juice decanter

4.13.3.1 Mass balance

This model aims to obtain the flow rate of sludge and clear water as a function of the flow rate of water with ash. Equation (4.214) is the mass balance of the clarifier and Equation (4.215) is the parametric equation where the parameters '*Ash retention efficiency*' and '*Concentration of ash in sludge*' must be known. The '*Ash retention efficiency*' is defined in Equation (4.216), and the '*Concentration of ash in sludge*' is defined in Equation (4.217).

These parameters are available in the literature, and the suspended solid concentration in the sludge is between 4.8% and 7% and the retention efficiency is 64% (REIN, 2007, p. 274).

$$Clearwater = Water\ with\ Ash - Sludge \quad (4.214)$$

$$Sludge = \frac{Ash\ retention\ efficiency\ _x\ Ash\ in\ water}{Concentration\ of\ Ash\ in\ Sludge} \quad (4.215)$$

$$Ash\ retention\ efficiency = \frac{Ash\ in\ mud}{Ash\ in\ clear\ water} \quad (4.216)$$

$$Concentration\ of\ ash\ in\ Sludge = \frac{Ash\ in\ Sludge}{Sludge} \quad (4.217)$$

Where:

Clearwater is the clear water flow rate, *tonne/h*;

Water with Ash is the feed flow rate to the clarifier, *tonne/h*;

Sludge is the bottom stream flow rate out of the clarifier, *tonne/h*.

4.13.3.2 Power

The electric power consumed in this step is due to the pumping of the clear water back to the gas scrubber and the sludge to the filtration. Therefore, the electrical power consumption in this unit operation is given by the equation described in Section 4.3.1. The sludge scraper uses a small power, which makes no difference in the electricity demand for this step, and thus is neglected.

4.13.4 Filtration:

In this step, the decanter sludge is dewatered and the cake produced is sent to the field as a fertilizer. In a belt-press filter, the sludge is first drained under gravity before being

sandwiched between two endless filtering belts. The pressure of the tensioned belts squeezes the water out of the sludge with a continuous discharge of the cake.

4.13.4.1 Mass balance

This model aims to obtain the Filtrated and Cake as functions of the sludge flow rate. The cake is obtained based on two parameters from the literature: filtering efficiency and cake moisture (MARTEL, 1993). The filtering efficiency is the parameter that gives the amount of solid retained by the filter at about 85%. The moisture of the cake is about 80%. The sludge is considered to be composed only of water and insoluble solids, ash. The filtrated stream is obtained by the overall mass balance, as given by Equations (4.218 and 4.219).

$$Cake = \frac{FiltEff \cdot Mud \cdot Ash\_Sludge}{(1 - Moisture)} \qquad (4.218)$$

$$Filtrated = Sludge - Cake \qquad (4.219)$$

Where:

FiltEff is the filter efficiency;

Sludge is the sludge flow rate, *tonne/h*;

Ash_Sludge is the ratio of insoluble solids to Sludge;

Moisture is the ratio of water to cake;

Filtrated is the filtrated flow rate, *tonne/h*;

Cake is the cake flow rate, *tonne/h*.

4.13.4.2 Power

The electric power consumed in this step is due to the pumping of the filtrated and the motor to move the belt. The electrical demand to move the belt press is estimated to be 0.75 kW per tonne of sludge. The electrical power consumption to pump the filtrated in this unit operation is given by the model described in Section 4.3.1.

4.14 Cooling water utility

This is the area in which the utility cooling water is cooled in a closed circuit. The production of ethanol requires water in the distillery condenser to cool the wine during fermentation and the broth before yeast inoculation. Sugar production requires cooling water at the barometric condensers for sugar crystallization and the last effect of multiple-effect evaporation. The turbine in electric power generation also requires water to cool the gear oil and bearing. When a condensation turbine is used, water is required to condensate the steam. Most sugarcane mills in Brazil do not use a closed circuit to cool the centrifugal pump seal and the vacuum pump seal because it requires a small amount of water. Therefore, to obtain a more realistic approach, this simulation platform considers that the open circuit is used to cool the seals, as shown in Section 4.16.

The aim of modeling the cooling water area is to obtain the evaporation of the water, the flow rate of the blowdown, and make-up water. The mathematical model is divided into two steps: cooling towers and cooling spray. The cooling spray system is used to cool the water from the sugar and multiple-effect evaporation, and the cooling tower is used to cool the water from the remaining areas.

4.14.1 Cooling tower

A cooling tower is a heat rejection device that rejects heat into the atmosphere through the evaporation of water. It is used to remove process heat and cool the utility fluid to near the wet-bulb air temperature. The aim is to obtain the evaporation rate, blowdown, and make-up water as shown in Figure 42; additionally, the power consumed is obtained.

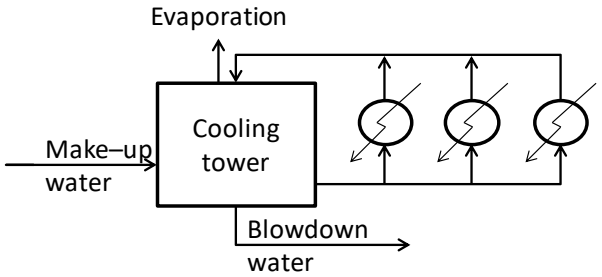

Figure 42 - Schematic flow diagram for a closed circuit cooling tower

4.14.1.1 Mass and energy balance

The evaporated water is calculated using Equation (4.220). The water discharged from the system to control the salt concentration is obtained by Equation (4.221). Make-up is obtained from the mass balance according to Equation (4.222). The term cycles of concentration, C, compares the level of salts of the recirculating cooling tower to the level of salts of the raw make-up water. Typically, circulating water has five times the salt concentration than the make-up water, so the concentration cycle is 5.

$$E = \frac{RR \cdot (H_{W,in} - H_{W,out})}{(DH_{vap}) - H_{W,out}} \qquad (4.220)$$

$$BV = \frac{E}{C - 1} \qquad (4.221)$$

$$M = E + BV \qquad (4.222)$$

Where:

RR is the circulating water, $tonne/h$;

$H_{w,in}$ is the enthalpy of the water into the tower, kJ/kg;

$H_{w,out}$ is the enthalpy of the water out of the tower, kJ/kg;

$\Delta H_{w,in}$ is the enthalpy of water vaporization, kJ/kg;

E is the water vaporization rate, $tonne/h$;

C is cycles of concentration (number of cycles)

BV is the blowdown water, $tonne/h$;

M is make-up water, $tonne/h$.

4.14.1.2 Power

The electric power consumed in this step is due to the pumping of the cooling water and driving the cooling tower fan. The electrical demand to drive the fan is estimated to be

$0.05\ kW$ per tonne of water. The electrical power consumption of the pumps is given by the model described in Section 4.3.1.

4.14.2 Cooling spray

The cooling spray is used in direct contact condensers, in which the coolant is brought into contact with the vapor, such as the barometric condenser described in Section 4.3.4. It has the advantage of being low cost and simple to use, but its use is restricted to those applications in which mixing of vapor and coolant is allowed. The aim is to obtain the evaporation rate, blowdown, and make-up water as shown in Figure 43; additionally, the power consumed is obtained.

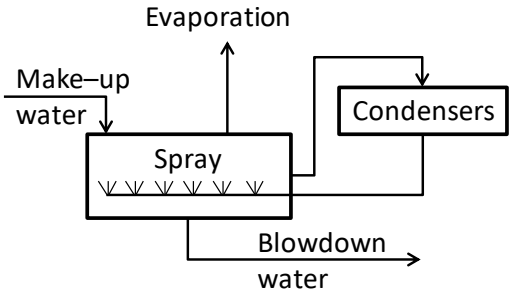

Figure 43 - Schematic flow diagram for a closed-circuit cooling spray system

4.14.2.1 Mass and energy balance

The evaporated water is calculated using Equation (4.223). Note that the condensed steam is incorporated with the cooling water. Consequently, the returning cooling water is different from the feed water and is obtained by Equation (4.224). Since some amount of water is incorporated into the returning stream, the water discharged from the system to control the salt concentration is obtained by Equation (4.225), and therefore no make-up is required in the cooling spray system.

$$E = \frac{RW \cdot H_{W,in} - FW \cdot H_{W,out}}{(DH_{vap})} \qquad (4.223)$$

$$RW = FW + St \qquad (4.224)$$

$$BV = RW - E - FW \qquad (4.225)$$

Where:

RW is the returning water, $tonne/h$;

FW is the feed water, $tonne/h$;

St is the vapor condensed at the direct contact condenser;

$H_{w,in}$ is the enthalpy of the water into the spray, kJ/kg;

$H_{w,out}$ is the enthalpy of the water out of the spray, kJ/kg;

$\Delta H_{w,in}$ is the enthalpy of water vaporization, kJ/kg;

E is the water vaporization rate, $tonne/h$;

C is cycles of concentration (number of cycles);

BV is the blowdown water, $tonne/h$;

M is make-up water (t/h).

4.14.2.2 Power

The electric power consumed in this step is due to the pumping of the cooling water. Thus, the electrical power consumption to pump the closed-circuit cooling water is given by the model described in Section 4.3.1.

4.15 Water treatment and demineralization

This is the area that supplies the water to feed the boiler. The make-up water in high-pressure boilers must be demineralized to avoid scale formation. Demineralized water can be obtained using a reverse osmosis membrane or ion exchange resin. This model considers only reverse osmosis, which is the most widely used one.

The aim of this area is to obtain industrial water consumption, wastewater, and concentrated water as a function of demineralized water. The mathematical model is divided into two steps: water treatment and demineralization, as shown in Figure 44.

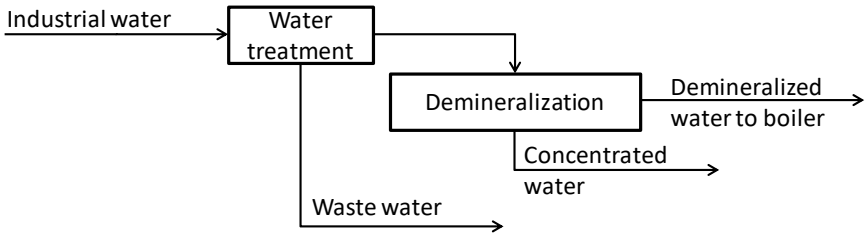

Figure 44 - Schematic flow diagram of a water treatment plant and demineralization

4.15.1 Water treatment

Wastewater and raw industrial water are obtained as a function of the treated water. Wastewater is obtained using the parametric equation in which the *WTP* relates the wastewater production per treated water. This parameter depends on the quality of industrial water and may vary according to the source of water abstraction and also during the seasons. An average value of *0.1* was considered. Industrial raw water and wastewater are obtained using Equations (4.226 and 4.227).

$$WasteWater = WTP \cdot TreatedWater \qquad (4.226)$$

$$IndustrialWater = WasteWater + TreatedWater \qquad (4.227)$$

Where:

TreatedWater, is the amount of water used in the demineralization process, *tonne/h*;

IndustrialWater is the amount of water used to produce the required treated water, *tonne/h*;

WTP is the ratio of wastewater to treated water;

WasteWater is the amount of water rejected, *tonne/h*.

4.15.2 Demineralization

Similar to the water treatment plant, reverse osmosis rejects part of the water as concentrated water, which is rich in salts. A parametric equation in which the *DMTP* is the ratio of concentrated water to demineralized water was used. An average value of *0.05* from a typical sugarcane industry was considered. The treated water, from the water treatment

plant, that feeds the reverse osmosis and the concentrated water are obtained using Equations (4.228 and 4.229).

$$ConcentratedWater = DMTP \cdot DemiWater \quad (4.228)$$

$$TreatedWater = ConcentratedWater + DemiWater \quad (4.229)$$

Where:

DemiWater is the amount of water necessary at the boiler, *tonne/h*;

DMTP is the ratio of concentrated water to demineralized water;

ConcentratedWater is the amount of water rejected due to the water demineralization process, *tonne/h*;

4.15.3 Power

The electric power consumed in this step is due to the pumping of raw industrial water, treated water, and demineralized water. Thus, the electrical power consumption of the pump is given as described in Section 4.3.1. Electricity consumption due to dosing pumps, mixers, electrical panels, illumination, etc. makes no difference in the electricity demand for this area, and it is neglected.

4.16 Water abstraction

In this unit, the total water consumption is inventoried. Water abstraction is calculated from the mass balance of the total water produced and consumed in the industry. As aforementioned, water is necessary for many steps of the sugarcane process. It can be added to juice streams for imbibition, must and yeast dilution, and filtering; make-up for cooling water systems; and for cleaning up. Sugarcane also contains approximately 70% water and the sugarcane water is removed from the sugarcane juice by evaporation. Thus, the condensed vapor is also used as a source of water in the industry.

This unit is responsible for the inventory of the consumption and production of water in all other areas. Thus, the aim is to obtain the total water abstraction and the surplus hot water. Figure 45 summarizes the hot water consumption, and Figure 46 summarizes the total

industrial raw water consumption. The aforementioned areas explain how water is used. The stream named 'Cleaning and other uses', shown in Figure 46, is calculated in this work using a specific consumption from a typical sugarcane mill industry, which is 0.15 m^3 of water per tonne of sugarcane.

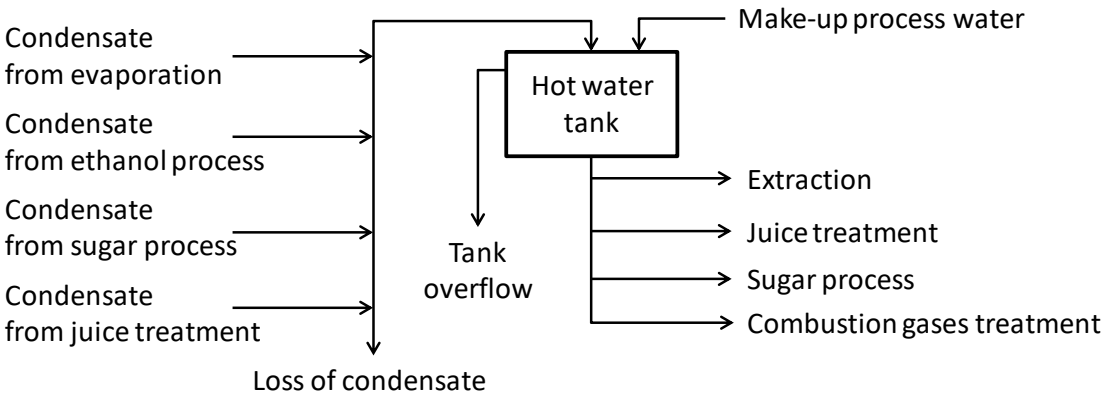

Figure 45 - Schematic hot water flowchart identifying mains consumers and producers

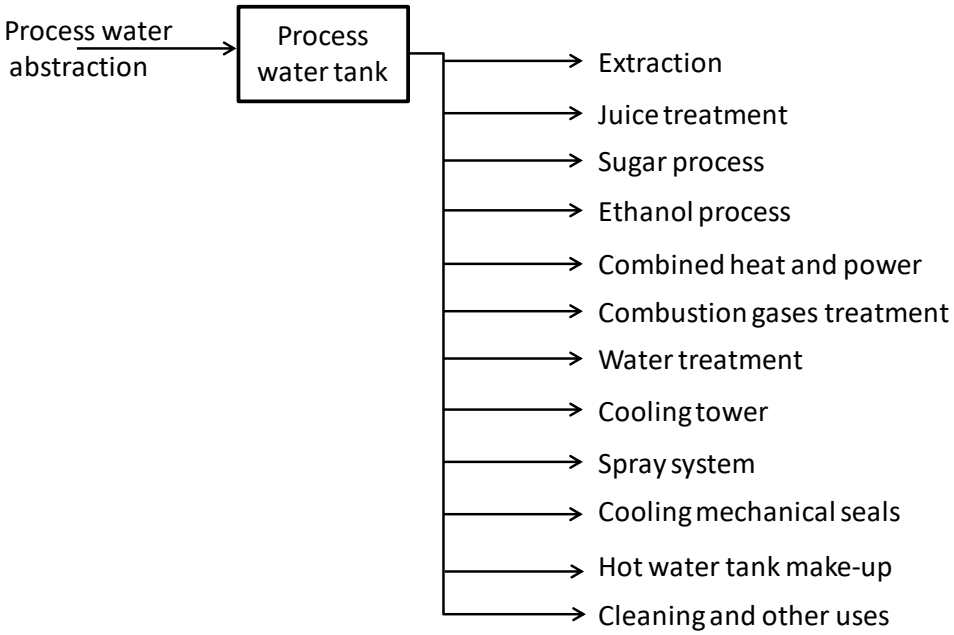

Figure 46 - Schematic process water flowchart identifying mains consumers

4.16.1 Power

The electric power consumed in this step is due to the pumping of the water abstraction. Thus, the electrical power consumption of the pump is given by the model described in Section 4.3.1. Electricity consumption due to electrical panels, illumination, etc. makes no difference in the electricity demand for this area and is neglected.

4.17 Convergence algorithm between areas

Figure 47 shows the area and the interconnections among them. The number indicates the sequence in which the areas are solved in the proposed model. The arrows represent the input and output in each area: an output from one area can be an input for another or a result of the simulation. The large arrows represent the feedstock and products of the whole industry. The thicker arrows are the recycling streams, which require this algorithm to converge. There are three convergence steps: first, the flow rate of vinasse is unknown when the regenerative heat exchange between sugar juice and vinasse is solved; second, the clear ethanol juice is unknown when the ethanol juice passes through the regenerative heat exchange; and third, the steam required in the sugar and ethanol process is also unknown when the evaporation area is solved. These recycling streams are inputs from an area that will be solved after the current area is solved. The direct substitution method was used to solve these recycling loops, and the initial guess of the flow rate of the recycling streams is either zero or the last simulation result.

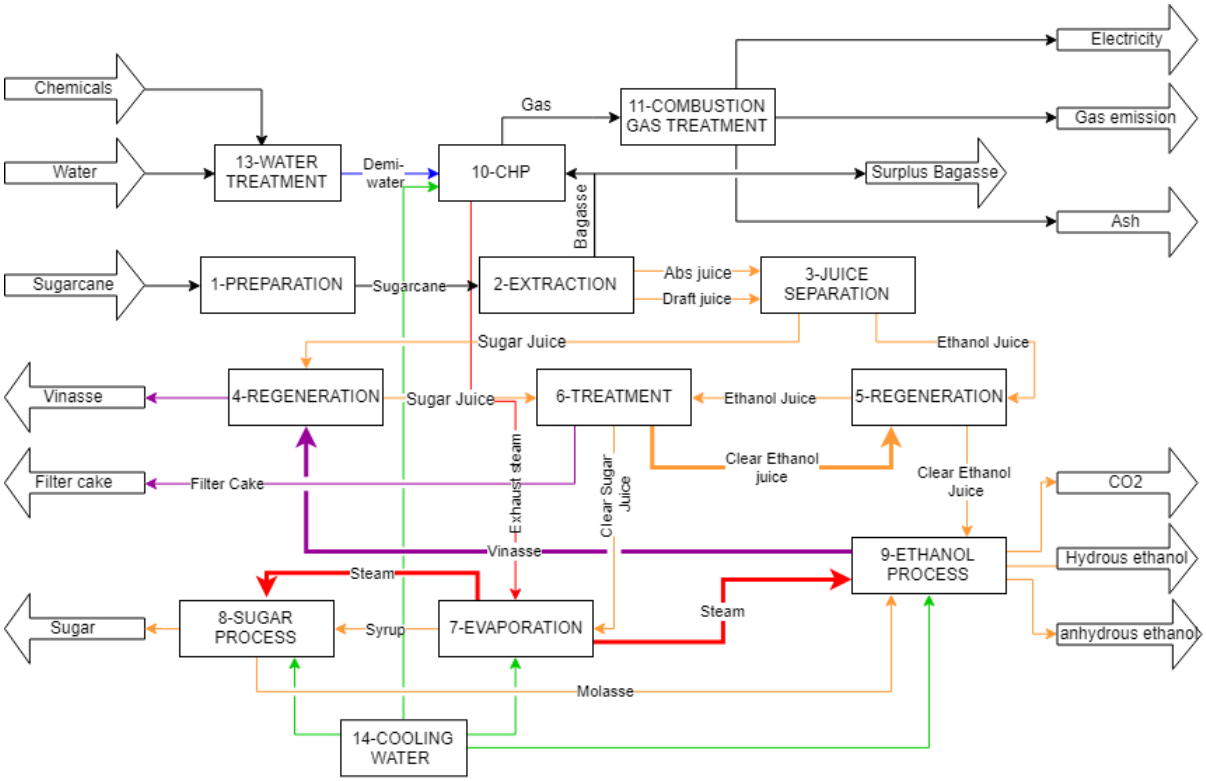

Figure 47 – Interconnection among the areas

4.18 Conclusion

This simulation platform demonstrates to be a powerful tool that can be used to obtain reliable information about the production of first-generation ethanol, sugar and electricity. Furthermore, this simulation platform was conceived to be constantly updated, for example, to include new technologies, such as vacuum distillation; to assess specific variables, such as fertilizer potential of residues (vinasse and filtering cake); or to widen the scope, such as include the agricultural production or supply chain. These updates could be carried out on one area or on one device, since they are independent but interconnected, or even a new area could be connected to this simulation platform.

References

ALFA LAVAL. **Alfa Laval centrifuge FESX 712B**, [s.d.]. Disponível em: <https://www.alfalaval.com/globalassets/documents/products/separation/centrifugal-separators/disc-stack-separators/fesx-712b-pchs00058en.pdf>. Acesso em: 19 fev. 2018.

ASTOLFI-FILHO, Zailer et al. Rheology and fluid dynamics properties of sugarcane juice. **Biochemical Engineering Journal**, [s. l.], v. 53, n. 3, p. 260–265, 2011. Disponível em: <https://www.sciencedirect.com/science/article/pii/S1369703X1000313X#bib0135>. Acesso em: 14 jun. 2018.

CASTRO, Bruno J. C. De et al. Sucrose crystallization: modeling and evaluation of production responses to typical process fluctuations. **Brazilian Journal of Chemical Engineering**, [s. l.], v. 36, n. 3, p. 1237–1253, 2019. a. Disponível em: <http://www.scielo.br/scielo.php?script=sci_arttext&pid=S0104-66322019000301237&tlng=en>

CASTRO, Rubens Eliseu Nicula De et al. Assessment of Sugarcane-Based Ethanol Production. In: BASSO, Thalita Peixoto; BASSO, Luiz Carlos (Eds.). **Fuel Ethanol Production from Sugarcane**. [s.l.] : IntechOpen, 2019. b. p. 3–22.

CASTRO, Sebastião Beltrão De; ANDRADE, Samara Alvachian C. **Tecnologia do açúcar**. 1ª edição ed. Recife: Editora Universitária da UFPE, 2007.

CHANDEL, Anuj Kumar et al. Techno-Economic Analysis of Second-Generation Ethanol in Brazil: Competitive, Complementary Aspects with First-Generation Ethanol. In: **Biofuels in Brazil**. Cham: Springer International Publishing, 2014. p. 1–29.

CHIAPPETA, A.; NASCIMENTO, C. A. O. do. Modelagem matematica e simulacao das operacoes da industria de acucar e alcool. I: moagem da cana. **Revista Brasileira de Engenharia Quimica**, [s. l.], v. 9, n. 4, 1989. Disponível em: https://www.osti.gov/etdeweb/biblio/654250.

CHIAPPETTA, A.; GIUDICI, R.; NASCIMENTO, C. A. O. do. Modelagem matematica e simulacao

das operacoes da industria de acucar e alcool: 2 - evaporacao. **Revista Brasileira de Engenharia Quimica**, [s. l.], v. 9, n. 5, 1986. Disponível em: https://www.osti.gov/etdeweb/biblio/6663O5.

CORTEZ, L. A. B.; GÓMEZ, E. O. A Methos for Exergy Analysis of Sugarcane Bagasse Boilers. **Brazilian Journal of Chemical Engineering**, [s. l.], v. 15, n. 1, p. 59–65, 1998. Disponível em: <http://www.scielo.br/scielo.php?script=sci_arttext&pid=S0104-66321998000100006&lng=en&tlng=en>. Acesso em: 15 fev. 2018.

DELFINI, Paulo. Revisão na moenda. In: 14º SEMINÁRIO BRASILEIRO AGROINDUSTRIAL 2013, Ribeirão Preto. **Anais**... Ribeirão Preto

DEMIRBAS, Ayhan. Higher heating values of lignin types from wood and non-wood lignocellulosic biomasses. **Energy Sources, Part A: Recovery, Utilization, and Environmental Effects**, [s. l.], v. 39, n. 6, p. 592–598, 2017. Disponível em: <https://www.tandfonline.com/doi/full/10.1080/15567036.2016.1248798>. Acesso em: 29 jul. 2020.

DIOGO JOSÉ HORST. **Avaliação da Produção Energética a Partir de Ligninas Contidas em Biomassa**. 2013. UNIVERSIDADE TECNOLÓGICA FEDERAL DO PARANÁ , [s. l.], 2013. Disponível em: <http://www.pg.utfpr.edu.br/dirppg/ppgep/dissertacoes/arquivos/216/Dissertacao.pdf>. Acesso em: 8 ago. 2018.

DOMALSKI, Eugene S.; EVANS, William H.; JOBE JR, Thomas L. **Thermodynamic Data for Waste Incineration**. New York, N.Y.

DOS SANTOS, Moacyr L. et al. ESTUDO DAS CONDIÇÕES DE ESTOCAGEM DO BAGAÇO DE CANA-DE-AÇÚCAR POR ANÁLISE TÉRMICA. **Quim. Nova**, [s. l.], v. 34, n. 3, p. 507–511, 2011. Disponível em: <http://quimicanova.sbq.org.br/imagebank/pdf/Vol34No3_507_23-NT10049.pdf>. Acesso em: 14 fev. 2018.

FAÇO. **Manual de Transportador de Correias**São PauloAllis Mineral System, , 1995.

FURLAN, Felipe Fernando et al. Assessing the production of first and second generation bioethanol from sugarcane through the integration of global optimization and process detailed modeling. **Computers and Chemical Engineering**, [s. l.], v. 43, p. 1–9, 2012.

GEBREEGZIABHER, Tesfaldet; OYEDUN, Adetoyese Olajire; HUI, Chi Wai. Optimum biomass drying for combustion – A modeling approach. **Energy**, [s. l.], v. 53, p. 67–73, 2013. Disponível em: <https://www.sciencedirect.com/science/article/pii/S0360544213001801>. Acesso em: 8 ago. 2018.

GHOSE, T. K.; TYAGI, R. D. Rapid ethanol fermentation of cellulose hydrolysate. II. Product and substrate inhibition and optimization of fermentor design. **Biotechnology and Bioengineering**, [s. l.], v. 21, n. 8, p. 1401–1420, 1979.

GIUDICI, R; NASCIMENTO, C. A. O. . Simulação de fermentador descontínuo alimentado em fermentação alcoólica em regime não-isotérmico. In: **VI Congresso Brasileiro de Engenharia**

Química, 1984. Anais**,** Campinas 1984. v. 3. p. 516-532

HATAKEYAMA, T.; NAKAMURA, K.; HATAKEYAMA, H. Studies on heat capacity of cellulose and lignin by differential scanning calorimetry. **Polymer**, [s. l.], v. 23, n. 12, p. 1801–1804, 1982.

HEI STANDARDS. **Performance Standard for Liquid Ring Vacuum Pumps and Compressors**. 5. ed. [s.l.] : Heat Exchange Institute, 2016. Disponível em: <http://www.heatexchange.org/pubs/03.html>

HOLMGREN, M. **IAPWS**. [s.d.]. Disponível em: <www.iapws.org>. Acesso em: 30 jun. 2017.

HUGOT, E. **Handbook of Cane Sugar Engineering**. 3. ed. [s.l.] : Elsevier, 1960. Disponível em: <https://linkinghub.elsevier.com/retrieve/pii/C20130124373>

IAPWS. **IAPWS The International Association for the Properties of Water and Steam**. [s.d.]. Disponível em: <http://www.iapws.org/release.html#GUIDE>.

IGLESIAS, Miguel Cardemil. **SIMULAÇAO DE SISTEMAS TÉRMICOS PARA GERENCIAMENTO ENERGÉTICO DE USINA SUCROALCOOLEIRA**. 2009. Universidade Federal de Santa Catariana, [s. l.], 2009.

KENT, G. A. A Model to Estimate Milling Unit Throughput. In: PROCEEDING OF AUSTRALIAN SOCIETY SUGARCANE TECHNOLOGY 2001, **Anais**... [s.l: s.n.]

LEAL, M. R. L. V. Energy cane. In: **Cortez, L. A. B. Sugarcane bioethanol**. [s.l.] : Blücher, 2014. p. 751–760.

LIONNET, G. R. E. The effect of the level of extraction on mixed juice purity. In: PROCEEDINGS OF THE SOUTH AFRICAN SUGAR TECHNOLOGISTS' ASSOCIATION 1981, **Anais**... [s.l: s.n.]

MARTEL, C. J. Fundamentals of Sludge Dewatering in Freezing Beds. Water. **Science & Technology**, [s. l.], v. 28, n. 1, p. 29–35, 1993.

MAUSA. **Centrífuga Contínua tipo Konti**. [s.l: s.n.]. Disponível em: <http://www.mausa.com.br/downloads/ficha_tecnica/Centrifuga_Continua_konti_evolution.pdf>. Acesso em: 1 fev. 2018.

MODESTO, Marcelo; ENSINAS, Adriano V.; NEBRA, Silvia A. SUGAR CANE JUICE EXTRACTION SYSTEMS COMPARISON - MILL. In: INTERNATIONAL CONGRESS OF MECHANICAL ENGINEERING 2005, Brazil. **Anais**... Brazil Disponível em: <http://www.abcm.org.br/anais/cobem/2005/PDF/COBEM2005-0836.pdf>. Acesso em: 30 jun. 2017.

MUSSATTI, Daniel; HEMMER, Paula. **Section 6 Particulate Matter Controls Chapter 2 Wet Scrubbers for Particulate Matter**. [s.l.] : United States Environmental Protection Agency, 2002. Disponível em: <https://www.epa.gov/economic-and-cost-analysis-air-pollution-regulations/cost-reports-and-guidance-air-pollution#cost manual>

NASH. **2be1 - 904 - cl - sc**BentleyvilleGardner Denver Nash, LLC, , 2017. Disponível em: <https://www.gardnerdenver.com/en-us/nash/liquid-ring-vacuum-pumps/cl-liquid-ring-

pump-compressor>

PATIENCE, Gregory S. **Experimental methods and instrumentation for chemical engineers**. [s.l.] : Elsevier, 2013.

PEDERSEN, Michael J.; KAY, Webster B.; HERSHEY, Harry C. Excess enthalpies, heat capacities, and excess heat capacities as a function of temperature in liquid mixtures of ethanol + toluene, ethanol + hexamethyldisiloxane, and hexamethyldisiloxane + toluene. **The Journal of Chemical Thermodynamics**, [s. l.], v. 7, n. 12, p. 1107–1118, 1975. Disponível em: <https://www.sciencedirect.com/science/article/pii/0021961475900300>. Acesso em: 13 fev. 2018.

PIMENTEL, I. M. C. et al. BALANÇO HÍDRICO, CARACTERIZAÇÃO E REÚSO DE ÁGUA DE COLUNAS BAROMÉTRICAS NA INDÚSTRIA SUCRO-ALCOOLEIRA - ESTUDO DE CASO -. In: XIII CONGRESSO BRASILEIRO DE ÁGUAS SUBTERRÂNEAS 2004, Cuiabá - MT. **Anais**... Cuiabá - MT Disponível em: <https://aguassubterraneas.abas.org/asubterraneas/article/download/23376/15466%0A>

POLING, Bruce E.; PRAUSNITZ, John M.; O'CONNELL, John P. **The Properties of Gases and Liquids**. 5. ed. [s.l.] : McGraw-Hill, 2004. Disponível em: <http://www.informaworld.com/openurl?genre=article&doi=10.1300/J111v23n03_01&magic=crossref>

REIN, P. W. A Comparison of Cane Diffusion and Milling. In: PROCEEDINGS OF THE SOUTH AFRICAN SUGAR TECHNOLOGY ASSOCIATION 1995, **Anais**... [s.l: s.n.]

REIN, Peter. **Cane Sugar Engineering**. Berlin: Bartens, 2007.

REIN, Peter W.; ECHEVERRY, Luis F.; ACHARYA, Sumanta. Circulation in vacuum pans. **Journal American Society of Sugar Cane Technologists**, [s. l.], v. 24, n. 5, p. 1–17, 2004.

ROCHA, George Jackson de Moraes et al. Influence of mixed sugarcane bagasse samples evaluated by elemental and physical-chemical composition. **Industrial Crops and Products**, [s. l.], v. 64, p. 52–58, 2015.

SILVEIRA, Luís Cláudio Inácio Da et al. Genetic diversity and coefficient of kinship among potential genitors for obtaining cultivars of energy cane. **Revista Ciência Agronômica**, [s. l.], v. 46, n. 2, p. 358–368, 2015. Disponível em: <http://www.ccarevista.ufc.br/seer/index.php/ccarevista/article/view/3382>. Acesso em: 24 jan. 2018.

THAVAL, Omkar P. **Modelling the Flow of Cane Constituents through the Milling Process of a Raw Sugar Factory**. 2012. Queensland University of Technology, [s. l.], 2012.

U.S. ENVIRONMENTAL PROTECTION AGENCY. **Emission Factor Documentation For AP-42 section 1.8 Bagasse Combustion in Sugar Mills**. Durham, NC.

WALSH, G. H. The Riviere Juice Extractor : a New Approach To the Extraction of Juice From Cane. In: PROCEEDINGS OF THE SOUTH AFRICAN SUGAR TECHNOLOGISTS ASSOCIATION 1998,

Anais... [s.l: s.n.]

WALTHER, John V. **Essentials of Geochemistry**. 2nd. ed. [s.l.] : Jones and Bartlett Publishers, 2009. Disponível em: <https://books.google.com.br/books?id=UhW58xSN-T4C&pg=PA622&lpg=PA622&dq=%22118+kJ%22+ethanol&source=bl&ots=IwPBOsSr7Z&sig=nu4DkuuDH2Cv1U4CuzlL9kti5ws&hl=pt-BR&sa=X&ved=0ahUKEwib9u25sofZAhXIxpAKHRfIBKEQ6AEIKTAA#v=onepage&q=%22118 kJ%22 ethanol&f=false>

WIENESE, By A. Mill settings and extraction. In: PROCEEDINGS OF THE SOUTH AFRICAN SUGAR TECHNOLOGISTIS' ASSOCIATION 1990, **Anais**... [s.l: s.n.]

WRIGHT, P. G.; STEGGLES, C. C.; STEINDL, R. J. TheBalanceBetweenCapacityAndPerformanceOfRotaryMudFilters. In: PROCEEDING OF AUSTRALIAN SOCIETY SUGARCANE TECHNOLOGY 1997, **Anais**... [s.l: s.n.]

Appendix A – Results from a sugar production simulation

72 hours of operation were simulated for the set of vacuum pans described in Section 4.10.1. Figures 48 to 53 show the results of the simulation for each vacuum pan. These figures present six variables in each vacuum pan: (a) the volume of the vacuum pan; note that when the vacuum pan reaches the maximum volume it is cut or discharged; (b) the percentage of crystal in massecuite; (c) the supersaturation coefficient; the value shown in this graph when the vacuum pan is in standby has no meaning; (d) the amount of crystal, water, impurity, sucrose, and total mass in the vacuum pan; (e) the feed vapor and the evaporated water from massecuite; (f) the evaporation flow rate; i.e. the water evaporated per heat exchange area; (g) kinetic coefficient; the value shown in this graph, when crystallization is not running, has no meaning; (h) the feed flow rate; (i) the massecuite brix and purity; the value shown in this graph has no meaning when the pan is empty.

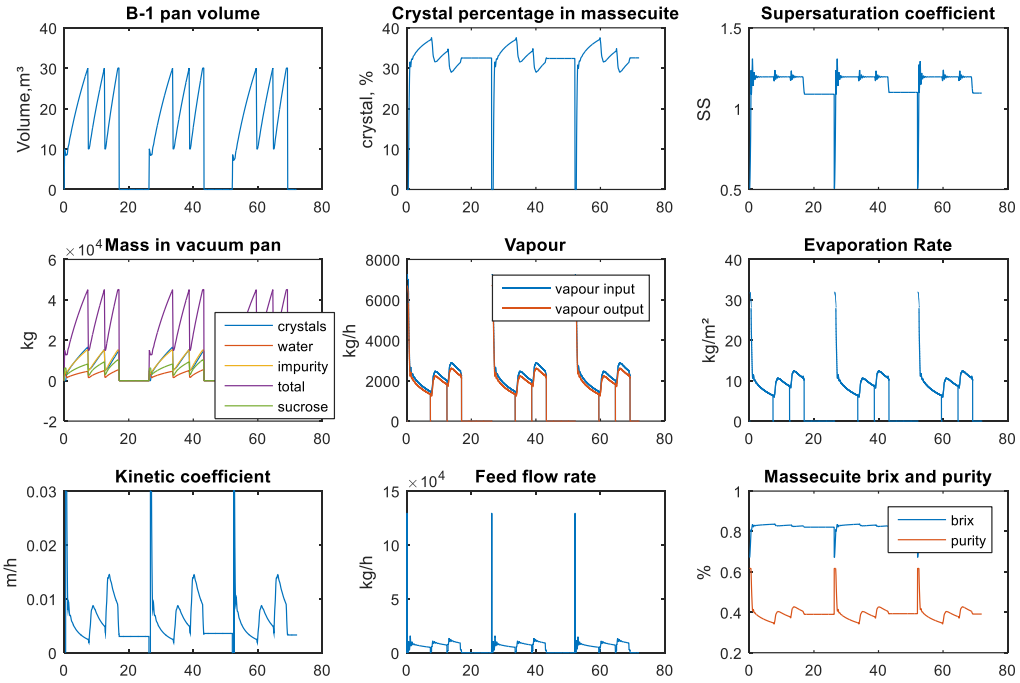

Figure 48 - B-1 vacuum pan run

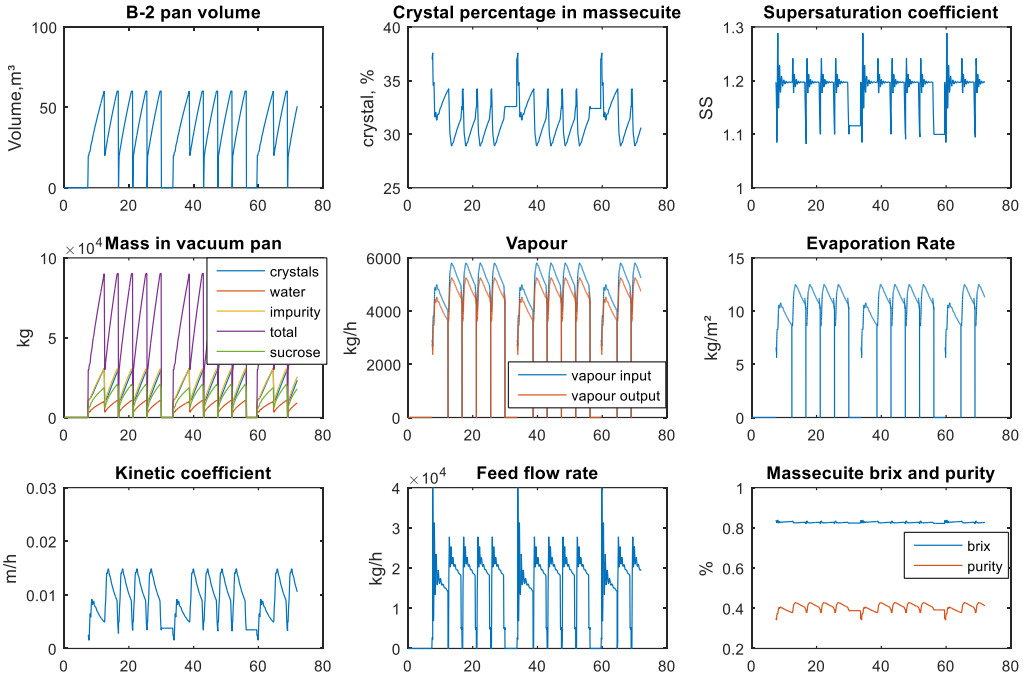

Figure 49 - B-2 vacuum pan run

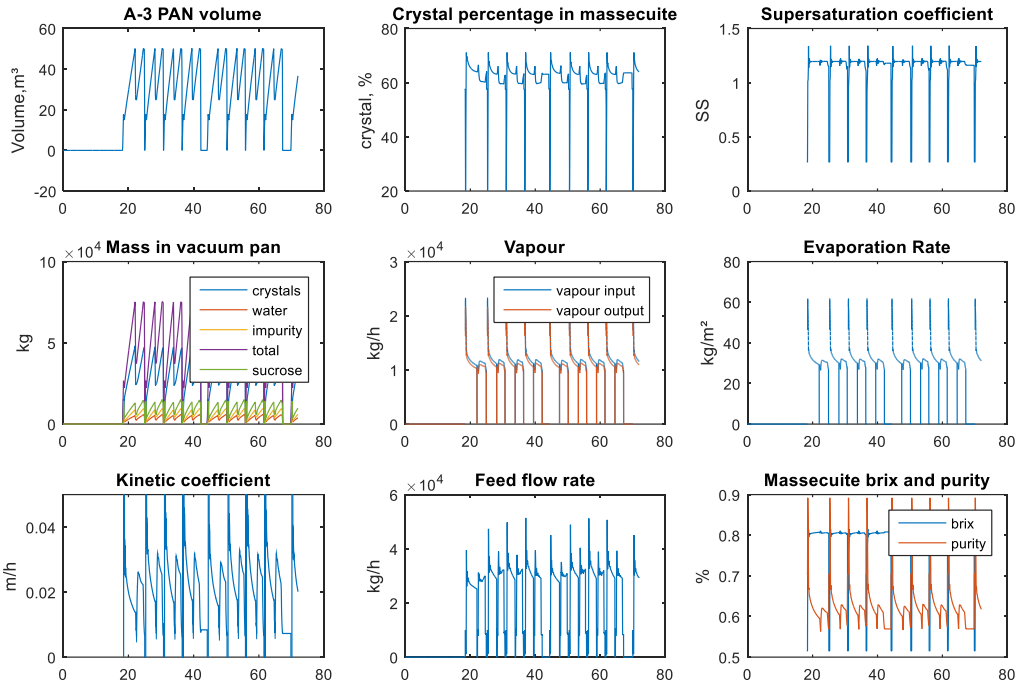

Figure 50 - A-3 vacuum pan run

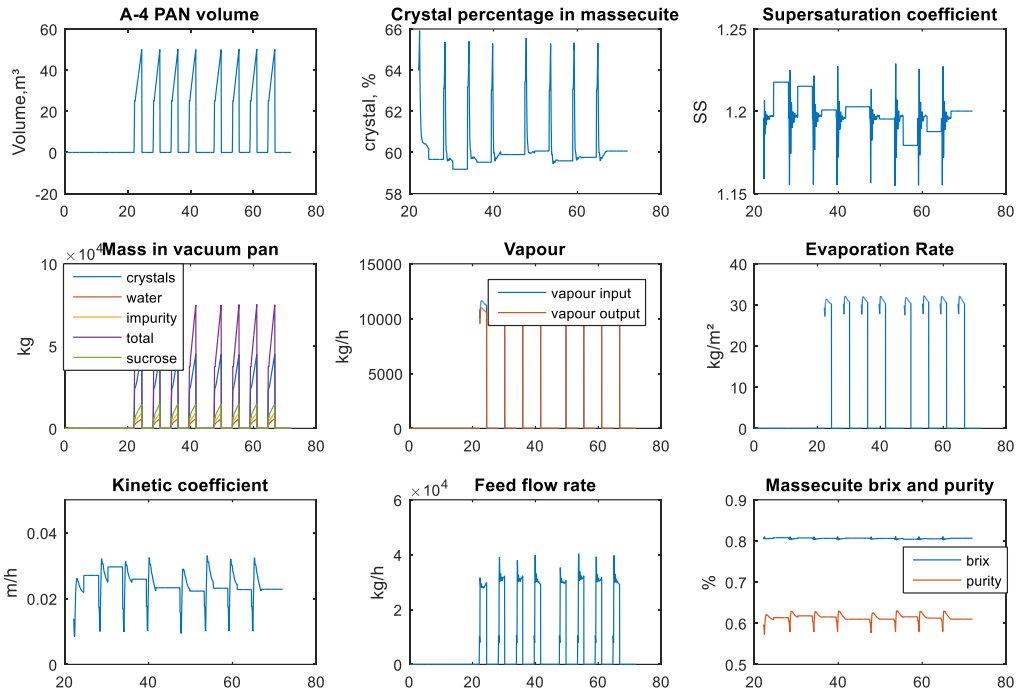

Figure 51 - A-4 vacuum pan run

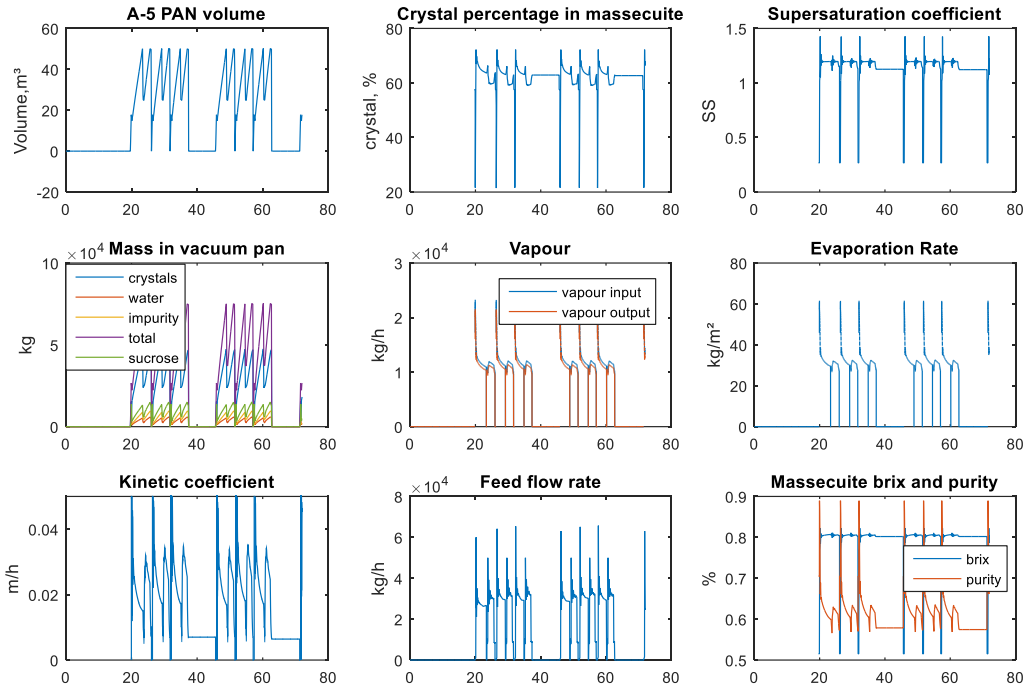

Figure 52 - A-5 vacuum pan run

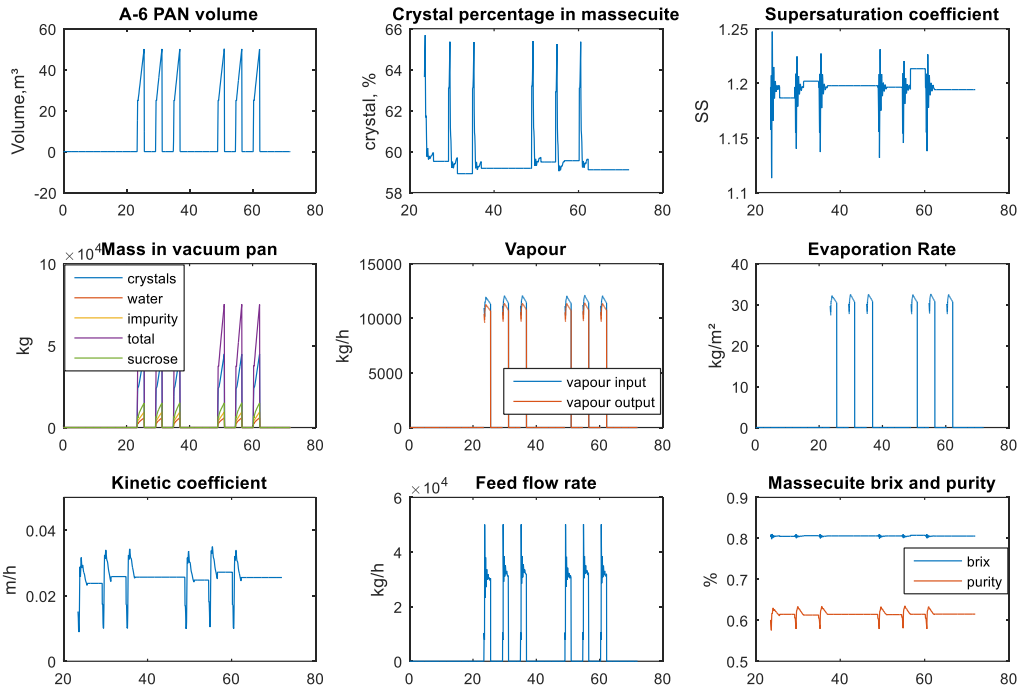

Figure 53 - A-6 vacuum pan run

Appendix B – Results from a fermentation simulation

Figure 54 to Figure 56 show, as an example, the result for a 72-hour simulation of a fed-batch fermentation with four reactors. The parameters and flow rate of the feed streams are summarized in Table 16.

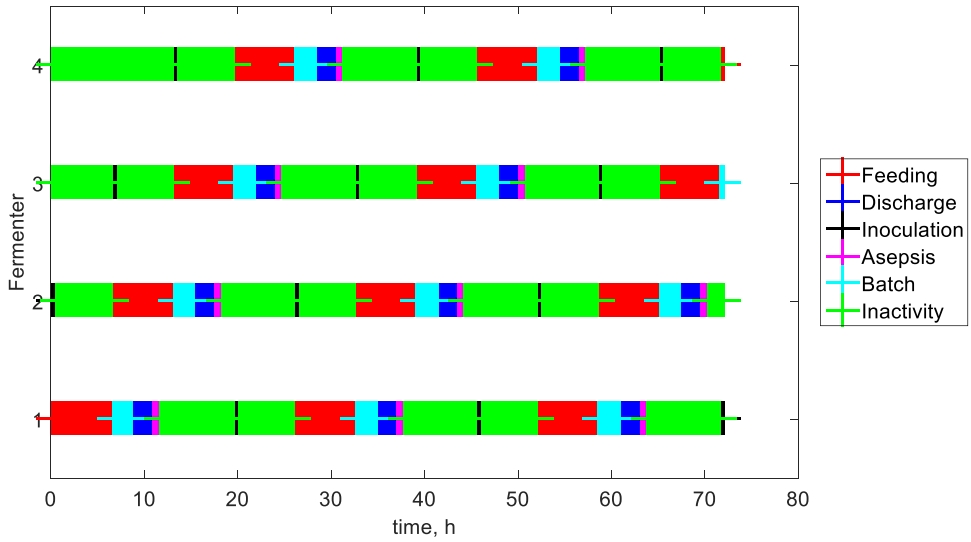

Figure 54 - Fermentation schedules

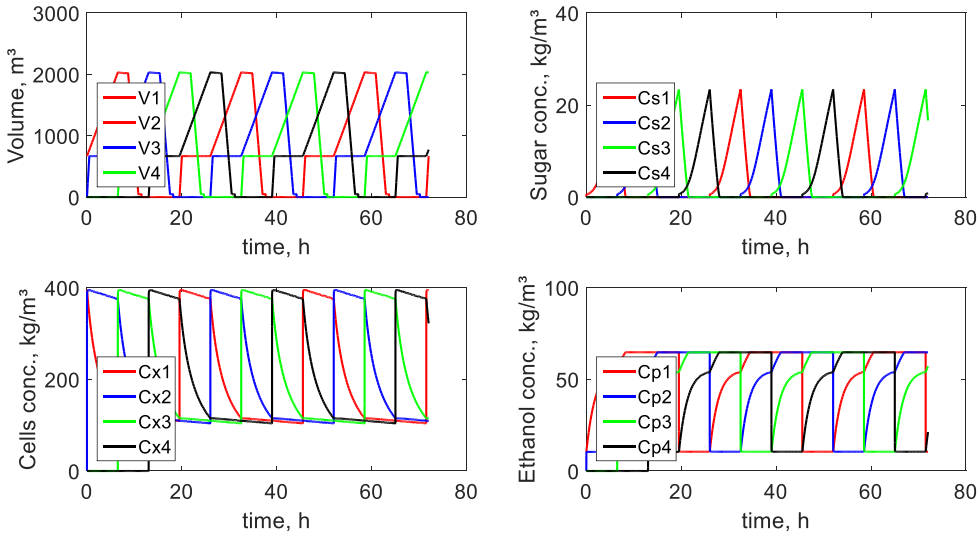

Figure 55 – Fed-batch 72 hours fermentation

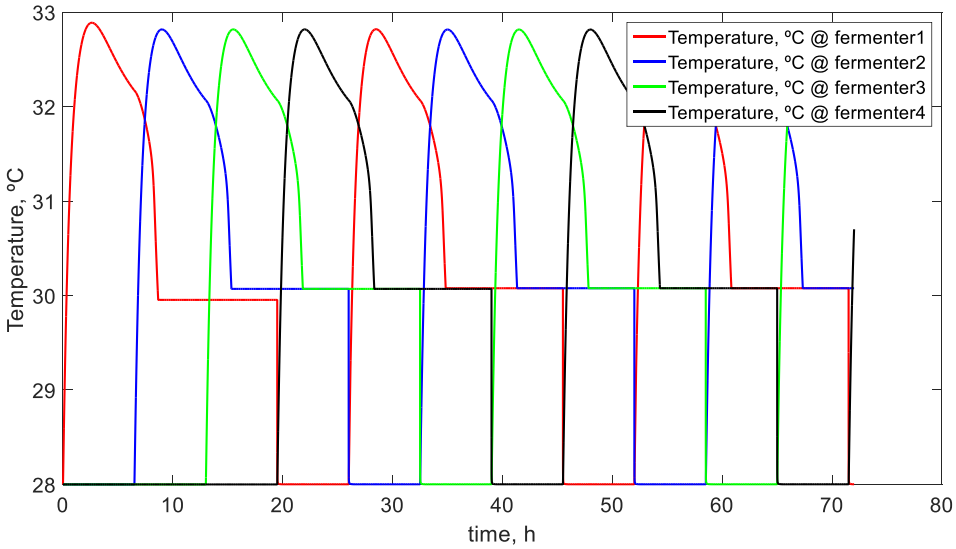

Figure 56 - Temperature change during simulation

Table 16 - Parameters used at simulation

Parameter	Value
kinetic	
μ_{max}	0.012
k_D	0.0083
k_s	0.48
k_i	203.5
C*	90.0
$Y_{X/SUB}$	0.035
$Y_{ETH/SUB}$	$0.9 \cdot \frac{92}{180} = 0.46$
Heat exchanger	
U ($kW/m^2 \cdot K$)	2
A (m^2)	500
$T_{in,f}$ (°C)	28
$F_{in,f}$ (m^3/h)	2000
Substrate inlet	
F_{sub}^{in} (m^3/h)	218.8
Cp_{sub}^{in} ($kJ/(kg \cdot K)$)	3.9
ρ_{sub}^{in} (kg/m^3)	1157
T_{sub}^{in}	32
Milk of yeast inlet	
F_{milk}^{in} (m^3/h)	109
Cp_{milk}^{in} ($kJ/(kg \cdot K)$)	3.9
ρ_{milk}^{in} (kg/m^3)	995
T_{milk}^{in}	28

CHAPTER 5: DYNAMIC SIMULATION OF MULTIPLE-EFFECT EVAPORATION

This chapter corresponds to a full-length article published in Case Studies in Thermal Engineering.

Rubens Eliseu Nicula de Castro, Rita Maria Brito Alves and Claudio Augusto Oller Nascimento. Dynamic simulation of multiple-effect evaporation. **Case Studies in Thermal Engineering**, [s. l.], n. 34, p. 102035, 2022.

Abstract

The main purpose of this work is to simulate multiple-effect evaporation and its variation as a result of the interconnection between batch and continuous unit operations. Therefore, the challenges posed by the hybrid continuous-discrete character of the model are addressed. The computer code is based on detailed fundamental material and energy balance equations, physical and thermodynamic properties, and well-proven correlations for the heat transfer coefficients. A sugarcane industry was used to demonstrate the effectiveness of the model; in this industry, there is an interconnection between a batch and a continuous process. The steam consumed in the batch process changes in each batch step. The results showed that changing the steam flow rate changes the pressure of the steam produced in a multiple-effect evaporation. Additionally, when a bypass valve and a relief valve are used to maintain constant steam pressure, it increases the overall steam consumption.

Keywords: multiple-effect evaporation, batch simulation, sugar crystallization, quasi-steady state, non-steady state.

Nomenclature

A	Area, m²
bpe	Boiling point elevation, K
$Brix$	Soluble solid concentration in kg of soluble solids per kg of solution
C	Concentration in kg of solute per kg of solution
Cp	Specific heat capacity, kJ/(kg·K)
CV	Condensate from a multiple-effect evaporator, kg/s
CVF	Condensate from a flash tank, kg/s
EV	Steam evaporated from a multiple-effect evaporator, kg/s
F	Streamflow rate, kg/s
H	Enthalpy, kJ/kg
ΔH	Enthalpy of vaporization, kJ/kg
J	Juice flow rate, kg/s
$LMTD$	Logarithmic mean temperature difference, K
m	Mass, kg
$\mathring{m}$	Mass flow rate, kg/s
P	Purity in kg of sucrose per kg of solids in solution
q	Heat transfer rate, W
t	Time, s
T	Temperature, °C
V	Feed steam in a multiple-effect evaporator, kg/s
VS	Steam bleed from MEE, kg/s
VFC	Steam flashed, kg/s
δT	Temperature difference,
U	Overall heat coefficient, W/(m²·K)
KG	Crystallization rate, m/h
kg	Kinetic crystallization parameter
ρ	Density, kg/m³

Subscript

c	Crystal
cv	Condensate
$E\ or\ 0$	Exhaust steam: in equations 5.3 to 5.7 the subscript ‘0’ is used instead of ‘E’
$heat$	Used to specify sensible heat when both latent and sensible heat, are exchanged
I	Impurities
i	Evaporation body effect
in	Vacuum pan feed
J	Juice
MC	Massecuite
s	Sucrose
st	Steam
T	Total
vap_out	Steam withdrawn from massecuite
vap_in	Steam consumed in the vacuum pan calandria
w	Water

5.1 Introduction

The multiple-effect evaporation system, MEE, was first adopted in the sugar mill industry in Florida in 1830. Invented by Norbert Rillieux (WAYNE, 2010-), it has since become widely used in many industries, such as pulp and paper,(DIEL *et al.*, 2016) salt production,(VAZQUEZ-ROJAS; GARFIAS-VÁSQUEZ; BAZUA-RUEDA, 2018) and water desalination.(ONISHI *et al.*, 2017) An evaporator is essentially a heat exchanger in which vapor is used to boil a liquid to produce vapor. It is hence possible to treat it as a low-pressure boiler, in which the steam thus produced is used in the following evaporator, and/or it can be used as a heat utility in the industrial process. Similarly, MEE is a thermal unit operation used in industrial processes to produce a concentrated stream. Therefore, MEE plays two roles in the industry: producing utility steam and concentrating a given stream. The higher the number of effects, the more efficient the evaporation process is, which means that the less energy is used to concentrate it.

A dynamic process is one that constantly changes, i.e., a non-steady state. To simulate the multiple-effect evaporation in a non-steady state, we assume a quasi-steady state: this is the situation where all parameters and variables change slowly enough for them to be considered constant for a short period. As an example to illustrate MEE in dynamic behaviour, we used a sugarcane industry process.

In a sugarcane industry, not all processes operate continuously. In some operations, such as sugar crystallization, the main steps operate discontinuously. A batch process delivers its product in discrete amounts. This means that heat, mass, temperature, concentration, and other properties vary with time. Most batch processes are made up of a series of batches and semi-continuous steps. A semi-continuous step runs continuously with periodic start-ups and shutdowns. A liquid stream from a continuous process interconnects to a batch process using buffers, i.e., storage containers. For example, sugar crystallization occurs in a batch vacuum pan; when the sugar crystals reach the required size, the syrup stops being fed and the massecuite is discharged into the massecuite tanks. The massecuite tanks vary their level to ensure the continuous supply of massecuite to centrifugation. Not only do liquid streams, such as syrup and massecuite, vary during the crystallization but also the steam consumed in the vacuum pan. Steam consumption varies because the crystallization process stops to discharge the massecuite and fill with magma before the start of the next crystallization; additionally,

steam consumption also varies during the crystallization process itself: the crystallization starts with a high steam consumption and ends with a lower one due to the increase in the viscosity of the massecuite (HUGOT, 1960, p. 662; PEACOCK; SHAH, 2013). The steam used in this process is bled from the multiple-effect evaporation and this is the reason why MEE operates in a non-steady state.

MEE allows many configurations to be designed; for example, Kaya (2007) has modelled many systems, such as counter-current, co-current, and parallel-current; Ahmetović (AHMETOVIĆ *et al.*, 2017, 2018) used vapor recompression to recycle steam. In the sugarcane industry, the co-current configuration is preferred to avoid sucrose degradation.(PURCHASE; DAY-LEWIS; SCHAFFLER, 1987) In addition to different configurations, many thermal integrations with different streams within the main industrial process are also possible (PINA *et al.*, 2017) or even with some by-processes, such as vinasse concentration (CORTES-RODRÍGUEZ *et al.*, 2018). The integration of MEE into the process has also produced many studies on process optimization (CHANTASIRIWAN, 2017; JIANG; KANG; LIU, 2018) and the application of the pinch analysis technique (HIGA *et al.*, 2009; PINA *et al.*, 2017). The complexity level of the mathematical model depends on the assumption each author made, which results in a number of possibilities in modeling, such as Heluane (2012), who considered fouling in their modeling, and Westphalen (2000), who considered boiling point elevation. The models used by the authors cited above usually consider the temperature (or saturation point pressure) as a constant parameter. This assumption simplifies the resolution of the model since the enthalpy, heat capacity, and heat transfer coefficient are calculated using equations that depend on the temperature and/or pressure. However, these assumptions would produce an imprecise answer and would not be able to simulate changes in steam bleed, such as those caused by the batch crystallization process in the sugarcane industry.

Unlike the models aforementioned, this study proposes a model in which the temperature and pressure of the produced steam are estimated based on the amount of steam consumed: i.e., different consumption of steam results in different steam temperatures. When the temperature of the steam produced in the MEE body increases near the temperature of the fed steam (steam from the previous body in the MEE or exhaustion for the first effect), the production of steam decreases due to the small temperature difference, δT. The steam produced, $\mathring{m}$ in the i^{th} effect, is obtained by Equation (5.1).

$$\mathring{m}_i = \frac{U_i \cdot A_i \cdot \delta T}{\Delta H_i} \qquad (5.1)$$

Therefore, changes in the steam consumption in the process, $\mathring{m}$, result in a change in the temperature difference to produce more or less steam in the MEE. Since the fed steam temperature cannot be modified by the evaporator, the temperature that changes close to or far from the fed steam temperature is that inside the evaporator (T_i in $\delta T = T_i - T_{i-1}$): therefore, even an evaporation body with a large evaporation area would not produce a large amount of steam when T_i approaches T_{i-1} also, a small area evaporator can produce a large amount of steam when the temperature of the produced steam is far from the inlet steam temperature. Additionally, if the temperature is not constant, the heat transfer coefficient, U, and the enthalpy, ΔH, are not constant either, since they are obtained using equations that use the temperature or pressure as a variable. As shown in Equation (5.1), both parameters are used to find the evaporation rate. Therefore, the temperature and pressure of the steam produced in the MEE are a function of the evaporation area (which is constant) and the rate of steam bleed (which varies due to the batch process). The evaporation rate is the sum of the steam bleed and the steam consumed in the next evaporation body. The model proposed in this work also includes the elevation of the boiling point and the sugar concentration in solution. The following hypotheses to reduce the complexity of the mathematical model were used in this study:

- The steam produced in the evaporator is free from sugar or other solutes;
- No degradation of sucrose during the evaporation process;
- No pressure drop in steam pipes.
- Heat dissolution was neglected

5.1.1 Process overview

The application of the proposed model is illustrated through a typical sugarcane industry, which uses batch crystallizers to produce sugar. We have considered that the sugar mill has a five-effect evaporation train, a cogeneration system, and an annexed ethanol process that uses the final molasse and part of the sugarcane juice.

Multiple-effect evaporation (MEE) is responsible for providing thermal energy for all industrial processes, such as the crystallization of sugar, distillation, and juice heating. Therefore, the total thermal energy input for the whole refinery is the exhaust steam, from the turbo-generator or straight from the boiler via a bypass valve, which enters the first-effect evaporator. As an example, Figure 57 shows a steam diagram. The blocks identified as $EVAP_i$ represent the i^{th} evaporation body. In this figure, vapor V_i is the vapor from the i^{th} evaporation body. Part of the vapor produced by the first and second evaporation bodies is used as a process utility heat.

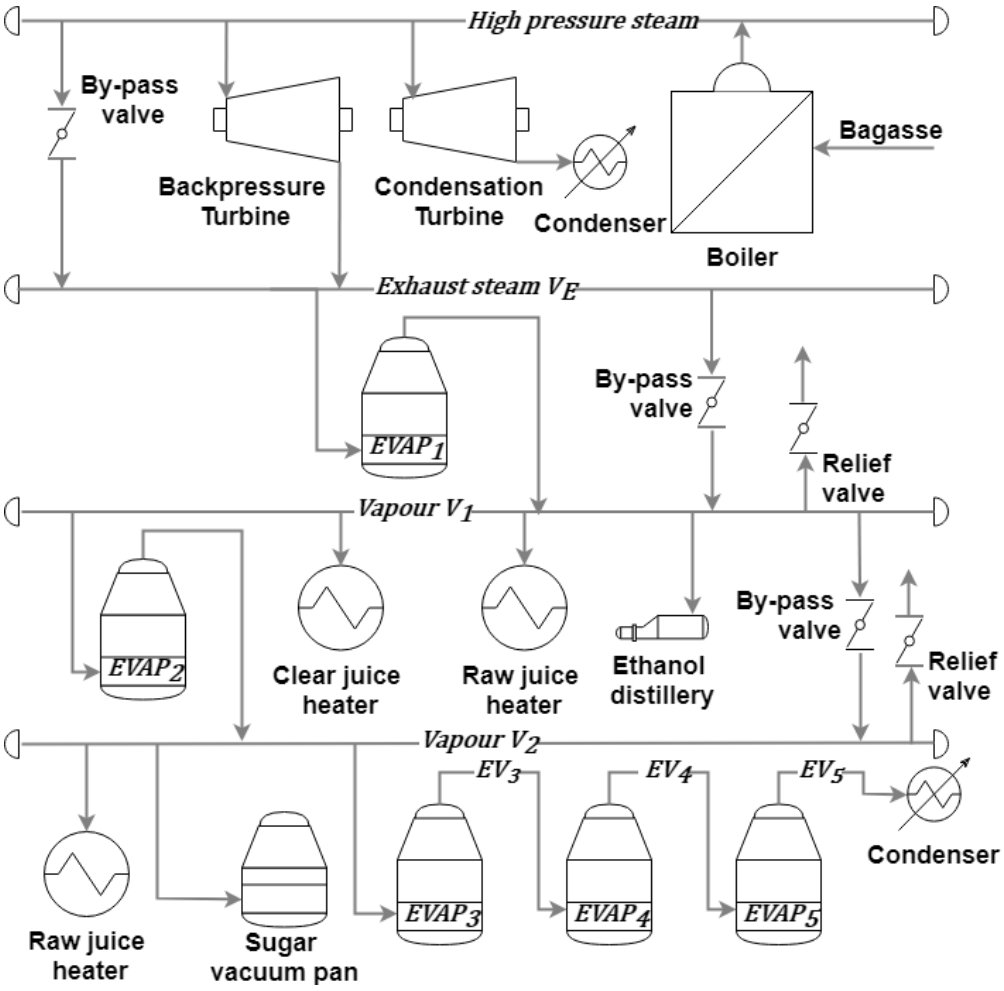

Figure 57 –Steam diagram

In general, evaporators consist of a heating section and an expansion vessel. The Robert evaporator type, which is the most used in sugar factories, consists of a calandria at the bottom and a flash space at the top. Heat is transferred through the tube wall in the calandria: the hotter fluid (fed steam) goes outside the tube and the cold (liquor), inside; thus, the steam condenses outside the tube, and the liquid evaporates inside. The driving force for heat transfer is based on the temperature difference between the steam and the liquor, as

shown by Equation (5.2). The greater the temperature difference, the greater the heat transfer, and thus the greater the production of steam.

$$q_i = U_i \cdot A_i \cdot \delta T, \qquad i = 1, \dots, N \tag{5.2}$$

Figure 58, shown here for explanatory purposes only, present two hypothetical scenarios of the temperature distribution in the same multiple-effect evaporator operating with different temperature distributions. Only the first and last temperatures are the same across the two distributions, because the first is the temperature of the steam from the turbine or boiler, and the last depends on the cooling water and on the efficiency of the barometric condenser. If the area and overall heat coefficient are assumed constant, the increase in the steam bleed results in an increase in the temperature difference. In the example shown in Figure 58, the distribution b) produces more steam in the 2nd effect than a); however, the temperature (and pressure) of the steam produced in b) is lower than a). Note, however, that this also results in a different concentration in the syrup, which causes a different steam consumption in the sugar crystallization process; besides, the different temperature of the steam affects the juice heaters and thus the temperature of the juice that enters the MEE.

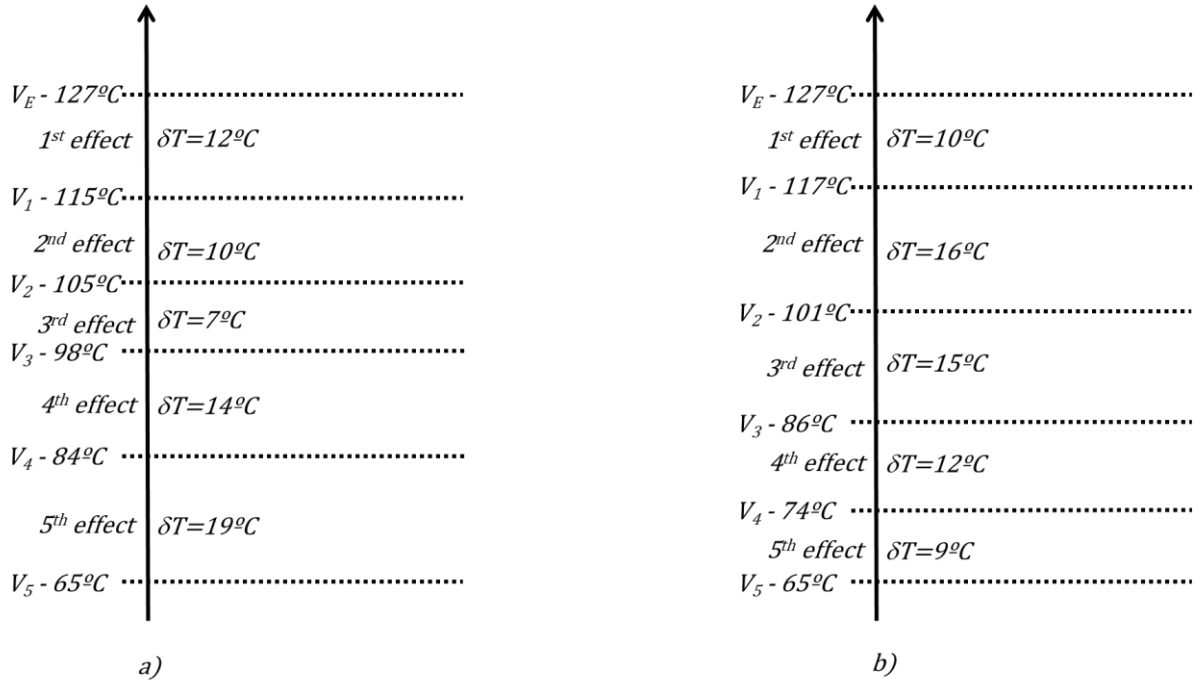

Figure 58 - Temperature distribution in a five-effect evaporation train

Thus, when sugar is crystallized in a batch vacuum pan instead of a continuous vacuum pan, the demand for energy (steam) is different during the batch cycle. To cope with this change in the energy demand, two alternatives are possible: first, one can let the temperature of the MEE oscillate to produce more or less steam as aforementioned; or second, they can keep the temperature of the steam constant by bypassing the higher pressure steam to boost the lower pressure steam when the demand is high or release the steam to the atmosphere when the steam demand is low. Here, we investigate these two possibilities, which require a mathematical model to find the temperature distribution. To our knowledge, there are no models in the literature that allow us to find the temperature distribution in multiple-effect evaporation: the previously mentioned papers use the temperature as a fixed input parameter; to do that, most of them considered the steam consumption as continuous, using the average steam consumption in batch processes.

5.2 Method

In this section, we describe the model used to simulate MEE and sugar batch crystallization. Other unit operations, such as heaters, clarifiers, distillation, extraction, fermentation, boiler, etc. are not shown in this article. These unit operations are described in Castro et al (2018).

5.2.1 Modeling of the Evaporator

The multiple-effect evaporator train is composed of four different unit operations: a) the evaporator itself, identified as $EVAP_i$ in Figure 59; b) the condensate tank, Tk_i, which extracts the condensate from the evaporation body and allows it to flash in the lower pressure steam; c) the mix/splitter, Sp_i, that plays three roles, which are to incorporate the steam flashed from the condensate Tk_i , divert steam to the industrial process (steam bleed) as a thermal utility, and feed the next effect evaporator $EVAP_{i+1}$ with the remaining steam. Therefore, the mathematical model is obtained by balancing the mass and energy in each unit operation and applying the design equation to the evaporator bodies.

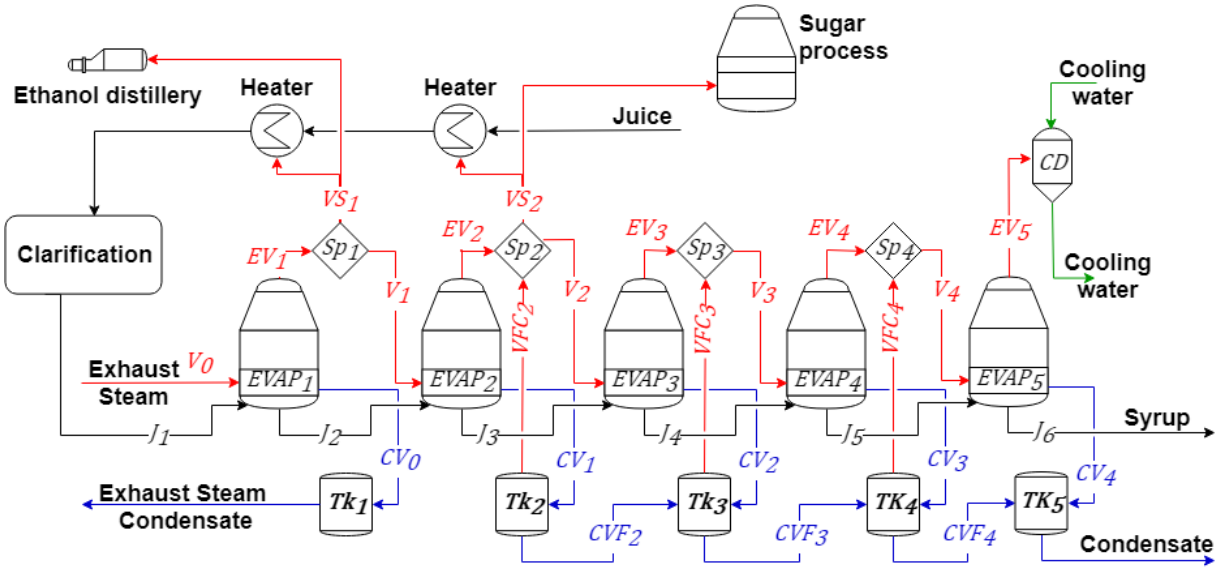

Figure 59 - Multiple effect evaporation representing the steam bleed in the Sugarmill

The expressions of the mass balance around the i^{th} effect evaporator ($EVAP_i$) are given by Equations (5.3) and (5.4). There are *2N* equations according to the number of evaporation effects, where N is the number of evaporation effects. In these equations, J_1 is a known variable that represents the juice stream that enters the MEE; all other variables are calculated.

$$J_i - J_{i+1} - EV_i = 0, \qquad i = 1, \dots, N \tag{5.3}$$

$$V_{i-1} - CV_{i-1} = 0, \qquad i = 1, \dots, N \tag{5.4}$$

The expressions of the energy balance around the i^{th} effect evaporator ($EVAP_i$) are given by Equations (5.5) and (5.6). Once again, there are *2N* equations according to the number of evaporation effects. In this case, the latent heat q_i produced by the condensation of the fed steam is assumed to be transferred entirely to the liquor to produce low-pressure steam. The boiling point elevation caused by the sugar concentration in the juice leads to the production of superheated steam, which quickly cools down and becomes saturated steam before entering the next evaporation body. We assume that this energy of cooling the steam until its saturation point is lost to the surrounding.

$$H_{st,i-1} \cdot V_{i-1} - H_{cv,i-1} \cdot CV_{i-1} - q_i = 0, \qquad i = 1, \dots, N \tag{5.5}$$

$$H_{J,i} \cdot J_i - H_{J,i+1} \cdot J_{i+1} + H_{st,i} \cdot EV_i + q_i = 0, \qquad i = 1, \dots, N \tag{5.6}$$

The heat transferred from the higher-pressure steam condensation to the liquor evaporation is given by Equation (5.7), which is the design equation for a heat transfer unit in the MEE. This equation is the same as Equation (5.1); however, it is rearranged. Thus, the amount of heat transferred depends on the evaporation area, the heat transfer coefficient, and the temperature difference. In this model, the temperature of the steam from the turbine, $T_{st,0}$, and the last effect evaporator, $T_{st,N}$, are known; the intermediary steam temperatures $T_{st,i}$ to $T_{st,N-1}$ are calculated. The term q_{heat} represents the heat necessary for the liquor to raise its temperature to the boiling point; q_{heat} is given by Equation (5.8). The liquor needs to be heated to its boiling point only in the first-evaporation effect: In a feedforward multiple-effect evaporation, this term is equal to zero from the second to the last evaporation body because the liquor enters the evaporation body above its boiling point.

$$U_i \cdot A_i \cdot T_{st,i-1} - U_i \cdot A_i \cdot T_{st,i} - q_i = U_i \cdot A_i \cdot bpe_i + q_{heat}, \qquad i = 1, \dots, N \tag{5.7}$$

$$\begin{aligned} q_{heat} &= U_i \cdot A_i \cdot LMTD, \qquad i = 1 \\ q_{heat} &= 0, \qquad\qquad i = 2, \dots, N \end{aligned} \tag{5.8}$$

The unit operation Mixer/Splitter (Sp_i) is responsible for incorporating steam flashed from the condensate tank and diverting steam between the next evaporation body and the process. The expression of the mass balance around the Mixer/Splitter is given by Equation (5.9). There are N–1 equations according to the number of evaporation bodies; the steam from the last evaporation body is not used as thermal energy. For the evaporation bodies where no steam is bled, the term VS is null.

$$EV_i - V_i + VFC_i - VS_i = 0, \qquad i = 1, \dots, N-1 \tag{5.9}$$

The condensate from the $EVAP_i$ evaporator goes to the Tk_i flash tank, where the condensate flashes into the lower pressure steam. The expressions of the mass and energy balance around the i^{th} flash tank are given by Equations (5.10) and (5.11). Usually, the condensate from the first tank is not allowed to flash on the lower pressure steam, because this condensate is used to feed the boiler in a closed circuit: if the condensate were allowed to flash, it would increase the amount of make-up water in the boiler, which would demand an additional amount of energy to heat this water. Moreover, the last flash tank does not flash in the lowest pressure steam, since this steam is not used as thermal energy: flashing this condensate would hinder the barometric condenser and increase the amount of cooling water. Therefore, there are $2N–2$ equations according to the number of evaporation effects.

$$CV_{i-1} + CVF_{i-1} - VFC_i - CVF_i = 0, \qquad i = 2, \dots, N-1 \tag{5.10}$$

$$H_{cv,i-1} \cdot CV_{i-1} - H_{st,i+1} \cdot VFC_i + H_{cv,i-1} \cdot CVF_{i-1} - H_{st,i-1} \cdot CVF_{i-1} = 0, \quad i = 2, \dots, N-1 \tag{5.11}$$

5.2.2 Thermodynamic Properties and Heat Transfer Coefficient

Thermodynamic properties of water and steam were obtained adjoining packages from the International Association for the Properties of Water and Steam, IAPWS IF – 97. The quality or range of the data is available in their release guidelines on their website (IAPWS, [*s. d.*]). The Matlab® correlation written for it was created by Holmgren and is available online (HOLMGREN, [*s. d.*]).

The specific heat and enthalpy of the juice are given by Equations (5.12a) and b adapted from Hugot (1960, p. 449).

$$Cp_J = \left(1 - \left(0.6 - 0.0018 \cdot T_J + 0.08 \cdot (1 - P)\right) \cdot \ Brix\right) \cdot 4.1868 \tag{5.12a}$$

$$H_J = Cp_J \cdot T_J \tag{5.12b}$$

As the concentration of dissolved solids increases, the boiling temperature of the juice increases above the temperature of saturated steam at the same pressure. The degree of boiling point elevation is determined as a function of the concentration of soluble solids, *Brix*, by Equation (5.13) (REIN, 2007, p. 271).

$$bpe = \frac{2 \cdot Brix}{1 - Brix} \tag{5.13}$$

Finally, the correlation of the heat transfer coefficient for conventional Robert evaporators is given by Equation (5.14), adapted from Wright (2008).

$$U = 0.00049 \cdot ((1.10 - Brix) \cdot 100)^{1.1616} \cdot T_J^{1.0808} \cdot \delta T^{0.266} \tag{5.14}$$

5.2.3 Sugar Batch Crystallization Process

In any crystallization process, the goal is to transfer sucrose from the mother liquor to the surface of the sugar crystal. This may take many steps and will depend on many factors, such as initial crystal size, sucrose concentration, impurities, machinery size, etc. Most Brazilian sugar mills use a batch vacuum pan to crystallize the sugar in a two-boiling pan scheme (CASTRO, R. E. N. De *et al.*, 2019). Thus, the batch processes that consume steam are A-Pan, B-Pan, and Graining-Pan. In this section, we briefly describe the sugar process using a batch vacuum pan. We will not detail the kinetic crystallization model because it is already detailed in the literature. (CASTRO, B. J. C. De *et al.*, 2019; GEORGIEVA; MEIRELES; FEYO DE AZEVEDO, 2003; REIN, 2007). Since the focus of this study is MEE, we describe only the crystallization operation schedule that occurs in the boiling pans with a focus on steam consumption during different batch operation steps. In Section 5.2.3.1, we describe the steps and stages in crystallization B, which are summarized in Table 17, and crystallization A, summarized in Table 18; Section 5.2.3.2 presents the mathematical model.

Table 17 – Stages and steps for crystalization B

Stage	Step	B-pan 1	B-pan 2
1	1	A-molasse feed	
	2	Concentration	
	3	Seeding and Crystallization	
2	1	Magma transfer (cut)	Magma transfer (cut)
	2	Crystal washing	Crystal washing
	3	Crystallization	Crystallization
3	1	Magma transfer (cut)	Magma transfer (cut)
	2	Crystal washing	Crystal washing
	3	Crystallization	Crystallization
	4	Tightening	Tightening
	5	Discharging	Discharging
4	1		Magma transfer (cut)
	2		Crystal washing
	3		Crystallization
	4		Tightening
	5		Discharging
5	1		Magma transfer (cut)
	2		Crystal washing
	3		Crystallization
	4		Tightening
	5		Discharging
6	1		Magma transfer (cut)
	2		Crystal washing
	3		Crystallization
	4		Tightening
	5		Discharging

Table 18 - Stages and steps for crystalization A

Stage	Step	A-pan 3	A-pan 5	A-pan 4	A-pan 6
1	1	Magma transfer (cut)	Magma transfer (cut)		
	2	Crystal washing	Crystal washing		
	3	Crystallization	Crystallization		
2	1	Magma transfer (cut)	Magma transfer (cut)	Magma transfer (cut)	Magma transfer (cut)
	2	Crystal washing	Crystal washing	Crystal washing	Crystal washing
	3	Crystallization	Crystallization	Crystallization	Crystallization
	4	Tightening	Tightening	Tightening	Tightening
	5	Discharging	Discharging	Discharging	Discharging

5.2.3.1 Sugar process recipe

In a two-boiling pan scheme, the crystals start growing in crystallization B, then continue growing in crystallization A: at the end of crystallization A, the crystals reach the desired size. The syrup, which contains a higher purity of sucrose, feeds crystallization A; A-molasse, which contains a lower purity of sucrose, feeds crystallization B, while B-molasse is the exhausted molasse used to produce ethanol. The term massecuite describes the mixture of crystals, which is the solid fraction, and mother liquor, which is the liquid fraction. The term magma describes the stream rich in crystals that provide the nuclei to initiate the growing process. Both crystallizations, A and B, occur in multiple vacuum pans; we use the term stage when massecuite or magma is transferred from one vacuum pan to another; thus, there are many steps in each stage. The flow of magma and massecuite among the vacuum pan is shown in Figure 28.

In crystallization B, the crystal growth process begins in graining (stage 1). The first step in this stage is to partially fill the vacuum pan with A-molasse. In the second step, the fluid is concentrated: the sucrose concentration must be above the solubility curve and below the labile curve. In this region, namely the metastable region, sugar crystals grow, but no new nuclei form. Crystallization is initiated by adding very fine seeds in the form of a slurry (about 4-µm size ground sugar crystals suspended in alcohol). Adding seeds starts the third step: as sucrose leaves the mother liquor and deposits on the crystal surface, more A-molasse is added to increase the amount of sucrose in the mother liquor; then, steam is used to withdraw the water and adjust the sucrose concentration. This stage ends when the volume of the graining pan reaches its maximum level. The graining pan product is the magma that contains the crystals used to start the B-crystallization in stage 2.

The amount of magma necessary to start the crystallization in each B-Pan is the volume that covers the calandria: typically, the graining-pan produces an amount of magma to start many B-Pans. After having the calandria filled with magma, which is the first step of stage 2, the second step of stage 2 starts, namely crystal washing: water is added to the massecuite; then, steam is fed to evaporate the water added; this step aims to start the circulation of the massecuite by convection forces. In the third step, the sugar crystals start to grow and molasse from A-Centrifuge is added as a source of sucrose to continue growing the crystals. Steam is used during crystallization to evaporate the water from the mother liquor. As crystallization

occurs, the viscosity of the massecuite increases due to the growth in the size of the crystals and the concentration of impurities: the higher the viscosity of the massecuite, the lower the heat transfer coefficient (REIN; ECHEVERRY; ACHARYA, 2004). Therefore, the steam consumption is higher at the beginning of batch crystallization and decreases as the crystal concentration increases and the concentration of mother liquor impurities increases. This stage stops when the maximum volume of the pan is reached; the magma is then partially transferred to the next vacuum pan, in a process, namely cut, to start the next stage.

Stage 3 repeats steps 1 to 3 described in stage 2; however, in stage 3, the crystals reach the desired size to be discharged and centrifuged. Thus, in step 4, namely tightening, the massecuite reaches the desired concentration of crystals, and then in step 5, the massecuite is discharged into massecuite buffer tanks. From these buffer tanks, massecuite goes to a centrifuge to separate the B-molasse from the crystals. The B-molasse is the final molasse in the two-boiling sugar production scheme; it goes to the ethanol fermentation process; the crystals from the B-centrifuges are mixed with water to produce magma for the A-pan. Stages 4, 5, and 6 repeat the steps from stage 3.

In crystallization A, the magma is the sugar produced in B and the sucrose source is the syrup from MEE. Step 1 in stage 1 of crystallization A is the magma transfer; the amount of magma necessary to start the crystallization in each A-Pan is the volume that covers the calandria. After having the calandria filled with magma, water is added to the massecuite (step 2 of stage 1), steam is then fed to evaporate the water added; this step aims to start the circulation of the massecuite by the convection forces (crystal washing). In step 3, the sugar crystals start growing and syrup from MEE is added as a source of sucrose to continue growing the crystals. Steam is used during crystallization to withdraw the water from the mother liquor in the vacuum pan. This step ends when the vacuum pan reaches its maximum level. Afterward, half of the massecuite is transferred to another vacuum pan, i.e., stage 2 and step 1. The next steps, steps 2 and 3, are the same as described in stage 1; then, when the vacuum pan reaches the maximum volume, before discharging the massecuite, the massecuite is tightened (step 4), then discharged (step 5).

In all the steps that involve heat transfer, the temperature of evaporation is controlled by maintaining the vacuum inside the heating chamber. The vapor, withdrawn from the product inside the vacuum pan, is conveyed through a condenser to a vacuum system, usually a water ejector or a vacuum pump.

5.2.3.2 Sugar crystallization mathematical model

In the recipe for sugar production, the steps named crystallization, crystal washing, concentration, and tightening are solved using the system of ordinary differential equations, ODE: the difference in each step is the fed stream as described above. These equations consist of an overall mass balance on the massecuite side of the vacuum pan, Equation (5.15), and on its components crystals, sucrose, impurities, and water, Equations (5.16) to (5.19), respectively; the energy balance on the calandria side and on the massecuite side is given by Equations (5.20) and (5.21), respectively. The kinetic crystallization is given by Equation (5.22) adapted from Castro et al (2019).

$$\frac{dm_T}{dt} = F_{in} - \frac{dm_{vap\_out}}{dt} \tag{5.15}$$

$$\frac{dm_c}{dt} = KG \cdot A_c \cdot \rho_c \tag{5.16}$$

$$\frac{dm_s}{dt} = F_{in} \cdot C_{s,in} - \left(\frac{dm_c}{m_t}\right) = F_{in} \cdot C_{s,in} - KG \cdot A_c \cdot \rho_c \tag{5.17}$$

$$\frac{dm_I}{dt} = F_{in} \cdot C_{I,in} \tag{5.18}$$

$$\frac{dm_W}{dt} = F_{in} \cdot C_{W,in} - \frac{dm_{vap\_out}}{dt} \tag{5.19}$$

$$\frac{dm_W}{dt} = F_{in} \cdot C_{W,in} - \frac{U \cdot A \cdot \left(T_{vap\_in} - T_{MC}\right) + F_{in} \cdot Cp_{in} \cdot T_{in} - F_{in} \cdot Cp_{MC} \cdot T_{MC}}{H_{vap\_out} - Cp_{MC} \cdot T_{MC}}$$

$$\frac{dm_{vap\_in}}{dt} = U \cdot A \cdot \frac{(T_{vap\_in} - T_{MC})}{\Delta H_{vap\_in}} \tag{5.20}$$

$$\frac{dm_{vap\_out}}{dt} = \frac{U \cdot A \cdot (T_{vap\_in} - T_{MC}) + F_{in} \cdot Cp_{in} \cdot T_{in} - F_{in} \cdot Cp_{MC} \cdot T_{MC}}{H_{vap\_out} - Cp_{MC} \cdot T_{MC}} \tag{5.21}$$

$$KG = kg \cdot exp\left(\frac{-57000}{R \cdot (T_{MC} + 273)}\right)(P - 1)\, exp\left(-8\frac{m_I}{m_s + m_I}\left(1 + 2\frac{\rho_{mc}}{\rho_c}\frac{m_c}{m_T}\right)\right) \tag{5.22}$$

5.2.4 Interactive algorithm

The sugar crystallization model is represented by the ODE system, which is solved using Runge-Kutta for a small time interval (one minute). At this time interval, the entire sugarcane industrial process is calculated taking into account the result from the sugar crystallization step. Depending on the step of the sugar crystallization process recipe, a different amount of steam is required from MEE. The calculation of the mathematical model of the sugar mill requires solving the equations of mass and energy balance, thermodynamic properties, and heat transfer coefficient. The MEE mass and energy balance equations can be rearranged into a set of linear equations. The thermodynamic properties and the heat transfer coefficient are a set of non-linear equations. To solve this set of linear and non-linear equations, an iterative method combining the Gaussian elimination for the matrix of linear equations and the fixed-point method is used. The calculation is repeated until all the steam temperature and the syrup concentration become constant.

To solve the MEE model, the mass and energy balance and the evaporator design equation are rearranged into *8N–5* linearly independent equations, where *N* is the number of effects. The fixed parameters are (a) the mass flow rate and temperature of the juice that enters the evaporation train; (b) the temperature and pressure of the exhaust steam from the turbine; (c) the temperature of the steam from the last evaporation body withdrawn by the barometric condenser; (d) the evaporation area of each body. The parameters calculated

previously are (a) the overall heat coefficient; (b) the juice boiling point elevation, which depends on the concentration of the juice; and (c) the steam bleed.

The intermediate temperature of the juice and steam streams and the concentration of the juice, in the multiple-effect evaporator, are results from the set of linear equations; however, before solving the mass and energy balance, a first guess of the temperature and juice concentration is made. Using this first guess, the enthalpy of the liquor, condensate, and steam; the boiling point elevation; and the heat transfer coefficient are estimated. Then the set of linear equations is solved and new values of temperature and concentration are obtained. Again, the thermodynamic properties are calculated using these obtained values of temperature and juice concentration. This is repeated until the values of the temperature and juice concentration become constant. A summary of this interaction is shown in Figure 60 and is represented by the dashed line identified as Interaction 1.

After finding the intermediate steam temperature, which balances the energy for a given amount of steam bleed, it is necessary to recalculate the steam bleed for juice heating. Changing the temperature of the steam utility changes the heat transferred to a given area. Additionally, changing the temperature distribution in MEE changes the syrup concentration; thus, different syrup concentrations require a different amount of steam to crystalize the sugar. Therefore, a new interaction is necessary to recalculate the temperature of the steam using the new values of steam bleed. In Figure 60, it is represented by the dashed line identified as interaction 2.

By applying this algorithm, it is possible to find the steam consumption for a given time considering a continuous process operation; however, the crystallization process is not continuous. Thus, the steam consumption in the crystallization process will depend on the batch crystallization stage. The steps and stages for sugar crystallization are represented by the dashed line identified as interaction 3 in Figure 60. Therefore, interaction 3 represents the small time interval at which the ODE for sugar crystallization is solved.

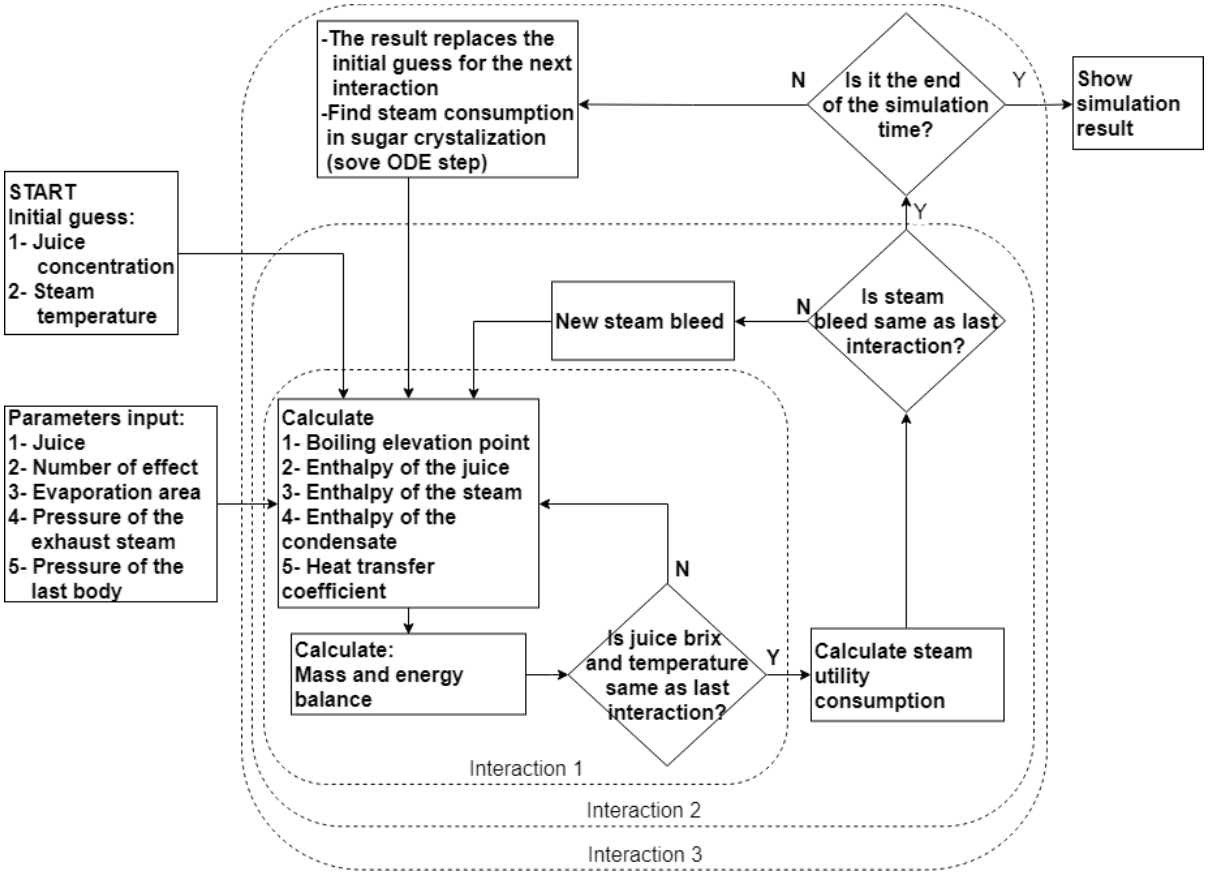

Figure 60 – Algorithm to solve multiple-effect evaporation in a Sugarmill industry

5.3 Results

In this section, we show the result of a 48-hour simulation of a sugarcane mill. We simulate two boundary scenarios and between these two scenarios. In the first scenario, the steam pressure changes according to the steam consumption on sugar crystallization. In the second, the pressure and thus the temperature of the steam are fixed; therefore, a by-pass valve from the higher-pressure steam to the lower one is used when the steam consumption rises above the average; analogously, a relief valve releases steam to the atmosphere when the steam consumption decreases below the average; in this way, the amount of steam bleed from the MEE is constant and corresponds to the average steam consumption in batch process. Since the steam bleed flow remains constant, the temperature and pressure of all of the vapors produced in MEE are constant as well. Then, in the third part (Section 5.3.3), we set the lower and upper boundaries; in this way, part of the steam is bypassed only when the steam consumption in sugar crystallization is above an upper limit, i.e., the average plus a delta; analogously, steam is released into the atmosphere when steam consumption is below

a lower limit, i.e., the average minus a delta. Here, this delta is a range around the average steam consumption.

5.3.1 Flexible Steam Pressure

The energy input for the whole sugarcane mill is produced by the boiler that feeds the first evaporation body of the MEE. Changing the steam bled from the MEE in any of the evaporation bodies changes the fed steam required in the first body. Figure 61 shows (during 48-hours simulation) the steam consumed in the crystallization process and the total steam from the boiler consumed by the entire industrial process. Depending on each crystalization step, different consumptions are expected. The steam used by the vacuum pan is bled from the second evaporator body. The higher the amount of steam required by the vacuum pan, the lower the pressure of the steam; this change in the steam pressure guarantees the amount of steam to feed the sugar process. The pressure of the steam from MEE is shown on the right-hand side of Figure 61; the steam extracted from the i^{th} body evaporator is identified as V_i and the steam that enters the first body of evaporation is identified as V_E. In this simulation, no bypass from the higher-pressure steam was considered to boost the lower-pressure steam. The total amount of V_E consumed during this operation interval is 1.2210x10^7 kg and the average steam flow rate used in the crystallization process (*V2*) is 28.425 x10^3 kg/h.

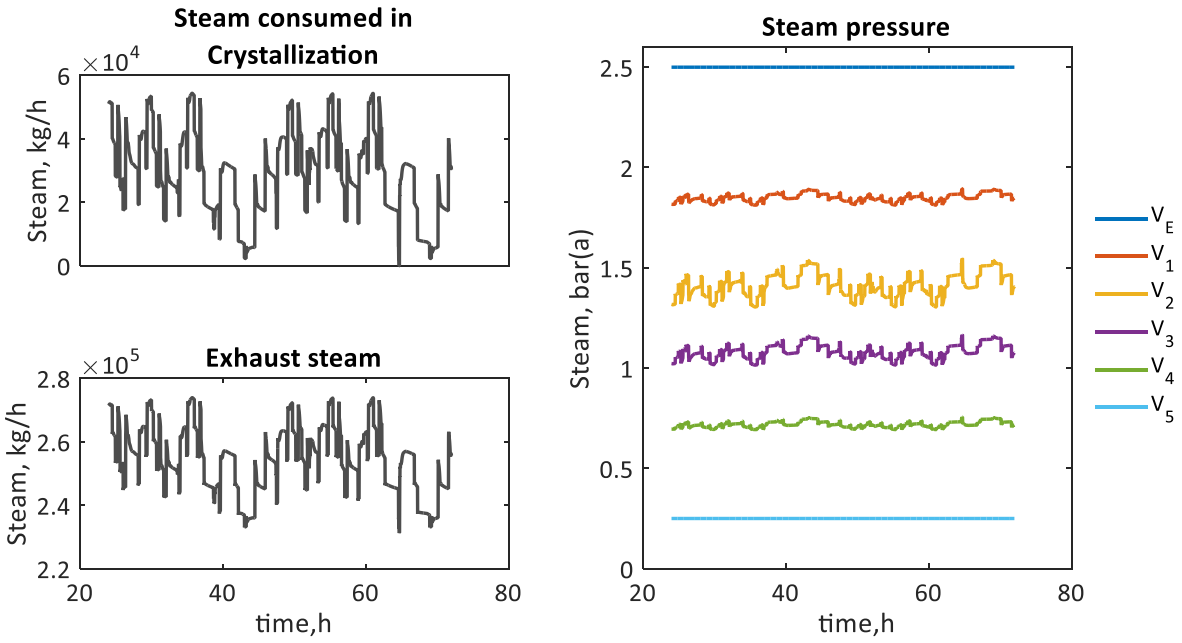

Figure 61 – Steam consumed during the crystallization process, steam fed in MEE and steam pressure produced at each multiple-effect evaporation body

5.3.2 Fixed Steam Pressure

In this simulation, the steam pressure is maintained unchanged; for this, a bypass valve is used to increase the pressure of the steam when the pressure drops, and a relief valve is used to relieve steam into the atmosphere when the pressure increases. Thus, the pressure of the steam remains constant during all the batch operation steps. We do not assess the control: we assume that the bypass and the relief valve can control the pressure with an immediate response; nonetheless, this might be an issue for a future study. Additionally, a controller study is a matter of seconds, and in this article, we assess 48-hour of operation aiming at the total steam consumption; i.e., the energy requirement. Figure 62 shows the steam consumed by the crystallization process; the exhausts steam, which is the total steam from the boiler consumed at the evaporation in the first body; and the amount of steam bypassed, V_E to V_1, V_1 to V_2, and V_2 to the atmosphere. The steam pressure remains constant during the simulation (V_1 = 1.857 bar(a); V_2 = 1.450 bar(a); V_3 = 1.085 bar(a); V_4 = 0.721 bar(a)). The total amount of V_E consumed during this operation interval is 1.2498x10^7 kg.

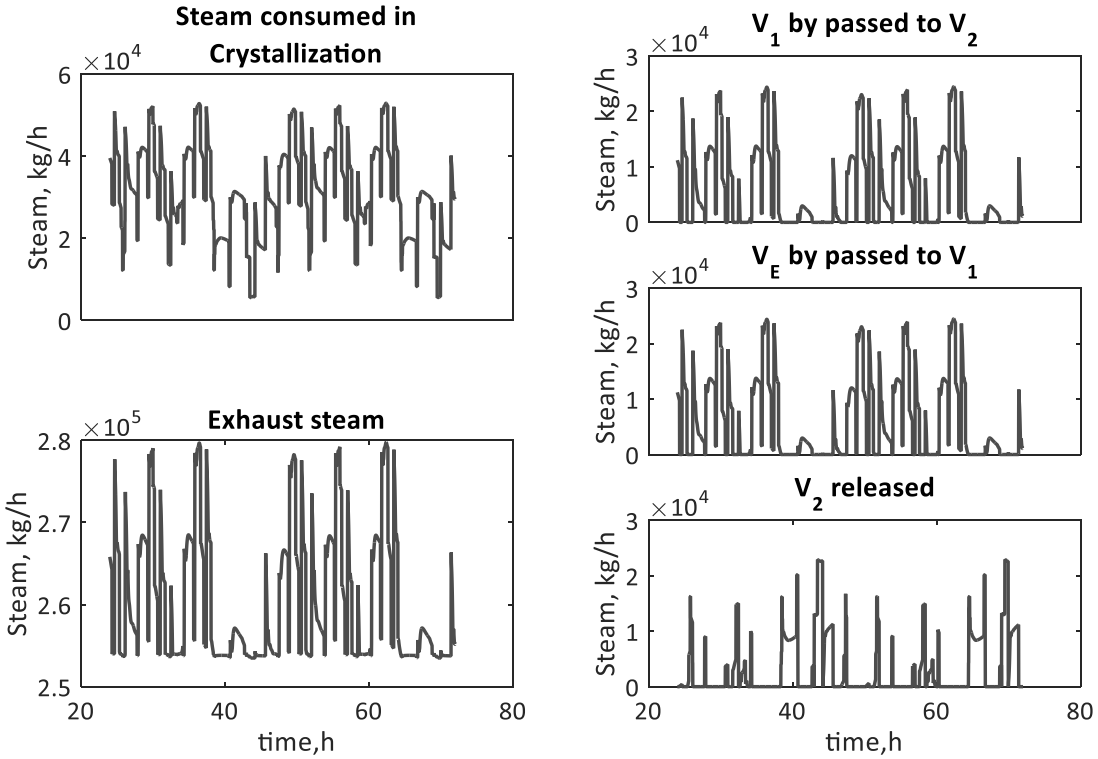

Figure 62 - Steam consumed at the crystallization process

5.3.3 Lower and upper boundaries condition

Industrial processes, in general, do not let the steam pressure oscillate freely (as described in Section 5.3.1), as well as heat exchange devices are not strict with a fixed steam pressure point (as described in Section 5.3.2). Therefore, the usual is that boundaries are created around an average steam consumption; then a control system, such as a bypass valve and a relief valve, actuate only when these boundaries are surpassed: knowing the average steam consumption, the bypass valve or relief valve actuates to increase or decrease the steam pressure. This boundary, namely Delta in this article, represents the amount of steam flow rate that is allowed to oscillate freely around the average steam flow rate. For example, when Delta is 5000 kg/h and the required steam is 37000 kg/h while average steam consumption is 28425 kg/h, only 3575 kg/h is by-passed; analogously, if steam consumed is 23000 kg/h, then 425 kg/h is released into the atmosphere. In this example, no bypass or relief valve is used when the steam consumed is between 23450 kg/h and 33450 kg/h.

Figure 63 shows the total exhaust steam consumed during the 48-hour of simulation against the boundary limit, Delta. The red line, at the top of the graph, considered the upper and lower limits, i.e., bypass and relief valve; while the blue line considered only the lower limit, i.e., only the bypass valve. In the second case, when the steam consumed is higher than the average, the steam is not released into the atmosphere; consequently, the steam pressure increases freely above the average plus Delta. Steam with a higher pressure should not be a problem in an industrial process since the heat exchange area reduces when temperature increases; conversely, a lower steam pressure would require a higher heat exchange area.

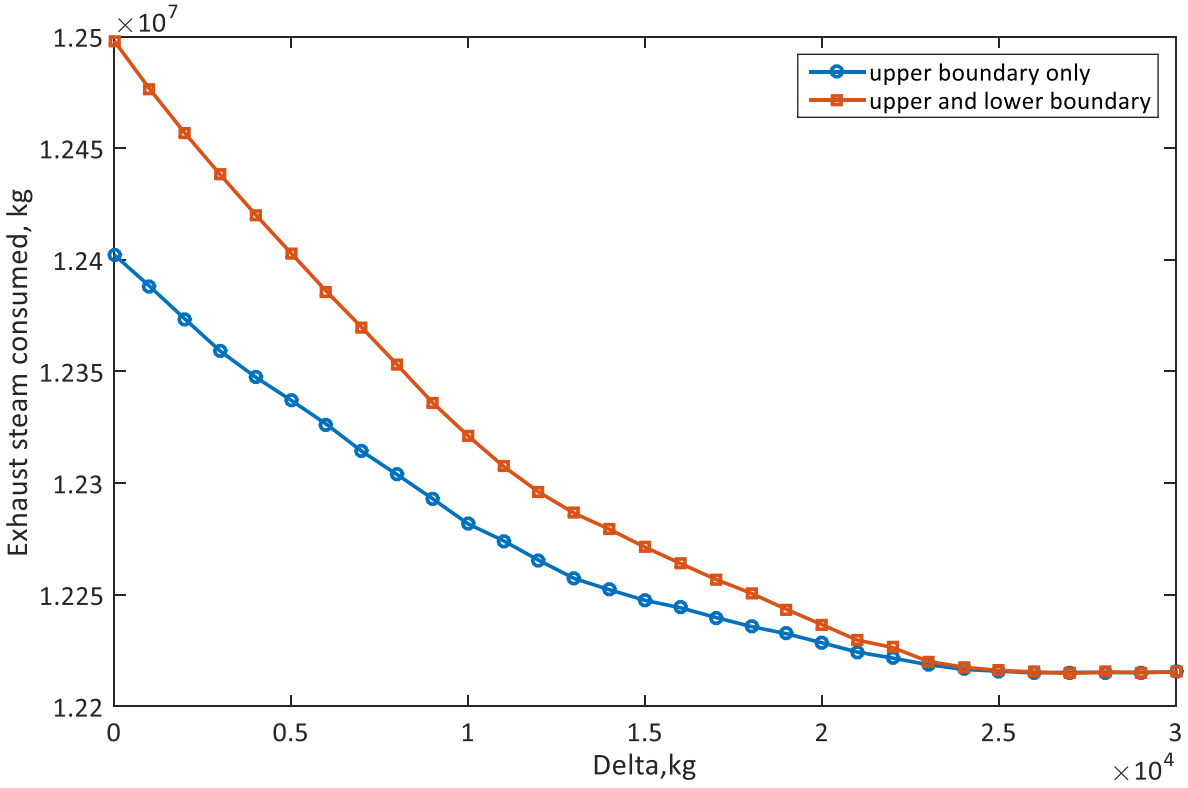

Figure 63 - Total exhaust steam consumed in a 48-hour simulation and Delta, lower and upper limit around average steam consumption.

5.3.4 Electricity production

Changing steam consumption changes the consumption of bagasse, which is considered a feedstock with many applications in the sugarcane industry (CASTRO; ALVES; NASCIMENTO, 2021). Here, we assess the production of electricity using a condensation turbine and a cogeneration system. A cogeneration system is defined as an energy system that produces two useful forms of energy simultaneously. Thus, the cogeneration system consists of a boiler and a backpressure turbine: the backpressure turbine produces electricity and steam (thermal energy), while the condensation turbine produces only electricity. Using less exhaustion steam results in using less high-pressure steam. In this simulation, the surplus high-pressure steam is used to produce electricity using a condensation turbine, which produces more electricity per kg of steam than the backpressure turbine, 267,8 W/kg and 187,7 W/kg, respectively.

We considered that all bagasse is burned to produce high-pressure steam is diverted to feed the backpressure turbine or condensation turbine, as shown schematically in Figure 57. Thus, the amount of steam diverted to the backpressure turbine depends on the amount

of exhaustion steam required on MEE. Figure 64 shows the power during the 48-hour simulation for the two scenarios described above; therefore, the area below the curve represents the total energy produced. The energy produced is 2,200.9 MW·h and 2,219.2 MW·h for the process that uses and does not use the bypass valve, respectively; that is, it is produced a surplus of 18.2 MW·h considering the scenario when no bypass valve is used or the steam pressure changes as a function of the crystallization process.

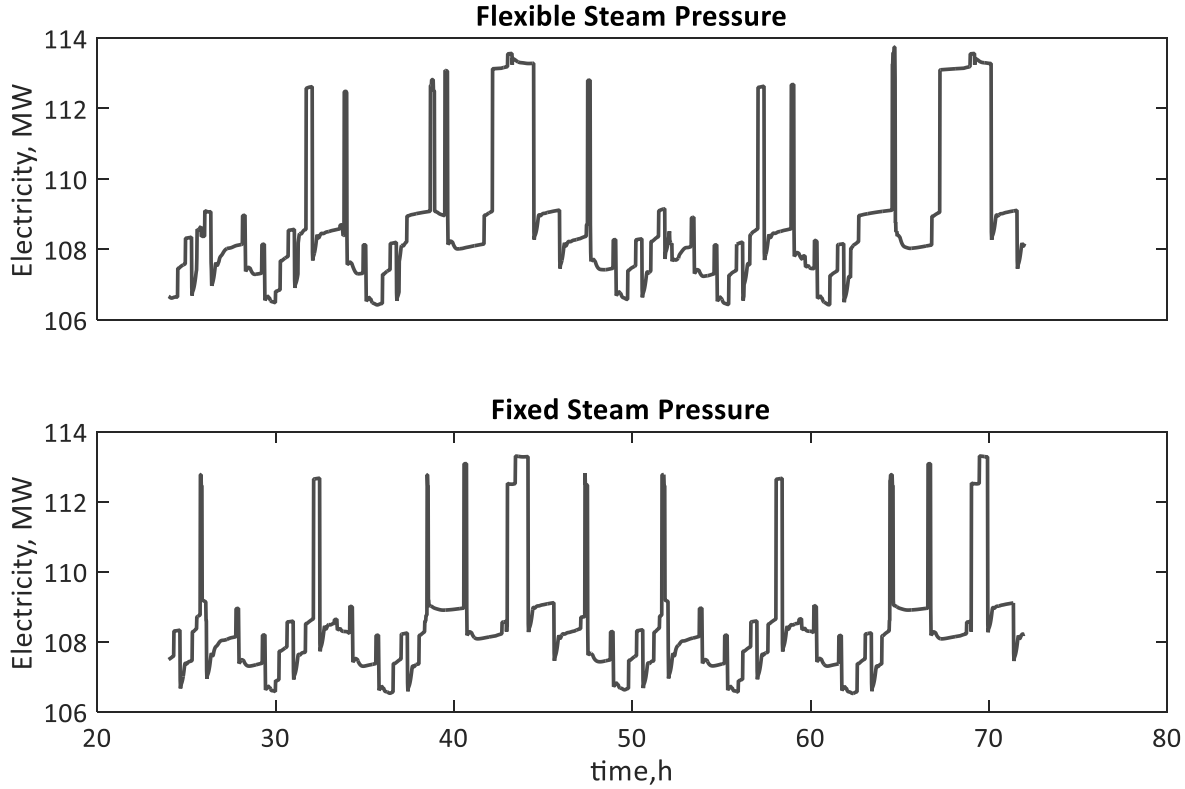

Figure 64 - Electricity production

5.4 Conclusion

The proposed algorithm was able to find the steam temperature when the amount of steam produced in a MEE changes. To our knowledge, there are no other works with this approach. Since the output of the simulation was the temperature or pressure, a much higher computational effort is required compared to the algorithms that use this variable as input. This is because the constitutive and thermodynamic equations which are used to calculate properties such as enthalpy, heat capacity, density, etc. require the temperature as an input variable. Thus, these properties were obtained initially by guessing the temperature and then solving them until they converge to a value that represents the heat transferred in both the thermodynamic and constitutive equations.

For the case in which this algorithm was used, it was possible to assess the consumption of exhaust steam due to the dynamics of batch sugar production: saving exhaust steam means saving bagasse. Surplus steam (produced using surplus bagasse) was used in a condensation turbine to produce electricity. The scenarios studied in this paper, in which steam is released or bypassed, increased the overall steam consumption (exhaust steam). Only bypassing steam reduces the overall consumption compared to that that also releases steam. The scenario that saved more steam was the one that did not bypass or release steam into the atmosphere. The drawback of not releasing or bypassing steam is the changes in steam temperature; steam with a lower temperature requires more area to perform the same heat exchange.

This algorithm was shown to be a powerful tool for assessing the energy consumption of the whole sugar mill considering a dynamic process. Besides this case study, the proposed model can be used to investigate different scenarios, such as the change in steam pressure due to fouling or due to a change in feed flow rate; additionally, it can be used to simulate MEE in different applications such as pulp and paper, desalinization, etc.

Acknowledgments

The authors acknowledge FAPESP-NERC (São Paulo Research Foundation and National Environment Research Council) process number 2015/50684-9 for its financial support.
We also gratefully acknowledge the support of the RCGI – Research Centre for Gas Innovation, hosted by the University of São Paulo (USP) and sponsored by FAPESP – São Paulo Research Foundation (2014/50279-4 and 2020/15230-5) and Shell Brasil, and the strategic importance of the support given by ANP (Brazil's National Oil, Natural Gas and Biofuels Agency) through the R&D levy regulation. This study was financed in part by the Personnel Coordination of Improvement of Higher Level - Brazil (CAPES) - Finance Code 001.

References

AHMETOVIĆ, E. *et al.* Simultaneous optimisation and heat integration of evaporation systems including mechanical vapour recompression and background process. **Energy**, [*s. l.*], v. 158, p. 1160–1191, 2018. Disponível em: https://linkinghub.elsevier.com/retrieve/pii/S0360544218311113. Acesso em: 7 mar. 2019.

AHMETOVIĆ, E. *et al.* Simultaneous optimisation of multiple-effect evaporation systems and

heat exchanger network. **Chemical Engineering Transactions**, [*s. l.*], v. 61, p. 1399–1404, 2017.

CASTRO, R. E. N. de *et al.* Assessment of Sugarcane-Based Ethanol Production. *In*: BASSO, T. P.; BASSO, L. C. (org.). **Fuel Ethanol Production from Sugarcane**. [*S. l.*]: IntechOpen, 2019. p. 3–22. *E-book*. Disponível em: https://www.intechopen.com/books/fuel-ethanol-production-from-sugarcane.

CASTRO, R. E. N. de *et al.* Open Sugarcane Process Simulation Platform. *In*: INTERNATIONAL SYMPOSIUM ON PROCESS SYSTEMS ENGINEERING – PSE 2018. San Diego: Elsevier B.V., 2018. p. 1819–1824. *E-book*. Disponível em: https://linkinghub.elsevier.com/retrieve/pii/B9780444642417502986.

CASTRO, B. J. C. de *et al.* Sucrose crystallization: modeling and evaluation of production responses to typical process fluctuations. **Brazilian Journal of Chemical Engineering**, [*s. l.*], v. 36, n. 3, p. 1237–1253, 2019. Disponível em: http://www.scielo.br/scielo.php?script=sci_arttext&pid=S0104-66322019000301237&tlng=en.

CASTRO, R. E. N. de; ALVES, R. M. B.; NASCIMENTO, C. A. O. Assessing the sugarcane bagasse and straw as a biofuel to propel light vehicles. **Sustainable Energy & Fuels**, [*s. l.*], n. 5, p. 2563–2577, 2021. Disponível em: http://pubs.rsc.org/en/Content/ArticleLanding/2021/SE/D1SE00129A.

CHANTASIRIWAN, S. Optimum Surface Area Distribution of Multiple-effect Evaporator for Minimizing Steam Use in Raw Sugar Manufacturing. **Chemical Engineering Transactions**, [*s. l.*], v. 61, p. 805–810, 2017. Disponível em: https://www.cetjournal.it/index.php/cet/article/view/CET1761132. Acesso em: 7 mar. 2019.

CORTES-RODRÍGUEZ, E. F. *et al.* Vinasse concentration and juice evaporation system integrated to the conventional ethanol production process from sugarcane – Heat integration and impacts in cogeneration system. **Renewable Energy**, [*s. l.*], v. 115, p. 474–488, 2018. Disponível em: https://doi.org/10.1016/j.renene.2017.08.036.

DIEL, C. L. *et al.* Optimization of multiple-effect evaporation in the pulp and paper industry using response surface methodology. **Applied Thermal Engineering**, [*s. l.*], v. 95, p. 1–6, 2016. Disponível em: http://dx.doi.org/10.1016/j.applthermaleng.2015.10.136.

GEORGIEVA, P.; MEIRELES, M. J.; FEYO DE AZEVEDO, S. Knowledge-based hybrid modelling of a batch crystallisation when accounting for nucleation, growth and agglomeration phenomena. **Chemical Engineering Science**, [*s. l.*], v. 58, p. 3699–3713, 2003. Disponível em: www.elsevier.com/locate/ces. Acesso em: 18 dez. 2020.

HELUANE, H. *et al.* Simultaneous re-design and scheduling of multiple effect evaporator systems. **Computers and Operations Research**, [*s. l.*], v. 39, n. 5, p. 1173–1186, 2012.

HIGA, M. *et al.* Thermal integration of multiple effect evaporator in sugar plant. **Applied Thermal Engineering**, [*s. l.*], v. 29, n. 2–3, p. 515–522, 2009. Disponível em: http://dx.doi.org/10.1016/j.applthermaleng.2008.03.009.

HOLMGREN, M. **IAPWS**. [*S. l.*], [*s. d.*]. Disponível em: www.iapws.org. Acesso em: 30 jun. 2017.

HUGOT, E. **Handbook of Cane Sugar Engineering**. 3. ed. [*S. l.*]: Elsevier, 1960. *E-book*. Disponível em: https://linkinghub.elsevier.com/retrieve/pii/C20130124373.

IAPWS. **IAPWS The International Association for the Properties of Water and Steam**. [*S. l.*], [*s. d.*]. Disponível em: http://www.iapws.org/release.html#GUIDE. .

JIANG, Y.; KANG, L.; LIU, Y. Simultaneous synthesis of a multiple-effect evaporation system with background process. **Chemical Engineering Research and Design**, [*s. l.*], v. 133, p. 79–89, 2018. Disponível em: https://www.sciencedirect.com/science/article/pii/S0263876218301023. Acesso em: 7 mar. 2019.

KAYA, D.; IBRAHIM SARAC, H. Mathematical modeling of multiple-effect evaporators and energy economy. **Energy**, [*s. l.*], v. 32, n. 8, p. 1536–1542, 2007.

ONISHI, V. C. *et al.* Shale gas flowback water desalination: Single vs multiple-effect evaporation with vapor recompression cycle and thermal integration. **Desalination**, [*s. l.*], v. 404, p. 230–248, 2017. Disponível em: http://dx.doi.org/10.1016/j.desal.2016.11.003.

PEACOCK, S. D.; SHAH, S. Recirculation rate for Robert evaporators. **Proc S Afr Sug Technol Ass**, [*s. l.*], n. 86, p. 334–349, 2013.

PINA, E. A. *et al.* Reduction of process steam demand and water-usage through heat integration in sugar and ethanol production from sugarcane – Evaluation of different plant configurations. **Energy**, [*s. l.*], v. 138, p. 1263–1280, 2017. Disponível em: https://doi.org/10.1016/j.energy.2015.06.054.

PURCHASE, B. S.; DAY-LEWIS, C. M. J.; SCHAFFLER, K. J. A comparative study of sucrose degradation in different evaporators. **Proc S Afr Sug Technol Ass**, [*s. l.*], p. 8–13, 1987.

REIN, P. **Cane Sugar Engineering**. Berlin: Bartens, 2007.

REIN, P. W.; ECHEVERRY, L. F.; ACHARYA, S. Circulation in vacuum pans. **Journal American Society of Sugar Cane Technologists**, [*s. l.*], v. 24, n. 5, p. 1–17, 2004.

VAZQUEZ-ROJAS, R. A.; GARFIAS-VÁSQUEZ, F. J.; BAZUA-RUEDA, E. R. Simulation of a triple effect evaporator of a solution of caustic soda, sodium chloride, and sodium sulfate using Aspen Plus. **Computers and Chemical Engineering**, [*s. l.*], v. 112, p. 265–273, 2018. Disponível em: https://doi.org/10.1016/j.compchemeng.2018.02.005.

WAYNE, L. B. **Sweet cane: The architecture of the sugar works of east Florida**. [*S. l.: s. n.*], 2010-. ISSN 0734-578X.

WESTPHALEN, D. L.; MACIEL, M. R. W. Pinch analysis of evaporation systems. **Brazilian Journal of Chemical Engineering**, [*s. l.*], v. 17, n. 4–7, p. 525–538, 2000. Disponível em: http://www.scielo.br/scielo.php?script=sci_arttext&pid=S0104-66322000000400017&lng=en&tlng=en.

WRIGHT, P. G. Heat transfer coefficient correlations for Robert juice evaporators. **Proceeding of Australian Society Sugarcane Technology**, [*s. l.*], v. 30, p. 547–558, 2008.

CHAPTER 6: ASSESSING THE SUGARCANE BAGASSE AND STRAW AS A BIOFUEL TO PROPEL LIGHT VEHICLES

This chapter corresponds to a full-length article published in Sustainable Energy and Fuels.

Rubens Eliseu Nicula de Castro, Rita Maria Brito Alves and Claudio Augusto Oller Nascimento. Assessing the sugarcane bagasse and straw as a biofuel to propel light vehicles. **Sustainable Energy & Fuels**, [s. l.], n. 5, p. 2563–2577, 2021.

Abstract

Sugarcane bagasse and straw are the residues from sugarcane production. They can be used to produce electricity, second-generation ethanol, and biogas. These three kinds of fuel are energy carriers that can be used to propel light vehicles. Thus, we assessed the use of these two residues as a primary fuel to propel light vehicles. For this assessment, this article takes into account, for the same amount of primary energy, the distance one can drive, the emission of CO2, the water usage, the expenditure to build the facilities, and some qualitative indicators, such as health and handleability. It is found that bringing straw from the field increases the production of biofuels and mitigates the environmental impact. Considering the different energy carriers (ethanol, electricity, and biogas), it is possible to conclude that depending on the criteria used to analyze these energy carriers, one carrier would be preferred to another. For example, taking into account the return on the investment, electricity would be the least preferable one, while analyzing health, electricity would be the most preferable one. The uncertainty associated with the analysis is captured using the Monte Carlo approach. Thus, some indicators, such as the distance one can drive and the CO2 emissions, show that they depend on the uncertainty associated with the conversion efficiency of the different processes and the vehicle mileage-rate.

6.1 Introduction

Transportation is currently crucial for society; hence, replacing fossil-based-fuels is urgent in order to stop global warming.(JACOBSON, 2009) Many kinds of biofuels are available, such as sugars (HUANG; PERCIVAL ZHANG, 2011; ZHANG, 2009) and lignocellulosic material;(TRIVEDI; MALINA; BARRETT, 2015) however, they cannot be used directly in vehicles. They need to be converted into a usable fuel, such as biogas, bioethanol, or

bioelectricity. Many studies included different fuel sources for vehicles equipped with different types of engines, such as internal combustion, battery electric vehicle, and fuel cell electric vehicle.(LUQUE *et al.*, 2008; RAMACHANDRAN; STIMMING, 2015) Choosing the best option (fuel and engine) is not simple: there are many indicators and conversion factors used to determine the pros and cons of a fuel-type; thus, it is necessary to build a model to assess their environmental, economic, and social impact. In this context, bagasse and straw from sugarcane are a primary source that can be used to produce electricity, ethanol, or biogas, then used in a light vehicle. Therefore, to answer the question: which fuel is better when they are produced from sugarcane lignocellulosic material, we examined CO_2 emission, air pollution, finances, water usage, handleability, and the distance one can drive in a light vehicle using the sugarcane lignocellulosic residue.

Lignocellulosic materials from agricultural residues are the most appealing raw materials for manufacturing biofuel because they do not compete with food production, they do not increase land usage, and they are abundant.(GOLDEMBERG, 2008; KONDE *et al.*, 2021) In the Brazilian sugarcane industry, bagasse is used to produce electricity and thermal energy by processing it in a combined heat and power plant (CHP). A well-designed Sugarmill does not consume all the bagasse to comply with its process requirement for thermal and electricity demand, and this results in surplus bagasse. Bringing straw from the field increases the amount of surplus lignocellulosic residue available in the industrial site. Here, we investigate the use of the surplus bagasse, which is an industrial residue, and straw, which is an agricultural residue, as the primary fuel used to propel light vehicles. Currently, the technology used in engine vehicles does not allow using bagasse directly; nevertheless, bagasse and straw can be converted into electricity, second-generation ethanol, and biogas. Cars that use these three kinds of fuels are currently available in the market. This means that these energy carriers are acceptable without affecting the current standard style of living.(GIAMPIETRO; ULGIATI, 2005) Brazil has been using sugarcane for large-scale bioethanol production since the 1980s(FERNANDES, 2011) and the United States started using ethanol from corn mixed with gasoline for fuel in 2001.(RFA RENEWABLE FUELS ASSOCIATION, 2002) Natural gas is an alternative fuel in which gasoline engines can be easily converted. Natural gas is composed essentially of methane gas, which is the same gas obtained during the anaerobic digestion of bagasse. Europe produced 1.2 billion m^3 of biomethane for use as a vehicle fuel or injection into the natural gas grid in 2015.(SCARLAT; DALLEMAND; FAHL, 2018) Despite the internal

combustion engine equipping most cars, the electric car emerges as a technology with great potential for the near future. In this regard, it is also important to introduce the distinction between energy carriers and primary energy sources; for example, if electricity is produced from fossil fuel the use of this in an electric car cannot be considered renewable energy

Bagasse and straw also play an important role in the country's energy security. In developing countries, energy security often means obtaining access to reliable and adequate energy supplies, taking into account the diversity of primary energy resources and where they come from (internal or external market).(KRUYT *et al.*, 2009) Bagasse and straw increase the security of sources reducing the fuel import dependence; increasing the diversity among fuel types and fuel suppliers; and increasing the share of zero-carbon fuels in the country.

Bagasse and straw also play an important role in the country's energy security. In developing countries, energy security often means obtaining access to reliable and adequate energy supplies, taking into account the diversity of primary energy resources and where they come from (internal or external market).(KRUYT *et al.*, 2009) Bagasse and straw increase the security of sources reducing the fuel import dependence; increasing the diversity among fuel types and fuel suppliers; and increasing the share of zero-carbon fuels in the country.

Figure 65 summarizes the problem; there is one source, which is the sugarcane lignocellulosic fraction; three possibilities of processing it, and one final use. Environmental, social, and economic indicators from the source material are the same when using these fuels because they came from the same source. The fiber fraction in sugarcane and the straw comprises the lignocellulosic materials which can be converted into three different energy carriers: a) electricity, by burning it in a boiler and then feed the steam to a condensation-turbine attached to a power generator; b) ethanol, by the second-generation process that converts the lignocellulosic material into ethanol; c) biogas, by the anaerobic digestion that converts the lignocellulosic material into biogas. The final use is in a light vehicle that can be fueled with electricity, ethanol, or biogas.

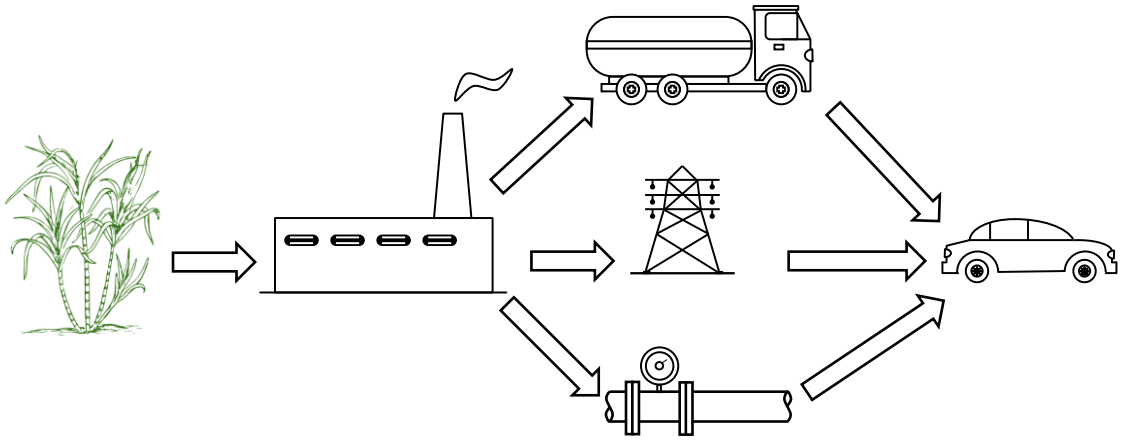

Figure 65 - Problem summary

There are many differences in the production of these three energy carriers, such as thermal energy, power, and water consumption and also waste, sewage, and gas emissions. To obtain these differences, it is necessary to develop a mathematical model. The mathematical model performs a mass and energy balance using parameters from a typical Brazilian Sugarmill processing 3.22×10^9 kg of sugarcane per year. The parameters used to simulate the processes that convert the surplus bagasse and straw into second-generation ethanol and biogas are taken from the literature. Some processes are used commercially, such as the Rankine Cycle to produce electricity; however, second-generation ethanol and anaerobic digestion of bagasse only recently left the laboratory scale; thus, the uncertainty of these processes is assessed using the Monte Carlo approach. The way the energy carrier is used in a light vehicle is also assessed: the differences in car fuel consumption for cities and highways. Additionally, different models and types of cars have different mileage rates, which result in uncertainty captured using the Monte Carlo approach.

This paper aims to investigate the social, economic, and environmental impacts of the use of sugarcane industrial and agricultural residues converted into ethanol biogas and electricity and then used in a light vehicle in cities and highways.

6.2 Methods

Simulations of the production of electricity, ethanol, or biogas were carried out by adding these processes to the Open Sugarcane Process Simulation Platform (CASTRO *et al.*, 2018), which simulates the Brazilian sugarcane first-generation process industry. For each of the three energy carriers, we considered bringing straw from the field in three different

amounts, and then we considered two different conditions of use of these fuels, i.e. in cities and highways, resulting in 18 different scenarios.

6.2.1 Bagasse processing into usable fuel for light vehicles

Figures 66, 67 and 68 show a typical Sugarmill process interconnected to three processes that convert bagasse into usable fuel for vehicles i.e., electricity, ethanol, and CNG (compressed natural gas). The blocks outlined in the dashed line represent the current Sugarmill industry that produces sugar and first-generation ethanol from sugarcane juice; this is the same for all three scenarios. The bagasse from the milling process is then used to produce one of the three fuels, nevertheless, the amount of surplus bagasse that feeds one of the three attached processes depends on the sugar and ethanol first-generation process.(CASTRO *et al.*, 2018)

The CHP, which is also outlined in the dashed line, is used in all three scenarios. However, different sizes are required depending on the heat and power demand from each scenario: the heat limits the CHP size for all scenarios, i.e., the three scenarios resulted in surplus power which is sent to the grid when thermal demand is complied with.

The sugarcane plant consists of stalk and straw; where straw is the leaves in the sugarcane plant. The maximum amount of straw is about 0.14 kg of straw per kg of sugarcane.(CARVALHO *et al.*, 2019) Bringing straw from the field presents an opportunity to increase the amount of surplus bagasse. For agricultural reasons, up to 50% of the straw can be removed without affecting soil quality (CHERUBIN *et al.*, 2019); the remainder is left on the field after harvesting.

The production of sugar and ethanol is modeled on a biorefinery with a capacity of 3.22×10^9 kg of sugarcane per year at a maximum milling rate of 700×10^3 kg/h. The leaves on the top of the plant are greener with higher moisture and the leaves in the bottom are drier; in this work, it has been considered that straw has an average moisture of 15%. The lower heating value (LHV) of the bagasse and straw is obtained by the equation (6.1) adapted from Hugot(HUGOT, 1960) wherein $\mathbf{19259}$ is the calorific value of fiber, kJ/kg; $\boldsymbol{f}$ is the ratio of fiber in bagasse; $\mathbf{16747}$ is the calorific value of sugar, kJ/kg; $\boldsymbol{S}$ is the ratio of sugar in bagasse; $\mathbf{196}$ is the energy lost to heat the dirty, kJ/kg; $\boldsymbol{D}$ is the ratio of dirt (like soil) in bagasse; $\Delta \boldsymbol{H_w}$ is the enthalpy to evaporate water, kJ/kg; $\boldsymbol{W}$ is the ratio of water in bagasse (moisture), wt%;

$\mathbf{0.585}$ is the water formed from fiber combustion reaction. $\boldsymbol{f}$, $\boldsymbol{D}$, and $\boldsymbol{W}$ are parameters obtained from simulation of sugarcane being processed in a six-mill tandem. Table 19 summarizes the main parameters used in the simulations concerning a typical Brazilian Sugarmill

$$\boldsymbol{LHV = 19259f + 16747S - 196D - \Delta H_w(W + 0.585f)} \qquad \textit{(6.1)}$$

Table 19 - Parameters for the first-generation ethanol and sugar production and CHP (backpressure turbine) processes.

Parameter	Value
Sugarcane (kg)	3.22×10^9
Pol [a]	14.7%
Brix [b]	17.0 %
Fiber [c]	13%
Boiler efficiency	85 %
Boiler temperature (°C)	520
Boiler pressure (bar(a))	67
Fermentation efficiency	90%
Distillation efficiency	99.5%
Production mix [d]	60 %
Driver and generator efficiency	97 %
BPT-MPS [e]	76 %
BPT-LPS [f]	86,5 %

[a] Amount of sucrose to total soluble solids; [b] Amount of soluble solids to total material; [c] Amount of insoluble material to total material; [d] amount of juice diverted to produce sugar, the remaining juice is used to produce ethanol; [e] Backpressure turbine isentropic efficiency with steam extracting at 22 bar(a); [f] Backpressure turbine isentropic efficiency with steam extracting at 2,5 bar(a);

Figure 66 shows a schematic representation of the surplus bagasse being converted to electricity using a condensation turbine and selling it to the power grid. Figure 67 shows the schematic process that converts bagasse into second-generation ethanol; in Brazil, ethanol is distributed to the fuel stations using trucks. In Figure 68, the surplus bagasse is converted into

biomethane using anaerobic digestion; and then, it is injected into the natural gas pipeline grid.

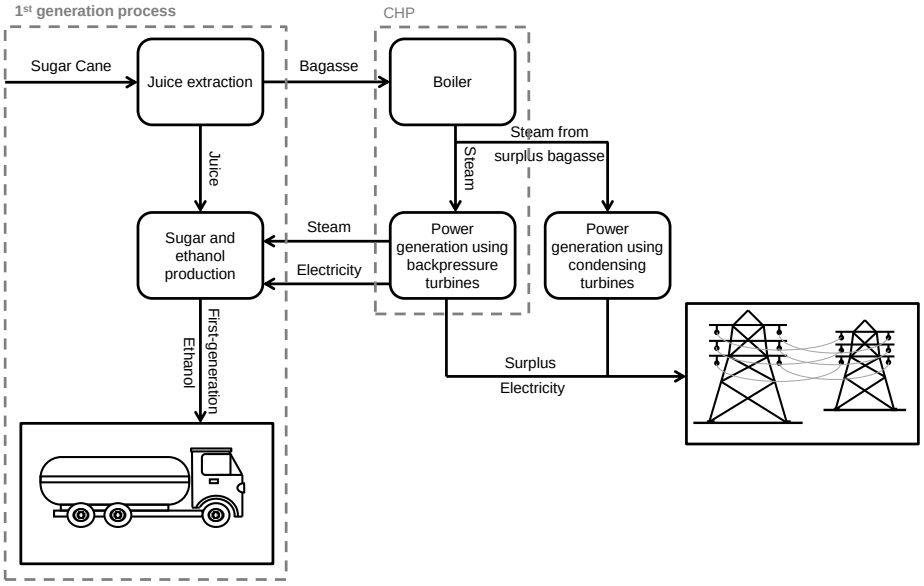

Figure 66 - Surplus lignocellulosic material being converted into electricity

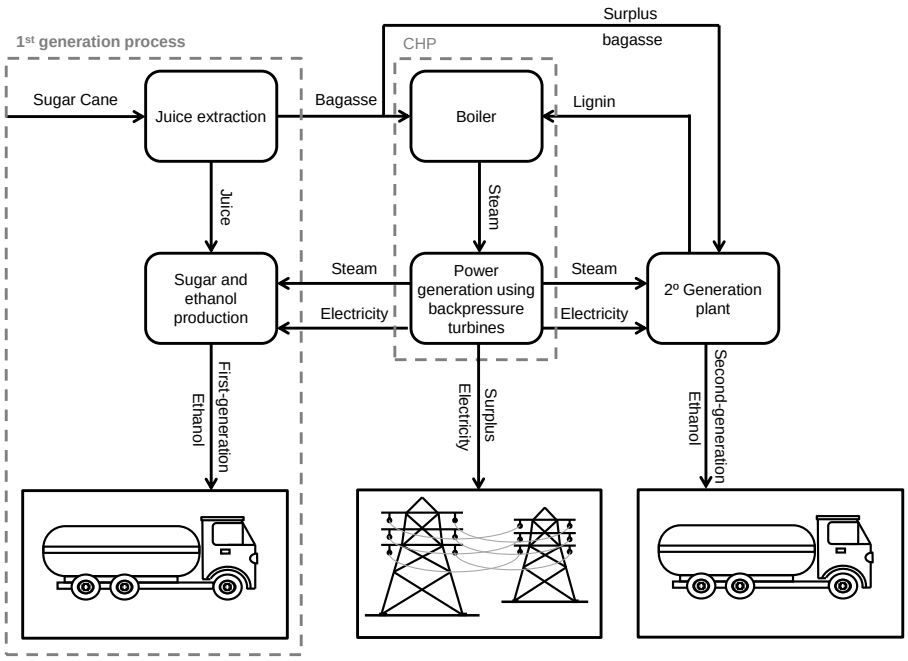

Figure 67 - Surplus lignocellulosic material being converted into second-generation ethanol

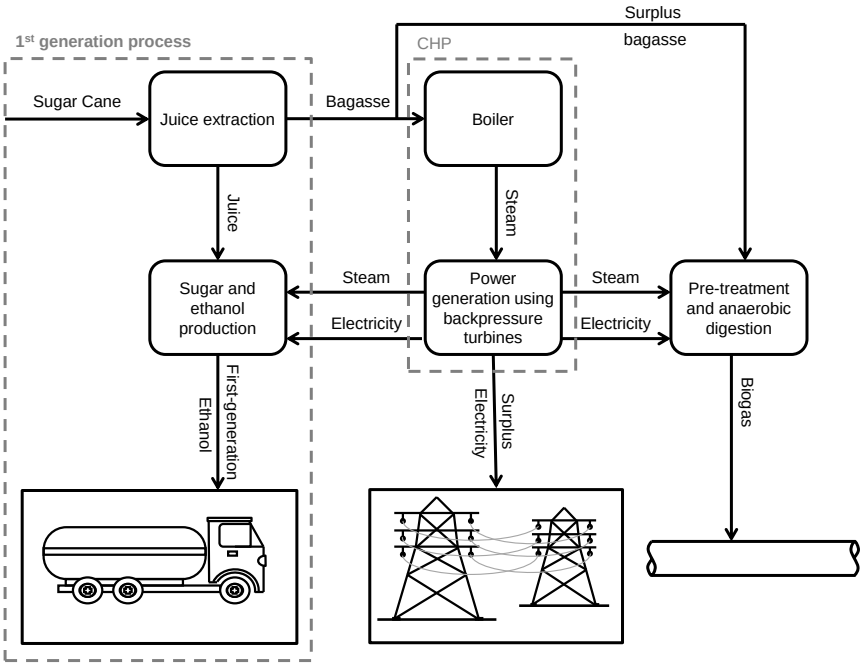

Figure 68 - Surplus lignocellulosic material being converted into biogas

6.2.1.1 Electricity production

The cogeneration system, which is comprised of a boiler and a back-pressure turbine, is a compulsory process in the sugarcane industry since the first-generation process requires thermal energy and electricity. The only decision is what type of process should be used, such as, thermodynamic cycle, steam pressure, burning technology, etc. Old sugar mill industries usually had a low-efficient process design that consumed all the bagasse to produce only heat in the process. Only after the regulation of the energy markets in 2001,(CASTRO, R. E. N. De *et al.*, 2019) did many sugar mills invest in higher efficiency cogeneration systems. A high-efficiency cogeneration process results in surplus bagasse. This can be used to produce electricity using a condensation turbine; in this process, only electricity is produced and no thermal energy is used. Table 20 shows the main parameters for the thermo-power unit using a condensation turbine. These parameters are well established since the electrical power production using the Rankine cycle has been known for over a hundred years. We design the lignocellulosic processing plant capacity based on 8000 operating hours per year while the first-generation process operates 4300 hours per year.

Table 20 - Parameters for the thermo-power unit with a condensation turbine

Parameter	Value
Driver and generator efficiency	97 %
CDT[a]	83 %
Driver and generator efficiency	97 %
Electricity losses [b] (ANEEL - AGÊNCIA NACIONAL DE ENERGIA ELÉTRICA, [*s. d.*])	13%.

[a] Condensation turbine isentropic efficiency with steam extracting at 0.17 bar(a); [b] Losses at the transformation stage, transport and distribution.

6.2.1.2 Bioethanol production

The second-generation ethanol process converts hexoses (glucan) from cellulose and pentoses (xylan) from hemicellulose to ethanol. Table 21 describes the composition of the fiber fraction in bagasse and straw in terms of the amount of glucan, xylan, and lignin on a dry basis. The straw fibrous part was considered to have the same composition as in the bagasse. The fiber fraction on sugarcane and straw comprises the lignocellulosic materials, which are composed principally of cellulose, hemicellulose, and lignin. The uncertainty regarding its composition is due to the different sugarcane varieties and the climate during the season crop.(ROCHA *et al.*, 2015)

Table 21 - Parameters used in the simulation for second-generation ethanol production

Parameter	Value
Glucan (kg / kg of bagasse dry) (ROCHA *et al.*, 2015)	[μ = 0.4219, σ = 0.0193] [a]
Xylan (kg / kg of bagasse dry) (ROCHA *et al.*, 2015)	[μ = 0.2760, σ = 0.0088] [a]
Lignin (kg / kg of bagasse dry) (ROCHA *et al.*, 2015)	[μ = 0.2156, σ = 0.0167] [a]
Electricity (W / kg of bagasse (dry)) (HUMBIRD *et al.*, 2011)	309
Lignin HHV (kJ/kg of lignin)(DIOGO JOSÉ HORST, 2013)	22460
MPS[b] (kg/kg of bagasse (dry)) (HUMBIRD *et al.*, 2011)	0.336
LPS[c] (kg/kg of bagasse (dry)) (HUMBIRD *et al.*, 2011)	0.566
Pre-treatment (ABRIL; MEDINA; ABRIL, 2012; HUMBIRD *et al.*, 2011; MAHAPATRA; MANIAN, 2017; MIURA *et al.*, 2012)	[75% 83% 95%] [d]
Fermentation efficiency of xylose (ABRIL; MEDINA; ABRIL, 2012; HUMBIRD *et al.*, 2011; MAHAPATRA; MANIAN, 2017; MIURA *et al.*, 2012)	[70% 80% 90%] [d]
Fermentation efficiency of glucose (ABRIL; MEDINA; ABRIL, 2012; HUMBIRD *et al.*, 2011; MAHAPATRA; MANIAN, 2017; MIURA *et al.*, 2012)	[87% 90% 95%] [d]

[a]Normal distribution; [b]Medium-pressure steam consumption, 22 bar(a); [c]Low-pressure steam consumption; [d]Comprises pre-treatment, conditioning, and enzymatic hydrolysis efficiency. [e]Nominal range for lower, most likely, and higher value in a triangular distribution;

The universal chemical reactions below convert cellulose and hemicellulose into ethanol. The two-step consists of enzymatic reaction followed by fermentation. Before the reaction occurs, a pretreatment on the lignocellulosic material is needed; the pre-treatment consists of a steam explosion which is aided by some chemical products.(HUMBIRD *et al.*, 2011) We assumed the efficiency conversions as shown in Table 21. Therefore, the uncertainty associated with the productions of ethanol is considered in these efficiency parameters using a triangular distribution. These uncertainties on the efficiency of the conversion of cellulose and hemicellulose into ethanol are because the industrial process has recently left the laboratory scale. Some industrial-scale second-generation ethanol plants have been implemented recently, and it seems that it may not be a feasible process so far.(CASTRO, R. E. N. De *et al.*, 2019)

$$(Glucan)_n + nH_2O \rightarrow nGlucose \rightarrow 2nEthanol + 2nCO_2 \quad (2)$$
$$C_6H_{10}O_5 \qquad C_6H_{12}O_6 \qquad C_2H_6O$$

$$(Xilan)_n + nH_2O \rightarrow nXylose \rightarrow {}^{5n}/_{3}Ethanol + {}^{5n}/_{3}CO_2 \quad (3)$$
$$C_5H_8O_4 \qquad C_5H_{10}O_5 \qquad C_2H_6O$$

As it is shown in Figure 67, the second-generation ethanol process is interconnected to the current Sugarmill process since this process requires utilities, such as steam, water, and electricity. The main interconnections, which affect the result of this analysis, are the supply of lignin to the boiler, and the consumption of steam and electricity. These change the amount of power exported by the CHP. In this simulation, not only was the efficiency of the conversion considered but also the internal loop of energy required for the process; i.e., steam and electricity that are consumed in the second-generation ethanol process. The steam production in the boiler due to the use of lignin was obtained using the lignin higher heating (DIOGO JOSÉ HORST, 2013) (HHV) shown in Table 21 and lignin moisture of 35% which is the output from the second-generation process.(HUMBIRD *et al.*, 2011) The boiler suitable to use simultaneously bagasse, straw, and lignin must be a fluidized bed boiler.

6.2.1.3 Biogas production

Biogas is produced by the conversion of the bagasse into methane.(MONLAU *et al.*, 2015) The conversion factor is usually given in cubic meters of methane per kg of volatile solids (m^3/kg-VS). Moreover, there are a number of methods for determining biomethane production in anaerobic digestion.(JINGURA; KAMUSOKO, 2017) For the bagasse, many different conversions can be found in the literature, ranging from 0.084 m^3/kg-VS(INYANG *et al.*, 2010) without any pre-treatment to 0.373 m^3/kg-VS(VATS; KHAN; AHMAD, 2019) using pre-treatment. Using data from the literature,(ANGELIDAKI; SANDERS, 2004; BADSHAH *et al.*, 2012; BOLADO-RODRÍGUEZ *et al.*, 2016; MAHAPATRA; MANIAN, 2017; MUSTAFA *et al.*, 2018; NOSRATPOUR; KARIMI; SADEGHI, 2018; Production of bioethanol, methane and heat from sugarcane bagasse in a biorefinery conceptRABELO *et al.*, 2011; SAJAD HASHEMI; KARIMI; MAJID KARIMI, 2019; VATS; KHAN; AHMAD, 2019) we build up the conversion parameter shown in Table 22 considering pre-treatment before anaerobic digestion: the steam explosion is the pre-treatment currently used in many lignocellulosic biogas plants in Europe.(ZORG BIOGAS BUILT BIOGAS PLANTS AROUND THE GLOBE | ZORG BIOGAS, [*s. d.*]) Moreover, the

bagasse sample itself shows different properties depending on the sugarcane variety, soil fertility, climate, maturity, etc.(BADSHAH *et al.*, 2012; MARTÍNEZ-GUTIÉRREZ, 2018; MUSTAFA *et al.*, 2018; ROCHA *et al.*, 2015) This uncertainty is also considered using the triangular distribution shown in Table 22. In the pre- treatment, we have considered the steam explosion,(AHMAD *et al.*, 2018; JANKE *et al.*, 2015; LIZASOAIN *et al.*, 2017; RIBEIRO *et al.*, 2017; STEINBACH *et al.*, 2019; THEURETZBACHER *et al.*, 2015; WEBER *et al.*, 2020) which consumes 0.336 kg of steam per kg of bagasse (dry).(HUMBIRD *et al.*, 2011)

Table 22 - Parameters used in the simulation for biogas production

Parameter	Value
VS(BADSHAH *et al.*, 2012; MARTÍNEZ-GUTIÉRREZ, 2018; MUSTAFA *et al.*, 2018) [a]	[70%, 80%, 90%] [b]
Methane conversion (m^3/kgVS) (AHMAD *et al.*, 2018; ANGELIDAKI; SANDERS, 2004; BADSHAH *et al.*, 2012; BOLADO-RODRÍGUEZ *et al.*, 2016; MUSTAFA *et al.*, 2018; Production of bioethanol, methane and heat from sugarcane bagasse in a biorefinery conceptRABELO *et al.*, 2011; SAJAD HASHEMI; KARIMI; MAJID KARIMI, 2019; VATS; KHAN; AHMAD, 2019)	[0.18, 0.25, 0.38] [b]
Methane concentration in raw biogas (HOYER *et al.*, 2016)	[48% 52.9% 60%] [b]
CO_2 concentration in raw biogas	[25% 30% 37%] [b]
Electricity demand (kWh/m^3) (HOYER *et al.*, 2016)	0.3
MPS for upgrading (kg/kg of bagasse (dry))	0.3363
Sulphuric acid (kg/kg of bagasse (dry))	0.02377
Ammonia (kg/kg of bagasse (dry))	0.01212

[a] Volatile solids in the substrate; [b] Nominal range for lower, most likely, and higher value in a triangular distribution;

The gaseous product leaving the bioreactor must uphold certain gas quality criteria, which are currently based on national specifications by ANP (National Petroleum and Biofuel Agency).(ANP - AGÊNCIA NACIONAL DO PETRÓLEO, Gás natural e biocombustíveis, [*s. d.*]) They are CH_4 = 90% min; CO_2 = 3% max; H_2S = 10 PPM max; N_3 = 3% max; O_2 = 0.8% max; this specification is obtained by a purification process. There are at least six processes currently being used in the market. We have adopted the Pressure Swing Adsorption (PSA) process. In this process, raw biogas is compressed to elevate pressure and then fed into an adsorption

column, which retains the carbon dioxide but not the methane. The energy and material inputs are shown in Table 22.

Water abstraction to dilute bagasse before anaerobic digestion was not considered. Instead of water, vinasse must be used to prepare the anaerobic substrate. Most studies of anaerobic digestion in the sugarcane sector consider vinasse as the substrate,(JANKE *et al.*, 2015; KOTARSKA; DZIEMIANOWICZ; ŚWIERCZYŃSKA, 2019; LONGATI *et al.*, 2019; LONGATI; CAVALETT; CRUZ, 2017; MORAES; ZAIAT; BONOMI, 2015) which is the stillage of the ethanol distillation. Vinasse presents lower values of organic matter content; for this reason, it would be possible to use and recycle vinasse to dilute bagasse. Moreover, vinasse is currently applied as organic fertilizer on the field without previous energy use; after anaerobic digestion, the digestant could still be used to partially replace the fertilizers in the sugarcane fields. Nevertheless, we want to access the production of biogas as a result of bagasse alone; therefore, only the volatile solids present in bagasse are considered to obtain the biomethane.

6.2.2 Mileage rate

To enable a fair comparison between the three processes, the total amount of ethanol, electricity, and biogas is converted in terms of the distance one can drive using a light vehicle; the mileage rate for each fuel is shown in Table 23. To access the ethanol fuel, we have considered the normal distribution among 427 ethanol cars, currently being commercialized in Brazil;(INMETRO, 2020) all ethanol cars use both ethanol and gasoline (flex-fuel technology). In Brazil natural gas vehicles are not commercialized by automobile manufacturers; therefore, consumers have to buy a gasoline car and convert it to use natural gas fuel. To determine the gas mileage rate, we assumed that a gasoline car that drives 10 km/L when converted to natural gas will drive 13.5 km/m^3; thus, to determine the mileage rate we have considered the normal distribution among 855 gasoline cars converted to be able to also use natural gas.(INMETRO, 2020) At the time we wrote this article, only 4 electric vehicles are available in the Brazilian market;(INMETRO, 2020) therefore, to access the electric cars mileage rate we used data from EPA,(EPA; US DEPARTMENT OF ENERGY, 2020) which presents 36 different electric cars being commercialized in the United States; the sample of 36 is statistically more reliable than a sample of 4. The mean mileage rate and the standard

deviation among them are shown in Table 23 as well. More detail about the car mileage rate distribution is shown in the Electronic Supplementary Information (ESI).†

Here, we did not take into account the use of hybrid and fuel-cell cars. The hybrid car is a car that combines the internal combustion engine with an electric motor. There are many kinds of hybrid cars, for example, some of them can be plugged in to charge the battery some cannot; some use the internal combustion engine to recharge the batteries so only the electric motor drives the car, some are driven by both motors. Since the focus of this article relies on the fuel, using a car that can use more than one fuel, would change the focus of the article evaluating the car instead of the fuel, and this would confuse the analysis and the conclusion; in fact, the hybrid car is an attempt to combine the advantages of both kinds of engines. Also, fuel cell cars were not included, this technology has great potential including the use of glucose(ZHANG, 2009) and ethanol(AN *et al.*, 2011) as a source to produce hydrogen; however, fuel cell cars are not widely currently available in the market.

Table 23 - Mileage rate for light vehicles

	City mileage rate	Highway mileage rate
EV[a] (km/kW·h) (INMETRO, 2020)	[μ=5.34 σ=1.08] [d]	[μ=4.80 σ=0.79] [d]
FLV[b] (km/L) (INMETRO, 2020)	[μ=7.72 σ=1.32] [d]	[μ=9.15 σ=1.44] [d]
GAS[C] (km/m³) (EPA; US DEPARTMENT OF ENERGY, 2020)	[μ=13.66 σ=4.15] [d]	[μ=16.25 σ=3.97][d]

[a]Electric vehicle; [b]Flex-fuel vehicle using ethanol-fuel; [c]Flex-fuel vehicle using biogas-fuel; [d] normal distribution.

6.2.3 Monte Carlo analysis

The uncertainties associated with the input values are evaluated using the Monte Carlo approach. Monte Carlo calculation runs a number of simulations to evaluate the mean and standard error of an output. As the number of simulations increases, the mean and standard error tend to reach a constant value;(LERCHE; MUDFORD, 2005) thus the output mean values from the last simulation are compared to the previous simulation. This process is repeated until the change in the mean values with the increase in the number of runs is less than a pre-

specified degree of accuracy; as shown by Equation (6.4), wherein $\boldsymbol{x}$ is the output, $\boldsymbol{k}$ is the number of outputs, and $\boldsymbol{n}$ is the number of Monte Carlo realizations.

$$\mathbf{0.9995} \leq \frac{\sum_{j=1}^{n} x_j^{(k)} \Big/ n}{\sum_{j=1}^{(n-1)} x_j^{(k)} \Big/ (n-1)} \leq \mathbf{1.0004}, \qquad \forall\, x^{(k)} \tag{6.4}$$

6.2.4 Gas emissions, water usage, and health

The CO_2 emissions are compared in the three alternatives. In this article, we do not study the whole lifecycle of sugarcane from plantation to the surplus bagasse, which is the input of the three investigated processes. The biomass production step and the first-generation process are the same across the options. Therefore, we investigate and compare the emission along the chain from the surplus bagasse through processing, manufacture, distribution, and use in a vehicle. We do not compare the greenhouse gas emission (GHG) to conventional fuels i.e. subtracting the CO_2 emitted by the biofuel to that emitted by conventional fossil fuel. Even so, many studies have compared GHG mitigation: they are first-generation ethanol compared to gasoline,(CONTRERAS *et al.*, 2009; MEZA-PALACIOS *et al.*, 2019; SOARES *et al.*, 2009) second-generation ethanol compared to gasoline,(SUN; FUJIMOTO; MINOWA, 2013; WATANABE *et al.*, 2016) electricity from bagasse compared to the one from fuel oil and natural gas,(AMEZCUA-ALLIERI *et al.*, 2019; HILOIDHARI; BANERJEE; RAO, 2021; MOHAMMADI *et al.*, 2020) and biogas compared to gasoline and natural gas from petroleum.(MORERO; RODRIGUEZ; CAMPANELLA, 2015; PATTERSON *et al.*, 2011) Therefore, the amount of CO_2 obtained in this simulation does not aim to determine the total GHG emission, or mitigation, but to compare the emission between the three alternative fuels; even though, most of the CO_2 emitted is from sugarcane photosynthesis.

The CO_2 emitted during the processing, distribution, and use are calculated using a mass balance and the emission factors shown in Table 24. The direct CO_2 emission is obtained applying mass balance using the developed simulation, and indirect CO_2 emission is calculated applying emission factors as it is listed hereafter. (a) When straw is brought from the field with sugarcane stalks using diesel trucks, we consider an average distance of 22 km(SOARES *et al.*, 2009) from the field to the industrial site. The CO_2 emission is calculated based on the amount

of straw being transported and does not include the weight of the sugarcane stalks. (b) Emission of CO_2 associated with the thermal and electric power production, for all the scenarios, is released to the atmosphere by the boiler.(AUL; PECHAN, 1993) This emission includes the internal consumption of electricity and steam, and the electricity exported to the grid (c) Emissions of CO_2 by the second-generation process comprises the fermentation, additive and enzymes, vinasse disposal, and ethanol transportation. Emission of CO2 by the second-generation ethanol process released during the fermentation is calculated according to chemical equations, Equations (6.2) and (6.3). The contribution due to the chemical additive and enzyme use is calculated according to Humbird.(HUMBIRD *et al.*, 2011) The vinasse produced in the second-generation process is used as a liquid fertilizer in the field; the emission of CO_2 in the field due to the use of vinasse is calculated in accordance with the emission factor shown in Table 24.(DE OLIVEIRA *et al.*, 2013) The ethanol is transported from the industrial site to the fuel stations using diesel heavy-load vehicles, using an average distance of 250 km.(SOARES *et al.*, 2009) (d) Emission of GHG by the biogas production comprises the anaerobic digestion, the biogas upgrading using PSA, biogas leakage during transportation and distribution, and the disposal of the digestate. The CO_2 in the raw biogas, the concentration of which is shown in Table 22, is released during the upgrading process,(ANGELIDAKI; SANDERS, 2004; BADSHAH *et al.*, 2012; BOLADO-RODRÍGUEZ *et al.*, 2016; MAHAPATRA; MANIAN, 2017; MUSTAFA *et al.*, 2018; Production of bioethanol, methane and heat from sugarcane bagasse in a biorefinery conceptRABELO *et al.*, 2011; SAJAD HASHEMI; KARIMI; MAJID KARIMI, 2019; VATS; KHAN; AHMAD, 2019) calculated using the concentration before and after the biogas is upgraded. CH_4 leakage in the production and upgrading process(HOYER *et al.*, 2016) and during transmission, storage, and distribution(BRADBURY; CLEMENT; DOWN, 2015) was obtained by the emission factors shown in Table 24. We assume that the digestate is used as a liquid fertilizer in the field: the emission of CO_2 in the field due to the use of the digestate is calculated following the emission factor used for vinasse shown in Table 24.(DE OLIVEIRA *et al.*, 2013) (e) Emission of CO_2 due to vehicle manufacture, using electric and combustion engines abides by the factor shown in Table 24. (f) Finally, the CO_2 released by the vehicles exhaust pipes is calculated using the combustion reaction of the bioethanol and biogas; additionally, CO, NOx, and NMHC (nonmethane hydrocarbon) due to incomplete combustion are calculated using the emission factors shown in Table 24. Emissions from the construction of facilities, such as the biorefinery, machinery,

pipeline, and power grid are not taken into account; these emissions are expected to make no difference in the overall GHG emissions.(TRIVEDI; MALINA; BARRETT, 2015) The CH_4, NOx, and CO when emitted, are converted to the CO_2 equivalent according to IPCC 2007.(IPCC, 2006)

Table 24 - Emission factors used to obtain the GHG emission

		Electricity	Ethanol	Biogas
HLV[a,1,2] (g-CO2eq/km-tonne)		[63.9 72.4 83.0][b]	[63.9 72.4 83.0] [b]	[63.9 72.4 83.0] [b]
BEF [c,3] CO_2 (kg-CO_2/kg-steam)		[0.303 0.390 0.476][b]	[0.303 0.390 0.476][b]	[0.303 0.390 0.476] [b]
BEF [c,3] NOx (g-NO_2/kg-steam)		[0.12 0.30 0.43] [b]	[0.12 0.30 0.43] [b]	[0.12 0.30 0.43] [b]
Vehicle[d,4] (kg-CO2eq)		11,996	9,744	9,744
Vehicle life time[4] (km)		150,000	150,000	150,000
Vehicle exhaust pipe emissions	CO_2 [e] (kg/m³)	–	1.5	0.48
	CO[5,6] (g/m³)	–	[μ = 3,363 σ = 1,593]	[3.75 4.50 6.00] [2]
	NOx[5,6] (g/L)	–	[μ = 172 σ = 90]	[0.08 0.26 0.56] [2]
	NMHC city[5,6] (g/L)	–	[μ = 172 σ = 85]	[0 0.14 0.39] [2]
E2G process [f,7] (g-CO2eg/kg-Bagasse)		–	[10.08 10.94 13.23] [b]	–
Biogas leakage[8,g]		–	–	1.5 %**
Biomethane loss[9,h]		–	–	0.055%**
Vinasse[i,10] (kg-CO2eq/m³-vinasse)			0.314	0.314

[a] Transportation emission factor by heavy load vehicle using diesel; [b] Nominal range for lower, most likely, and higher value in a triangular distribution;[c] Boiler emission factor; [d] Emission Cradle-to-Gate of the vehicle manufacturing; [e] From the stoichiometric conversion of ethanol and methane in CO2 by combustion; [f] Emission factor due to the use of enzyme during the production of second-generation ethanol; [g] Raw biogas leakage during production and upgrading; [h] Biomethane loss during transmission storage and distribution. [i] Emission of CO_2 from vinasse being applied to the sugarcane field

Source: [1](COYLE, 2007); 2 (MCKINNON; PIECYK, 2010);3 (AUL; PECHAN, 1993);4(QIAO et al., 2019); 5(INMETRO, 2020); 6(BIELACZYC; SZCZOTKA; WOODBURN, 2016); 7(SUN; FUJIMOTO; MINOWA, 2013); 8(HOYER et al., 2016); 9(BRADBURY; CLEMENT; DOWN, 2015); 10(DE OLIVEIRA et al., 2013)

Water abstraction is also obtained using the developed simulation. The first-generation process produces surplus hot water from the sugarcane juice concentration. Therefore, adding a subsequent process to the current process, such as the ones in this study, reduces the overall water abstraction when compared with the sum of each separate process. We have assumed no water from abstraction is used to dilute the bagasse before anaerobic digestion; the dilution of bagasse must be done by the vinasse and industrial wastewater.

Nowadays, the vehicle emission of pollutants at the exhaust pipe responsible for causing diseases such as particulate matter (PM), nitrogen oxides (NOx), carbon monoxide (CO), and hydrocarbons (HCs) has decreased significantly. For example, PM emitted from tires and brakes is of the same order of magnitude as the exhaust pipe emission.(WINKLER *et al.*, 2018) Besides, the data available do not allow a quantitative comparison between biogas and ethanol fuel.(ANP - AGÊNCIA NACIONAL DO PETRÓLEO, Gás natural e biocombustíveis, [*s. d.*]) Even so, it is clear that a zero-emission car, such as the electric vehicle, would lower the burden of disease caused by air pollution.(ZARANTE; SODRÉ, 2018) For this reason, we only qualitatively compare the use of the electric vehicle with the other two internal-combustion vehicles.

6.2.5 Financial appraisal

There is often some confusion between financial analysis and economic analysis of projects. The financial analysis studies the performance of a project from the point of view of the investors and lenders. The economic analysis aims at identifying economic, social, and environmental benefits from the perspective of the national economy. (KONSTANTIN; KONSTANTIN, 2018) Nevertheless, prices are always distorted by customs duties, taxes, subsidies, and other restrictions.

Here, we assess the investment in facilities to produce and distribute the fuel: the point of view of the owner of the industry. We do not assess the cost of the cars for the final user: the difference in price between an electrical and an internal-combustion engine vehicle. This is because the cost strongly depends on how much the final user uses the car; additionally, the end-user decision on what car to buy relies on many intangible parameters besides financial such as design, size, accessories, etc.

To examine any technical-economic phenomenon, it is necessary to build its mathematical model. The model to access the economic effectiveness of any investment project is designed by using geometric series, commonly used in three different forms: the total discounted net present value, NPV; internal rate return, IRR; and discounted payback period DPBP. Cash flow is the sum of disbursement and revenues, as represented in Figure 69. We here use NPV as shown in Equation (6.5); therefore, the option with the highest positive NPV is the preferred option, provided that the investment risk and lifetime are the same across the options. Cash flow is the sum of disbursement and revenues; the capital disbursed in a project like this is usually not made at the beginning of the project but rather in many installments during the construction. Moreover, part of the money invested is usually funded by a financial institution or government. The capital expenditure, $Capex$, is a function of the facilities capacity. The investment for the different capacities, which depends on the amounts of straw from the field, is calculated using a capacity function model that uses a capacity parameter to estimate the facility cost as shown in Equation (6.6). Larger facilities cost more, but usually, there are economies of scale in their construction.(ESCHENBACH, 2011) Table 25 shows the parameters used to access NPV. The NPV accessed refers to the earnings before taxes and retail costs.

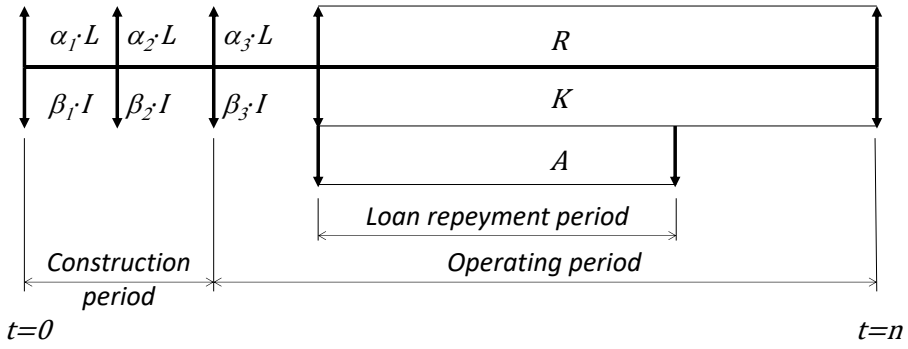

Figure 69 - Cashflow diagram

$$NPV = \sum_{t=0}^{n} \frac{L - I + R - A - k}{(1+r)^t} \qquad (6.5)$$

$$Capex(S) = \frac{Capex_b}{{S_b}^m} S^m \qquad (6.6)$$

$$Capex(S) = \sum_{j=1}^{3} \alpha_j I + \beta_j L\,, \qquad \sum \alpha_j + \beta_j = 1 \qquad (6.7)$$

Wherein: $\boldsymbol{n}$ is the calculation period of the company's lifetime expressed in years; $\boldsymbol{t}$ is subsequent years of operating the enterprise; $\boldsymbol{L}$ is the loan; $\boldsymbol{I}$ is the equity installment; $\boldsymbol{R}$ is the annual revenue; $\boldsymbol{A}$ is the annuity loan repayment.

The base capital expenditure for a given size, $Capex_b$, is estimated from values given by industries(BNDES, 2020; GRANBIO, 2020) and the literature (HOYER *et al.*, 2016; HUMBIRD *et al.*, 2011; ZORG BIOGAS BUILT BIOGAS PLANTS AROUND THE GLOBE | ZORG BIOGAS, [*s. d.*]). For the scenarios where the condensation turbine is used, no power grid infrastructure was considered; i.e. we assumed that the Sugarmill is connected to the national power grid. For the scenario where biogas is produced, we have considered an additional expenditure, which comprises two possibilities; first, to build a facility to distribute natural gas locally or second, to build 10 km of pipeline to connect the Sugarmill to the national pipeline grid; both are expected to have about the same cost; therefore, an increment of 14×10^6 USD(EPE - EMPRESA DE PESQUISA ENERGÉTICA, [*s. d.*]) was added to the biogas Capex alternative. A third possibility, not considered in this study, is to use the biogas to replace diesel used in agriculture machinery; nevertheless, an additional expenditure to adapt the fleet would be necessary.

The cost of the feedstock is assumed to be the cost of the delivered sugarcane straw. Bagasse is assumed to be cost-free; this is because the facilities must be placed in the same industrial site.

Table 25 - Parameters used to obtain the net present value of the investments

	Electricity production	Ethanol production	Biogas Production
$Capex_b$ (USD)	56,751,000.00	116,600,000.00	26,180,000.00
S_b (m³/y)[a] (MW)[b]	55	230,910.00	36,630,000.00
m – scaleable parameter	0.75	0.8	0.8
Construction period (year)	2	2	2
Loan repayment period (years)	15	15	15
Operating period (years)	25	25	25
r - discount rate (year^{-1})	12%	12%	12%
Intrest on loan (year^{-1})	3.4%	3.4%	3.4%
Inflation (year^{-1})	[1% 2% 5%]	[1% 2% 5%]	[1% 2% 5%]
k - operation costs M&I[c]	5%	5%	5%
k - operation costs ADM[d] (USD/year)	1,100,000	1,100,000	1,100,000
k - operation costs Variable (USD/(km·kg)	2.40x10^{-4}	2.40x10^{-4}	2.40x10^{-4}
$\alpha_1 - \alpha_2 - \alpha_3$	15% – 15% – 20%	15% – 15% – 20%	15% – 15% – 20%
$\beta_1 - \beta_2 - \beta_3$ [f]	15% – 15% – 20%	15% – 15% – 20%	15% – 15% – 20%
Price (USD/m³)[1] (USD/MWh)[2]	[μ = 36.82 σ = 11.27] [2]	[μ = 329.69 σ = 25.16] [3]	[μ = 0.3572 σ = 0.0453] [4]

[a] The unit applies for the second-generation ethanol and Biogas; [b] The unit applies for the condensation turbine; [c] M&I maintenance and insurance as a percentage of CAPEX; [d] ADM fixed costs such as administrative expenses; [e] Equity disbursement; [f] Loan parcel.
Source: 1 (FRANÇOSO et al., 2017); 2 (ANEEL - AGENCIA NACIONAL DE ELENRGIA, [s. d.]); 3(UDOP - UNIÃO NACIONAL DE BIOENERGIA, [s. d.]); 4(ANP - AGÊNCIA NACIONAL DO PETRÓLEO, Gas natural e biocombustíveis, [s. d.])

The administrative expenses, i.e. wages, benefits, executive compensation, etc, shown in Table 25, comprise only the direct staff since the non-direct staff is considered to be shared with the current industry. We have used an exchange rate of 5.45 BRL to 1.00 USD and 1.19 USD to 1.00 EUR. Revenue is calculated according to the fuel price: to determine the fuel price uncertainty, we considered the average fuel price and its standard deviation from the last ten years applying the inflation correction index according to IPCA(IBGE - INSTITUTO BRASILEIRO DE GEOGRAFIA E ESTATISTICA, [*s. d.*]) index.

6.3 Results and discussion

The better scenario for the use of sugarcane bagasse and straw will depend on the stakeholders (governments, private industry, and individual consumers). Each one will prioritize the result differently. In this section, we compare different simulation results and at the end, of this section, we use the radar plot to give the overall view. Uncertainty calculated using the Monte Carlo is represented by the error bar. Simulations were repeated using the different inputs as described in Section 6.2.3. The repeating simulation is stopped once the mean value of the output remains constant: 548 Monte Carlo realizations were conducted to reach the stopping criterion as described in section 6.2.3.

6.3.1 Total mileage

Here, total mileage is the distance one can drive using the surplus bagasse and straw when they are converted into fuel a light vehicle can use. Side-by-side comparison of the sugarcane bagasse and straw being converted into ethanol, electricity, and biogas is shown in Figure 70. The simulations comprise bringing straw from the field in three different ratios of straw (kg) to sugarcane (kg): 0:1, 0.035:1, and 0.07:1. Additionally, the simulations take into account the driving condition in cities and highways. Therefore, this figure depicts the distance a vehicle can travel in 18 different scenarios using the bagasse and straw as a primary fuel; produced by a sugarcane industry that mills 3.22×10^9 kg of sugarcane per year. The figure also shows the ethanol produced from sugarcane sucrose, namely first-generation process, and the surplus-power produced using a back-pressure turbine, i.e. when the thermal energy from the CHP is also used in the industrial process. The volume of first-generation ethanol remains the same across all the simulations; however, the surplus electricity depends on the industrial-process scenario. Table 26 shows the distance that 1kg of sugarcane can provide when transformed in fuels and used in a light vehicle. The base scenario is the one that no straw is brought from the field nor fuel is produced using bagasse. It is important to mention that part of the service provided by the sugarcane plantation is sugar. Therefore, this table does not present all the services provided by the sugarcane as feedstock: i.e., if this data is used to compare sugarcane to another feedstock, the production of sugar must be taken into account. We have considered that 60% of the juice is diverted to produce sugar; in this case, the amount of sugar produced is 73g/kg of sugarcane.

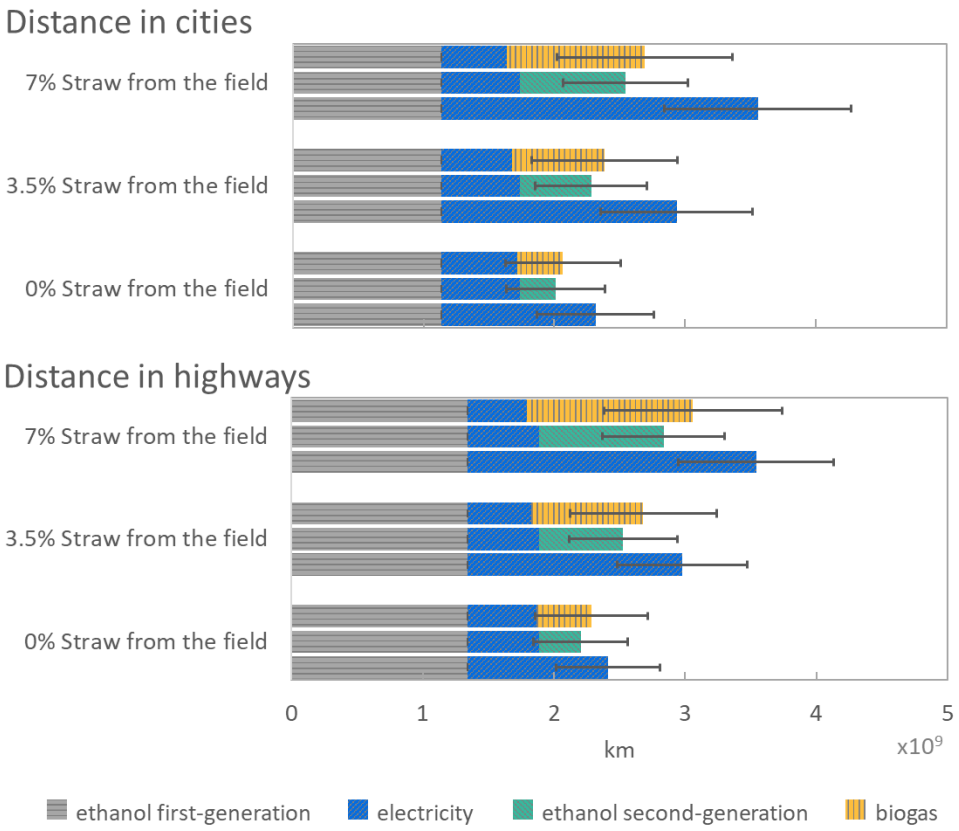

Figure 70 - Total distance one can drive in a light vehicle using different types of fuel obtained from bagasse

Table 26 - Distance per kg of sugarcane

	Straw from the field	City $Km/kg_{sugarcane}$	Highway $Km/kg_{sugarcane}$
Base scenario[a]	0%	0.380±0.066	0.447±0.071
Biogas	0%	0.688±0.147	0.762±0.144
	3.5%	0.795±0.186	0.893±0.186
	7%	0.897±0.223	1.020±0.227
Second-generation ethanol	0%	0.669±0.125	0.735±0.120
	3.5%	0.760±0.142	0.842±0.138
	7%	0.848±0.159	0.945±0.155
Electricity	0%	0.771±0.150	0.803±0.132
	3.5%	0.978±0.194	0.992±0.165
	7%	1.186±0.238	1.180±0.197

[a]No fuel is produced from lignocellulosic material, i.e. only first-generation ethanol, that uses sucrose is considered.

Bringing straw from the field increases the mileage in all the scenarios. However, it shows a non-conclusive result when comparing across the fuel type. This is because of the mileage-rate variation among the different vehicles. As described in section 2.2, Monte Carlo (used to access the uncertainty) considered a number of vehicles available in the market; in this list, there are variable efficiency cars that result in a high mileage-rate variation. Electricity is better than ethanol or biogas provided that we compare an average mileage-rate. A previous study(CASTRO, R. E. N. De *et al.*, 2019) which had used an electric and a flex-fuel version of the same car showed that electricity performs better in cities and is equivalent to ethanol on highways. In fact, the closer one gets to encompassing all the relevant elements the less straightforward the resulting outcome is.

6.3.2 Financial appraisal

Figure 71 shows the net present value obtained considering that a Sugarmill could alternatively invest in one of the three fuel-production processes, using its surplus bagasse and straw from the field. Bringing straw from the field was a profit opportunity in all the simulated scenarios. The ethanol and biogas have a better NPV than electricity due to the lower price of electricity when compared with the price of vehicular-gas and ethanol.

Although this result outlines the view of the investor, considering other aspects, such as national energy security, health, and environmental aspects, a less profit option could be preferable; in this case, incentive from the government is required to make the less attractive investment more attractive to Sugarmill owners.

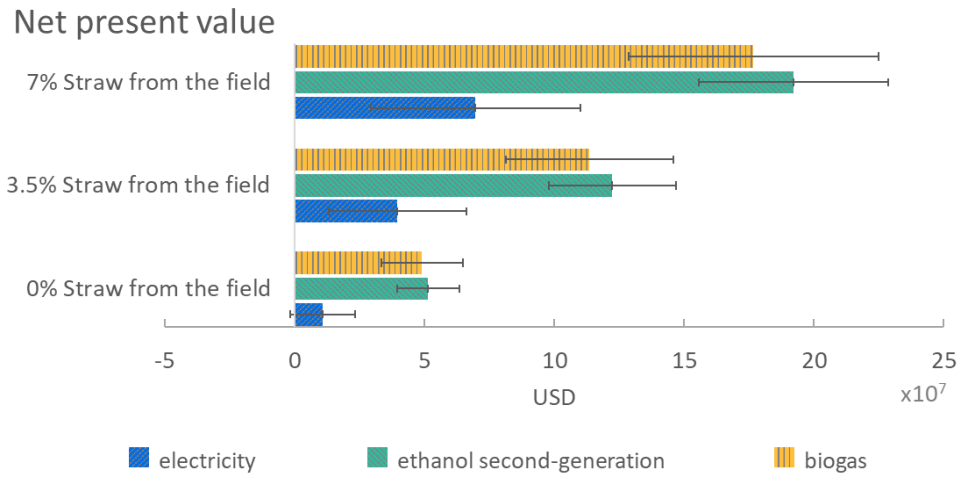

Figure 71 - The net present value of the investment in the surplus bagasse processing plant

6.3.3 CO_2 emission

Figure 72 shows the specific values for the emission of CO_2 per km; the absolute value is in the (ESI).† However, this study compares the values of CO_2 emission across the scenarios; the value of the CO_2 emission shown in this graph cannot be analyzed alone because this article does not comprise the whole life cycle analysis from the sugarcane plantation to the final use. In fact, the agricultural and industrial residue, such as sugarcane bagasse and straw, when used as a fuel source is often considered as having net zero emission of CO_2;(WATANABE *et al.*, 2016; YAN; INDERWILDI; KING, 2010) thus, a mitigation analysis which compares it with the conventional fossil fuel would result in a negative CO_2 emission.

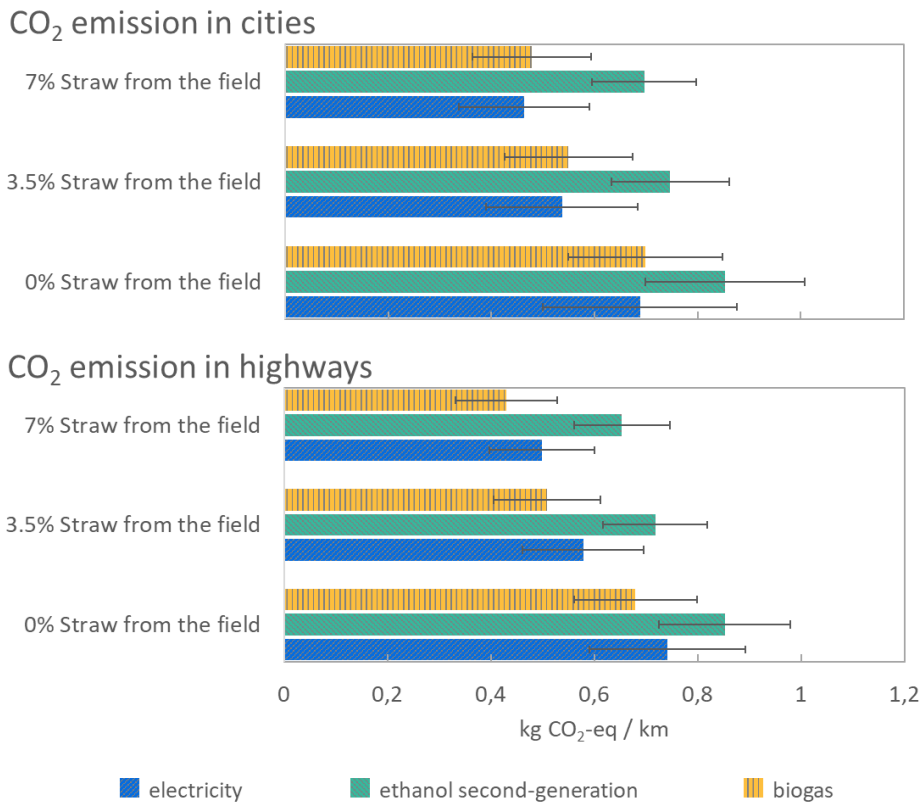

Figure 72 - CO2 equivalent emitted from the surplus bagasse being processed to use in a light vehicle

Bringing straw from the field lowers the emission of CO_2 in all the scenarios. Examining across fuel alternatives, the average values of CO_2 emission for the electric and biogas are better than second-generation ethanol. Comparing the biogas and electric car, the electric one performs better in cities, and biogas on highways; this is because of the higher mileage rate that the electric car has in cities, and the higher mileage rate of biogas car on highways.

Currently, CO_2 is the major environmental concern when transportation is evaluated. This is because fossil-based fuel is by far the most used source. However, it is important to

mention that although the use of an electric vehicle lowers GHG emission, it depletes some critical metal resources such as lithium.(HAO *et al.*, 2019)

6.3.4 Water abstraction

Figure 73 shows the total water abstraction in the Sugarmill industry when the surplus bagasse and straw are converted into fuel for light vehicles by adding an industrial plant to the current Sugarmill industry. The water abstraction when the condensation turbine is used is mainly due to the make-up of the cooling tower used to condense the steam output from the condensation turbine. The volume of water abstraction when biogas is produced is only used in the pre-treatment step; i.e. water is not used to dilute the lignocellulosic material before the anaerobic digestion. Instead of water, vinasse from first-generation ethanol, industrial wastewater, and part of the digestate is recycled and used to dilute(MONLAU *et al.*, 2015) the bagasse and straw that enter the anaerobic digestor. If raw water alone were used to prepare the substrate in the anaerobic digestion, the water abstraction would skyrocket.

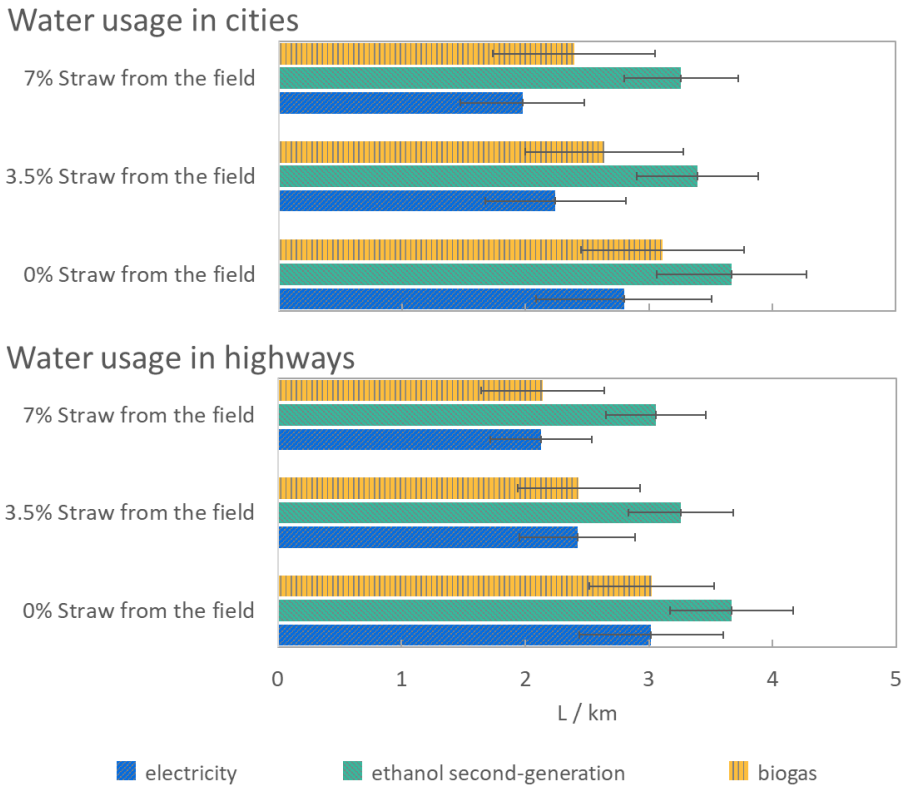

Figure 73 - Total water abstraction considering a Sugarcane mill industry when a process that converts bagasse and straw into fuel for light vehicles is added

To access the potential that sugarcane bagasse and straw can represent in the national scenario, we extrapolate the current simulation considering all the sugarcane produced in Brazil in 2019. In that year, 642.7x10^9 kg of sugarcane were harvested.(CONAB, 2017) In the same year, 37.24x10^6 m³ of gasoline(FELIPE KURY, 2020) was consumed. If all the sugarcane surplus bagasse and straw were used to replace the gasoline by converting them into ethanol, it would have been possible to replace 59% of the gasoline used in that year. It is also possible to compare biogas with natural gas; in the same year, Brazil consumed 35.8x10^9 m³ of which 28% was imported.(BP, 2020) Again, if all the surplus bagasse and straw produced in Brazil were transformed into biogas, it would have been possible to replace all the natural gas consumed in 2019. This shows that sugarcane bagasse and straw can play an important role not only because of their environmental benefits but also securing the country's energy.

Regardless of the other variables, bringing straw from the field in a ratio of 0.07:1 (straw:sugarcane) showed better performance; thus, to access the three different fuels in this ratio of straw, a radar plot is used as shown in Figure 74. In this figure, each axis drawn from the center corresponds to an attribute. The values toward the outer edges of the radar plot are preferred. As the metrics are all in different units, the scale along each dimension is normalized.

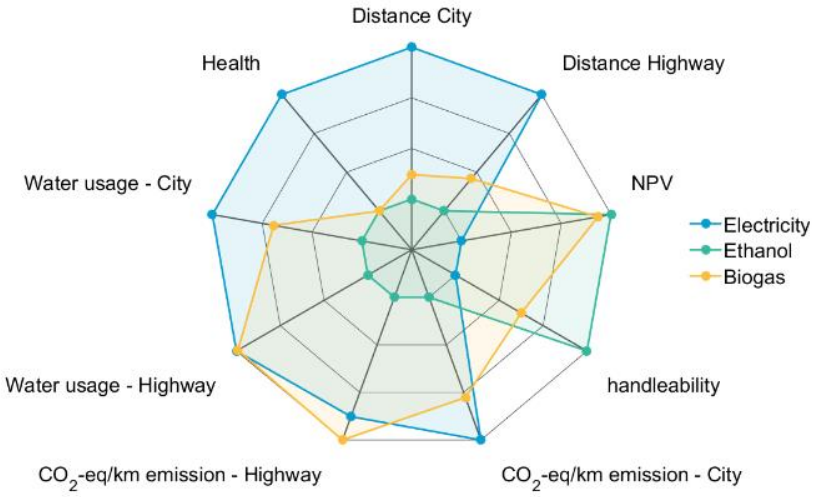

Figure 74 - Representation of the performance of electricity, second-generation ethanol, and biogas used as fuel in light vehicles.
Straw is brought from the field in a ratio of 0.07 kg/kg-bagasse

We included in this plot the health category that stands for the emission of pollutants in populated areas and that causes diseases. The data available(ANP - AGÊNCIA NACIONAL DO PETRÓLEO, Gás natural e biocombustíveis, [*s. d.*]) does not allow the quantitative comparison

between biogas and ethanol fuel; even so, it is clear that a zero-emission car, such as the electric vehicle, would lower the burden of diseases caused by air pollution in large cities.(RAMACHANDRAN; STIMMING, 2015) Ethanol may increase the emission of acetaldehyde(ANDERSON, 2009) near fuel stations and both biogas and ethanol release $PM_{2.5}$ and CO during combustion.(HOLNICKI *et al.*, 2017; PAOLINI *et al.*, 2018; SEMPLE *et al.*, 2014) Therefore, to include this criterion, we attribute a better grade for the electric car and the same grade for the other two types of internal-combustion engine vehicles.

We also included the handleability among the three fuels: people in general, are willing to pay more for a fuel that is easier to be handled, as happened with gas replacing coal in Europe for heating systems.(GIAMPIETRO; ULGIATI, 2005) Liquid fuel, because of its high energy density, state, and stability, is easier to handle when compared to gas. The use of compressed gas requires a hermetic cylinder, and a number of accidents are reported annually caused by gas leakage. Hence, ethanol is selected as the easiest fuel to handled. The energy density and the time necessary to recharge the battery is the main drawback of the electric vehicle. Most electric vehicles have low autonomy (the distance one can travel using a fully charged battery set) when compared with similar internal-combustion engine vehicles. For this reason, we classified electricity as the worst fuel in the handleability criterion.

6.4 Conclusion

This study investigated the use of lignocellulosic agricultural and industrial residue from the sugarcane industry. Bringing straw from the field increased the production of biofuels and mitigated the environmental impact. This study also concludes that, depending on the point of view of the stakeholder involved in the analysis, different decisions on what fuel to produce using bagasse and straw could be made; therefore, the decision will depend on the weight each stakeholder gives to each criterion. The three types of fuel have different advantages and disadvantages when considering different aspects, such as climate, air pollution, health, economy, energy security, and handleability. A stricter system boundary, considering a more specific use, for example, the use of cars in cities or the model and type of the car, would reduce the uncertainty and tend toward one of the options. Additionally, the high uncertainty gives insight to policymakers:(LOVETT *et al.*, 2011) for example, the high variance in the car mileage rate (shown in ESI) indicates that a higher efficiency technology is

available and a law imposed on manufactures will improve the average mileage rate of the cars available in the market. It also illustrates the opportunity for the private sector to invest in research to reach high-efficiency conversion factors in the second-generation ethanol and biogas processing; uncertainty in these conversion factors arises due to upscaling the two processes. In fact, all are possible depending on the particularities of each producer and consumer; thus, all can be produced and used simultaneously with a predominance of one according to the regional variation of the country.

Conflicts of interest

There are no conflicts to declare.

Acknowledgments

The authors gratefully acknowledge the support of the RCGI – Research Centre for Gas Innovation, hosted by the University of São Paulo (USP) and sponsored by FAPESP – The São Paulo Research Foundation (2014/50279-4) and Shell Brasil.

This study was financed in part by the Personnel Coordination of Improvement of Higher Level - Brazil (CAPES) - Finance Code 001.

References

ABRIL, D.; MEDINA, M.; ABRIL, A. Sugar cane bagasse prehydrolysis using hot water. **Brazilian Journal of Chemical Engineering**, [*s. l.*], v. 29, n. 1, p. 31–38, 2012.

AHMAD, S. *et al.* Prospects for pretreatment methods of lignocellulosic waste biomass for biogas enhancement: opportunities and challenges. **Biofuels**, [*s. l.*], v. 9, n. 5, p. 575–594, 2018. Disponível em: https://www.tandfonline.com/doi/full/10.1080/17597269.2017.1378991. Acesso em: 10 ago. 2020.

AMEZCUA-ALLIERI, M. A. *et al.* Techno-economic analysis and life cycle assessment for energy generation from sugarcane bagasse: Case study for a sugar mill in Mexico. **Food and Bioproducts Processing**, [*s. l.*], v. 118, p. 281–292, 2019. Disponível em: https://linkinghub.elsevier.com/retrieve/pii/S0960308519300422.

AN, L. *et al.* A novel direct ethanol fuel cell with high power density. **Journal of Power Sources**, [*s. l.*], v. 196, n. 15, p. 6219–6222, 2011. Disponível em: https://linkinghub.elsevier.com/retrieve/pii/S0378775311006550.

ANDERSON, L. G. Ethanol fuel use in Brazil: air quality impacts. **Energy & Environmental Science**, [*s. l.*], v. 2, n. 10, p. 1015, 2009. Disponível em: http://xlink.rsc.org/?DOI=b906057j.

ANEEL - AGENCIA NACIONAL DE ELENRGIA. **Resultados dos Leilões (preço, potência e quantidade de empreendimentos) ANEEL - Agencia Nacional de Elenrgia Elétrica**. [*S. l.*], [*s. d.*]. Disponível em: https://app.powerbi.com/view?r=eyJrIjoiYmMzN2Y0NGMtYjEyNy00OTNlLWI1YzctZjI0ZTUwMDg5ODE3IiwidCI6IjQwZDZmOWI4LWVjYTctNDZhMi05MmQ0LWVhNGU5YzAxNzBlMSIsImMiOjR9. Acesso em: 22 ago. 2020.

ANEEL - AGÊNCIA NACIONAL DE ENERGIA ELÉTRICA. [*S. l.*], [*s. d.*]. Disponível em: http://www2.aneel.gov.br/area.cfm?idArea=801&idPerfil=4. Acesso em: 30 jul. 2020.

ANGELIDAKI, I.; SANDERS, W. Assessment of the anaerobic biodegradability of macropollutants. **Reviews in Environmental Science and Bio/Technology**, [*s. l.*], v. 3, n. 2, p. 117–129, 2004. Disponível em: https://link.springer.com/article/10.1007/s11157-004-2502-3. Acesso em: 10 ago. 2020.

ANP - AGÊNCIA NACIONAL DO PETRÓLEO, gas natural e biocombustíveis. **CSA Sistema de Levantamento de Preços | ANP - Agência nacional do petróleo, gas natural e biocombustíveis**. [*S. l.*], [*s. d.*]. Disponível em: http://preco.anp.gov.br/include/Resumo_Mensal_Regiao.asp. Acesso em: 22 ago. 2020.

ANP - AGÊNCIA NACIONAL DO PETRÓLEO, gás natural e biocombustíveis. **RESOLUÇÃO ANP Nº 685, DE 29.6.2017 - DOU 30.6.2017**. [*S. l.*], [*s. d.*]. Disponível em: http://legislacao.anp.gov.br/?path=legislacao-anp/resol-anp/2017/junho&item=ranp-685--2017. Acesso em: 17 ago. 2020.

AUL, E.; PECHAN, E. H. **Emission Factor Documentation for Ap-42 Section 1.8 Bagasse Combustion In Sugar Mills**. [*S. l.: s. n.*], 1993.

BADSHAH, M. *et al.* Use of an Automatic Methane Potential Test System for evaluating the biomethane potential of sugarcane bagasse after different treatments. **Bioresource Technology**, [*s. l.*], v. 114, p. 262–269, 2012.

BIELACZYC, P.; SZCZOTKA, A.; WOODBURN, J. A comparison of exhaust emissions from vehicles fuelled with petrol, LPG and CNG. **IOP Conference Series: Materials Science and Engineering**, [*s. l.*], v. 148, n. 1, p. 012060, 2016. Disponível em: https://iopscience.iop.org/article/10.1088/1757-899X/148/1/012060.

BNDES. **Com R$97,1 mi do BNDES, Cocal investe em geração de energia apartir de biogás de cana**. [*S. l.*], 2020. Disponível em: https://agenciadenoticias.bndes.gov.br/detalhe/noticia/Com-R$-971-mi-do-BNDES-Cocal-investe-em-geracao-de-energia-a-partir-de-biogas-de-cana/. Acesso em: 2 nov. 2020.

BOLADO-RODRÍGUEZ, S. *et al.* Effect of thermal, acid, alkaline and alkaline-peroxide pretreatments on the biochemical methane potential and kinetics of the anaerobic digestion of wheat straw and sugarcane bagasse. **Bioresource Technology**, [*s. l.*], v. 201, p. 182–190, 2016.

BP. **Statistical Review of World Energy**. [*S. l.: s. n.*], 2020. Disponível em: https://www.bp.com/en/global/corporate/energy-economics/statistical-review-of-world-energy/natural-gas.html. .

BRADBURY, J.; CLEMENT, Z.; DOWN, A. **Greenhouse Gas Emissions and Fuel Use within the Natural Gas Supply Chain – Sankey Diagram Methodology**. [*S. l.: s. n.*], 2015. Disponível em: https://www.energy.gov/sites/prod/files/2015/07/f24/QER Analysis - Fuel Use and GHG Emissions from the Natural Gas System%2C Sankey Diagram Methodology_0.pdf. .

CARVALHO, J. L. N. *et al.* Multilocation Straw Removal Effects on Sugarcane Yield in South-Central Brazil. **Bioenergy Research**, [*s. l.*], v. 12, n. 4, p. 813–829, 2019.

CASTRO, R. E. N. de *et al.* Assessment of Sugarcane-Based Ethanol Production. *In*: BASSO, T. P.; BASSO, L. C. (org.). **Fuel Ethanol Production from Sugarcane**. [*S. l.*]: IntechOpen, 2019. p. 3–22. *E-book*. Disponível em: https://www.intechopen.com/books/fuel-ethanol-production-from-sugarcane.

CASTRO, R. E. N. de *et al.* Open Sugarcane Process Simulation Platform. *In*: INTERNATIONAL SYMPOSIUM ON PROCESS SYSTEMS ENGINEERING – PSE 2018. San Diego: Elsevier B.V., 2018. p. 1819–1824. *E-book*. Disponível em: https://linkinghub.elsevier.com/retrieve/pii/B9780444642417502986.

CHERUBIN, M. R. *et al.* Sugarcane Straw Removal: Implications to Soil Fertility and Fertilizer Demand in Brazil. **BioEnergy Research**, [*s. l.*], v. 12, n. 4, p. 888–900, 2019. Disponível em: https://doi.org/10.1007/s12155-019-10021-w. Acesso em: 15 jan. 2020.

CONAB - COMPANHIA NACIONAL DE ABASTECIMENTO. **Conab - Boletim da Safra de Cana-de-açúcar**. [*S. l.*], [*s. d.*]. Disponível em: https://www.conab.gov.br/info-agro/safras/cana/boletim-da-safra-de-cana-de-acucar. Acesso em: 2 set. 2020.

CONTRERAS, A. M. *et al.* Comparative Life Cycle Assessment of four alternatives for using by-products of cane sugar production. **Journal of Cleaner Production**, [*s. l.*], v. 17, n. 8, p. 772–779, 2009. Disponível em: https://linkinghub.elsevier.com/retrieve/pii/S0959652608003004. Acesso em: 17 ago. 2020.

COYLE, M. **Effects of payload on the fuel consumption of trucks research for the department for transport (DFT) funded through the department for environment food and rural affairs (DEFRA) aggregates levy sustainability fund (ALSF)**. [*S. l.: s. n.*], 2007. Disponível em: https://imise.co.uk/wp-content/uploads/2017/09/RR5-Effects-of-Payload-on-the-Fuel-Consumption-of-Trucks.pdf. Acesso em: 23 ago. 2020.

DE OLIVEIRA, B. G. *et al.* Soil greenhouse gas fluxes from vinasse application in Brazilian sugarcane areas. **Geoderma**, [*s. l.*], v. 200–201, p. 77–84, 2013. Disponível em: https://linkinghub.elsevier.com/retrieve/pii/S0016706113000487. Acesso em: 29 ago. 2020.

DIOGO JOSÉ HORST. **Avaliação da Produção Energética a Partir de Ligninas Contidas em Biomassa**. 2013. - UNIVERSIDADE TECNOLÓGICA FEDERAL DO PARANÁ , [*s. l.*], 2013. Disponível em: http://www.pg.utfpr.edu.br/dirppg/ppgep/dissertacoes/arquivos/216/Dissertacao.pdf.

Acesso em: 8 ago. 2018.

EPA; US DEPARTMENT OF ENERGY. **2020 Fuel Economy Guide**. [*S. l.: s. n.*], 2020. Disponível em: https://fueleconomy.gov/feg/pdfs/guides/FEG2020.pdf. Acesso em: 11 ago. 2020.

EPE - EMPRESA DE PESQUISA ENERGÉTICA. **Plano Indicativo de Gasodutos de Transporte | EPE Empresa de pesquisa energética**. [*S. l.: s. n.*], [*s. d.*]. Disponível em: http://www.epe.gov.br. Acesso em: 22 ago. 2020.

ESCHENBACH, T. G. **Engineering Economy Applying Theory to Practice**. [*S. l.: s. n.*], 2011.

FELIPE KURY. **Seminário Anual de Avaliação do Mercado de Combustíveis 2020**. Rio de Janeiro: ANP, 2020. Disponível em: http://www.anp.gov.br/arquivos/palestras/seminario-mercado-combustiveis-2020/sdl.pdf. Acesso em: 1 set. 2020.

FERNANDES, A. C. **Cálculos na agroindústria da cana-de-açúcar.** 3. ed. Piracicaba: Sociedade dos Técnicos Açucareiros e Alcooleiros do Brasil, 2011.

FRANÇOSO, R. F. *et al.* Relação do custo de transporte da cana-de-açúcar em função da distância. **Revista IPecege**, [*s. l.*], v. 3, n. 1, p. 100–105, 2017. Disponível em: https://revista.ipecege.org.br/Revista/article/view/123. Acesso em: 22 ago. 2020.

GIAMPIETRO, M.; ULGIATI, S. Integrated assessment of large-scale biofuel production. **Critical Reviews in Plant Sciences**, [*s. l.*], v. 24, n. 5–6, p. 365–384, 2005.

GOLDEMBERG, J. The challenge of biofuels. **Energy & Environmental Science**, [*s. l.*], v. 1, n. 5, p. 523, 2008. Disponível em: http://xlink.rsc.org/?DOI=b814178a.

GRANBIO. **GranBio e NextChem assinam parceria para desenvolver mercado de etanol celulósico**. [*S. l.*], 2020. Disponível em: http://www.granbio.com.br/press-releases/granbio-e-nextchem-assinam-parceria-para-desenvolver-mercado-de-etanol-celulosico/. Acesso em: 2 nov. 2020.

HAO, H. *et al.* Impact of transport electrification on critical metal sustainability with a focus on the heavy-duty segment. **Nature Communications**, [*s. l.*], v. 10, n. 1, p. 1–7, 2019. Disponível em: http://dx.doi.org/10.1038/s41467-019-13400-1.

HILOIDHARI, M.; BANERJEE, R.; RAO, A. B. Life cycle assessment of sugar and electricity production under different sugarcane cultivation and cogeneration scenarios in India. **Journal of Cleaner Production**, [*s. l.*], v. 290, n. xxxx, p. 125170, 2021. Disponível em: https://linkinghub.elsevier.com/retrieve/pii/S0959652620352148.

HOLNICKI, P. *et al.* Burden of Mortality and Disease Attributable to Multiple Air Pollutants in Warsaw, Poland. **International Journal of Environmental Research and Public Health**, [*s. l.*], v. 14, n. 11, p. 1359, 2017. Disponível em: http://www.mdpi.com/1660-4601/14/11/1359.

HOYER, K. *et al.* **Biogas upgrading - a technical review**. [*S. l.: s. n.*], 2016. Disponível em: http://vav.griffel.net/filer/C_Energiforsk2016-275.pdf. .

HUANG, W.-D.; PERCIVAL ZHANG, Y.-H. Analysis of biofuels production from sugar based on

three criteria: Thermodynamics, bioenergetics, and product separation. **Energy Environ. Sci.**, [*s. l.*], v. 4, n. 3, p. 784–792, 2011. Disponível em: http://xlink.rsc.org/?DOI=C0EE00069H.

HUGOT, E. **Handbook of Cane Sugar Engineering**. 3. ed. [*S. l.*]: Elsevier, 1960. *E-book*. Disponível em: https://linkinghub.elsevier.com/retrieve/pii/C20130124373.

HUMBIRD, D. *et al.* **Process Design and Economics for Biochemical Conversion of Lignocellulosic Biomass to Ethanol**. Colorado: [*s. n.*], 2011. Disponível em: https://www.nrel.gov/research/publications.html. .

IBGE - INSTITUTO BRASILEIRO DE GEOGRAFIA E ESTATISTICA. **Índice Nacional de Preços ao Consumidor Amplo - IPCA | IBGE**. [*S. l.*], [*s. d.*]. Disponível em: https://www.ibge.gov.br/estatisticas/economicas/precos-e-custos/9256-indice-nacional-de-precos-ao-consumidor-amplo.html?t=downloads. Acesso em: 22 ago. 2020.

INMETRO. **Tabela de consumo/eficiência energética de veículos automotores leves 2020**. [*S. l.: s. n.*], 2020. Disponível em: http://www.inmetro.gov.br/consumidor/pbe/veiculos_leves_2020.pdf. Acesso em: 11 ago. 2020.

INYANG, M. *et al.* Biochar from anaerobically digested sugarcane bagasse. **Bioresource Technology**, [*s. l.*], v. 101, n. 22, p. 8868–8872, 2010. Disponível em: https://linkinghub.elsevier.com/retrieve/pii/S0960852410010692. Acesso em: 10 ago. 2020.

IPCC. **Publications 2006 IPCC Guidelines for National Greenhouse Gas Inventories**. [*S. l.*], 2006. Disponível em: https://www.ipcc-nggip.iges.or.jp/public/2006gl/vol1.html. Acesso em: 23 ago. 2020.

JACOBSON, M. Z. Review of solutions to global warming, air pollution, and energy security. **Energy Environ. Sci.**, [*s. l.*], v. 2, n. 2, p. 148–173, 2009. Disponível em: http://xlink.rsc.org/?DOI=B809990C.

JANKE, L. *et al.* Biogas Production from Sugarcane Waste: Assessment on Kinetic Challenges for Process Designing. **International journal of molecular sciences**, [*s. l.*], v. 16, n. 9, p. 20685–20703, 2015.

JINGURA, R. M.; KAMUSOKO, R. Methods for determination of biomethane potential of feedstocks: A review. **Biofuel Research Journal**, [*s. l.*], v. 4, n. 2, p. 573–586, 2017.

KONDE, K. S. *et al.* Sugarcane bagasse based biorefineries in India: Potential and challenges. **Sustainable Energy and Fuels**, [*s. l.*], v. 5, n. 1, p. 52–78, 2021. Disponível em: http://dx.doi.org/10.1039/D0SE01332C.

KONSTANTIN, P.; KONSTANTIN, M. **Power and Energy Systems Engineering Economics**. Cham: Springer International Publishing, 2018. *E-book*. Disponível em: http://link.springer.com/10.1007/978-3-319-72383-9.

KOTARSKA, K.; DZIEMIANOWICZ, W.; ŚWIERCZYŃSKA, A. Study on the Sequential Combination of Bioethanol and Biogas Production from Corn Straw. **Molecules**, [*s. l.*], v. 24, n. 24, p. 4558,

2019. Disponível em: https://pubmed.ncbi.nlm.nih.gov/31842493/. Acesso em: 10 ago. 2020.

KRUYT, B. *et al.* Indicators for energy security. **Energy Policy**, [*s. l.*], v. 37, n. 6, p. 2166–2181, 2009. Disponível em: https://linkinghub.elsevier.com/retrieve/pii/S0301421509000883.

LERCHE, I.; MUDFORD, B. S. How Many Monte Carlo Simulations Does One Need to Do?. **Energy Exploration & Exploitation**, [*s. l.*], v. 23, n. 6, p. 405–427, 2005. Disponível em: http://journals.sagepub.com/doi/10.1260/014459805776986876.

LIZASOAIN, J. *et al.* Corn stover for biogas production: Effect of steam explosion pretreatment on the gas yields and on the biodegradation kinetics of the primary structural compounds. **Bioresource Technology**, [*s. l.*], v. 244, n. Pt 1, p. 949–956, 2017. Disponível em: https://pubmed.ncbi.nlm.nih.gov/28847085/. Acesso em: 9 ago. 2020.

LONGATI, A. A. *et al.* Biogas Production from Anaerobic Digestion of Vinasse in Sugarcane Biorefinery: A Techno-economic and Environmental Analysis. **Waste and Biomass Valorization**, [*s. l.*], v. 1, p. 3, 2019. Disponível em: https://doi.org/10.1007/s12649-019-00811-w. Acesso em: 16 jul. 2020.

LONGATI, A. A.; CAVALETT, O.; CRUZ, A. J. G. Life Cycle Assessment of vinasse biogas production in sugarcane biorefineries. *In*: COMPUTER AIDED CHEMICAL ENGINEERING. [*S. l.*]: Elsevier, 2017. v. 40, p. 2017–2022. Disponível em: https://www.sciencedirect.com/science/article/pii/B978044463965350338X. Acesso em: 21 dez. 2017.

LOVETT, J. C. *et al.* Multiple objectives in biofuels sustainability policy. **Energy Environ. Sci.**, [*s. l.*], v. 4, n. 2, p. 261–268, 2011. Disponível em: http://xlink.rsc.org/?DOI=C0EE00041H.

LUQUE, R. *et al.* Biofuels: a technological perspective. **Energy & Environmental Science**, [*s. l.*], v. 1, n. 5, p. 542, 2008. Disponível em: www.uco.es/senecagreencat.

MAHAPATRA, S.; MANIAN, R. P. Bioethanol from Lignocellulosic Feedstock: a Review. **Research Journal of Pharmacy and Technology**, [*s. l.*], v. 10, n. 8, p. 2750, 2017. Disponível em: https://www.scopus.com/record/display.uri?eid=2-s2.0-85040836339&origin=resultslist&zone=contextBox. Acesso em: 26 fev. 2018.

MARTÍNEZ-GUTIÉRREZ, E. Biogas production from different lignocellulosic biomass sources: advances and perspectives. **3 Biotech**, [*s. l.*], v. 8, n. 5, p. 233, 2018. Disponível em: https://link.springer.com/article/10.1007/s13205-018-1257-4. Acesso em: 10 ago. 2020.

MCKINNON, A. C.; PIECYK, M. **Measuring and Managing CO2 Emissions in European Chemical TransportCefic**. [*S. l.: s. n.*], 2010. Disponível em: www.cefic.org. .

MEZA-PALACIOS, R. *et al.* Life cycle assessment of cane sugar production: The environmental contribution to human health, climate change, ecosystem quality and resources in México. **Journal of Environmental Science and Health, Part A**, [*s. l.*], v. 54, n. 7, p. 668–678, 2019. Disponível em: https://www.tandfonline.com/doi/full/10.1080/10934529.2019.1579537. Acesso em: 17 ago. 2020.

MIURA, T. *et al.* Improvement of enzymatic saccharification of sugarcane bagasse by dilute-alkali-catalyzed hydrothermal treatment and subsequent disk milling. **Bioresource Technology**, [*s. l.*], v. 105, p. 95–99, 2012. Disponível em: http://dx.doi.org/10.1016/j.biortech.2011.11.118.

MOHAMMADI, F. *et al.* Life cycle assessment (LCA) of the energetic use of bagasse in Iranian sugar industry. **Renewable Energy**, [*s. l.*], v. 145, p. 1870–1882, 2020. Disponível em: https://doi.org/10.1016/j.renene.2019.06.023.

MONLAU, F. *et al.* New opportunities for agricultural digestate valorization: current situation and perspectives. **Energy & Environmental Science**, [*s. l.*], v. 8, n. 9, p. 2600–2621, 2015. Disponível em: www.rsc.org/ees.

MORAES, B. S.; ZAIAT, M.; BONOMI, A. Anaerobic digestion of vinasse from sugarcane ethanol production in Brazil: Challenges and perspectives. **Renewable and Sustainable Energy Reviews**, [*s. l.*], v. 44, p. 888–903, 2015. Disponível em: http://dx.doi.org/10.1016/j.rser.2015.01.023.

MORERO, B.; RODRIGUEZ, M. B.; CAMPANELLA, E. A. Environmental impact assessment as a complement of life cycle assessment. Case study: Upgrading of biogas. **Bioresource Technology**, [*s. l.*], v. 190, p. 402–407, 2015. Disponível em: http://dx.doi.org/10.1016/j.biortech.2015.04.091.

MUSTAFA, A. M. *et al.* Effect of hydrothermal and Ca(OH)2 pretreatments on anaerobic digestion of sugarcane bagasse for biogas production. **Bioresource Technology**, [*s. l.*], v. 259, p. 54–60, 2018.

NOSRATPOUR, M. J.; KARIMI, K.; SADEGHI, M. Improvement of ethanol and biogas production from sugarcane bagasse using sodium alkaline pretreatments. **Journal of Environmental Management**, [*s. l.*], v. 226, p. 329–339, 2018.

PAOLINI, V. *et al.* Environmental impact of biogas: A short review of current knowledge. **Journal of Environmental Science and Health, Part A**, [*s. l.*], v. 53, n. 10, p. 899–906, 2018. Disponível em: https://www.tandfonline.com/action/journalInformation?journalCode=lesa20.

PATTERSON, T. *et al.* Life cycle assessment of biogas infrastructure options on a regional scale. **Bioresource Technology**, [*s. l.*], v. 102, n. 15, p. 7313–7323, 2011. Disponível em: http://dx.doi.org/10.1016/j.biortech.2011.04.063.

QIAO, Q. *et al.* Life cycle greenhouse gas emissions of Electric Vehicles in China: Combining the vehicle cycle and fuel cycle. **Energy**, [*s. l.*], v. 177, p. 222–233, 2019. Disponível em: https://doi.org/10.1016/j.energy.2019.04.080. Acesso em: 23 ago. 2020.

RABELO, S. C. *et al.* Production of bioethanol, methane and heat from sugarcane bagasse in a biorefinery concept. **Bioresource Technology**, [*s. l.*], v. 102, n. 17, p. 7887–7895, 2011. Disponível em: http://dx.doi.org/10.1016/j.biortech.2011.05.081.

RAMACHANDRAN, S.; STIMMING, U. Well to wheel analysis of low carbon alternatives for road

traffic. **Energy & Environmental Science**, [*s. l.*], v. 8, n. 11, p. 3313–3324, 2015. Disponível em: www.rsc.org/ees.

RFA RENEWABLE FUELS ASSOCIATION. **Ethanol Industry Outlook 2002**. Washington: [*s. n.*], 2002. Disponível em: https://ethanolrfa.org/wp-content/uploads/2015/09/outlook_2002.pdf. Acesso em: 14 jul. 2020.

RIBEIRO, F. R. *et al.* Anaerobic digestion of hemicellulose hydrolysate produced after hydrothermal pretreatment of sugarcane bagasse in UASB reactor. **Science of the Total Environment**, [*s. l.*], v. 584–585, p. 1108–1113, 2017.

ROCHA, G. J. de M. *et al.* Influence of mixed sugarcane bagasse samples evaluated by elemental and physical-chemical composition. **Industrial Crops and Products**, [*s. l.*], v. 64, p. 52–58, 2015.

SAJAD HASHEMI, S.; KARIMI, K.; MAJID KARIMI, A. Ethanolic ammonia pretreatment for efficient biogas production from sugarcane bagasse. **Fuel**, [*s. l.*], v. 248, n. March, p. 196–204, 2019. Disponível em: https://doi.org/10.1016/j.fuel.2019.03.080.

SCARLAT, N.; DALLEMAND, J. F.; FAHL, F. Biogas: Developments and perspectives in Europe. **Renewable Energy**, [*s. l.*], v. 129, p. 457–472, 2018. Disponível em: https://doi.org/10,1016/j.renene2018.03.006.

SEMPLE, S. *et al.* Commentary: Switching to biogas – What effect could it have on indoor air quality and human health?. **Biomass and Bioenergy**, [*s. l.*], v. 70, p. 125–129, 2014. Disponível em: http://dx.doi.org/10.1016/j.biombioe.2014.01.054.

SOARES, L. H. de B. *et al.* **Mitigação das emissões de gases efeito estufa pelo uso de etanol da cana-de-açúcar produzido no Brasil.Embrapa**. Seropédica - RJ: [*s. n.*], 2009. Disponível em: http://www.cnpab.embrapa.br/publicacoes/ download/cit027.pdf. .

STEINBACH, D. *et al.* Steam Explosion Conditions Highly Influence the Biogas Yield of Rice Straw. **Molecules**, [*s. l.*], v. 24, n. 19, p. 3492, 2019. Disponível em: https://pubmed.ncbi.nlm.nih.gov/31561500/. Acesso em: 9 ago. 2020.

SUN, X.-Z.; FUJIMOTO, S.; MINOWA, T. A comparison of power generation and ethanol production using sugarcane bagasse from the perspective of mitigating GHG emissions. **Energy Policy**, [*s. l.*], v. 57, p. 624–629, 2013. Disponível em: http://dx.doi.org/10.1016/j.enpol.2013.02.020.

THEURETZBACHER, F. *et al.* Steam explosion pretreatment of wheat straw to improve methane yields: Investigation of the degradation kinetics of structural compounds during anaerobic digestion. **Bioresource Technology**, [*s. l.*], v. 179, p. 299–305, 2015. Disponível em: https://pubmed.ncbi.nlm.nih.gov/25549903/. Acesso em: 9 ago. 2020.

TRIVEDI, P.; MALINA, R.; BARRETT, S. R. H. Environmental and economic tradeoffs of using corn stover for liquid fuels and power production. **Energy & Environmental Science**, [*s. l.*], v. 8, n. 5, p. 1428–1437, 2015. Disponível em: http://xlink.rsc.org/?DOI=C5TC02043C.

UDOP - UNIÃO NACIONAL DE BIOENERGIA. :: **:: UDOP - União Nacional de Bioenergia ::**. [*S. l.*], [*s. d.*]. Disponível em: https://www.udop.com.br/index.php?item=alcool_historico&op=13. Acesso em: 22 ago. 2020.

VATS, N.; KHAN, A. A.; AHMAD, K. Observation of biogas production by sugarcane bagasse and food waste in different composition combinations. **Energy**, [*s. l.*], v. 185, p. 1100–1105, 2019.

WATANABE, M. D. B. *et al.* Hybrid Input-Output Life Cycle Assessment of First- and Second-Generation Ethanol Production Technologies in Brazil. **Journal of Industrial Ecology**, [*s. l.*], v. 20, n. 4, p. 764–774, 2016. Disponível em: http://doi.wiley.com/10.1111/jiec.12325.

WEBER, B. *et al.* Agave bagasse response to steam explosion and anaerobic treatment. **Biomass Conversion and Biorefinery**, [*s. l.*], p. 1–11, 2020. Disponível em: https://doi.org/10.1007/s13399-020-00619-y. Acesso em: 13 jul. 2020.

WINKLER, S. L. *et al.* Vehicle criteria pollutant (PM, NOx, CO, HCs) emissions: how low should we go?. **npj Climate and Atmospheric Science**, [*s. l.*], v. 1, p. 26, 2018. Disponível em: www.nature.com/npjclimatsci.

YAN, X.; INDERWILDI, O. R.; KING, D. A. Biofuels and synthetic fuels in the US and China: A review of Well-to-Wheel energy use and greenhouse gas emissions with the impact of land-use change. **Energy Environ. Sci.**, [*s. l.*], v. 3, n. 2, p. 190–197, 2010. Disponível em: www.rsc.org/ees.

ZARANTE, P. H. B.; SODRÉ, J. R. Comparison of aldehyde emissions simulation with FTIR measurements in the exhaust of a spark ignition engine fueled by ethanol. **Heat and Mass Transfer**, [*s. l.*], v. 54, n. 7, p. 2079–2087, 2018. Disponível em: https://doi.org/10.1007/s00231-018-2295-5.

ZHANG, Y.-H. P. A sweet out-of-the-box solution to the hydrogen economy: is the sugar-powered car science fiction?. **Energy & Environmental Science**, [*s. l.*], v. 2, n. 3, p. 272, 2009. Disponível em: http://xlink.rsc.org/?DOI=b818694d.

ZORG BIOGAS BUILT BIOGAS PLANTS AROUND THE GLOBE | ZORG BIOGAS. [*S. l.*], [*s. d.*]. Disponível em: https://zorg-biogas.com/. Acesso em: 11 ago. 2020.

Supplementary Information

1 Vehicle mileage rate distribution

The 75, 76, and 77 show the mileage rate distribution in a histogram plot for ethanol, biogas, and electric vehicles.

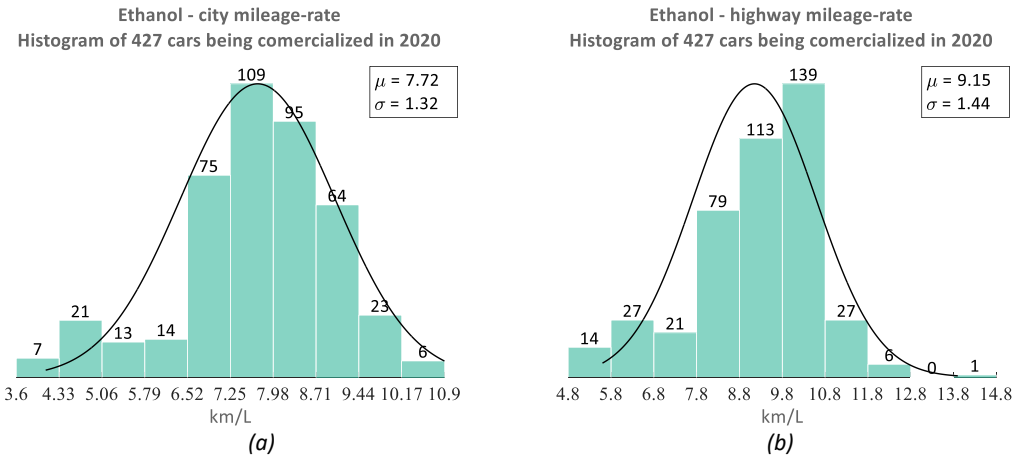

Figure 75 - Ethanol cars mileage rate. (*a*) city mileage rate (*b*) highway mileage rate

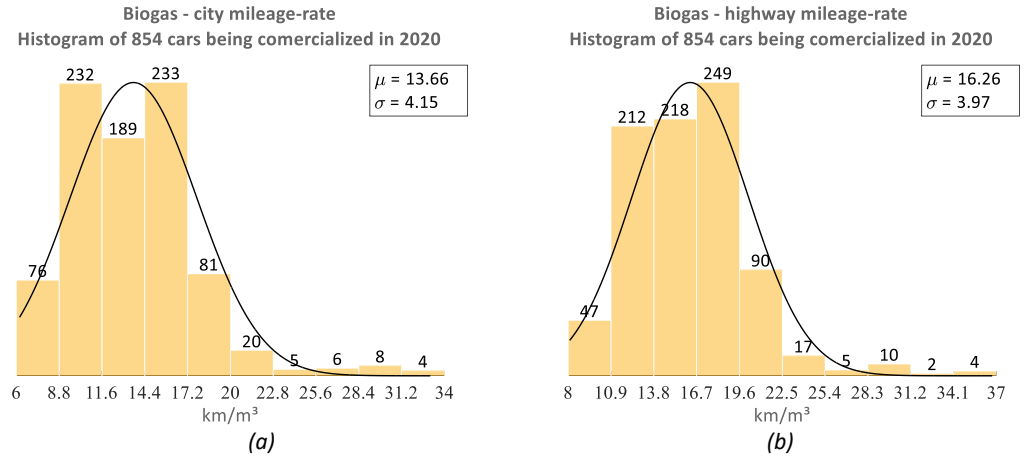

Figure 76 - Biogas cars mileage rate. (*a*) city mileage rate (*b*) highway mileage rate

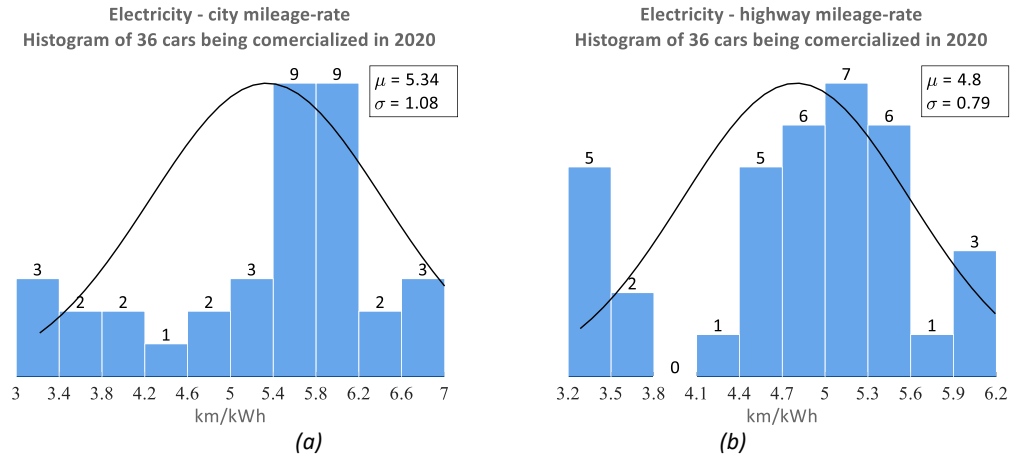

Figure 77 - Electric cars mileage rate. (*a*) city mileage rate (*b*) highway mileage rate

2 CO2 emission

Figure 78 shows the CO_2 emission along the chain from the surplus bagasse and straw from the field through processing, manufacture, distribution, and use in a vehicle. The value of CO_2 emission in terms of kilograms equivalent comprises the sugarcane mill processing $3x10^9$ kg of sugarcane per year. When the bar color does not appear in the plot, such as straw transportation, it is because it is insignificant when compared to the others emission step. The calculated value is shown in Table 27.

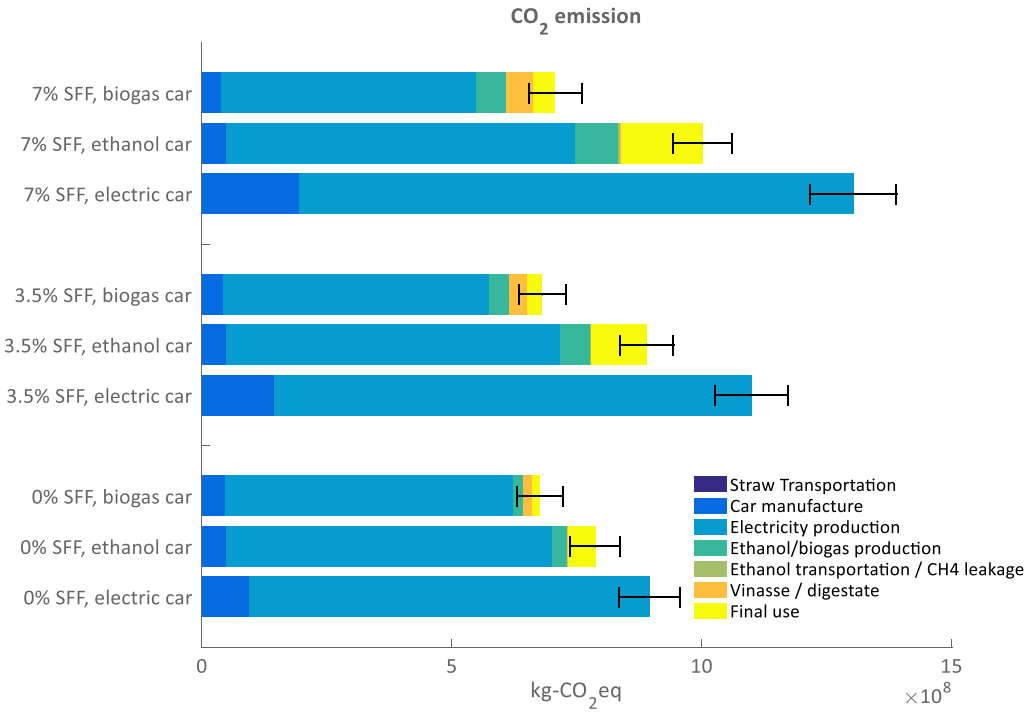

Figure 78 - CO2 emitted during the process of producing and using each fuel

Table 27 - CO2 emission given in kg of CO2 equivalent

	Straw transportation [a]	Car manufacture [b]	Electricity production [c]	Biogas/ethanol production [d]	Ethanol transportation of biogas leakage [e]	Vinasse / digestate	Final use
0% SSF, electric car	0	9.41E+07	8.00E+08	0.00E+00	0.00E+00	0.00E+00	0.00E+00
0% SSF, ethanol car	0	4.82E+07	6.53E+08	2.94E+07	1.36E+06	1.36E+05	5.46E+07
0% SSF, Biogas car	0	4.55E+07	5.78E+08	1.97E+07	3.34E+05	1.78E+07	1.44E+07
3.5% SSF, electric car	1.73E+05	1.44E+08	9.55E+08	0.00E+00	0.00E+00	0.00E+00	0.00E+00
3.5% SSF, ethanol car	1.73E+05	4.82E+07	6.69E+08	5.92E+07	2.74E+06	4.05E+05	1.10E+08
3.5% SSF, Biogas car	1.73E+05	4.15E+07	5.33E+08	4.00E+07	6.78E+05	3.61E+07	2.93E+07
7% SSF, electric car	3.45E+05	1.94E+08	1.11+09	0.00E+00	0.00E+00	0.00E+00	0.00E+00
7% SSF, ethanol car	3.45E+05	4.82E+07	6.97E+08	8.76E+07	4.06E+06	6.01E+05	1.63E+08
7% SSF, Biogas car	3.45E+05	3.76E+07	5.10E+08	5.96E+07	1.01E+06	5,38E+07	4.36E+07

[a] Refers to the contribution of the straw being transported using diesel trucks in an average distance from the filed to the industrial site of 22km; [b] Emission of CO2 due to vehicle manufacture, using electric and combustion engines is according to Qiao(QIAO *et al.*, 2019); [c] Refers to the emission by the boiler; [d] Refers to the emission in the industrial process to produce second-generation ethanol or biogas; [e] Refers to the emission due to transportation of ethanol from the industrial site to the fuel stations or due to leakage of CH_4 in the pipeline grid and during cars fueling;

3 - Price of Ethanol Biogas and Electricity

In Figures 79, 80, and 81 are shown the price of the fuels and its correction by the inflation rate when necessary. It is also shown the average value and standard deviation used in the article analysis. The ethanol price was taken from UDOP (UDOP - UNIÃO NACIONAL DE BIOENERGIA, [*s. d.*]); the vehicular-natural-gas price was taken from ANP(ANP - AGÊNCIA NACIONAL DO PETRÓLEO, Gas natural e biocombustíveis, [*s. d.*]). Ethanol and vehicular-natural-gas price were corrected by the inflation rate index IPCA from IBGE(IBGE - INSTITUTO BRASILEIRO DE GEOGRAFIA E ESTATISTICA, [*s. d.*]). The electricity price was taken from national electricity agency ANEEL(ANEEL - AGENCIA NACIONAL DE ELENRGIA, [*s. d.*]): those prices are the average price paid to producers at power ouctions. The price released by ANEEL is already corrected by inflation rate index.

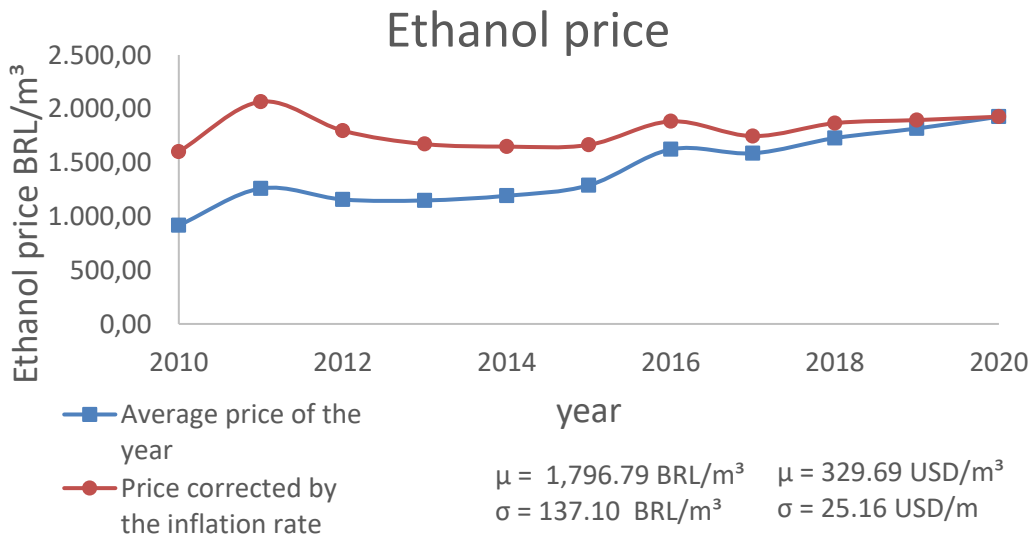

Figure 79 - Ethanol price paid at Paulínea - SP fuel distribution center

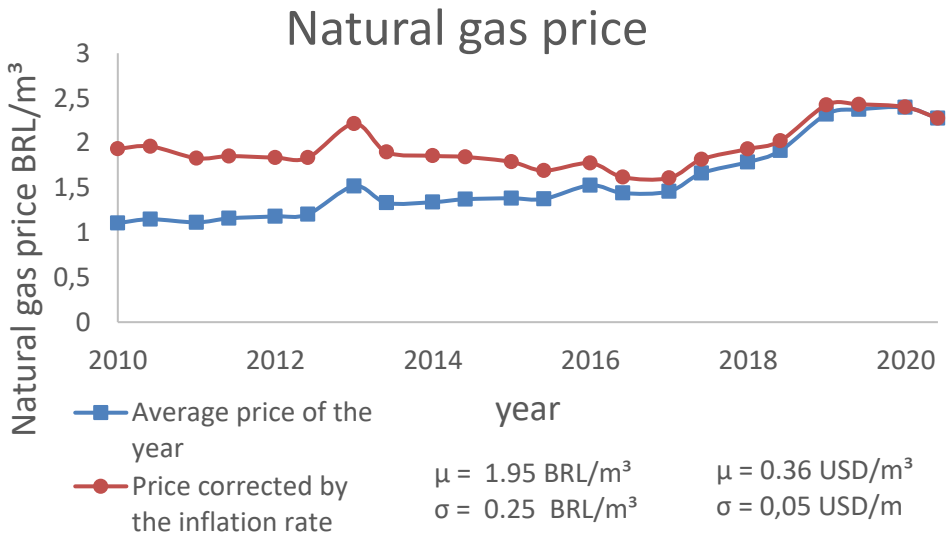

Figure 80 - Vehicular natural gas average price at São Paulo State

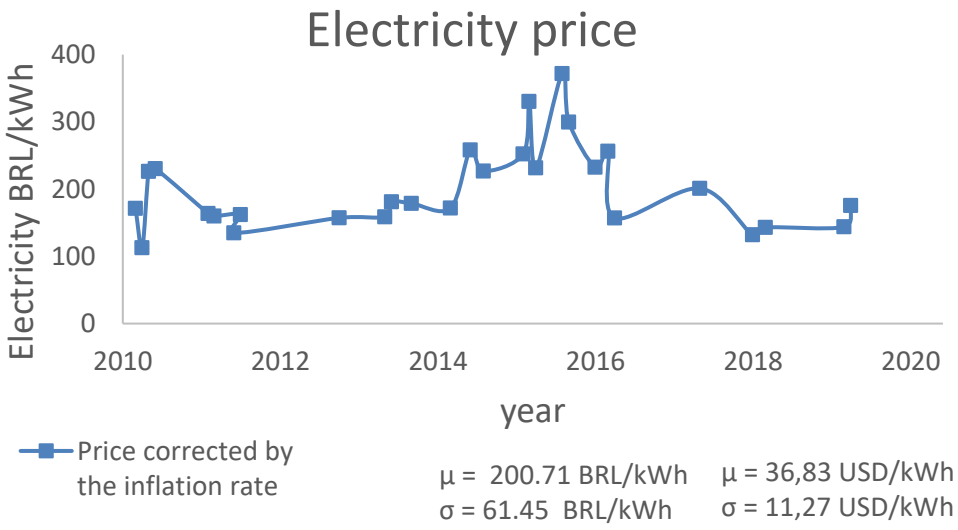

Figure 81 - Average price paid at power auctions

CHAPTER 7: FINAL CONSIDERATIONS

The purpose of this chapter is to highlight the main contribution of this thesis and to offer recommendations for future research by identifying some research gaps. This thesis shows the mathematical model, methodology and computational tools for the simulation of the sugarcane industry. Its use aims to improve the performance of the industrial process in many aspects such as energy, environment and economics.

7.1 General conclusions

Detailed studies on the main unit operations used in the Sugarmill were carried out. Then a mathematical model, based on the energy and mass balance of each unit operation, was developed; some unit operations also required a parametric equation. Each unit operation model was solved and the result was compared with industrial data, and, when necessary, the parameters were adjusted. These unit operations were clustered in areas, which simplifies the resolution of the mathematical model and makes the platform simple for future modifications, adjustments, corrections, or improvements. The areas were then assembled to simulate the entire industrial process. Adding a process such as second-generation ethanol consists of adding an area to the industry.

Multiple-effect evaporation is a key operation in the sugarcane industry, as it is responsible for the supply of thermal energy for the entire industrial process. It was shown that changing the operation mode can save bagasse, which can be used to produce more electricity, second-generation ethanol, or biogas.

The sugarcane industrial process was shown to be improved through the use of bagasse and straw to produce advanced biofuels. The feedstocks used to produce these fuels are industrial and agricultural residues or other residues that cannot be used directly as food for humans. The evaluation of the process that uses the residues, when interconnected with the current sugarcane industry, showed a synergetic effect. This synergy is due to the exchange of feedstock and utilities with the first-generation process. The type of fuel to be produced was shown to depend on the investigated aspects, i.e., social, economic, environmental, handleability, and health. The use of residues to produce fuel is not only profitable for the producer but also plays an important role in the Brazilian environmental-friendly fuel matrix.

7.2 Future work suggestions

Any simulation aims to explore an issue; therefore, some areas, in this work, were detailed modeled because are a key operation to provide the result to an issue, while others have a simplified model. For example, multiple-effect evaporation, to allow the study of dynamic simulation, requires a complex mathematical model; conversely, distillation has a simple model. For example, when different concentrations of ethanol in wine are used (which were not done in this work), the mathematical model of distillation needs to be updated to obtain the right steam consumption.

The first-generation process has been modeled using modern techniques and technology that have been tested for many years in the industry; conversely, the process that converts industrial and agricultural residues has recently left the laboratory scale. Therefore, there are many uncertainties associated with the conversion efficiency of different processes. Thus, narrowing the result of bagasse and straw conversion to second-generation ethanol, biogas, or another product could provide a more realistic approach to determine which fuel is the best (CASTRO; ALVES; NASCIMENTO, 2021). This narrowing approach should also consider the specifics, such as the location of the industry and current facilities.

Vinasse and filter cake are residues that have great potential to be used as an energy source to enhance the industrial process (BARROS *et al.*, 2017). Currently, both are used as fertilizers, therefore, the impact of the removal of these agricultural fertilizers (PRADO; CAIONE; CAMPOS, 2013) must also be evaluated in a study in which they are used as feedstock for another process.

Another suggestion is to include new modules in the simulation platform, such as agricultural production, supply chain, and product distribution. This would be useful to assess the greenhouse gas inventory.

Also, the investment in a new plant to produce advanced fuel can consider feedstock from more than one Sugarmill. This is the situation where, for example, for reasons of economies of scale, a joint venture is set up and thus the feedstock would be exchanged or centralized between industries (CHIAO; LO; YU, 2010).

References

BARROS, Valciney Gomes De; DUDA, Rose Maria; VANTINI, Juliana da Silva; OMORI,

Wellington Pine; FERRO, Maria Inês Tiraboschi; OLIVEIRA, Roberto Alves De. Improved methane production from sugarcane vinasse with filter cake in thermophilic UASB reactors, with predominance of Methanothermobacter and Methanosarcina archaea and Thermotogae bacteria. **Bioresource Technology**, *[S. l.]*, v. 244, n. May, p. 371–381, 2017. DOI: 10.1016/j.biortech.2017.07.106. Disponível em: http://dx.doi.org/10.1016/j.biortech.2017.07.106.

CASTRO, Rubens Eliseu Nicula De; ALVES, Rita Maria Brito; NASCIMENTO, Claudio Augusto Oller. Assessing the sugarcane bagasse and straw as a biofuel to propel light vehicles. **Sustainable Energy & Fuels**, *[S. l.]*, n. 5, p. 2563–2577, 2021. DOI: 10.1039/D1SE00129A. Disponível em: http://pubs.rsc.org/en/Content/ArticleLanding/2021/SE/D1SE00129A.

CHIAO, Yu Ching; LO, Fang Yi; YU, Chow Ming. Choosing between wholly-owned subsidiaries and joint ventures of MNCs from an emerging market. **International Marketing Review**, *[S. l.]*, v. 27, n. 3, p. 338–365, 2010. DOI: 10.1108/02651331011047998.

PRADO, Renato de Mello; CAIONE, Gustavo; CAMPOS, Cid Naudi Silva. Filter Cake and Vinasse as Fertilizers Contributing to Conservation Agriculture. **Applied and Environmental Soil Science**, *[S. l.]*, v. 2013, p. 1–8, 2013. DOI: 10.1155/2013/581984. Disponível em: http://www.hindawi.com/journals/aess/2013/581984/.